Process stratigraphy: from numerical simulation to lithology prediction

Karamitopoulos, Pantelis

DOI
10.4233/uuid:1a21c6a6-0412-4ea1-b8b4-c1c84c19d68e

Publication date
2020

Document Version
Final published version

Citation (APA)
Karamitopoulos, P. (2020). *Process stratigraphy: from numerical simulation to lithology prediction*. [Dissertation (TU Delft), Delft University of Technology]. https://doi.org/10.4233/uuid:1a21c6a6-0412-4ea1-b8b4-c1c84c19d68e

Process stratigraphy: from numerical simulation to lithology prediction

Pantelis Karamitopoulos

Process stratigraphy: from numerical simulation to lithology prediction

Dissertation

for the purpose of obtaining the degree of doctor
at Delft University of Technology
by the authority of the Rector Magnificus prof.dr.ir. T.H.J.J. van der Hagen
chair of the Board for Doctorates
to be defended publicly on
Monday 10 February 2020 at 10:00 o'clock

by

Pantelis KARAMITOPOULOS
Master of Science in Geoscience for Subsurface Exploration, Appraisal and Development,
Heriot-Watt University, Scotland, United Kingdom
born in Thessaloniki, Greece

This dissertation has been approved by the promotors.

Composition of the doctoral committee:

Rector Magnificus	chairman
Prof. dr. A.W. Martinius	Delft University of Technology, promotor
Prof. dr. G.J. Weltje	Katholieke Universiteit Leuven, Belgium, promotor
Dr. M.E. Donselaar	Delft University of Technology, copromotor

Independent members:

Prof. dr. A. Amorosi	University of Bologna, Italy
Prof. dr. G. Hampson	Imperial College London, United Kingdom
Prof. dr. ir. Z.B. Wang	Delft University of Technology
Dr. M.B. Brommer	International Geothermal Association, Germany
Prof. dr. G. Bertotti	Delft University of Technology, reserve member

This research was funded by the Netherlands Organization for Scientific Research (NWO) and GRASP Marie Curie Research Training Network.

Keywords: chronosome, avulsions, bifurcation intensity, depositional connectivity, process-based geological modelling

Printed by: Gildeprint

Cover design by P. Karamitopoulos

ISBN 978-94-6402-097-7

An electronic version of this dissertation is available at:
https://repository.tudelft.nl

Preface

When I started this PhD research, I didn't know much about numerical modelling of river systems. Until then I had mainly done research on seismic sequences and forward seismic modelling of turbidite geometry and facies architecture as part of my bachelor's and master's thesis, respectively. After completing a master's degree in Geosciences, I was eager to explore further sedimentary systems dynamics, for I realized its importance when interpreting and modelling multi-scale heterogeneity in three dimensions. Having gained some experience with outcrop-based reservoir modelling, I joined the Applied Geology Section at TU Delft, a group that cultivates a vibrant and sustained research culture and shares the common vision to bridge Geoscience and Engineering disciplines. I was surprised that my new colleagues were so keen to integrate multiscale surface and subsurface technical data and to utilize new data types derived from numerical simulation in order to improve physical property predictions in shallow and deep subsurface reservoirs. During the course of my PhD research, my colleagues have made me increasingly enthusiastic about numerical simulation, sedimentary systems and reservoir sedimentology, and have taught me a lot. Without them I could never have finished this thesis, for which I am truly grateful.

My first words of gratitude go to my promotor Gert Jan Weltje. Gert Jan dedicated a lot of his time to share his knowledge while giving me the freedom to follow my own intuition. Besides contributing and reviewing all of my manuscripts, discussing results and research ideas we could also talk about other things in life, which I much appreciated. Gert Jan, I've learned a lot from you and I deeply thank you for that! I would like to thank Rory Dalman for being an excellent co-supervisor and a very good friend. His advice and comments were accurate and truly valuable for the fulfilment of most of the chapters of this thesis. Special thanks go to Hans Bruining who invited me to contribute to an EU-funded research project on carbon capture and sequestration (CCS) as a Marie-Curie Early Stage Researcher, and gave me a strong theoretical and technical foundation of CCS technology, from capture to underground storage. Many thanks go out to my promotor Allard Martinius and my co-promotor Rick Donselaar whose comments and suggestions significantly improved the contents of this thesis. The committee members are acknowledged for their thorough and constructive comments and suggestions.

Most of the chapters presented in this thesis describe collaborative work, which would have not been possible without the comments of people who were somehow involved. Chapter 2 was written together with Gert Jan Weltje and Rory Dalman. It comprises a rework of a stranded manuscript,

previously submitted by the former authors under the title: ‘High-resolution marine to continental correlation in fluvio-deltaic systems: analysis of the morphodynamic feedback governing autogenic parasequence formation’. Careful reviews by Matthew Wolinsky, Jean Lynch-Stieglitz and three anonymous reviewers greatly improved the quality of the original manuscript. Chapter 3 was written together with Gert Jan Weltje and Rory Dalman. The thoughtful reviews of Peter van der Beek, Kyle Straub, Rudy Slingerland and two anonymous reviewers helped to improve the text significantly. Chapter 4 was written together with Gert Jan Weltje and Rory Dalman, and was greatly improved by the careful reviews of Zoltan Sylvester, Joshua Dixon, Jinyu Zhang and Jory Pacht. Chapter 5 was written together with Rick Donselaar, who also provided me the field data for the model initiation and calibration. Perceptive reviews by Gert Jan Weltje, Dario Ventra and Rory Dalman, were very helpful in shaping this chapter. Chapter 6 was written together with Gert Jan Weltje, Rory Dalman, Quinto Sacchi and Adriaan Janszen. A big thanks to Adriaan who provided some figures from his Master’s thesis.

I would like to thank all the people at TU-Delft who supported me this period of my life as a PhD, making the past years fun, interesting and diverse: Adriaan, Alex, Andrea, Anke, Araz, Bob, Carlos, Claudio, Daria, Elisa, Elmer, Geertje, Giacomo, Guy, Ilja, Ioannis, Jiaguang, Joelle, Joost, Jürg, Kevin, Koen, Louise, Marcin, Nathalie, Nico, Negar, Panos, Roozbeh, Remco, Sanaz, Saskia, Thomas, Wieske, Wiebke, Walter, Xiaoxi, all the current research staff at the Applied Geology Section, Akeel, Aulia, Annemarie, Giovanni, Hemmo, Jan Kees, Joep, Maaike, Maria, Martha, Pierre-Oliver, Rahul, Rémi, Runhei, Helena, Hiranya, Santosh, Siddharth, Stefan, Stephan, Thais, Tim, Youwei and of course the secretarial staff of the department Lydia, Margot, Marijke, Marja, Marlijn, Myrthe and Ralf, you guys are the best!

I would also like to thank my colleagues from TNO, where I worked for a couple of years as a consultant. Many thanks to Denise, Dirk, Frank, Freek, Friso, Geert, Geert-Jan, Hanneke, Isabel, Johan, Kees, Lindsay, Mart, Rader, Renaud, Roel, Susanne, Thijs, Xander, Ymke for the support, ideas and fruitful discussions during the projects we did together and the thoughtful comments regarding applications of this PhD research.

Finally, I wish to thank all the collaborators from Polytechnic University of Turin, Costanzo, Christoforos, Eloisa, Francesca and Quinto, whose excellent contribution and research methods have taken this type of research to a whole new level.

Besides my colleagues, I would like to thank my family, especially Natalie and all my friends - you have always been there for me and have always supported me, not only throughout my PhD, but with everything that comes in life. For that, I am very grateful.

Enjoy reading the remaining part of the thesis!

Chapter 1

Introduction

1.1 General introduction

The essence of geoscience is to map the physical properties of the earth, extract spatio-temporal trends and build models that represent, explain and predict new observations in the stratigraphic record. In this perspective, the geoscientist's main task is to reconcile the quantitative descriptions of the available data sets with the qualitative storylines of a conceptual geological framework and build a multi-scale numerical/categorical representation of the subsurface, i.e. the geological model. The data sets available are typically sparse, of varying sampling intensity and resolution, spanning km to nm scales, and originate from single- or multi-purpose discontinuous surveys. Hence, the geological model build-up relies largely on data integration (upscaling or downscaling methods) and sequential time-stepping (data assimilation) procedures. Ultimately, the goal is to reduce the inherent uncertainties in geological modelling and to improve predictions of key subsurface properties such as size, shape, spatial distribution and internal heterogeneity of sedimentary units, as these may host recoverable volumes of water and energy resources.

Geostatistical tools (e.g. pixel- and/or object-based simulation, multipoint statistics) have been customarily used for the modelling of aquifers/aquitards and reservoirs/seals (Hoeksema and Kitanidis, 1985; Haldorsen and Chang, 1986; Journel, 1986; Matheron et al., 1987; Dubrule, 1989; Journel and Alabert, 1989, 1990; Haldorsen and Damsleth, 1990; Cressie, 1991; Anderson and Woessner, 1992; Xu et al., 1992; Dimitrakopoulos and Desbarats, 1993; Desbarats and Bachu, 1994; Yarus and Chambers, 1994; Bratvold et al., 1995; Goovaerts, 1997; Webster and Oliver, 2001; Deutsch, 2002; Strebelle et al. 2002; Caers and Zhang, 2004; Liu et al. 2004; Harding et al. 2005; Felleti et al., 2006; Arpat and Caers 2007; Daly and Caers, 2010; Straubhaar et al., 2011), yet inevitable questions related to geostatistical model validation, space of uncertainty, non-uniqueness reduction of inverted geophysical models and the underlying processes that generated the observed data highlighted the importance for adapting multi-step approaches able to connect data space (i.e. predictive model distributions) to observed data and model parameter space in a

consistent way, representative of spatial distribution and internal heterogeneity captured in the stratigraphic record (Soares, 1993; Armstrong and Dowd, 1994; Dimitrakopoulos, 1994; Soares et al., 1997; Gómez-Hernández et al., 1999; Monestiez et al., 2001; Leuangthong and Deutsch, 2003; Sanchez-Vila, 2004; Soares et al., 2008; Atkinson and Lloyd, 2010; Abrahamsen et al., 2012; Agterberg, 2014; Gómez-Hernández et al., 2017; Arnold et al., 2019).

Numerical process-based stratigraphic models in forward (Allen, 1978; Leeder, 1978; Bridge, 1979; Tetzlaff and Harbaugh, 1989; Martinez and Harbaugh, 1993; Slingerland et al., 1994; Mackey and Bridge, 1995; Koltermann and Gorelik, 1996; Heller and Paola, 1996; Miall, 1996; Wendebourg and Harbaugh, 1997; Granjeon and Joseph, 1999; Griffiths et al., 2001; Meijer, 2002; Storms et al., 2002; Clevis et al., 2003; Lesser et al., 2004; Burgess et al., 2006; Jerolmack and Paola, 2007; Hutton and Syvitski, 2008; Burgess, 2012; Hajek and Wolinsky, 2012; Zhang et al., 2018) and inverse mode (Bornholdt et al., 1999; Cross and Lessenger, 1999; Karssenberg et al., 2001; Wijns et al., 2004; Karssenberg et al., 2007; Sharma and Imhof, 2007; Charvin et al., 2009, 2011; Weltje, et al, 2013; Falivene et al., 2014; Sacchi et al., 2015, 2016; Skauvold and Eidvik, 2018) provide attractive tools to simulate sedimentary system dynamics spanning a wide range of stratigraphic spatial scales (basin, architecture, event), timescales (0.1-10 yr, 1-10 kyr, 100 kyr-1 myr) (Cowell et al., 2003a, b; Keogh et al., 2007; Hajek and Wolinsky, 2012) and segments (or compartments) of the sediment routing system (Swenson et al., 2000; Swenson et al., 2005; Kim et al., 2006a, b; Sømme et al., 2009; Carvajal and Steel, 2012) while allowing full access to the model responses, i.e. the spatial distribution of discriminant lithologies and physical properties as a function of the intervening processes and environmental conditions at the time of deposition. The realism and predictive power of model responses may be quantitatively assessed by comparison with the geophysical/geological data available.

1.2 Background

1.2.1 The sediment routing system: from erosional source to depositional sink

The study of sediment routing systems comprises an integral part of basin analysis as it provides quantitative information regarding the fairways of sediments and dissolved solutes from upland regions (sources) down to regions of long-term deposition (sinks), and their contribution to global biogeochemical cycles (i.e. the long-term carbon cycle) (Fig. 1.1) (Meybeck, 1987; Allen, 1997; Hay 1998; Galy et al., 2007; Sømme et al., 2009; Allen and Heller, 2012; Allen and Allen, 2013,

Allen, 2017). Sediment mass flux (or yield) is generated at upland catchments under 'the decay and disintegration of rock *in situ* at the Earth's surface' (Allen and Allen, 2013), and expelled down-system, mainly by runoff. Sediments accumulate to depositional sites (or sinks) for short-term or long-term storage. Short-term storage implies that fluvial sediment supply is directly connected to deep sea sinks, and thus sediment supply signals are propagated to a large extent unaltered from source to sink (Allen, 2008; Romans et al., 2009). By contrast, depositional systems that have the capacity to store sediments along their transport fairways, transform (or shred) sediment supply signals and are characterized by long response times (Allen, 2008; Somme et al., 2011).

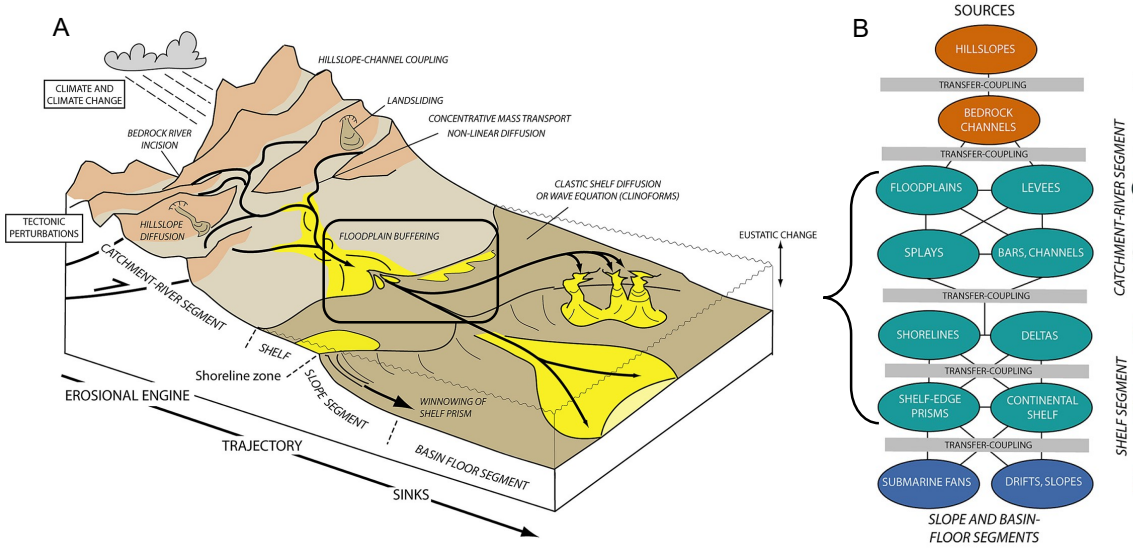

Figure 1.1: (A) Concept of the sediment routing system and its mutually coupled subsystems (or segments) (From Allen and Heller (2012, p. 113, fig. 6.2), modified from Somme et al. (2009). (B) Sediment sources (orange), sites of temporary (green) and permanent (blue) sediment storage. From Allen and Heller (2012, p. 113, fig. 6.1). Black square and curl in figures A and B respectively, outline the sediment routing system segments studied in this thesis.

Sediment routing systems consist of mutually coupled subsystems (or segments), each characterized by a distinct set of sedimentation processes (Fig. 1.1) (Allen and Allen, 2013; Allen, 2017). These processes involve internal (or autogenic) dynamics (i.e. crevassing, avulsions, mouthbar-induced bifurcations) and external (or allogenic) forcing mechanisms (i.e. climate, tectonics) and occur over a wide range of spatial and temporal scales: some operate over very small areas and are effectively instantaneous, others are less localized and active over long periods of time (Tipper, 2016). The moving boundaries between the sediment routing system segments (i.e. alluvial valleys, coastal zones, shelf-edge prisms) act as staging areas (or buffer zones) for temporary sediment storage (Swenson et al., 2000; Malmon et al., 2003; Swenson et al., 2005; Kim

et al., 2006a, b; Sømme et al., 2009; Sømme et al., 2011; Allen and Heller, 2012; Carvajal and Steel, 2012; Romans et al., 2016). Thus, investigating the complex interplay of sedimentation processes occurring in staging areas is elemental, not only for understanding their functioning and sensitivity to upstream sediment flux signals, but also for quantifying the amount and distribution of ancient sediment budgets critical to predict large-scale stratigraphic trends in depositional basins (Marr et al., 2000; Strong et al., 2005).

The total amount of sediment released to the ocean is estimated to be c.18×10^{9} t yr^{-1} (Milliman and Syvitski, 1992; Walling and Webb, 1996; Syvitski and Milliman, 2007). This is conditioned by a large number of geologic, geomorphic and geographic factors, as well as the ever-increasing human activities. According to Hovius et al. (1998), half of the variance in global sediment yield is explained by environmental factors (i.e. precipitation rate, temperature) and topographic effects, i.e. maximum elevation, local relief, slope and drainage basin area. Models of sediment yield utilized measurements of sediment load data obtained at the mouths of large rivers and were typically used as indices of sediment yield (Milliman and Meade, 1983; Summerfield and Hulton, 1994; Berner and Berner, 1997; Hay, 1998; Hovius, 1998). Figure 1.2 illustrates an inverse relationship between drainage basin area and sediment yield which partly reflects the storage effect (floodplain buffering) likely to increase in larger drainage basins (Allen and Allen, 2013). Milliman and Meade (1983) addressed several problems regarding the use of sediment load data measured at river mouths, and were mainly related to human activities, the scarcity of 'pristine' rivers and the inefficacy to compare measurements from different surveys over different periods of time. In addition, sediment-load measurements at the river mouth account for suspended load only. Consequently, sediment budget estimates are subject to high uncertainty in active systems, let alone ancient ones. Similarly, the estimation of catchment-averaged erosion rates in palaeo-catchments that have now vanished has its own limitations (Hovius et al., 2000; Dadson et al., 2003; Braun, 2005; Reiners et al., 2005; Heffern et al., 2008; Leeder, 2011).

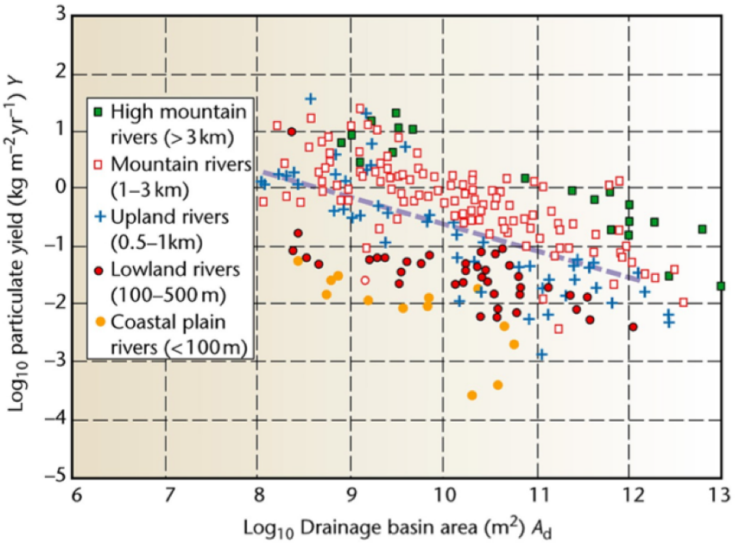

Figure 1.2: Plot of drainage basin area versus particulate sediment yield for five elevation classes of Milliman and Syvitski (1992). From Allen and Allen (2013), after Hay (1998).

The *BQART* model accounts for the contribution of the different sediment-yield producing factors (geologic, geomorphic and geographic influences, and human activities) and provides a more comprehensive prediction of long-term sediment fluxes to the coastal zones (Syvitski and Milliman, 2007), assuming that certain catchment characteristics have been approximated:

$$Q_s = \omega B Q_w^{0.31} A^{0.5} R T \qquad (1),$$

where Q_S is sediment discharge at the river mouth, ω is a dimensional factor, Q_W is the estimated water discharge, B is the anthropogenic-geological influence factor, R is the catchment maximum relief and T is basin-averaged temperature.

1.2.2 Process stratigraphy

Process stratigraphy comprises an evolutionary branch of sequence stratigraphy (see §1.2.4) and is concerned with the dynamics of the controls on stratigraphic patterns, regulated by the interplay of sediment supply (volume, grain sizes) and the rate of generation and spatial distribution of accommodation (Allen and Allen, 2013). Sediment supply and accommodation (the space available for sediments to accumulate) vary strongly over space and time, causing complex stacking and architectural arrangement of stratal units (Catuneanu, 2006; Catunenanu et al., 2009). Sediments filling this available space may underfill or overfill sedimentary basins, which makes process stratigraphy 'essentially a mass or volume balance exercise' (Allen and Allen, 2013). Process

stratigraphy comprises a kind of integrated stratigraphy, combining elements of chronostratigraphy, lithostratigraphy, chemostratigraphy, biostratigraphy and magnetostratigraphy, yet discriminating stratal categories is not its primal aim. Its fundamental aim is to understand the driving mechanisms behind the architectural arrangement and stratigraphic cycles found in sedimentary basins (Barrel, 1917; Tipper, 2000; Miall, 2010). These mechanisms are associated with the sedimentary system's internal (autogenic) dynamics and external (allogenic) forcing (i.e. dynamic topography, changes in crustal/lithospheric thickness, loading and unloading of the lithosphere causing subsidence and uplift respectively, the orbit of the earth around the sun and greenhouse gas concentrations in its atmosphere) (Reading, 1996; Einsele, 2000; Ruddiman, 2001; Leeder, 2011), with the frequency of autogenic dynamics related to the rate of change in allogenic forcing relative to basin response (or equilibrium) time (Paola et al., 1992; Blum et al., 2013; Postma, 2014). Under this process-stratigraphic approach, 'sedimentary basins should not be regarded as passive receptacles but instead as dynamic entities occupied by complex physical and biological process systems' (Allen and Allen, 2013), which interact over different orders of magnitude and duration. Towards this direction, identifying the role and relative contribution of sedimentary processes to the stratigraphic record requires detailed investigation of recent and ancient depositional systems.

1.2.3 Depositional Systems

Depositional systems record the sedimentary fabrics associated with the interplay of allogenic and autogenic processes at the time of deposition. They may be classified according to the geomorphic elements (or landforms) found along the proximal, medial and distal segments of the sediment routing system. In this section, a brief overview of depositional systems relevant to this thesis is presented (i.e. continental, coastal and nearshore and continental shelf depositional systems).

Alluvial fans are widespread depositional landforms, found over a wide range of tectonic and climatic settings, bordering highland regions and actively subsiding continental basins (Fig. 1.3). Alluvial fans are occupied by coupled systems involving hillslope and fluvial processes and are highly sensitive to upstream sediment flux signals. Debris, grain flows and mudflows are common processes occurring at the fan apex. In cases where sediment and water discharges are high, river channels become braided, whereas groundwater-fed fan channels are generally smaller with meandering channel pattern (Bridge, 2003). The overbank areas are characterized by sparse channelized flow and episodic sheet-floods while channel diversions (avulsions) are also common (Schumm et al., 1987). Variations in water and sediment discharge from the catchments relative to

basin subsidence rate regulate fan aggradation or degradation rates and thus control the size and geometry of the alluvial fan (Bull and Schick, 1979; Bull, 1991; Blair and McPherson, 1994; Whipple and Trayler, 1996; Allen and Hovius, 1998; Parker et al., 1998; Allen and Densmore, 2000; Gawthorpe and Leeder, 2000; Duller et al., 2010; Allen et al., 2013). Detailed reviews on alluvial-fan sedimentation processes are provided by Bull (1977), Miall (1996), Nichols and Fisher (2007), North and Warwick (2007), Ventra and Clark (2018).

Alluvial (or transfer) valleys stretch from upland catchment confluences down to the distal reaches of the catchment-river sediment routing segment (Fig. 1.1) where subaerial delta-lobes grow. The different sediment-transfer trajectories across the valley involves various transit times which result in temporary or prolonged periods of sediment storage. Sediment discharge patterns may directly reflect the erosional processes in the upland catchments, or may be modulated by base-level fluctuations across the valley or at the river mouth (Blum and Hattier-Womack, 2009). Alluvial valleys consist of alluvial ridges and floodplains (or flood basins). The former comprise active and abandoned channels, bars with accretion topography, levees, crevasse channels and splays, whereas the latter refer to marshes, lakes, windblown sediments and drainage channels (Fig. 1.4).

Figure 1.3: A dry river channel carves through the Zagros Mountains in southern Iran and spreads out across the valley floor in a silvery fan (Google Earth - October 12, 2004, NASA image created by Jesse Allen, using data from NASA/GSFC/METI/ERSDAC/JAROS, and the U.S./Japan ASTER Science Team. Caption by Rebecca Lindsey, based on interpretation provided on the ASTER Project Science Imagery Gallery Website).

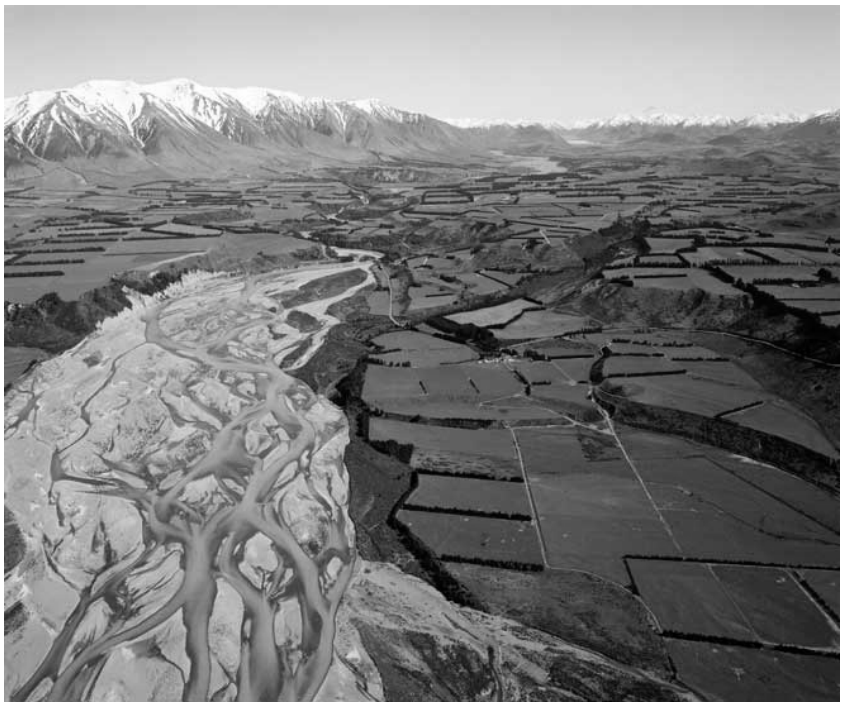

Figure 1.4: Rakaia River and the Southern Alps in the background (New Zealand) (GNS Science, CN24034/27, Original coloured photograph by Lloyd Homer).

The channel 'is distinctive in that it has a finite width and depth, a permeable boundary composed of erodible sediment and a free water surface' (Bridge, 2003). It comprises the major conveyor of water and sediments downstream. Channel geometry is principally controlled by the flow and the sedimentation processes occurring during seasonal floods (Wolman and Miller, 1960; Leopold et al., 1964; Carlston, 1965; Schumm, 1968, 1969; Daniel, 1971; Pickup and Werner, 1976; Andrews, 1980; Knighton, 1998). The rise of channel banks alters channel flow and sedimentation pattern, forming bars whose dimensions are regulated by channel flow width and depth (ASCE Task Force on Bed Forms 1966).

Channels scale to water discharge (Leopold and Maddock,1953; Wolman and Miller, 1960; Williams, 1978). 'The vertical dimension between the depth of scour and the bar top is a proxy for bankfull depth, and bankfull cross-sectional areas are known to adjust to flood discharge, the so-called bankfull discharge' (Blum et al., 2013). Channel bankfull discharge scales in turn to drainage area with high amount of variability explained by topographic relief and climate characteristics (Syvitski and Milliman, 2007).

Levees are discontinuous wedge-shaped ridges framing active and abandoned channels. Levee height relates to river size, grain size of sediment load and aggradation rate, whereas levee width is typically around four channel widths (Brierley et al., 1997; Bridge, 2003). Newly formed levees are narrow and steep due to initial high deposition rate of coarse-grained sediments, which gradually decreases away from the crest (Cazanacli and Smith, 1998).

Levee continuity may be interrupted by ephemeral smaller distributary channels (crevasse channels), which divert flow by breaching the banks of the main channel and deposit fan or lobe-shaped mounds of sediment called crevasse splays (Fig. 1.5) (Coleman, 1969; Smith et al., 1989; Bristow et al., 1999). By contrast, vegetation and/or early lithification (e.g. calcretes, silcretes) increase tensile and shear strength of river bank and bar surfaces and thus stabilize river flow and mitigate lateral migration of the main channel (Smith, 1976; Gibling and Rust, 1990; Fielding et al., 1997; Huang and Nanson; 1997; Gran and Paola, 2001). Levees consist occasionally of stacked adjacent crevasse splays (Coleman, 1969) which over the long-term act as natural bank stabilizers and thus play a key role to the progradation of alluvial ridges (Van Toorenenburg et al., 2018).

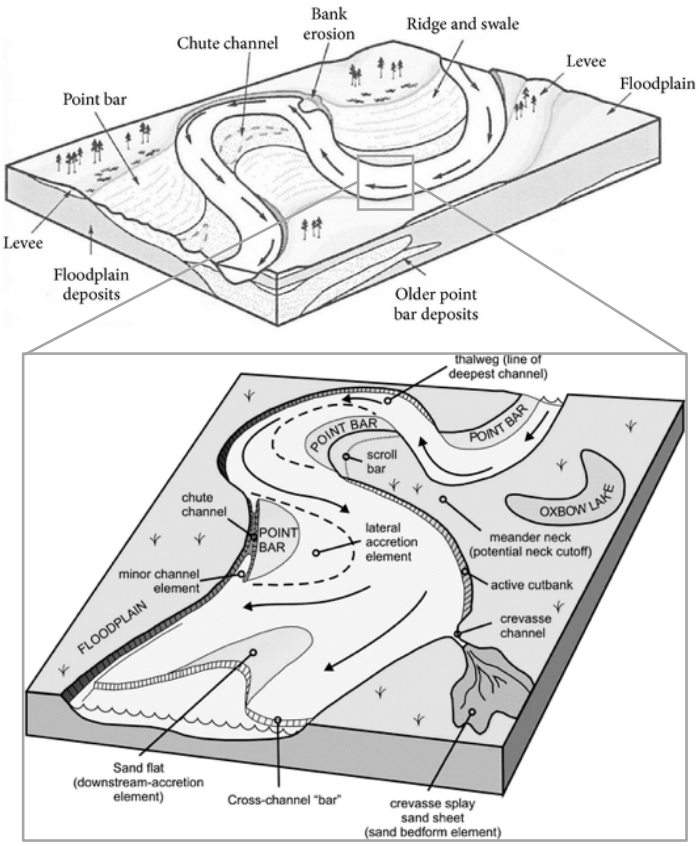

Figure 1.5: Sedimentation processes and landforms of a meandering single channel river (modified from Mount,1995). Inset: terminology of river sub-environments (modified from Miall, 2015).

Coastal and nearshore depositional systems comprise staging areas for temporary deposition before further transport to sites for permanent storage (sinks). Deltas are 'mounds of sediment deposited where river channel enters a body of water (such as a lake or sea) and supplies more sediment than can be carried away by currents in the water body' (Bridge, 2003). They are categorized according to characteristics within the delta plain i.e. the outflow dynamics (river flow velocity, friction between effluent and river bed, shear stress and water level/depth) which regulates the transport distances of the different-size particulates, and the density contrast between the water of the river and the basin waters (Bates, 1953; Wright and Coleman, 1974; Coleman and Wright, 1975; Galloway, 1975; Wright, 1977; Bhattacharya and Walker, 1992; Orton and Reading, 1993; Nemec, 1995; Boggs, 1995; Van Wagoner et al., 2003; Bhattacharya, 2006). Based on outflow dynamics there are three main categories: inertia-dominated jets, friction-dominated jets and buoyancy-dominated outflows. The first category is associated with high flow velocities and turbulence leading to rapid deposition of sediments close to the feeder stream (or main channel). The second category is characterized by high bed friction, shear stress and shallow water levels at the river-basin boundary. These conditions decelerate river flow and deposit sediments with a wider lateral extent compared to the first category, favouring as such the formation of subaqueous levees, fining basinward middle ground bars and bifurcated channels. The third category is characterized by deeper water levels compared to friction-dominated deltas and form subaqueous levees, distributary mouthbars, distal bars and prodelta clays. Deltas are also characterized by: a) homopycnal flow (density of fluvial discharge approximates the density of basin waters) favouring rapid mixing and abrupt deposition of sediments, b) hyperpycnal flow (density of fluvial discharge greater than the density of basin waters) which creates favourable conditions for river flow below the receptive waters while concomitantly eroding the previously deposited sediments and c) hypopycnal flow (density of fluvial discharge lower than the density of basin waters) which favours river flow over the basin waters and the gradual deposition of the suspended clay portion to the prodelta. Lacustrine deltas (and depositional systems in general) occupy tectonically active depressions and are very sensitive to climatic changes. They are subdivided based on their hydrological status into open (in the presence of an outlet) or closed (lacking an outlet to other external bodies of water), also known as endorheic (flowing within) lacustrine systems (Allen and Collinson, 1986; Talbot and Allen, 1996). The former is dominated by terrigenous clastic input, whereas the latter are characterized by the abundance of chemical/biochemical sedimentation. A more detailed description of terminal endorheic basins is provided in Chapter 5 of this thesis.

Deltas may also be subdivided into three geomorphological elements as a function of decreasing effect of fluvial processes and increasing subaqueous influence towards the distal part of the basin: delta top, delta front and prodelta. Delta morphology reflects the type and intensity of the dominant hydrodynamic processes including: a) river-dominated deltas, which are characterized by elongated distributary channels and mouthbars, b) wave-dominated deltas and c) tide-dominated deltas (Galloway, 1975; Heward, 1981; Postma, 1990; Boyd et al., 1992; Dalrympe et al., 1992; Reading and Collinson, 1996; Martinius et al., 2001) (Fig. 1.6). Under low wave and tide energies, river systems prograde into coastal areas and form 'birdfoot' deltas (i.e. Mississippi Delta) (Fig.1.7E, 1.8). Wave energy reduces the delta-lobe progradation because sediments entering the basin waters are resuspended and redistributed along the coastline, forming arc-shaped sandy ridges (i.e. São Francisco), while the finer-grained sediments are carried further offshore. Higher tidal energy (compared to river and wave energies) reworks mouth bars into longitudinal channel bars (or shoals) and govern local accumulation of fine-grained sediments in estuaries by flocculation (i.e. Ganges-Brahmaputra, Mahakam and Fly Deltas).

Finally, continental shelf depositional systems (or cross-shelf segments, sensu Blum et al., 2013) are sensitive to sea-level fluctuations and are similarly classified according to the hydraulic regime (wave-, tide-, storm- or current-dominated) and the nature of sediments (modern vs relict) (Swift, 1974; McManus, 1975; Johnson and Baldwin, 1986).

This PhD thesis focuses on sedimentation processes occurring in river systems and homopycnal flows in river-dominated deltas under the influence of internal (autogenic) dynamics and allogenic forcing in the form of relative base-level cycles.

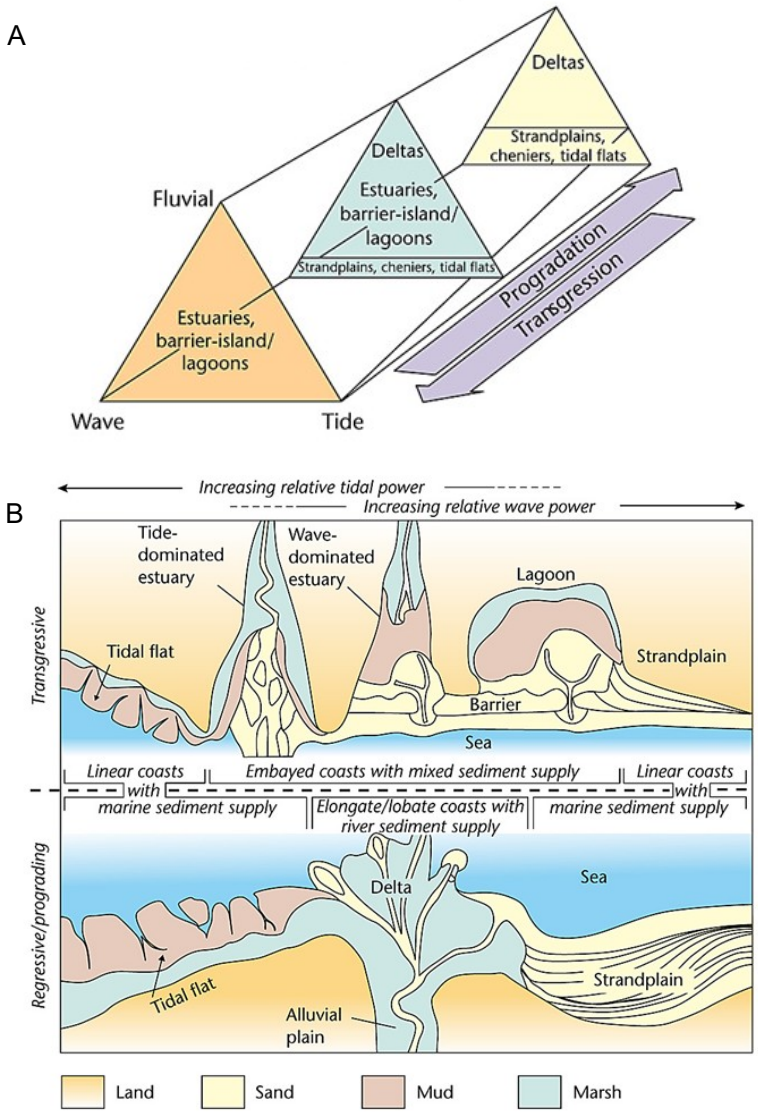

Figure 1.6: (A) Delta classification according to fluvial discharge, wave power and tidal range (from Allen and Allen (2013), following Galloway (1975), Postma (1990), Reading and Collinson (1996)). (B) Plan views of transgressive/retrogradational and regressive/progradational coasts under varying wave power and tidal range and marine and fluvial sediment supply (from Allen and Allen, 2013, based on Heward 1981 and Boyd et al., 1992).

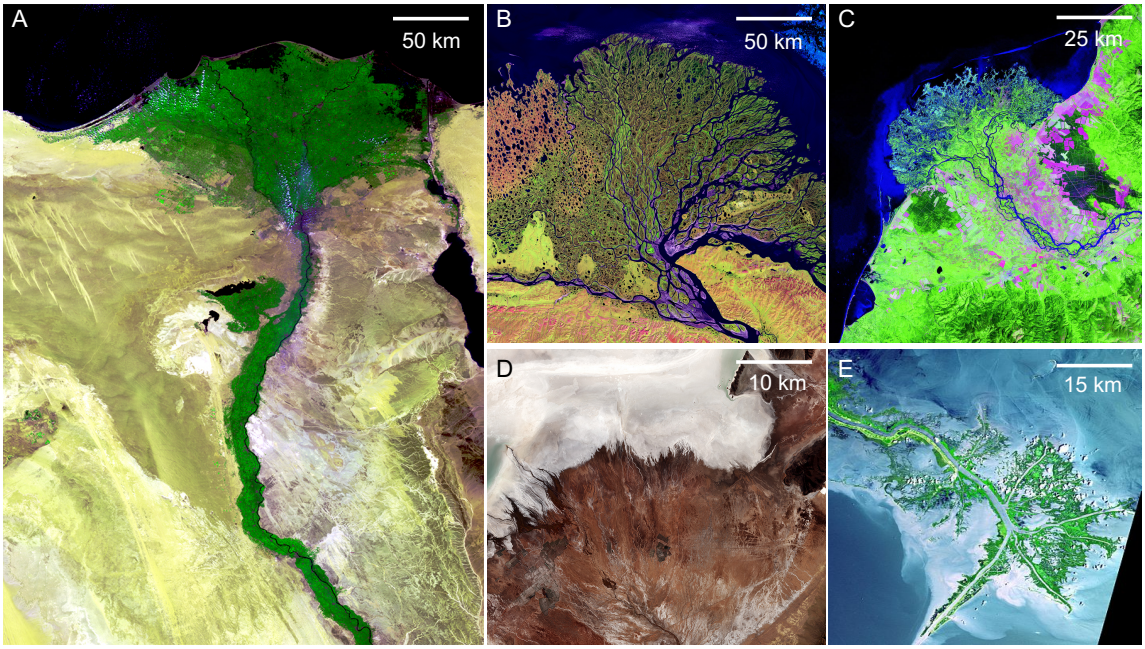

Figure 1.7: Real-world examples of river-dominated deltas. (A) The Nile Delta in Egypt acquired by Proba-V on 24 March 2014 (Source: ESA/VITO, Id 310511). (B) Lena Delta, north-east Siberia (Satelite image: NASA-landsat). (C) Selenga River Delta satellite image (Landsat 5 image acquired on August 23, 2010). (D) Rio Grande de Lípez Delta, Uyuni salt flat, Bolivia (Source ESA, contains modified Copernicus Sentinel data (2017), processed by ESA, CC BY-SA 3.0 IGO, Id 380675). (E) Mississippi River Delta acquired on May 24, 2001 by the Advanced Spaceborne Thermal Emission and Reflection Radiometer (ASTER) on NASA's Terra satellite. Hurricanes Katrina and Rita destroyed much of the Mississippi River Delta in 2005.

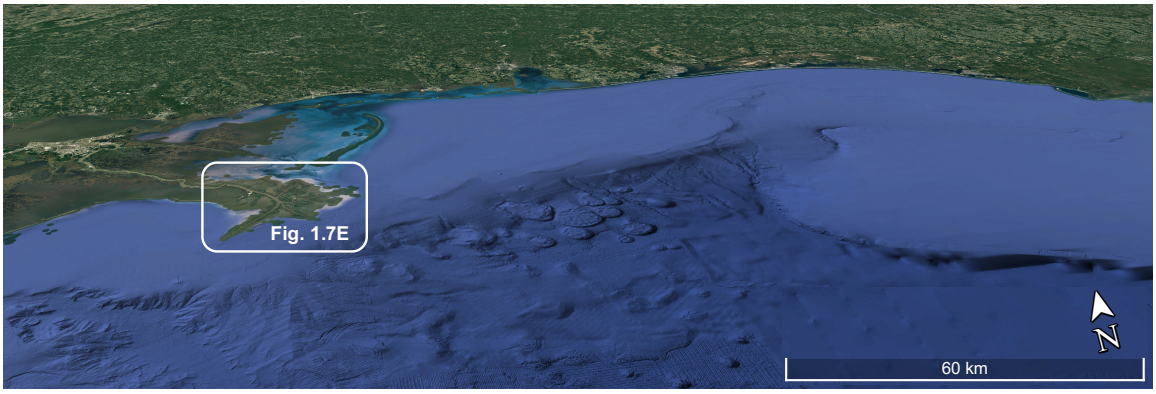

Figure 1.8: Oblique projection of Gulf of Mexico using Google Earth, Inset: Mississippi River Delta.

Sandstone reservoirs are formed by the deposition of sediments. Owing to the various processes involved in their formation, they are highly heterogeneous and host a vital network of interconnecting pore spaces. After deposition, sediments are buried, compacted and cemented to various degrees and spatial scales, resulting into the formation of subsurface reservoir units. Albeit the fact that these units may be subsequently folded or faulted during different phases of tectonic

deformation, their depositional fabric appears to be preserved in the stratigraphic record, which provides a source of calibration or validation for new theories and models of geological processes.

1.2.4 Elements of sequence stratigraphy

The geological record of fluvial, coastal, nearshore and continental shelf depositional systems has been customarily explained in terms of allogenic forcing by invoking conceptual models of fluvial and paralic architecture embedded in a sequence-stratigraphic framework (Shanley and McCabe, 1993; Wright and Marriott, 1993; Emery and Myers, 1996; Holbrook et al., 2006). Fundamental notions of sequence stratigraphy resulted from observations of conspicuous patterns on continental-margin seismic lines (Payton, 1977; Mitchum et al., 1977; Vail et al., 1977). In this context, the observed seismic reflection events were interpreted to outline basin-fill segments whose architectural arrangement is regulated by base level changes, controlling the rate of generation and spatial distribution of accommodation space (Fig. 1.9, 1.10, 1.11). Sequence stratigraphy applies base level concepts with the aim to improve predictions in the spatial distribution and physical properties of potential subsurface resources (i.e. water, hydrocarbon and/or geothermal reservoirs). This is achieved by providing a geometric framework to subdivide sedimentary sequences based on observational changes in stacking pattern and their bounding surfaces, which are typically attributed to fluctuations of base level and climatic change (Mitchum et al., 1977; Vail et al., 1977; Jervey, 1988; Posamentier and Vail, 1988; Galloway, 1989; Wright and Marriott, 1993; Shanley and McCabe, 1994; Emery and Myers, 1996; Neal and Abreu, 2009). This idea dates back to mid-1900's, when sedimentary successions were subdivided into rock packages based on regionally extensive unconformities (Sloss, 1950, 1963).

Base level is 'the conceptual surface of equilibrium that separates erosion from deposition' (Shanley and McCabe, 1994), an idea introduced by Powel (1875), who described base level as an imaginary level below which a river cannot erode further, and was later refined by Dana and Rice (1897) as 'the surface of balance (equilibrium) between erosion and deposition'. Barrel (1917, p.778) described base level as 'the surface toward which the external forces strive, the surface at which neither erosion nor sedimentation takes place'. He viewed base level as a controlling surface whose oscillatory behaviour over multiple timescales leads to the formation of unconformities of different magnitudes. Wheeler (1964) on the other end saw base level as a descriptive surface (synonymous with stasis) rather than a controlling one.

The concept of base level is applicable to any depositional environment, from continental to deep water. For river systems entering the basin waters (i.e. coastal and nearshore depositional systems) over long timescales, base level corresponds to sea level, also known as the ultimate base level (Bates and Jackson, 1987) (Fig. 1.9A). Over short timescales, temporary base levels are established and correspond to three-dimensional surfaces that reshape the lithic surface as a function of the changing equilibrium conditions and thus describe the equilibrium profile towards which deposition proceeds (i.e. Chapter 2). The position of temporary base levels in response to changing equilibrium conditions, explains also the discrimination between local and regional sedimentation processes and their expression in the stratigraphic record (see Chapter 3). Temporary base level is typically referred as the 'graded stream profile' in fluvial environments, which is graded to sea-level or lake-level at its distal end (Mackin, 1948; Jervey, 1988; Schumm, 1993; Emery and Myers, 1996; Cross and Lessenger, 1998; Posamentier and Allen, 1999; Holbrook et al., 2006). In shallow marine systems fairweather wave base can form a temporary base level (i.e. 'graded shelf profile') (Emery and Myers, 1996). In deep water environments, the base level lies far below the sea level (Hübscher et al., 2016). The position of temporary base levels in such environments (referred as 'deep base level') is not directly related to the sea level fluctuations but rather to their consequences on the hydrodynamic conditions at the sediment-water interface and the layering of the water column densities (Rebesco and Camerlenghi, 2008; Qayyum et al., 2017).

Accommodation space (i.e. the space available for sediment to accumulate) is controlled by base level, since long-term sediment accumulation may occur up to base level (Emery and Myers, 1996; Allen and Allen, 2013). The change of accommodation space *(ΔA)* may be written as:

$$\Delta A = \Delta E + \Delta S + \Delta C \qquad (2),$$

where *A* is accommodation, *E* is eustasy, *S* is subsidence and *C* is compaction. The change in water depth can be written as:

$$\Delta W = \Delta A - \Delta D = (\Delta E + \Delta S + \Delta C) - \Delta D \qquad (3),$$

where *D* is the amount of sediment deposited. These concepts are summarized in Figure 1.9A. Sediment supply controls the amount of accommodation space that is filled., i.e. high sediment supply rate fills accommodation space rapidly leading to bypassing of excessive sediment and the cutting and filling of unconformities or disconformities (Holbrook and Bhattacharya, 2012; Allen and Allen, 2013). On the other end, at low sediment supply rates the available accommodation space is underfilled, leaving an excess of base level (or water depth) to be filled.

Shoreline transgression and regression is regulated by the rate of relative sea-level change and rate of subsidence (Sloss, 1962). Figure 1.9B illustrates a simple 1D forward model of relative sea-level variation through a cycle of eustatic change with wavelength λ and amplitude h_0 in a basin subdued to linear tectonic subsidence rate a (see more details in Allen and Allen, 2013; Appendix 51). This forward model, which was based on the work of Barrel (1917), is applied here in three dimensions as an external forcing mechanism, representative of relative base-level cycles (Chapter 3 and 4).

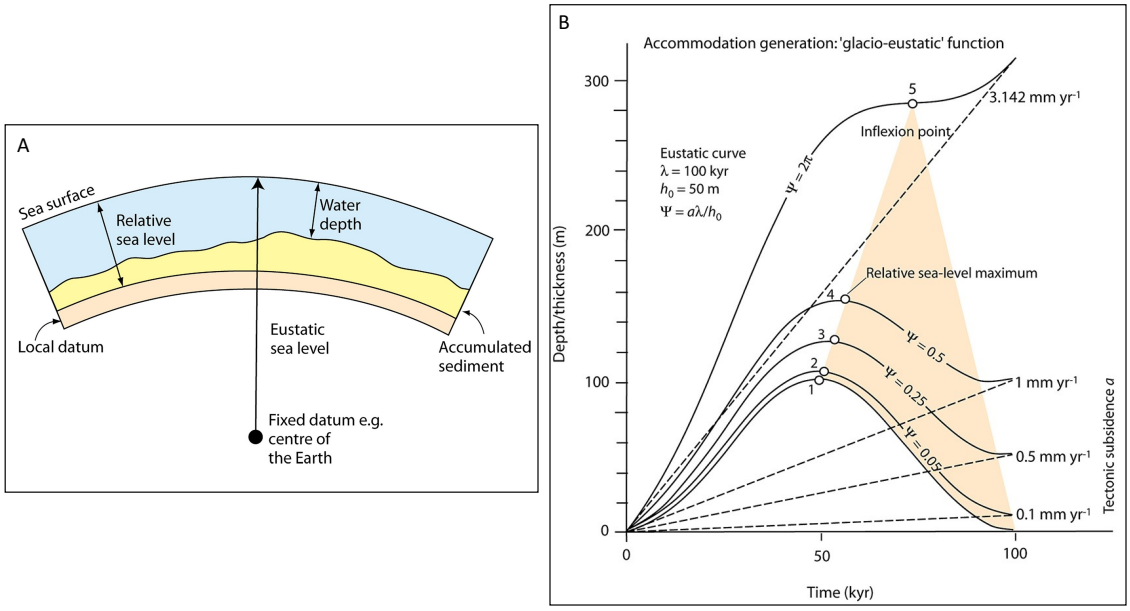

Figure 1.9: (A) Definitions of terms used in process (or sequence) stratigraphy (i.e. eustatic sea level, relative sea level and water depth) (after Jervey; Emery and Myers, 1996). (B) Variations in relative sea level through a cycle of eustatic change with wavelength λ and h_0 in a basin with linear tectonic subsidence rate a. The dimensionless parameter Ψ varies from 0.05 to 2π, corresponding to tectonic subsidence rates of 0.1 to π mmyr^{-1}. Increasing values of Ψ cause the relative sea level curve maximum (open circle) to be delayed in the cycle. For the 'glacial' eustatic parameters used, tectonic subsidence must be >πmmyr^{-1} in order for the relative sea-level fall to disappear (after Allen and Allen, 2013).

Figure 1.10A illustrates a reference curve of base-level changes along the coastline and the four main events that occur over a full base-level cycle (from Catuneanu, 2006). 'The timing of the four events is unique along each dip line, but it may change along strike due to variations in sediment supply and/or subsidence rates: (1) onset of a forced regression (onset of base-level fall at the shoreline); (2) end of a forced regression (end of base-level fall at the shoreline); (3) end of a regression (during base-level rise, when the rate of base-level rise creates accommodation that overwhelms the rate of sedimentation at the shoreline); (4) end of a transgression (during base-level rise, when the rate of sedimentation at the shoreline once again exceeds the accommodation created by base-level rise at that location)' (Catuneanu, 2009). Depending on the interplay of the

various driving mechanisms responsible for base level fluctuations, the reference curve may be symmetrical or asymmetrical.

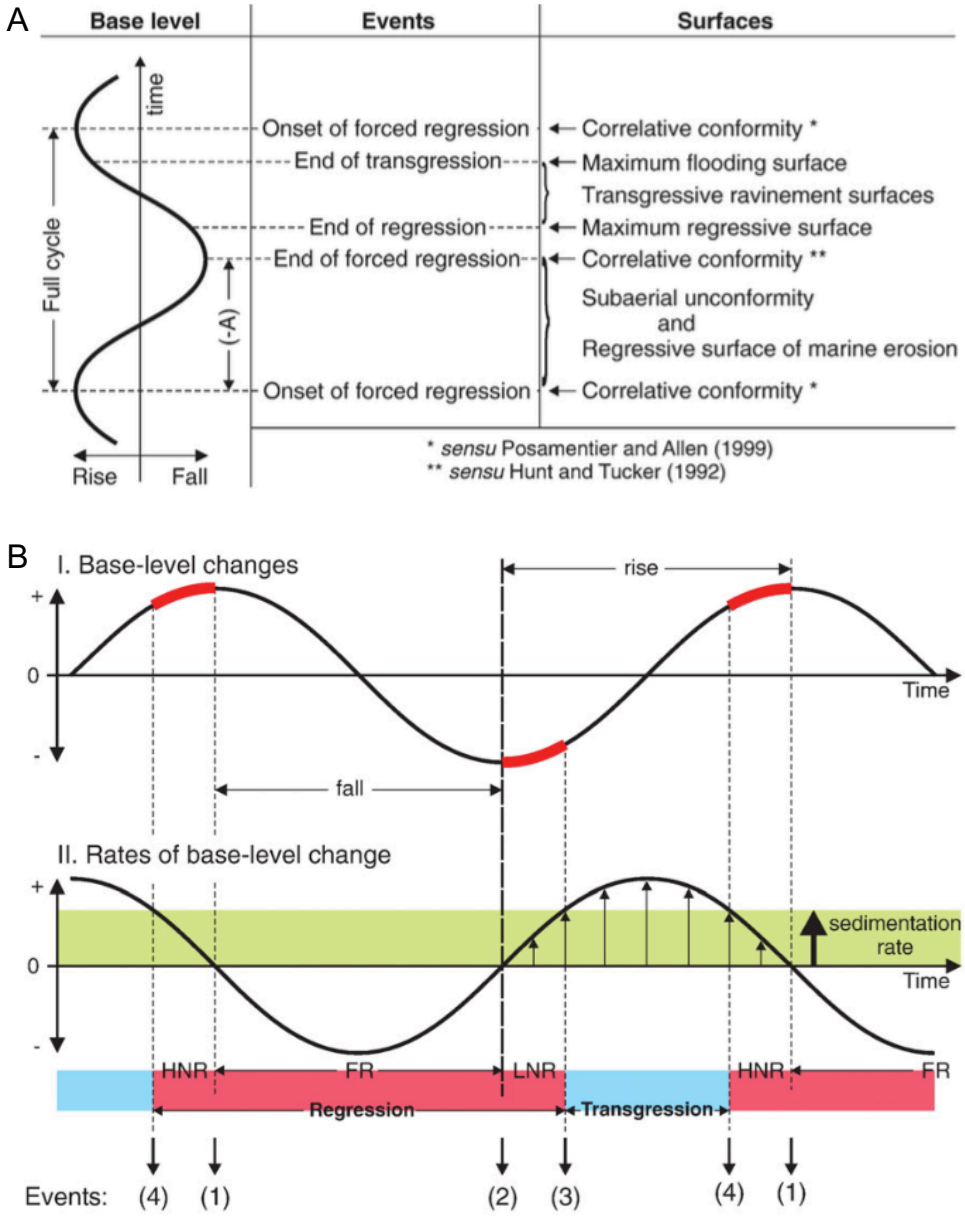

Figure 1.10: (A) Timing of sequence-stratigraphic surfaces relative to the four events the on the reference base-level curve. Abbreviation: (−A) negative accommodation. (B) Concepts of transgression, normal regression, and forced regression, defined by the interplay of base-level changes and sedimentation at the shoreline. Top sine curve shows the magnitude of base-level changes through time, whereas the sine curve below shows the rates of base-level changes. Abbreviations: FR, forced regression; LNR, lowstand normal regression; HNR, highstand normal regression. The four events of the base-level cycle are: (1) onset of forced regression; (2) end of forced regression; (3) end of regression; (4) end of transgression (from Catuneanu, 2006).

Stratal stacking patterns within the coastal area of any marine (or lacustrine) setting are linked to these four events because they regulate changing rates of coastal accommodation creation and sediment fill (also known as accommodation succession, sensu Neal and Abreu, 2009) (Fig. 1.11C, 1.13). The onset-of-forced-regression event marks a shift from progradation to aggradation to degradation (or downstepping). End of forced regression marks a shift from downstepping to aggradation with continued progradation. End of regression marks a sharp shift from progradation to retrogradation and the end-of-transgression event punctuates the shift from stratal retrogradation to progradation, following the shoreline backstepping and forestepping, respectively (Catuneanu, 2009). These four events control also the timing of formation of sequence-stratigraphic surfaces (Fig. 1.10A, 1.12). Detailed description of sequence-statigraphic surfaces is provided by Zecchin & Catuneanu (2013). A genetic linkage of these surfaces to their fluvial counterparts is thoroughly discussed by Holbrook and Bhattacharya (2012).

Using these key sequence-stratigraphic surfaces, geoscience practitioners have forged a series of two-dimensional models (Fig. 1.11, 1.12), aiming at landward and basinward prediction of lithological composition (Frazier, 1974; Mitchum et al., 1977; Vail et al., 1977; Jervey, 1988; Galloway, 1989; Posamentier and Vail, 1988; Hunt and Tucker, 1992; Wright and Marriott, 1993; Shanley and McCabe, 1994; Embry, 1995; Posamentier and Allen, 1999; Plint and Nummedal, 2000; Neal and Abreu, 2009). There are six types of sequences distinguished in the literature: depositional sequence I (sensu Mitchum et al., 1977), II (sensu Haq et al., 1987; Posamentier et al., 1988), III (sensu Van Wagoner et al., 1988, 1990; Christie-Blick, 1991), IV (sensu Hunt and Tucker, 1992, 1995; Helland-Hansen and Gjelberg, 1994) the genetic stratigraphic sequence (sensu Frazier, 1974; Galloway, 1989) and the transgressive-regressive sequences (sensu Johnson and Murphy, 1984; Embry and Johannessen, 1992) (Fig. 1.12). Each sequence type consists of a set genetically related depositional (statal) units (or stages of deposition) with characteristic stacking pattern, also known as systems tracts. Detailed description of coastal and shallow marine systems tracts may be found in Zecchin & Catuneanu (2013) and www.sepmstrata.org.

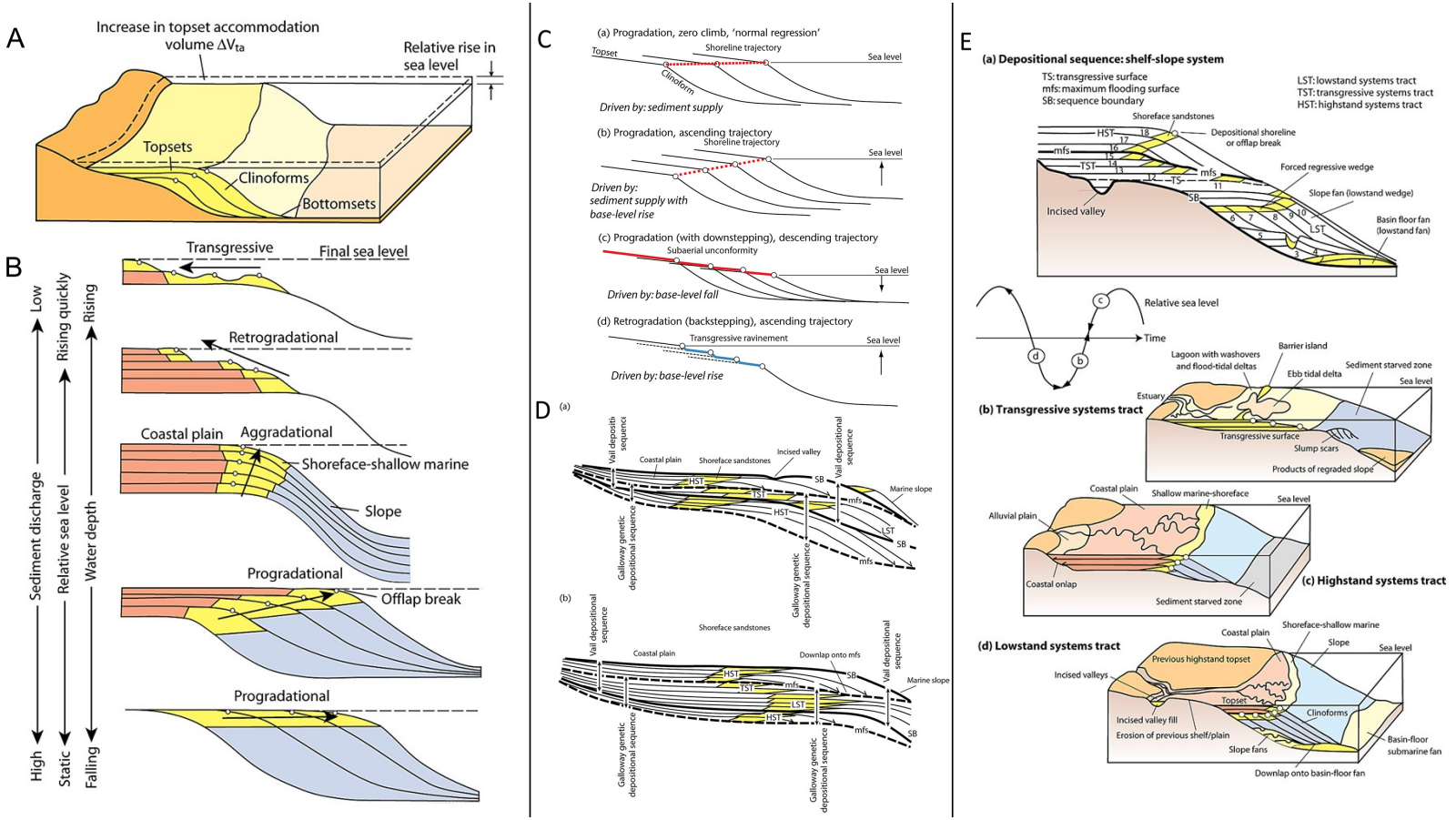

Figure 1.11: Large-scale depositional architecture of depositional units relative to accommodatin and sediment supply (from Allen and Allen, 2013): (A) Relative sea level rise increases topset accomodation volume ΔV_{ta} equal to the product of relative sea-level rise and the topset area. (B) Large-scale stratigraphic patterns are conformed to the balance between sediment supply and topset accommodation and alter from transgressive to retrogradational, aggtadational and progradational. (C) Shoreline trajectory associated with progradation and retrogradation, showing ascending and descending trends (after Catuneanu et al., 2009). (D) Distinction between a Vail-type depositional sequence and genetic one (sensu Galloway) based on their bounding unconformities and maximum flooding surfaces, respectively. HST, Highstand systems tract; TST, Transgressive systems tract; LST, Lowstand systems tract; SB, Sequence boundary; mfs, maximum flooding surface. (E) Systems tracts and their relation to relative sea-level curve according to the Exxon Group (Posamentier et al., 1988; modified by Emery and Myers, 1996). Open circles correspond to depositional shoreline or offlap break.

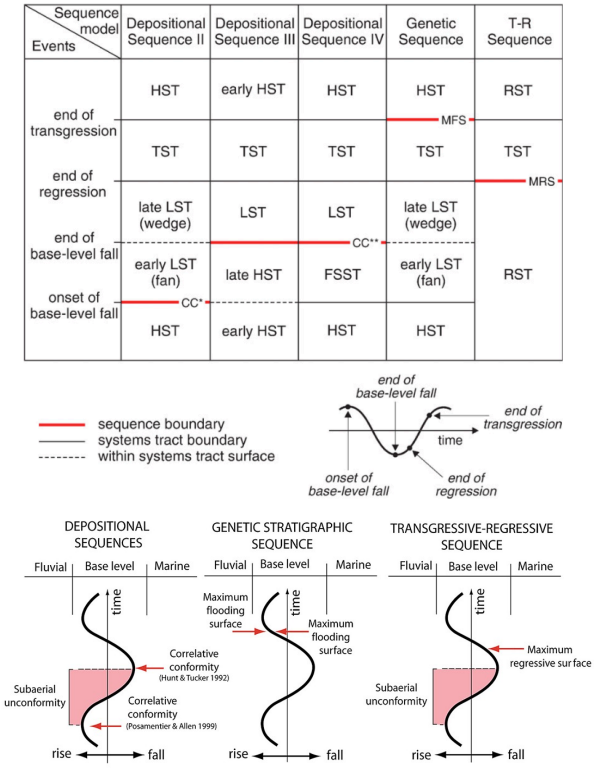

Figure 1.12: Terminology: sequences (or cycles of relative sea-level change), stages of deposition (systems tracts) relative to a cycle of relative sea level and timing of sequence and systems tracts boundaries. Abbreviations: LST, lowstand systems tract; TST, transgressive systems tract; HS, highstand systems tract; FSST, falling-stage systems tract; RST, regressive systems tract; T–R, transgressive–regressive; CC*, correlative conformity sensu Posamentier and Allen (1999); CC**, correlative conformity sensu Hunt and Tucker (1992); MFS, maximum flooding surface; MRS, maximum regressive surface (from Catuneanu, 2006; Catuneanu et al., 2009) (see text for more details).

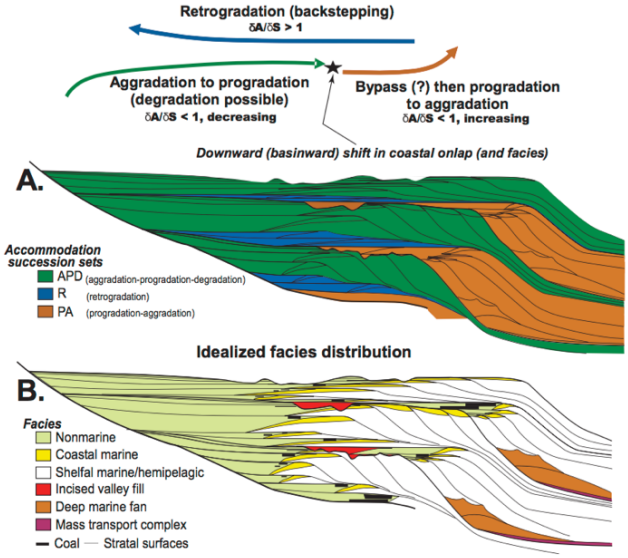

Figure 1.13: Accommodation successions. A: Depositional sequences. B: Idealized facies distribution (from Neal and Abreu, 2009).

The concept of stratigraphic cycles invoking rises and falls of relative-sea level involves a coarse resolution (tens to hundreds of meters in thickness) and has been termed 'low-resolution sequence stratigraphy' by Posamentier and Weimer (1993). High-resolution sequence stratigraphy deals with small-scale sedimentary cycles, commonly referred to as parasequences (e.g., Van Wagoner et al., 1988, 1990; Posamentier and Allen, 1999), and correspond to the 4th to 6th order of cyclicity of Vail et al. (1991). Zecchin and Catuneanu (2013) stressed that 'sedimentary cycles associated with shoreline shifts are high-frequency sequences, irrespective on their allocyclic or autocyclic origin, whereas sedimentary cycles unrelated to shoreline shifts correspond to bedsets'.

Advances in seismic technology and inversion methods improve subsurface imaging and mediate the detection of relic geomorphic features and geobodies in three dimensions (Posamentier, 2004; Posamentier et al., 2007). The stacking arrangement of stratal units that fall below seismic resolution can be partly characterized using conventional sequence-stratigraphic terms (Deveugle et al., 2011). Several studies have demonstrated that the subdivision of systems tracts down to discrete bed set-scale units is possible in the presence of high-resolution datasets (Li et al., 2011; Zhu et al., 2012; Zecchin and Catuneaunu, 2013). The latter consisted of outcrop-based data which enabled the subdivision of strata into sedimentary facies, as interpreted by the sedimentary structures and trace fossils. High-resolution stratal units may then be grouped into systems tracts (Posamentier et al., 1992; Dalrympe, 1992; Posamentier and Allen, 1999; Plint and Nummedal, 2000; Catuneanu et al., 2009, Catuneanu and Zecchin, 2013), allowing as such gross stratal geometries (i.e. systems tracts) to be linked to internal lithology. Despite these few examples, sparse subsurface datasets (i.e. one-dimensional sections or well-logs) together with the fragmented nature of the stratigraphic record cannot guarantee rigorous assessments of the time-stratigraphic relationships of high-resolution stratal units in three-dimensional space and thus any the subdivision of sedimentary sequences into time-bounded facies assemblages is highly likely to be biased (Bhattacharya, 2011).

1.2.5 Stratigraphic completeness

'Time transforms sediment routing systems into geology, and like history, selectively samples from the events that actually happened to create a narrative of what is recorded' (Allen, 2008). The earth's surface is being shaped by fluctuations of base level and global climate. These fluctuations regulate the sedimentary systems states (erosion, transport, deposition and stasis) and variability in sediment accumulation, producing patterns of stratigraphic cyclicity and incompleteness (Barrel,

1917; Tipper, 2000, 2014; Ruddiman, 2001; Miall, 2010; Allen and Allen, 2013). Figure 1.14A illustrates the sediment accumulation variability as a function of sinusoidal variation with superimposed background subsidence. Sediments deposited during periods of net positive accommodation (i.e. sediments in the rising limb of the sediment accumulation curve) are preserved in the stratigraphic record, assuming they 'survive' the younger erosional time intervals. Increasing background subsidence rates will increase the fraction of time represented by preservation (Allen and Allen, 2013). According to Sadler (1981) and Sadler and Strauss (1990), stratigraphic completeness, critical for the interpretation of trends in sediment accumulation rates, is a function of the time interval over which sediment accumulation rates are measured (1.14B). What is always missing in the stratigraphic record 'is that part of the history before the oldest preserved horizon, which for systems that are in long-term balance will on average be half of the total time' (Tipper, 2015).

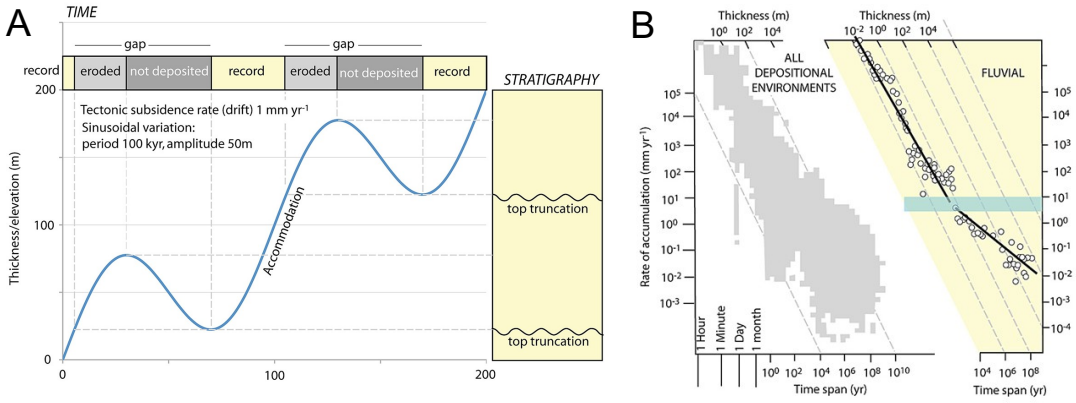

Figure 1.14: (A) Accommodation represented by relative sea level: sinusoidal sea-level change superimposed on background tectonic subsidence. Accommodation generation marks periods of deposition, whereas accommodation loss is represented by erosional and non-depositional gaps which are expressed as unconformities in the stratigraphic record (based on Barrel, 1917). (B) 'Sadler plot' for all depositional environments (left) illustrating relationships between time span of observation, rate of sediment accumulation and bed thickness. (Right) Subset of fluvial environments showing a decrease in net sediment accumulation rate for longer timespans (from Allen and Allen, 2013).

1.2.6 Numerical modelling of clastic sedimentary basins

Numerical models comprise idealized representations of certain naturally occurring processes. They allow to simulate the behaviour of dynamic physical systems and make predictions about certain variables of interest at various spatial and temporal scales. In clastic sedimentary basins, process-based numerical models evoke fundamental equations of water discharge and sediment

transport in order to simulate erosional, transportational and depositional processes of sedimentary systems and approximate large-scale basin-fill parameters.

Long-range sediment transport is typically modelled using various forms of the diffusion equation, representing sediment transport and deposition as a function of topographic gradient (Fig. 1.15) (Bridge and Leeder, 1979; Parker, 1978a, b; Paola et al., 1992; Howard, 1994; Mackey and Bridge; 1995; Paola and Seal, 1995; Dade and Friend; 1998; Bowman and Vail, 1999; Granjeon and Joseph, 1999; Marr et al., 2000; Paola, 2000; Meijer, 2002; Bridge, 2003; Clevis et al., 2003; Karssenberg et al., 2001; Fagherazzi and Overeem, 2007).

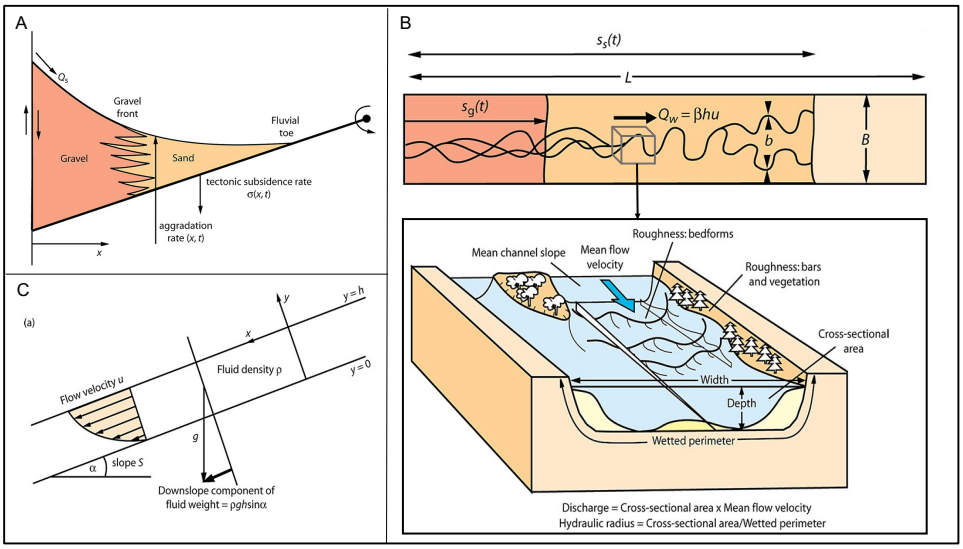

Figure 1.15: Diffusion-based model for long-range sediment transport of a mixture of gravel and sand. (A) Cross-section and (B) map view of alluvial basin of length *L*, width *B*, containing channels with cumulative width b undergoing tectonic subsidence σ(x). (Inset) Wetted perimeter and hydraulic radius of a river. If flow depth, *h* is large compared to channel width, depth should be replaced by hydraulic radius. From Allen and Allen (2013), after Marr et al. (2000). (C) Steady uniform flow of channel down an inclined plane of slope *a* (after Allen and Allen, 2013).

Diffusion-based models typically assume that: a) long-term flow of water approximates a steady uniform flow down an inclined plane, b) moving fluid over bed and banks loses energy by friction and c) water and sediment discharges are conserved through the system (Allen and Allen, 2013). Heller and Paola (1992) used a diffusion-based model to understand the origin of gravel progradation in three Neogene alluvial basins. They made a differentiation between short-term and long-term sedimentation patterns and underlined that the most important terms to systems which are in long-term balance are subsidence and sedimentation rate. The meaning of long-term balance has been specified by Tipper (2015). He wrote: 'long-term balance assumes that: (1) the proportions of deposition and erosion in the system over the long term should be assumed to have been equal, (2) net change in sediment thickness produced by the system over the long term should be assumed

to have been zero, and (3) that the frequency distributions of the system's deposition and erosion rates over the long term should be assumed to have been the same'. By contrast, 'on short time scales, the subsidence term becomes progressively less important and behaves like the conventional diffusion equation involving only the surface topography' (Paola et al., 1992). This differentiation between short-term and long-term processes is summarized metaphorically in the latter paper by writing that: 'slow changes are felt in the body of the basin while rapid changes are felt in its skin'.

Numerical models of clastic sedimentary basins can simulate the evolution of sedimentary systems over geological timescales and produce numerical analogues, similar to reference cases obtained by physical experiments. 'Where such reference cases do not provide detailed predictions of specific field cases, they can still provide a baseline to separate local, case-specific features from generic system behavior.' (Paola and Martin, 2012). Paola and Leeder (2011) pointed out that these such reference models (or reference states, sensu Power, 1998) are analogous to the geoid reference in gravity studies. They wrote: 'one does not expect that the geoid value at a given location will give exactly the measured value, but rather uses it to subtract off that part of the measurement that represents the generic and well understood part of the signal, leaving behind the part (the anomaly) that is interesting, and that represents local conditions.'

1.2.6.1 Numerical models of river systems and alluvial stratigraphy: a short review

The first two-dimensional qualitative model of alluvial stratigraphy (Allen, 1965) was based on the hypothesis that fluvial style (i.e. low-sinuosity braided, high-sinuosity meandering) affects the spatial distribution of channel-belt deposits. It did not account critical parameters such as alluvial plain dimensions, varying aggradation rate and relative sea-level fluctuation which are prominent contributors to alluvial architecture (Shanley and McCabe, 1993; Wright and Marriot, 1993, Bridge, 2003). Leeder's alluvial stratigraphic model (1978) comprises the first two-dimensional quantitative approach that relates autogenic geological process (random avulsions) with channel-belt proportion and degree of connectedness. The latter highlighted the coherency between intrinsic geological processes (i.e. avulsions) and alluvial architecture. Subsequent versions of the latter model included controlling factors such as varying topographic relief (Allen, 1979), varying sedimentation rates and the effects of compaction and tectonic tilting (Bridge and Leeder, 1979), recorded spatial distribution of channel belt deposits as a function of local and regional avulsions (Heller and Paola, 1996) and simulated avulsions and alluvial architecture on a three-dimensional

floodplain geometry (Mackey and Bridge, 1995). This constructive three-dimensional model usually referred as the *LAB* model (after Leeder, Allen and Bridge). It was also concluded that the next critical step was to cross-validate simulated fluvial stratigraphy (i.e. estimated avulsion frequencies, spatial distribution of channel belt deposits) with experimental observations and data acquired from modern and ancient fluvial systems (Törnqvist, 1994; Mackey and Bridge, 1995; Bryant et al. 1995; Khan et al. 1997, Karssenberg and Bridge, 2008).

Slingerland et al. (1994) highlighted the importance of nesting/dynamic coupling of various processes occurring in different depositional environments (i.e. fluvial, deltaic, shoreface), paving as such the notion of building coupled interacting models of single-environments able to simulate complete sedimentary systems (Martinez, 1987; Martinez and Harbaugh, 1993; Tetzlaff, 2004b; Hutton, et al., 2008). Hydraulic models solve fundamental equations of fluid flow and sediment transport based on Lagrangian simplifications of Navier-Stokes equations (Tetzalff and Harbaugh, 1989; Griffiths et al., 2001) or depth-averaged versions of the Reynolds-averaged Navier-Stokes equations (i.e. Lesser et al., 2004). The full Navier-Stokes equations describing the fluid flow in three dimensions is currently impossible to solve due to computing speed limitations. Leveraging, however, the computing power of high-performance computing infrastructures may allow the usage of full Navier-Stokes equations to simulate morphodynamic evolution of river systems and downstream grain-size variations over geological timescales.

1.2.7 Geostatistical reservoir modelling

Geological reservoir models used in hydrocarbon and groundwater exploitation studies are typically based on stochastic-geometric interpolation methods (Deutsch, 2002). Such methods generate solutions that are locally optimal (honouring borehole information) but are not constrained by the large-scale geological setting of the reservoir, which is critical for estimates of reservoir flow performance. Before such methods became a convention in geological modelling workflows, interpolation of properties (i.e. discrete lithologies) between boreholes was achieved using well correlation methods. The latter methods were unable to capture heterogeneity over large well-spacings as well as to quantify uncertainty associated with architecture and property predictions at the reservoir scale. This was largely tackled by kriging geostatistical methods. Kriging is a two-point statistics method based on the semivariogram, which is used to describe the spatial correlation between the data, and provides an insight into trends and the uncertainty in the data (Krige, 1951; Matheron, 1962; Cressie, 1990; Olea, 1994; Deutsch, 2002). The semivariogram can be inferred from existing datasets or selected from an outcrop analogue or some previous ‘reliable’ subsurface

dataset (Dubrule and Damsleth, 2001). Kriging requires information on the distribution and variability of the property one wishes to interpolate. Cokriging allows the estimation of a property value (i.e. porosity) based on different attributes (i.e. measured sample porosity and related acoustic impedance value). Albeit the fact that kriging-based interpolation methods honour all the existing data, they provide only one, most likely outcome (realization), which is not enough to account for the uncertainty of the model. In addition, a bias is introduced by overestimating the overall proportion of reservoir/aquifer facies (i.e. clustering of wells around a good quality reservoir/aquifer) which needs to be modified by using a declustering procedure (Deutsch, 1989; Deutsch and Journel, 1998).

Geostatistical conditional simulation is often preferable to traditional interpolation approaches because their stochastic approach allows the generation of many equiprobable realizations which may be used to quantify and to assess the uncertainty of the models. There are two basic categories of conditional simulation methods: cell- (or pixel-) based and object-based methods. Both categories have been widely used for modelling facies distributions because petrophysical properties are highly correlated with facies types which are used to constrain the range of variability in the property of interest (Deutsch, 2002).

Cell-based modelling (i.e. sequential indicator, truncated Gaussian simulations) similar to deterministic and kriging methods are based on two-point statistics. They operate on one cell at a time and have each cell visited sequentially (i.e. sequential indicator simulation) in a random path. Multiple realizations are generated by repeating the procedure with a different random seed number (Deutsch, 2002). This procedure generates different results at unsampled locations and all outcomes honour all the 'hard' data available (i.e. borehole information). Truncated Gaussian simulation allows the definition of both vertical and lateral facies relationships deeming it particularly well with transitional facies (i.e. foreshore to offshore) A disadvantage of the cell-based modelling is that often their results show unrealistic short-scale variations (Daly and Caers, 2010), and may be treated by some cleaning algorithm used in image processing (Geman and Geman, 1984; Besag, 1986; Ripley, 1989).

Object-based methods on the other end (also known as Boolean or marked-point methods), deploy only categorical data (i.e. facies types) and provide visually attractive results because they operate on groups of pixels which are arranged to represent idealized geometries interpreted in outcrop and modern analogues (Deutsch, 2002; Pyrcz and Deutsch, 2014). Owing their 'geological realism', object-based models became very popular during the mid-1980's, especially for their use in fluvial reservoirs (Haldorsen and Chang, 1986; Clemensten et al., 1989; Haldorsen and Damsleth, 1990;

MacDonald and Halland, 1993; Yarus and Chambers, 1994; Deutsch and Wang, 1996; Journel et al., 1998; Deutsch and Tran, 2002). The algorithms for an object-based model generate geometries (channels, crevasse splays, reefs) with dimensions (i.e. orientation, sinuosity, length, width) inferred from proprietary databases based on well-exposed outcrops, modern analogues and/or well-understood susbsurface datasets (Ravenne et al., 1987; Dreyer et a., 1993; Reynolds, 1999). The method, which generally works best in settings with a low net-to-gross ratio and widely spaced wells (low data density), simulates many grid cells at one time and introduces simulated geometries over background shales. Object-based models typically demonstrate lower error variance comparing to pixel-based ones, and thus have a smaller space of uncertainty. However, the algorithm is frequently unable to honour borehole data, especially when borehole spacing is small comparing to the simulated objects. Finally, if the original conceptual model is wrong, there is little chance to capture the correct solution which may in turn have negative consequences in the estimate of reservoir flow performance.

Multiple-point statistics (MPS) provided new additions to the toolbox of geostatistical algorithms (Caers and Zhang, 2004; Daly and Caers, 2010). MPS realizations can capture complex geometries with sharp transitions similar to object-based methods, while honouring borehole data even at high borehole densities. The sedimentary bodies generated are not limited to some database with preconfigured dimensions but are based on the so-called training image which is equivalent to the semivariogram. Training image construction is possible using all sort of two- or three-dimensional models, including conceptual depositional models, maps, outcrop and satellite images or process-based modelling results. Choosing the right training image (stationary or non-stationary) is the most critical modelling decision in MPS and requires a trade-off between statistical representation and empirical realism (or subjectivity) (Mariethoz and Caers, 2014). In any case, the statistical structure (basic statistics, semivariogram) of the outcome (realization) must be comparable with the statistics derived from the available data (borehole information, outcrops or subsurface datasets). Statistics, however are often not satisfactory to describe natural processes and thus obtaining a realistic model of natural systems able to reproduce statistical quantities does not guarantee that the physical processes are correctly represented (Mariethoz and Caers, 2014).

1.3 Objectives

Improving the capacity to decipher the functioning and composition of modern and ancient sediment routing systems is essential not only for the sustainable recovery and storage of water and

energy resources in the subsurface but also for predicting the systems' biogeochemical responses to climate changes. The objective of this PhD thesis is twofold: a) to illustrate how a high-resolution quantitative model of geological heterogeneity in clastic sedimentary basins may serve to enhance our understanding of clastic sedimentary systems as a whole, and b) provide a new data type that captures the spatial distribution of lithology at the time of deposition, at a resolution directly comparable to subsurface data. For this purpose it is important to: i) understand how river systems evolve over geological timescales under the influence of intrinsic (autogenic) dynamics and external (allogenic) forcing mechanisms (i.e. relative sea level fluctuations) and how their associated sedimentary processes are expressed in the stratigraphic record; ii) extract genetic stratal units from process-based stratigraphic (volumetric) data in order to assess their architectural arrangement and depositional connectivity at basin-scale; iii) validate numerical simulations by comparing them with real-world ('pristine') river systems, providing as such robust numerical analogues representative of ancient ones and iv) propose a workflow in order to integrate process-based knowledge into the geological modelling of aquifer, hydrocarbon and geothermal reservoirs, minimize exploration risk and provide cost-effective solutions for production and sustainable management of shallow and deep subsurface resources, complementing integrated geo-technologies in the fields of subsurface imaging, reservoir characterisation and engineering.

1.4 Approach

Stratigraphic forward models that combine topographic diffusion and advective transport equations are well suited for investigating the morphodynamic evolution of sediment dispersal systems over a wide range of spatial and temporal scales (Granjeon and Joseph, 1999; Paola, 2000; Meijer, 2002; Hajek and Wolinsky, 2012). Albeit their nonlinear behaviour and various input parameters, they provide attractive tools for incorporating basin-scale information at the reservoir scale (Cross and Lessenger, 1999; Karssenberg et al., 2001, 2007; Wijns et al., 2004; Imhof and Sharma, 2006; Charvin et al., 2009; Falivene et al., 2014). In this PhD study, fluvio-deltaic and shallow marine stratigraphy was obtained using Simclast (Dalman and Weltje, 2008, 2012), a basin-scale stratigraphic forward model that includes subgrid parameterizations (modules) of alluvial and coastal (shoreface) processes for efficient multi-scale simulation of basin-fill architecture. Physical experiments, designed to understand the formation of alluvial and basin stratigraphy (Martin et al., 2009; Straub et al., 2009; Wang et al., 2011; Li et al., 2016; Hajek and Straub, 2017; Esposito et al., 2018), supported by field observations of modern and ancient river systems can point out the

dominant small-scale processes (modules) needed to be incorporated in the simulations of process-based stratigraphic models, improving as such their predictive capabilities when dealing with the systems past morphodynamic behaviour and the exploration and production of subsurface resources enclosed in buried quaternary and ancient river systems.

SimClast was built upon the loading and accounting schemes developed by Meijer (2002). The model is capable of simulating channel network dynamics, floodplain interactions (including compaction, groundwater and peatland dynamics) and wave-induced longshore and cross-shore transport. The fluvial module simulates channel-network development, including dispersive flow routing on the floodplain (Freeman, 1991) and river avulsions through a simplified bifurcation-stability routine (Slingerland and Smith, 1998). This allows to assess the spatial distribution and geometry of high-resolution fluvio-deltaic sedimentary products (stratal units) as a function of fluvial avulsion cycles without compromising computational efficiency. Potential avulsion sites are associated with the development and stabilization of randomly initiated crevasses (Fig. 1.16). Crevassing initiates channelized flows outside the parent channel (Slingerland and Smith, 2004; Edmonds et al., 2009; Hajek and Edmonds, 2014). The newly formed crevasse channel is assigned a random depth of incision and discharge is redistributed over both active channels. Cases where sediment transport capacity of the crevasse channel exceed the sediment load received from the parent channel allow the former to incise and thus remain active. The equilibrium configuration of the crevasse channel depends on local threshold conditions, including channel-belt superelevation, and in-channel sediment-concentration profile (Dalman and Weltje, 2008). Field and experimental studies have confirmed this avulsion-initiation mechanism (Mohrig et al., 2000; Martin et al., 2009). Crevasse channels which do not heal develop into partial avulsions, nodal avulsions or reoccupy abandoned channel segments (Jerolmack and Paola, 2007). The SimClast model does not include delta avulsions based on morphodynamic backwater controls (Jerolmack and Swenson, 2007; Hoyal and Sheets, 2009; Edmonds et al., 2009). For all numerical experiments presented in this study, the marine processes are represented by a simplified plume routine with diffusion-based mass wasting.

Simulations require several environmental parameters to be set including: initial topographic surface, subsurface sediment properties, spatially variable subsidence (or uplift) rates, initial sea level and sea level change, sediment entry point(s), water discharge and sediment supply (volume, grain sizes) and wave regime (Fig. 1.17). The model output consists of multiple topographic, sedimentation-pattern and water-discharge maps and volumetric (stratigraphic) data covering the entire grid (i.e. net sediment accumulation, grain size and age of deposition).

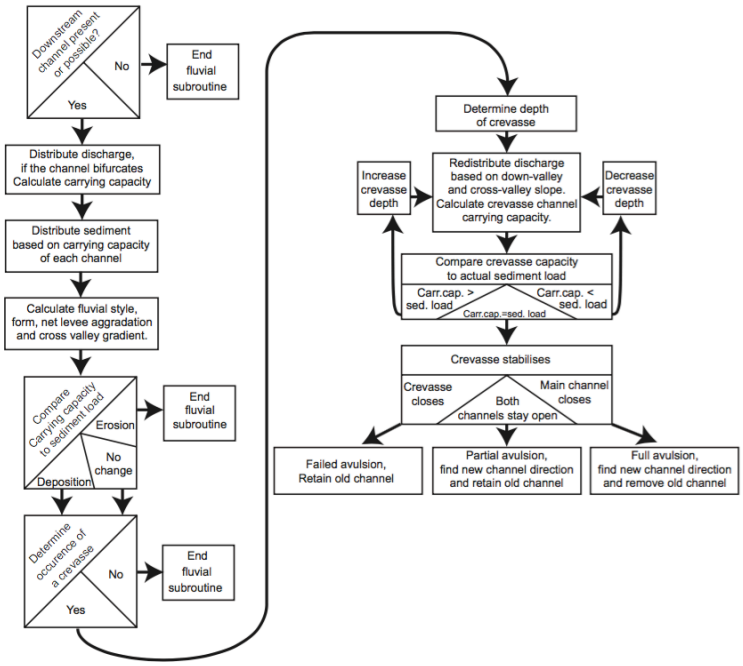

Figure 1.16: Flowchart of the routines developed to calculate water discharge, sediment transport and channel evolution (from Dalman & Weltje, 2008).

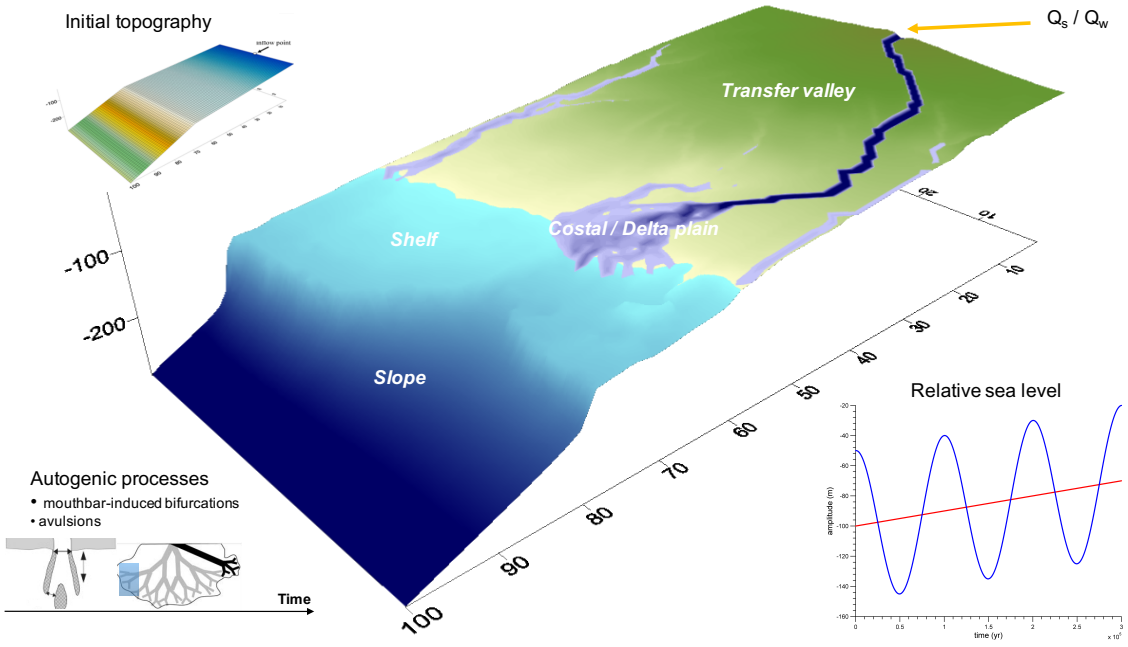

Figure 1.17: Overview of SimClast version used in this PhD study: initial and boundary conditions include initial topography, location of water/sediment entry point(s), presence (or absence) of relative base level fluctuations (background subsidence superimposed). Inset: sedimentation processes include alluvial ridge and overbank aggradation, crevassing, and threshold phenomena i.e. avulsions and mouthbar induced bifurcations (modified from Jerolmack and Swenson, 2007).

A post-processing software suite of object-based post-processing algorithms was developed in order to quantify local and stratigraphic variability and extract genetically related channel-belt and delta-lobe units. A stack data structure was designed to load synthetic stratigraphy (net sediment accumulation) in dynamic arrays. The algorithm implements sequentially a series of post-processing methods, including: a) constrained cubic spline interpolation of cumulative net sediment accumulation, b) a first order central difference operator for the approximation of net sediment accumulation rates and c) a binary transformation and thresholding of the estimated rates. Finally, a cellular automaton simulation algorithm was used to outline the boundaries of the genetically related channel-belt and delta-lobe units (chronosomes).

1.5 Thesis outline

This chapter provided a concise introduction to the role process stratigraphy in geosciences, an outline of depositional systems relevant to this thesis, elements of sequence stratigraphy, a brief overview of the numerical modelling tools developed to simulate clastic sedimentary basins (and alluvial stratigraphy in particular) and the geostatistical methods used to build static reservoir models. In addition, the objectives of this thesis were formulated and the approach followed was outlined. Chapter 2 captures the relation between alluvial sedimentation and deltaic deposition under time-invariant forcing. The channelized drainage network evolution of the delta and the stratigraphic expression of high-resolution stratal units associated with avulsion-induced depocentre shifts (chronosomes) are analyzed using the post-processing software explained in the following two chapters. Chapter 3 investigates the role of autogenic processes throughout a sequence (i.e. a cycle of accommodation to sediment supply rates). The numerical experiments were conducted under the influence of external (allogenic) forcing mechanisms (i.e. relative sea level fluctuations). Post-processing of the stratigraphic, shoreline trajectory and palaeodischarge output allows to quantify stratigraphic variability, extract isochronous surfaces and major (or large-scale) avulsions sites, respectively. The metric bifurcation intensity is introduced as the total number of bifurcations over a unit time, divided by subaerial area. Chapter 4 demonstrates the design and implementation of object-based post-processing operations able to extract genetically related channel-belt and delta-lobe units. The simulations involved accommodation-to-sediment-supply (A/S) cycles (by means of relative sea level fluctuations) of varying wavelength and amplitude. The analysis permitted to extract chronostratigraphically constrained lithosomes (or chronosomes) and to quantify large-scale depositional connectivity throughout an A/S cycle.

Chapter 5 explores the stratigraphic expression of the avulsion process in terminal fluvial systems (and its control on basin-fill architecture) by comparing a modern-day dryland terminal basin (Altiplano Basin, Bolivia) filled by fluvio-lacustrine sediments with the simulation results obtained using SimClast. The model boundary and initial conditions (i.e. catchment area, smoothed initial topographic surface, grain size of sediment supply and water discharge) were extracted from the area of interest. Chapter 6 discusses a workflow able to improve predictive capacity of geostatistical modelling algorithms by incorporating process-based stratigraphic modelling results. Finally, a synthesis is made of the findings, and recommendations are made for future research.

Chapter 2

High-resolution sequence stratigraphy of fluvio-deltaic systems: prospects of system-wide chronostratigraphic correlation[1]

Abstract

A basin-scale numerical model with a sub-grid parameterization of fluvio-deltaic processes and stratigraphy was used to study the relation between alluvial sedimentation and marine deltaic deposition under conditions of time-invariant forcing. The experiments show that delta evolution is governed by a robust morphodynamic feedback loop, which provides a link between major avulsions, delta-lobe switches, and sequestration of sediments on the delta plain. Major avulsions, driven by local superelevation, result in abandonment of delta lobes and initiation of new lobes. Progradation of the delta front lengthens the fluvial profile and reduces its gradient, which induces aggradation upstream. The aggradation, in turn, causes local superelevation of the channel belt. Each major avulsion causes a wave of incision to migrate upstream, whereas downstream of the avulsion point, the rate of aggradation temporarily increases until a new equilibrium situation has been established. The feedback loop explains storage and release of fluvial sediments without the need to invoke changes in upstream or downstream controls and provides a plausible mechanism for the generation of high-frequency incision-aggradation cycles as the sole result of compensational stacking.

[1] Based on: Dalman, R.A.F., Weltje, G.J., Karamitopoulos, P., published. High-resolution sequence stratigraphy: prospects of system-wide chronostratigraphic correlation. EPSL, 412, 10-17. https://doi.org/10.1016/j.epsl.2014.12.030.

The stratigraphic expression of a depocentre shift is an essentially isochronous surface. Hence, the stratigraphic record of fluvio-deltaic systems may be subdivided into a series of units representing intervals during which a channel belt and delta lobe were forming at a fixed location in the basin, so-called chronosomes. Fluvio-deltaic chronosomes are bounded by abandonment surfaces, which are clearly expressed in the marine as well as the fluvial domain. The surface marking the abandonment of a particular channel belt and delta lobe correlates with the surface at the base of a new delta lobe. Landward, this surface forms the base of an aggradational package of fluvial sediments downstream of an avulsion site associated with a lobe switch. Upstream of this site, the conformable surface passes into a surface of fluvial incision and terrace formation onlapped by aggradational channel-belt deposits. Identification of the isochronous bounding surfaces of chronosomes in the field offers the attractive prospect of high-resolution chronostratigraphic correlation throughout fluvio-deltaic systems.

2.1 Introduction

The geological record of fluvial systems has been customarily explained in terms of allogenic forcing by invoking conceptual models of fluvial architecture embedded in a sequence-stratigraphic framework (Emery and Myers, 1996; Shanley and McCabe, 1994; Wright and Marriott, 1993; Holbrook et al., 2006). Rigorous tests of these models are unavailable, because the practical limitations of field-based studies of ancient sediment dispersal systems rarely allow high-resolution system-wide reconstructions to be made (Bhattacharya, 2011). There is a clear need for high-resolution correlation in fluvio-deltaic systems, if only because they display conspicuous stratigraphic patterns of metre to decametre-scale lithological variability in well logs and cores, whose lateral dimensions are of substantial interest to hydrologists and reservoir geologists (Schultz, 1982; Van Wagoner et al., 1988, 1990). A substantial part of this short-range variability has been attributed to autogenic mechanisms such as compensational stacking (Sheets et al., 2002; Straub et al., 2009; Miall, 2014). The depocentre shifts by which compensational stacking in fluvial systems is achieved are primarily governed by channel avulsion (Jones and Schumm, 1999; Slingerland and Smith, 2004). Other explanations of small-scale lithological variability observed in well logs and cores require changes in the system's boundary conditions, such as rapid relative sea-level rise or abrupt changes in sediment supply. Rigorous criteria to distinguish autogenically from allogenically induced lithological variability based on subsurface or outcrop data have not been formulated (Zecchin, 2007; Catuneanu and Zecchin, 2013), although modelling studies

suggest that the covariance structure of sediment properties may be used for this purpose (Weltje et al., 1998).

Numerical models provide attractive tools for investigating morphodynamic and stratigraphic patterns generated by sediment-dispersal systems on different spatial and temporal scales (Hajek and Wolinsky, 2012), because they allow full access to stratigraphy produced under known conditions. The generation of small-scale lithological variability in fluvio-deltaic systems may be studied within a sequence-stratigraphic framework with a model that encompasses the full range from alluvial to shallow-marine environments. Many existing numerical models of fluvial architecture (Mackey and Bridge, 1995; Heller and Paola, 1996; Karssenberg and Bridge, 2008) cannot be easily placed in a sequence-stratigraphic context, because they lack a direct connection with the marine domain. This paper describes a series of numerical experiments in which the morphological evolution of fluvio-deltaic systems and the resulting stratigraphic record have been simulated with the SimClast model (Dalman and Weltje, 2008, 2011). SimClast covers the entire distributive portion of a sediment-dispersal system from the alluvial plain to the outer shelf. We will focus on the role of fluvial system dynamics, specifically avulsion, in the formation of delta lobes under time-invariant forcing, in order to characterize the morphodynamic feedback loop responsible for the generation of small-scale stratigraphic patterns in the fluvio-deltaic geological record as a result of compensational stacking.

2.2 Methods

Fluvio-deltaic stratigraphy was acquired by employing a basin-scale forward stratigraphic model that includes sub-grid parameterizations of alluvial and marine processes for efficient simulation of basin-fill architecture (Simclast: Dalman and Weltje, 2008, 2011). The fluvial module simulates channel-network development, including dispersive flow routing on the floodplain (Freeman, 1991) and river avulsions through a simplified bifurcation-stability routine (Slingerland and Smith, 1998). Potential avulsion sites are associated with the development and stabilization of randomly initiated crevasses. Crevassing initiates channelized flows outside the parent channel (Slingerland and Smith, 2004; Edmonds et al., 2009). The newly formed crevasse channel is assigned a random depth of incision and discharge is redistributed over both active channels. Cases where sediment transport capacity of the crevasse channel exceed the sediment load received from the parent channel allow the former to incise and thus remain active. The equilibrium configuration of the

crevasse channel depends on local threshold conditions, including channel-belt superelevation, and in-channel sediment-concentration profile. Field and experimental studies have confirmed this avulsion-initiation mechanism (Mohrig et al., 2000; Martin et al., 2009). Crevasse channels which do not heal develop into partial avulsions, nodal avulsions or reoccupy abandoned channel segments (Jerolmack and Paola, 2007). The SimClast model does not include delta avulsions based on morphodynamic backwater control (Jerolmack and Swenson, 2007; Hoyal and Sheets, 2009; Edmonds et al., 2009). Marine hydrodynamics were simplified by switching off wave- and current-induced sediment transport. Hence, suspended sediment was transported by river plumes entering still water. Redeposition of bedload by mass wasting is the only mechanism to prevent oversteepening of subaqueous slopes.

River and marine delta development were simulated by several numerical experiments under time-invariant external forcing (Table 1). The initial topography represented low-gradient shelf systems extended over an area of 5×10^3 km^2. The grid-cell size (1×1 km) was set equal to the finest spatial discretization at which the model can operate (Dalman and Weltje, 2008). Two grain size end-members were used (0.5 mm and 0.001mm) to represent sandy and muddy sediments.

Parameter	Experiment 1	Experiment 2	Experiment 3
Time simulated (kyr)	20	20	100
Discharge (m^3/yr)	5×10^9	2.5×10^9	2.5×10^9
Shelf slope (-)	5×10^{-3}	5×10^{-3}	1.5×10^{-3}

Table 2.1: Input parameters used in numerical experiments.

Experiments 1 and 2 represent short (20 kyr), low-gradient shelf system under time-invariant forcing, which allow the basic pattern of sediment sequestration and redistribution to be studied. Experiment 3 was allowed to run for 100 kyr, in order to study the linkage between the ratio of continental/marine deposition and erosion and avulsions over longer time intervals.

2.3 Results

The evolution of delta morphology over 20 kyr on a largely unconfined low-angle shelf is illustrated by Experiment 1 (Fig. 2.1). The smooth initial surface and time-invariant forcing allow a symmetrical delta to form. The active delta-plain area increases over time, because upstream migration of major avulsion sites at the apex of the delta (Fig. 2.1) coincides with overall progradation, thereby creating a fully autogenic avulsion sequence (cf. Mackey and Bridge 1995; Stouthamer and Berendsen, 2007). Initial deposition is progradational in the centre section and compensational offset stacking of later delta lobes results in a classic delta with a mounded lens shape.

Figure 2.2 illustrate the development of the channelized drainage network of the delta of Experiment 1 (exceeding a threshold value of 2×10^9 m^3 yr^{-1}) and its analysis by post-processing software (Karamitopoulos et al., 2014). Figures 2.2A and 2.2B display a frontal and top view of the full drainage network in a Wheeler (space-time) diagram. Channel-flow paths associated with avulsions occurring more than 5 km from coastline have been used to identify major river-mouth shifts (Fig. 2.2C) and shifts of the apex of the delta (Fig. 2.2D).

The stratigraphic record produced by Experiment 1 is shown in Figure 2.3. Under conditions of limited delta-plain aggradation, avulsion scours erode and rework older deposits to create amalgamated fluvial sediment bodies. The facies contact between subaerial and subaqueous deposits roughly coincides with the sand-to-mud transition at the shoreline.

Figure 2.4 shows that each major avulsion creates a wave of channel incision which migrates upstream, whereas downstream of the avulsion point, a high rate of aggradation is recorded on the delta-plain area occupied by the new channel belt. The rate of aggradation decreases as soon as a new equilibrium profile has been established. Hence, the net effect of a major avulsion on the marine domain is a temporary drop in the rate of sediment supply to the delta front. As soon as the channel network has recovered from a major avulsion, local sedimentation rate at the coastline will increase and a new delta lobe will develop. Upstream of the avulsion point, the aggrading channel-belt deposits will begin to onlap the incision that was formed as the initial response to avulsion. Meanwhile, the previously active delta lobe drowns and is covered by marine muds, because it is not receiving any more sediment from its inactive feeder channel.

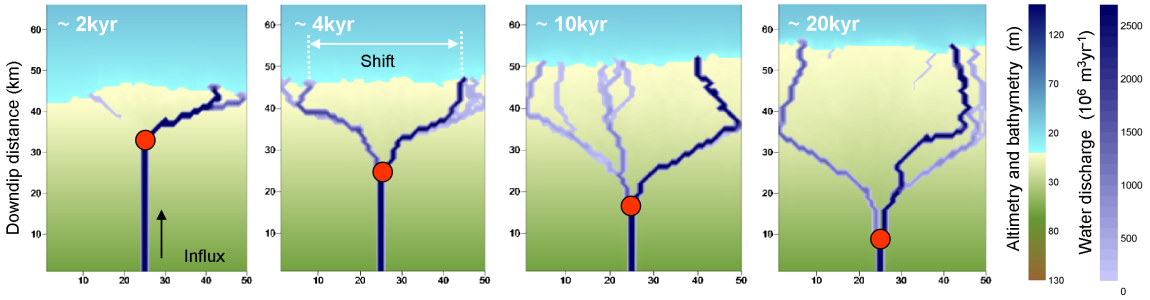

Figure 2.1: Plan-view morphology snapshots of Experiment 1 with superimposed fluvial drainage patterns. Red dots indicate position of major avulsion sites forming the apex of the delta. Backstepping of the apex resembles an avulsion sequence.

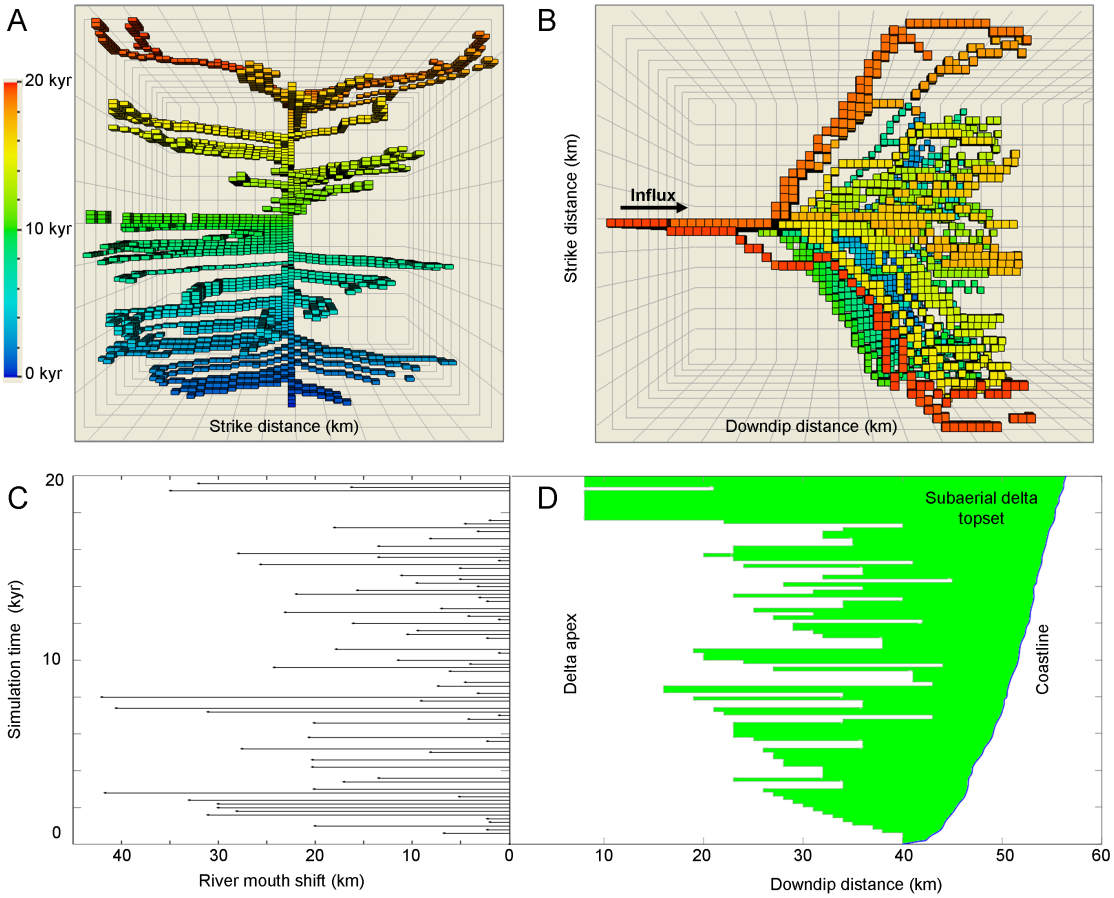

Figure 2.2: Development of the channelized drainage network of Experiment 1 in space-time (Wheeler) domain. A) upstream view; B) top view; C) river mouth shifts; D) 2D-subaerial delta topset (green area) defined by the length of delta apex (grey line) to the mean (crossdip) coastline position (blue line).

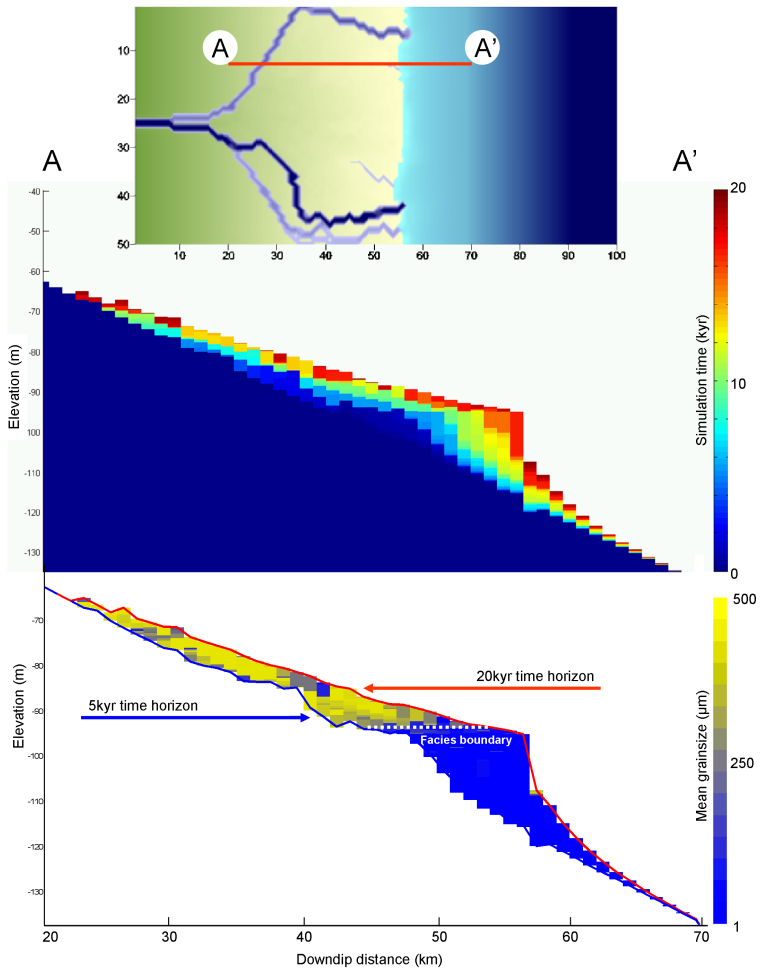

Figure 2.3: Longitudinal section (top) generated in Experiment 1. Simulated stratigraphy is represented by age of deposition (middle) and mean grain size (bottom). Chronostratigraphic correlation surfaces are marked in blue and red. Dashed white line indicates facies boundary between sandy/silty fluvio-deltaic deposits and marine muds.

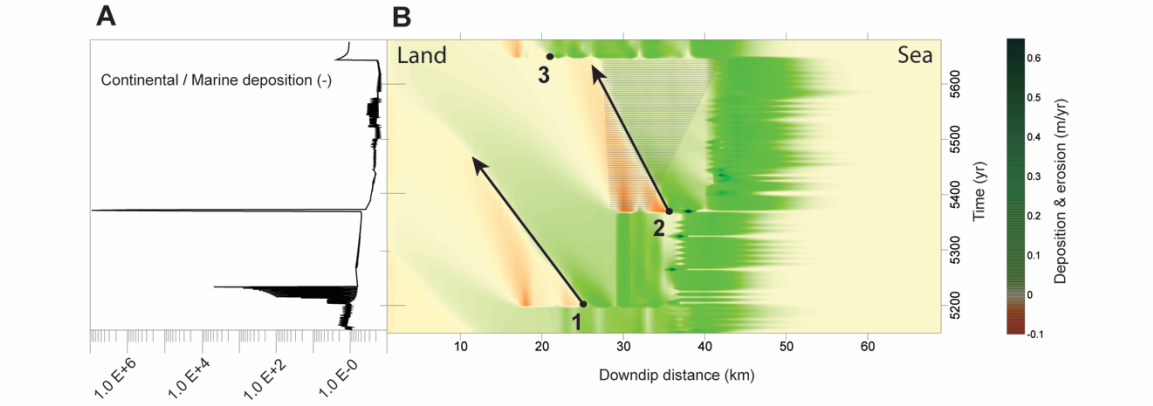

Figure 2.4: Detailed view of representative 450-year interval of Experiment 3. A) Ratio of continental/marine deposition. Major avulsions occur at points 1, 2, and 3. Event surface is isochronous and marked by an abrupt drop of sediment supply to the delta front; B) Strike-averaged dip section in time-space (Wheeler) domain. Dots mark avulsion sites. Arrows mark boundary between channel incision and fluvial onlap (boundary between red and green at right-hand side of figure) and delta-lobe progradation (at left-hand side of figure).

2.4 Discussion

2.4.1 Morphodynamic feedback loop

The central assumption embodied in SimClast is that avulsions driven by super-elevation (Slingerland and Smith, 2004; Jerolmack and Mohrig, 2007) are the main control on channel-network evolution on geological timescales. The model output clearly illustrates the consequences of this assumption: delta evolution may be described in terms of a series of events, which tie major avulsions, delta-lobe switches, fluctuations of delta-plain equilibrium profiles, and sequestration of sediments on the delta plain together in a robust feedback loop.

Under conditions of stable sea level, aggradation on the delta plain is fully controlled by progradation. If the equilibrium profile of the river system would be constant, progradation may be directly translated into a fixed rise of base level across the entire delta plain. However, progradation is to some extent neutralized by minor avulsions which increase the total number of active distributaries over the time interval in which a delta lobe grows. An increase in the number of concomitant distributaries decreases the ratio of the total cross-sectional channel area and the total wetted perimeter, which implies an increase in friction and therefore a decrease of the equilibrium gradient (Dalman and Weltje, 2008). Hence, the base-level rise caused by progradation under conditions of stable sea level will be smaller in the proximal part of the fluvial system than in the distal part, where the direct coupling to sea level is strongest. After a major avulsion, the system returns to a low-friction, high-gradient state in which all water and sediment are transported by a single channel, which explains the lateral expansion of the delta.

This morphodynamic feedback loop thus ensures that fluvial profiles will fluctuate around their equilibrium state without any changes in upstream or downstream controls. It also explains why sediment supply to the shoreline is expected to fluctuate in the absence of external forcing. After a nodal avulsion, the area of the alluvial plain that was previously subject to soil formation or peat growth is being invaded by a new channel belt. In its initial stage of development, this new channel belt will aggrade rapidly in order to approach local base level. Hence, sediment sequestration on the delta plain right after a nodal avulsion implies that the growth of the new delta lobe does not start immediately, but is preceded by a time interval of a few hundred years during which sediment supply to the marine realm is severely reduced. In summary, our results indicate that high-frequency cycles of fluvial incision and aggradation, as well as storage and release of delta-plain

sediments (cf. Kim et al, 2006; Holbrook et al, 2006), may be entirely attributable to self-organisation.

2.4.2 High-resolution sequence stratigraphy

The persistent feedback between aggradation, avulsion, and delta-lobe growth is expected to govern the architecture of fluvio-deltaic systems formed under conditions which permit delta-plain aggradation to occur. The complex response to nodal avulsion which rapidly propagates through the entire system leaves clear traces in the stratigraphic record. New major avulsions occur after timescales of 10^2-10^3 years and result in discrete sequences two orders of magnitude in thickness (10^0-10^1 m) (Fig. 2.3). As shown in Figure 2.4, each depocentre shift arising from a major avulsion produces a geologically brief episode of readjustment which provides the key to high-resolution chronostratigraphic correlation from the marine to the fluvial part of a delta. Figure 2.5 aims to summarize the readjustments in a series of cartoons, starting from a situation in which superelevation has developed. The abrupt change in flow path resulting from avulsion triggers concomitant upstream erosion and downstream aggradation, which ends as soon as the channel belt approaches its equilibrium profile. In the marine realm, the episode of readjustment is marked by a depocentre shift which takes place during a drop in sediment supply resulting from rapid aggradation directly downstream of the avulsion site. The stratigraphic expression of these changes marks an essentially isochronous surface. Hence, the stratigraphic record of fluvio-deltaic systems may be subdivided into a series of units representing intervals during which a channel belt and delta lobe were forming at a fixed location in the basin.

As shown in Figure 2.6, the lower bounding surface of each unit in the marine realm is marked by the transition from mudstone deposition to more silty/sandy deposits announcing the arrival of a new delta lobe. The fluvial equivalent of this surface would be a transition from floodplain sediments characterized by low rates of accumulation (a peat/coal horizon or a palaeosol, depending on the climatic regime) to an active channel belt characterized by crevasse splays acting as precursors to fully developed channel deposits. Upstream of the avulsion site, this conformable surface passes into a localized erosional surface (incision) which is expected to be associated with terrace formation (see Figure 2.6 upstream of the avulsion site). The upper bounding surface in the marine portion of the system would be marked by an abrupt change in the local rate of sediment supply (a flooding surface), which may be identified by a blanket of hemipelagic sediments on top of a previously active delta lobe. In the fluvio-deltaic part of the system, this surface would show

similar signs of abandonment. Abrupt or gradual abandonment may be marked by clay plugs in formerly active channels, or decreasing cross-sectional areas of channels, respectively.

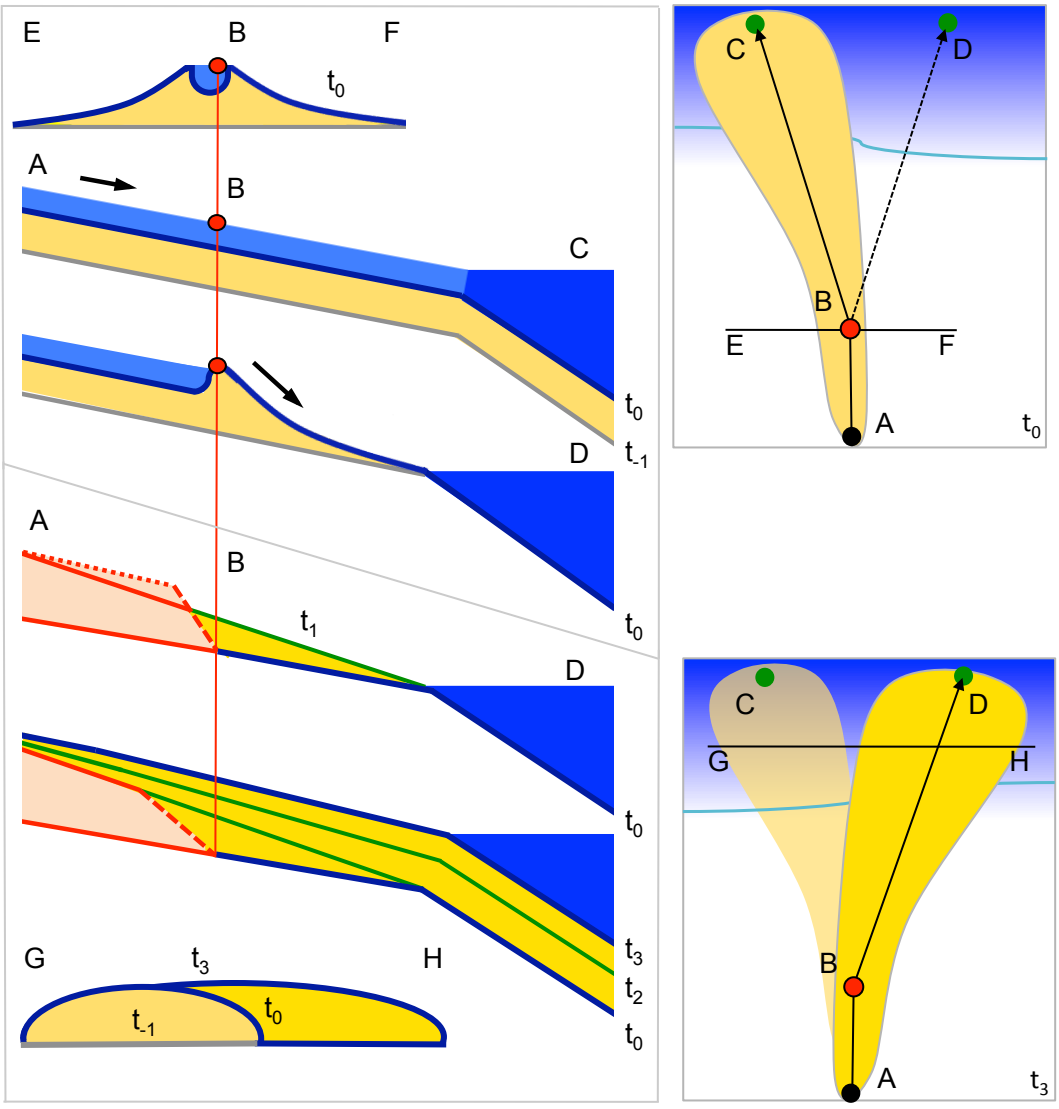

Figure 2.5: Schematic representation of processes and stratigraphic expression associated with delta-lobe switching. Left: vertical sections; Right: map views. Top: Situation at time t_0. Cross-valley section (E-F), longitudinal sections through existing (A-C) and future (A-D) flow paths. Red dot at B marks the avulsion site. Bottom: At t_1, fluvial incision occurs upstream of the avulsion site (A-B), while rapid aggradation occurs in the new channel belt downstream (B-D). No sediment reaches the coastline. At t_3, the backstepping incision has been onlapped by deposits of the new channel belt (A-B), and the morphology has been restored to that of t_0. Offshore, the time horizon at t_1 marks the abandonment of the old lobe and the initiation of the new one (section G-H). See text for full discussion.

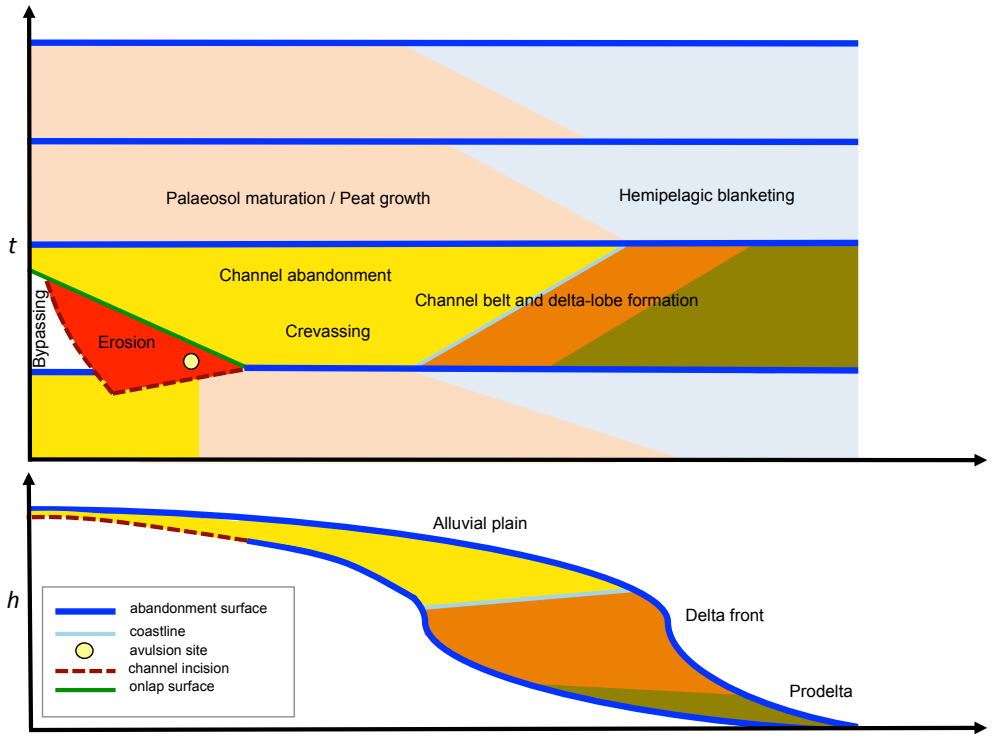

Figure 2.6: Conceptual model illustrating a longitudinal section through four stacked fluvio-deltaic chronosomes in space-time (Wheeler) domain (top) and depth (bottom). Note that a channel belt is active during formation of each chronosome, even though it is visible in the first and second chronosomes only. The upper two chronosomes (and a large part of the lowermost one) are assumed to represent condensed facies. They are very thin and therefore not visible in the bottom section. Some of the characteristic sedimentary processes and environments are listed in the upper and lower panels, respectively. Note that the term bypassing assumes that the upstream portion of the channel belt is in equilibrium, which need not be the case. See text for full discussion.

The marine portion of the units described above conforms to the definition of a classic parasequence, i.e., a relatively conformable succession of genetically related beds or bed sets bounded by marine flooding surfaces and their correlative surfaces (Van Wagoner et al., 1988). We have deliberately avoided use of this term, because it has been the subject of a lot of discussion recently. The problems associated with the parasequence concept have been summarized elsewhere (Catuneanu, 2006; Zecchin, 2010; Zecchin and Catuneanu, 2013). The lower-order chronostratigraphic units we describe may be termed chronosomes (Schultz, 1982), a neutral term entirely devoid of interpretation. The nature of the isochronous bounding surfaces of the fluvio-deltaic chronosomes may be clarified by referring to Tipper (2000), who provides generalizations of the concepts of accommodation and supply that are also applicable to areas of stasis and net erosion. In areas where the lithic surface lies below base level, changes in the vertical distance between the two may be interpreted in terms of deepening and shallowing. According to this view,

the lower bounding surface of a fluvio-deltaic chronosome marks the start of an episode of shallowing and the upper bounding surface marks a return to deepening conditions everywhere in the system. Because one unit's lower bounding surface coincides with another unit's upper bounding surface, we propose to use the generic term abandonment surface for chronostratigraphic subdivision of fluvio-deltaic stratigraphy.

In parts of the floodplain far away from active channel belts, abandonment surfaces are likely to be cryptic, just like one would expect them to be in marine parts of the system far away from active delta lobes (Fig. 2.6). In both environments, the lithology of inactive chronosomes most likely reflects the distance to the nearest active part of the system (channel belt or delta lobe), and an abrupt change in this distance may therefore be expressed in the stratigraphic record.

2.4.3 Application to real-world stratigraphy

The synthetic stratigraphy produced in the numerical experiments displays a strong short-range lateral variability governed by the morphodynamic feedback loop discussed above. Similar patterns of stratigraphic variability have been cited in various field studies of Quaternary and ancient fluvio-deltaic sequences. Detailed field studies of the Mississippi (Frazier, 1967; Autin et al., 1991; Aslan and Autin, 1999), the Rhine-Meuse (Törnqvist, 1994; Stouthamer, 2011) and the Cumberland Marshes of Saskatchewan (Smith et al., 1989) provided evidence of rapid river avulsions controlling the spatial distribution of channel-belt and overbank deposits in sedimentary basins. Studies of ancient avulsion deposits (Kraus and Wells, 1999; Mohrig et. al, 2000; Slingerland and Smith, 2004; Jones and Hajek, 2007) recorded major sheet-like sandstones directly overlying, or locally scouring, heterolithic overbank deposits, supporting the threshold nature of avulsions. The upstream migrating wave of erosion directly following a major avulsion (Fig. 2.4) has been documented in the case of the 1855 Yellow River avulsion which initiated a wave of erosion that migrated ca.100 km upstream from the avulsion site resulting in extensive terrace formation (Qian, 1990).

Rapid downstream aggradation, filling lower areas of the floodplain was inferred from analysis of Miocene overbank deposits of the Chinji Formation, Himalayan Basin (Willis and BehrensMeyer, 1994). Unfortunately, their data do not permit a distinction between continuously shifting localized overbank deposition or wide-spread but short-lived events associated with river-channel avulsion,

which underscores the difficulties of diagnosing systematic patterns of overbank sedimentation in the field due to lack of kilometer-wide outcrops and low bedding angles of overbank deposits.

The genetic and geometric relationship between avulsion sites and floodplain sequences was highlighted by Kraus (1987), Kraus and Aslan (1999) and Kraus and Wells (1999), who described large-scale floodplain sequences characterized by alternations of crevasses and overbank deposits. These alternations are in accordance with patterns of palaeosol variability caused by channel avulsions. The maturity of palaeosols in floodplain environments is inversely proportional to the sediment accumulation rate, which is highest in the active channel belt. Kraus and Aslan (1999) concluded that an unusually mature palaeosol should develop in association with the thick sandstone at the base of a new avulsion sequence, i.e. at the base of a chronosome. This is fully consistent with our inference that mature palaeosols develop in areas which have not received sediment for a long time and are therefore far below base level, which makes them particularly attractive to gravitationally driven processes such as avulsion. The style of avulsion may vary throughout a floodplain sequence (Hajek and Edmonds, 2014), yet the intrinsic stratigraphic response is expected to be consistent with the morphodynamic feedback loop proposed here.

2.5 Conclusions

A feedback loop linking major avulsion, delta-plain aggradation, and delta-lobe switching is responsible for the generation of compensational stacking patterns in fluvio-deltaic systems. These stacking patterns occur in all settings where delta-plain accommodation is sufficient to permit local top-set aggradation. The abrupt nature of depocentre shifts permits subdivision of the fluvio-deltaic stratigraphic record along isochronous surfaces. Each conformable abandonment surface may be traced from the marine into the fluvial domain. Upstream of the avulsion site, the abandonment surface changes to a local incision associated with terrace formation. The chronostratigraphic units thus defined have been termed chronosomes (Schultz, 1982). The recognition of system-wide chronosomes potentially allows high-resolution chronostratigraphic correlation of marine to continental deposits. The main differences between our simulations and real-world stratigraphy are the absence of floodplain processes (vegetation growth and soil formation), marine hydrodynamics (waves and tides), and sea-level rise in our simulations. These factors affect the stratigraphic expression, completeness, and resolution, respectively (Swenson, 2005, Karamitopoulos et al., 2014). In practice, high-resolution dating of Quaternary systems and detailed studies of modern

systems will be necessary to investigate whether physical continuity of the continental and marine portions of fluvio-deltaic chronosomes can be demonstrated.

Chapter 3

Allogenic controls on autogenic variability in fluvio-deltaic systems: inferences from analysis of synthetic stratigraphy [2]

Abstract

Fluvio-deltaic stratigraphy develops under continuous morphodynamic interactions of allogenic and autogenic processes, but the role and relative contribution of these processes to the stratigraphic record are poorly understood. We analysed synthetic fluvio-deltaic deposits of several accommodation-to-supply cycles (sequences) with the aim to relate stratigraphic variability to autogenic and allogenic controls. The synthetic stratigraphy was produced in a series of long time-scale (10^5 yrs) numerical experiments with an aggregated process-based model using a typical passive-margin topography with constant rates of liquid and solid river discharge subjected to sinusoidal sea level fluctuation. Post-processing of synthetic stratigraphy allowed us to quantify stratigraphic variability by means of local and regional net sediment accumulation over equally spaced time intervals (1 to 10 kyr). The regional signal was subjected to different methods of time-series analysis. In addition, major avulsion sites (> 5 km from the coastline) were extracted from the synthetic stratigraphy to confirm the interpretations of our analyses. Regional stratigraphic variability as defined in this study is modulated by a long-term allogenic signal, which reflects the rate of sea-level fluctuation, and it preserves two autogenic frequency bands: the intermediate and high-frequency components. The intermediate autogenic component corresponds to major

[2] Based on: Karamitopoulos, P., Weltje, G.J., Dalman, R.A.F., published. Allogenic controls on autogenic variability in fluvio-deltaic systems: inferences from analysis of synthetic stratigraphy. Basin Research, 26, 767-779. https://doi.org/10.1111/bre.12065.

avulsions with a median inter-avulsion period of ~3 kyr. This component peaks during time intervals in which aggradation occurs on the delta plain, because super-elevation of channel belts is a prerequisite for large-scale avulsions. Major avulsions occur occasionally during early stages of relative sea-level fall, but they are fully absent once the coast line reaches the shelf edge and incision takes place. These results are consistent with a number of field studies of falling-stage deposition in fluvial systems. The high-frequency autogenic component (decadal to centennial time scales) represents mouthbar-induced bifurcations occurring at the terminal parts of the system, and to a lesser extent, partial or small-scale avulsions (< 5km from the coastline). Bifurcation intensity correlates strongly with the rate of progradation, and thus reaches its maximum during forced regression. However, its contribution to overall stratigraphic variability is much less than that of the large-scale avulsions, which affect the entire area downstream of avulsion nodes. The results of this study provide guidelines for predicting fluvio-deltaic stratigraphy in the context of co-existing autogenic and allogenic processes and underscore the fact that the relative importance and the type of autogenic processes occurring in fluvio-deltaic systems are governed by allogenic forcing.

3.1 Introduction

Quantitative stratigraphic analysis of fluvio-deltaic sedimentary systems is hampered by the incompleteness of the stratigraphic record and by our inability to identify laterally extensive isochronous surfaces (Jerolmack and Paola, 2010; Bhattycharya, 2011). In addition, the extent to which allogenic and autogenic processes contribute to the morphological evolution of fluvio-deltaic systems is still under debate (Kim et al., 2006; Van Dijk et al., 2009; Tomer et al., 2011). Recent experimental and field research suggest that fluvio-deltaic stratigraphy is controlled by the evolution of channel networks and is closely linked to shoreline migration (Jerolmack, 2009). Delta-front progradation by mouthbar-induced bifurcation is an example of an autogenic process occurring exclusively at the river mouth (Edmonds and Slingerland, 2007). Major (or nodal) avulsions have a much larger impact on the fluvio-deltaic drainage system, and appear to be characterized by system-specific inter-avulsion periods (Ashmore, 1991; Törnqvist, 1994; Bryant et al., 1995; Jerolmack and Mohrig, 2007, Jerolmack, 2009; Stouthamer and Berendsen, 2007). Both phenomena reflect the system's self-organization across a range of spatial and temporal scales (Werner, 1999; Murray, 2003; Paola et al., 2009; Kleinhans, 2010).

At present, our knowledge of the relative roles of different autogenic processes is scant at best. It is not known whether these processes interact, or whether they are ultimately driven by allogenic forcing mechanisms. As a baseline for further discussion we propose that the role of autogenic processes should be investigated throughout a sequence, i.e., a cycle of accommodation to sediment supply rates (Neal and Abreu, 2009) which may be viewed as a natural stratigraphic unit (Catuneanu et al. 2009, 2012). The most convenient way to achieve this goal is to employ a numerical model, which includes nodal avulsions and mouthbar-induced bifurcations as autogenic processes (SimClast; Dalman and Weltje, 2008, 2012) in order to acquire synthetic stratigraphy. We quantify stratigraphic variability in terms of local and regional standard deviations of net sediment accumulation integrated over equally-spaced time intervals. Time-series analysis of regional stratigraphic variability permits the recognition of distinct allogenic and autogenic components in the time and frequency domains, which are investigated in more detail by post-processing of the synthetic stratigraphy.

3.2 Methods

3.2.1 Generation of synthetic stratigraphy

A series of numerical experiments were performed with SimClast to test the relative contribution of sea level fluctuation and channel network dynamics to autogenic stratigraphic variability. The model combines diffusive and advective transport with sub-grid algorithms of channel network dynamics in the fluvial domain. Crevasses are treated as sub-grid phenomena and occur randomly. Their subsequent evolution is determined by the sediment concentration profile in the river channel and the ratio of in-channel and cross-valley gradients. Stable bifurcations or full avulsions will develop under favourable conditions, such as local superelevation (Mohrig et al., 2000; Törnqvist and Bridge, 2002; Slingerland and Smith, 2004; Jerolmack and Mohrig, 2007) or through bifurcations due to mouth-bar deposition at the terminal parts of the distributive channel network (Jerolmack and Swenson, 2007). All of the experiments were conducted on a typical passive margin topography (50 x 100 km; Fig. 3.1). We used grid cells of 1 x 1 km, which represents the finest spatial discretization at which the model can operate, because the width of the grid cells should be larger than the width of the channel (Dalman and Weltje, 2008).

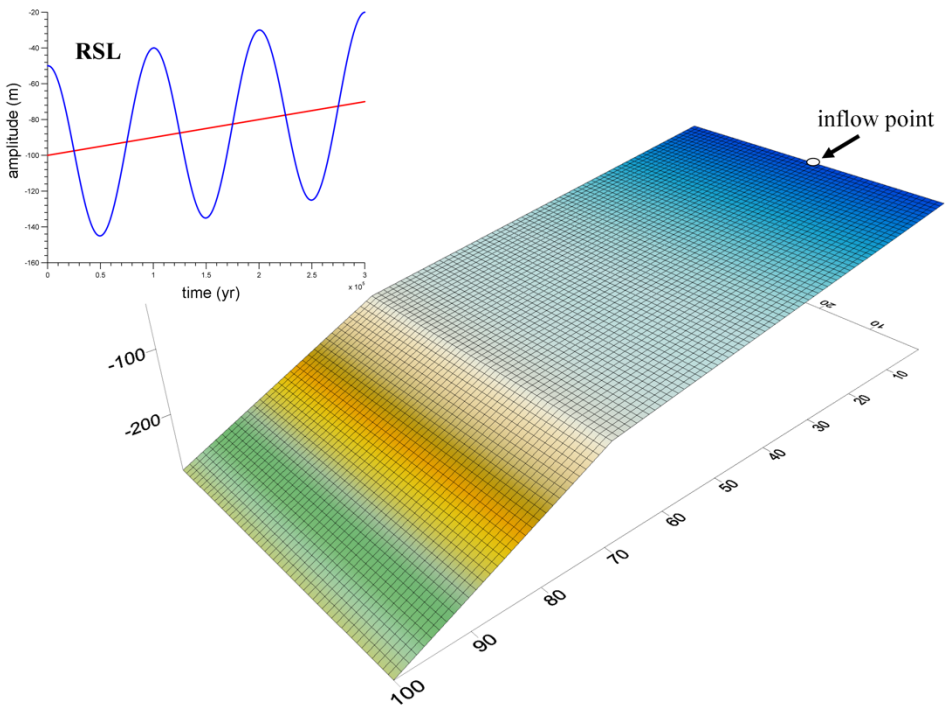

Figure 3.1: Initial model topography and inflow point. Inset: Relative sea-level curve and superimposed subsidence (red).

Scenarios	Q_s (m^3/yr)	Q_w (m^3/yr)	S_L (-)	Subsidence rate (mm/yr)
Base case (BS)	1×10^6	5×10^9	5×10^{-3}	0.1
HQ_s	2×10^6	5×10^9	5×10^{-3}	0.1
Low angle (LA)	1×10^6	5×10^9	3.5×10^{-3}	0.1
MQ_s	1.5×10^6	5×10^9	5×10^{-3}	0.1
LQ_w	1×10^6	4×10^9	5×10^{-3}	0.1
HQ_w	1×10^6	5.25×10^9	5×10^{-3}	0.1

Table 3.1: Input parameters: sediment and water discharge rates, shelf angle and subsidence rate.

Throughout the experiments which lasted for 300kyr, sediment and water discharge rates were kept constant (Table 3.1) with Q_s/Q_w ratio ranging between 1.9×10^{-4} and 4×10^{-4}, i.e. on the same order as major river systems such as the Rhine (Törnqvist, 1994; Stouthamer and Berendsen, 2001). An additional experiment with a lower shelf angle (S_L) was carried out to test the effect of initial topography on autogenic stratigraphic variability. We used two grain size end-members (1 mm and 0.001mm) representative of sandy and muddy sediments (50% of each by volume). Substratum thickness is 50m (grain-size distribution identical to sediment feed). Dimensionless bank erodibility and riverbed friction coefficients were set equal to 0.01 and 0.05 respectively (Dalman and Weltje, 2008). Sea level fluctuation was modelled as a sinusoid with wavelength of 100 kyr and amplitude of 50 m, to be comparable to the glacio-eustatic sea-level fluctuations of the Pleistocene (Emiliani,

1955; Shackleton and Opdyke, 1973, 1976; Carter, 1998, 2005). Linear spatially uniform subsidence was superimposed on the sinusoidal sea-level curve. Sedimentation was recorded as a time series of bulk net sediment accumulation, $d(t_k)$ in meters. Wave activity and tides were assumed to be absent, so as to maximize the preservation of shelf deposits and facilitate the interpretation of the simulated stratigraphic record.

3.2.2 Quantification of stratigraphic variability

The fluvio-deltaic stratigraphic record reflects intermittent shifts in the locus of deposition, a phenomenon known as compensational stacking (Straub et al. 2009; Hajek et al., 2010; Wolinsky et al., 2010; Wang et al., 2011). We constructed a stratigraphic column for each grid cell and throughout the model run we recorded net sediment accumulation (stratal thickness in meters) at variably spaced stratigraphic markers (time steps). We defined the standard deviation of net sediment accumulation at time interval z_i as:

$$lsv_{x,y,z}(t_k) = \sqrt{\frac{1}{n_{x,y,z}} \sum_{t_k} (d(t_k) - d(t_k + \Delta t_i))^2} \quad (1)$$

$$z : \left\{ \begin{pmatrix} d(t_1) \\ d(t_2) \\ . \\ . \\ d(t_k) \end{pmatrix} \begin{pmatrix} t_1 \\ t_2 \\ . \\ . \\ t_k \end{pmatrix} \right\}, \Delta t_i = t_1 - t_2$$

where $d(t_i)$ is thickness of net sediment accumulation corresponding to variably spaced time steps (t_i) and n is the number of net sediment accumulation differences encountered at time interval z_i. Constant net sediment accumulation will produce predictable stratal patterns (with standard deviations approaching zero). Sudden changes associated with shifting of the locus of deposition will produce progradational or retrogradational stacking as well as lateral shifting of local depocentres and hence increase local stratigraphic variability. This metric has some similarity to the decay of standard deviation of sedimentation rate divided by subsidence with increasing time intervals (Sheets et al., 2002; Straub et al., 2009).

Time interval selection *(z_i)* divides the time-depth axis into equally-spaced stratigraphic spans, whose lengths represent the tradeoff between stratigraphic resolution and robustness of these measures. We selected equally spaced time intervals that range from 1 kyr to 10 kyrs. This range

of intervals allows us to attain high signal-to-noise ratios and is adequate to resolve periodic recurrence of autogenic geological processes such as large-scale avulsions and formation of channel belts (Törnqvist et al., 1994; Stouthamer et al., 2001; Blum et al., 2000, 2013).

Regional stratigraphic variability (*rsv*) results from summation of the *lsv* estimates across the entire model domain:

$$rsv_{x,y}(z) = \sum_{x}\sum_{y} lsv(t_{k,x,y}), \quad (2)$$

We used the *rsv* signal for time series and spectral analysis. De-trending, low-pass and high-pass filtering were applied successively in order to reveal trends, identify low-frequency features and isolate the high-frequency content respectively. The frequency-domain representation allowed us to decompose the *rsv* signal into several bands and identify significant peaks corresponding to modelled allogenic and autogenic processes. We used the Fast Fourier Transform (FFT) and the multi-taper method (Thomson, 1982; Percival and Walden, 1993) as implemented in the SSA-MTM toolkit (Ghil et al., 2002) to convert time to frequency domain. The former was used to analyze broadband variability whereas the latter was applied to extract the midrange and high-frequency components of variability and identify statistically significant peaks.

3.2.3 Extraction of isochronous surfaces and avulsion sites

Throughout the experiments, for each time step (1yr) we calculated:

$$\alpha(t_i) = \frac{n_{continental\_cells}}{n_{marine\_cells}}, \quad (3)$$

where $\alpha(t_i)$ is the ratio of the number of continental to marine grid cells. Minima and maxima of $\alpha(t_i)$ correspond to the ages of maximum flooding surfaces (MFSs) and maximum regressive surfaces (MRSs), respectively. Both sequence-stratigraphic surfaces are thus isochronous by definition. We extracted the number and location of avulsion sites by applying a post-processing operation. This involves the application of a Boolean transformation with thresholding:

$$Q_{w_{x,y,z}} > Q_{thr} = 1$$

$$Q_{w_{x,y,z}} < Q_{thr} = 0,$$

followed by calculation of differences for the successive Boolean channel networks:

$$D_{z_i} = B_{i-1}^{Q_{w(z_{i-1})}} - B_i^{Q_{w(z_i)}}, \quad (4)$$

where $Q_{x,\,y,\,z}$ is water discharge corresponding to time interval z_{ii}, Q_{thr}=1.0×10^9 m^3 yr^{-1}, B^Q is a Boolean value of water discharge (0 or 1) and D_z refers to the successive differences of Boolean channel networks. Avulsion sites were identified as intersections of old and new channel branches. The magnitude of an avulsion was quantified by its distance from the coast line (Fig. 3.2). Avulsions occurring more than 5 km away from the coastline were considered major, because they tend to be associated with large lateral displacements of depocentres at the coastline (i.e. major lobe switches). This category does not include cases of regional reoccupation (sensu Jerolmack and Paola, 2007), a phenomenon that is clearly visible inside both the old and the new channel belts linked by a major avulsion (Fig. 3.2).

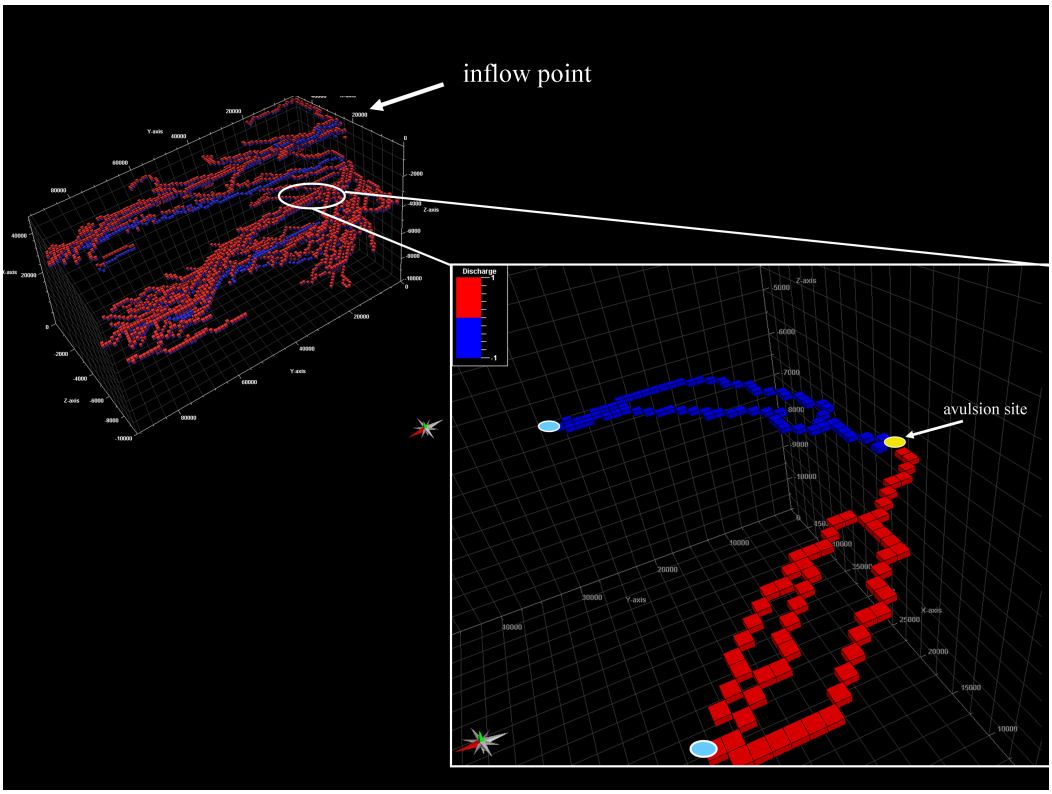

Figure 3.2: Post-processing: Boolean transformation for avulsion site extraction. Red and blue grid cells correspond to the old and new channel branches, respectively. Both branches terminate at the coastline (cyan). Major avulsion site (yellow) lies at the intersection of the two branches (>5km from coastline).

The total number of bifurcations (N_{bif}) was defined as the sum of all avulsions, crevasses, and mouthbar-induced bifurcations. The bifurcation intensity was defined as the total number of bifurcations over a unit time, divided by the subaerial area:

$$I_{bif} = \frac{N_{bif}}{A_c}. \qquad (5)$$

Overall, these post-processing operations provided frequency distributions of autogenic processes that occur throughout a relative sea-level cycle and contribute to regional stratigraphic variability.

3.3 Results

3.3.1 Synthetic stratigraphy

The ages of the MFS and MRS allow a subdivision of the stratigraphic record into conformity-bounded genetic sequences (Galloway, 1989). Figure 3.3A to 3.3C illustrate the stratigraphic record of the base-case scenario (Table 3.1). The distinction of MFSs and MRSs allows us to separate the stratigraphic record into transgressive systems tracts (TST; bounded below by an MRS and above by an MFS) on the one hand, and into units comprising successions of highstand (HST), falling-stage (FSST) and lowstand (LST) systems tracts on the other hand. The medial cross section (Fig. 3.3A) shows that genetic sequences on the alluvial plain are characterised by an overall coarsening up from the MFS to the MRS, reflecting the succession of aggradation, progradation and degradation. The TST (fining upwards from the MRS to the MFS) shows that the fluvial valleys are preferentially filled with sand, and finally the areas surrounding the formerly active channel belts are blanketed with fine-grained sediment, indicative of retrogradational stacking (transgression). Essentially the same phenomena may be recognized in the distal cross section of Figure 3.3B, although it is apparent that there is much less lateral confinement and incision in these lobate units. In both sections, compensational stacking is clearly visible in the genetic sequences bounded by MFSs. The longitudinal central section (Fig. 3.3C) illustrates that compensational stacking is largely responsible for the apparent deviations from the expected shifts in depocentres throughout genetic sequences. In fact, only the lowermost HST-FSST-LST unit displays a well-developed wedge-type geometry, because the depocentres of the other two sequences are out of the plane of the longitudinal section.

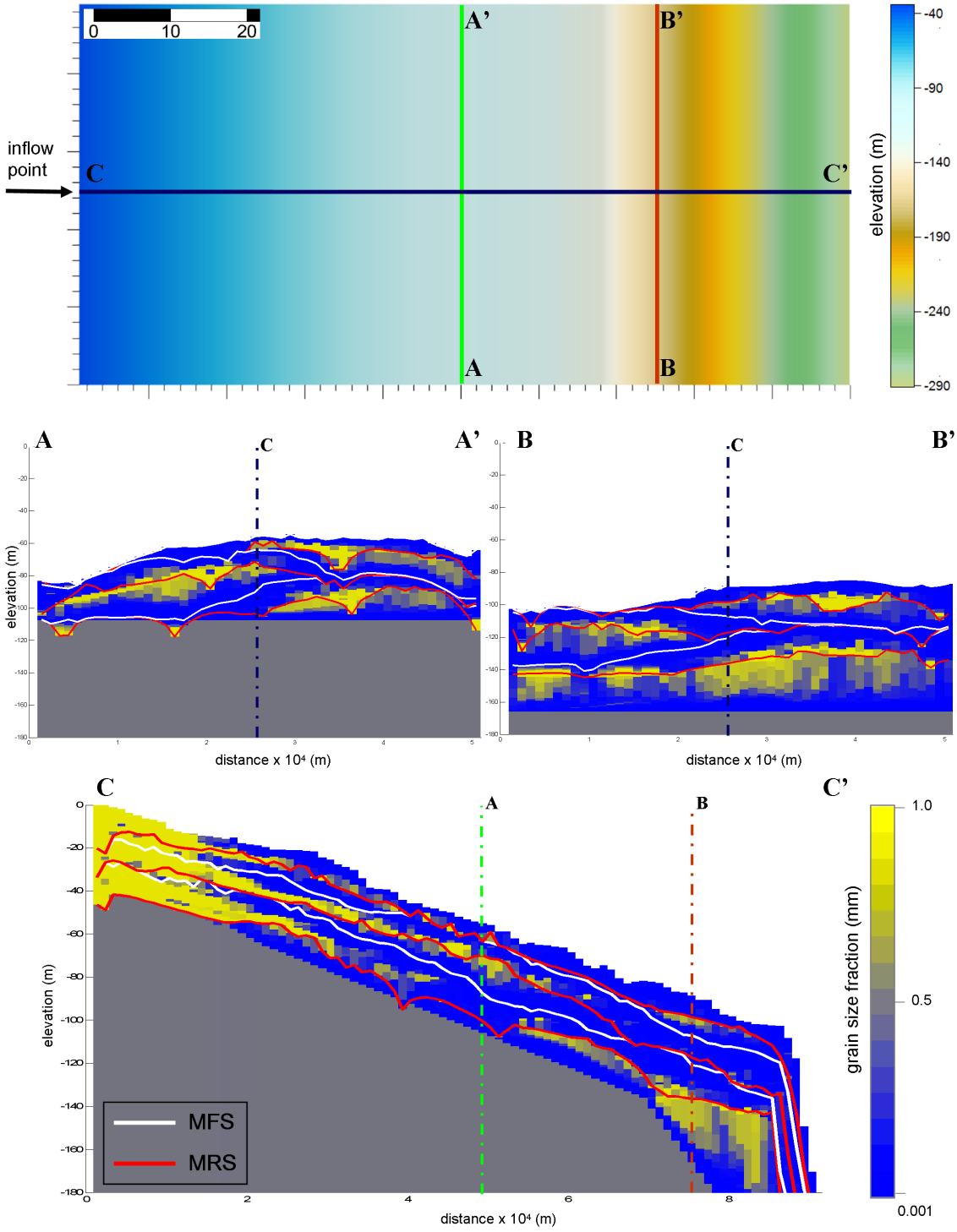

Figure 3.3: Vertical sections of synthetic stratigraphy (base case model run) represented by median grain sizes and bounding surfaces. (A) Medial cross section. (B) Distal cross section. (C) Longitudinal central section.

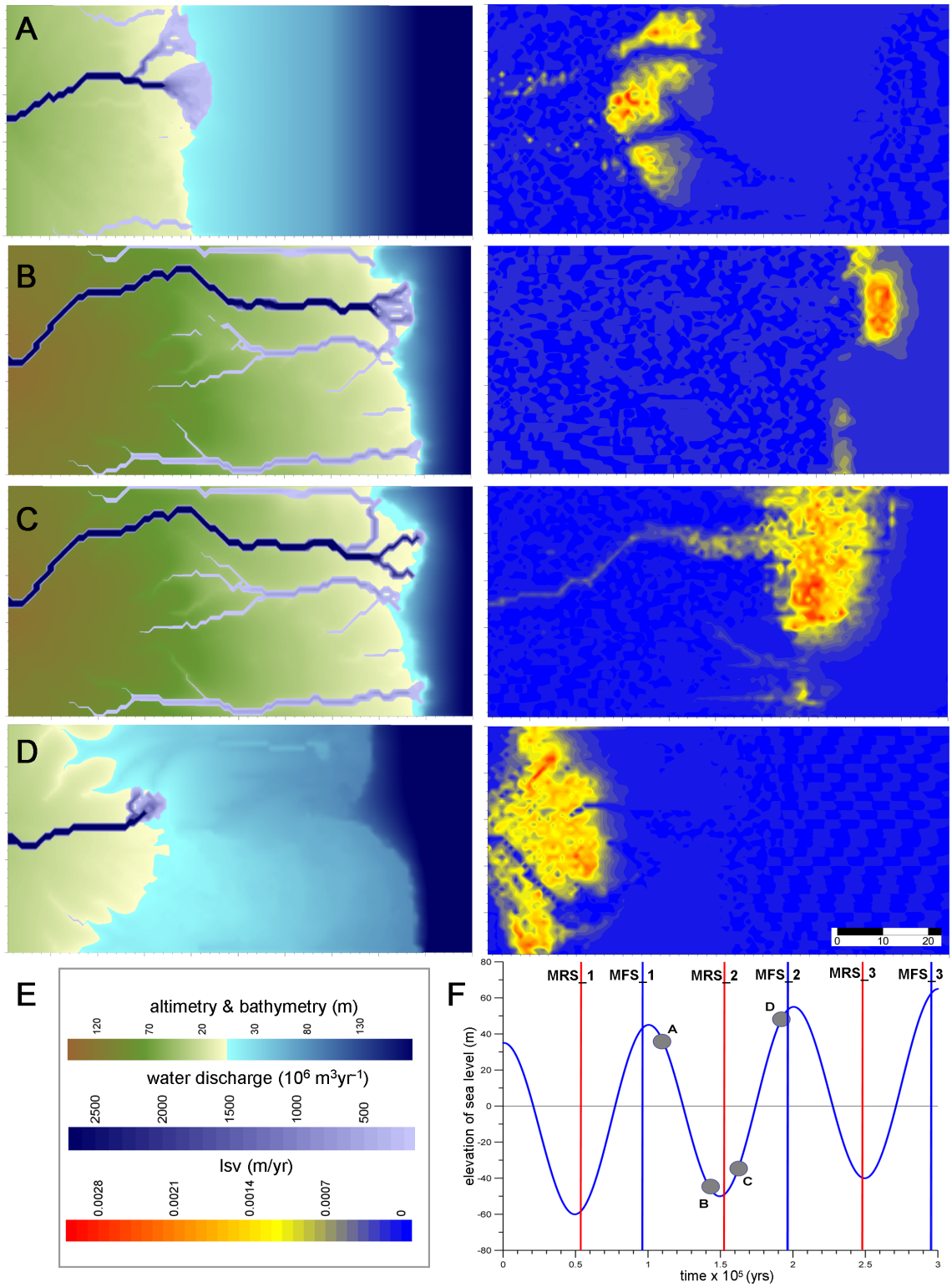

Figure 3.4: Snapshots of morphology and 10-kyr average local stratigraphic variability. (A) Early falling stage. (B) Late falling stage. (C) Early rising stage. (D) Late rising stage. (E) Legends to figures A-D. (F) Normalized relative sea level curve (blue); snapshots of model run (A to D) are marked by grey dots. Red and blue lines mark times of Maximum Regressive and Maximum Flooding surfaces, respectively.

3.3.2 Patterns of local stratigraphic variability

The patterns of stratigraphic variability throughout sequences are illustrated in Figure 3.4. During early falling stage (Fig. 3.4A), the sediment dispersal system is regulated by the interplay of relative sea-level fall and a few major avulsions. At this stage, progradation of the delta-front by mouthbar-induced bifurcations occurs simultaneously with delta-plain aggradation. During late falling stage (Fig. 3.4B) sea level drops below the shelf break, which initiates a phase of fixed drainage marked by erosive features (canyons). The main depocentre migrates further basinwards where localized, highly variable sequences are formed in the absence of major avulsions. During the early stage of sea-level rise (Fig. 3.4C), progradation gives way to retrogradation and the major trunk channels are back-filled with sediment. High rates of aggradation in the active channel belt favour alluvial ridge super-elevation, which in turn increases the probability of avulsion. Finally, during late rising stage (Fig. 3.4D), the sedimentary system becomes highly dispersive.

The events extracted from the stratigraphic record (Fig. 3.5) show that mouthbar-induced bifurcations are the dominant autogenic process occurring during intervals characterized by negative rates of sea-level change. Bifurcation intensity has a median equal to ~0.003 yr^{-1} km^{-2} (Fig. 3.6A). During intervals characterized by positive rates of relative sea-level change, major avulsions are the dominant autogenic process (Table 3.2), although major avulsions still occur during the early falling stage (cf. Fig. 3.4A). The median inter-avulsion period equals ~3 kyr (Fig. 3.6B). Bifurcation intensity is lowest during periods of relative sea-level rise, reflecting low or even negative rates of progradation.

3.3.3 Time-series analysis of regional stratigraphic variability

Time-series and spectral analysis of regional stratigraphic variability (*rsv)* was conducted as follows. Initially we remove the linear trend from the *rsv* signal which reflects basin subsidence (Fig. 3.7A). The frequency-domain representation of the *rsv* signal is not very informative (Fig. 3.7D), which is why we split the signal into a low- and high-frequency part. The low-pass filter (cut-off frequency = 1cycle/100 kyrs) returns the low-frequency *rsv* signal which corresponds to the rate of sea-level fluctuation (Fig. 3.7B and 3.7E).The high-pass filter (2cycle/100kyrs 'low-cut') returns the high-frequency content which is characterized by two frequency-bands: an intermediate component that corresponds to major avulsions and associated delta-lobe switches with periods ranging from 2 kyr to 50 kyr, and high-frequency noise associated with mouthbar-

induced bifurcations and partial or small-scale avulsions occurring at timescales <2 kyr (Fig. 3.7C and 3.7F). These results are consistent with the time scales derived from extraction of autogenic events (Fig. 3.5 and 3.6).

The multi-taper method (Fig. 3.8A) was used to acquire continuous spectra and estimate statistically significant peak frequencies (exceeding 90%, 95% and 99% confidence levels). We calculate periodic recurrence for these significant peaks by dividing the sampling interval (1 kyr) with the corresponding frequencies. The resulting wavelengths fall in the same band (2 kyr to 6 kyr) as the ones estimated with the FFT and are compared to the Q_s/Q_w ratios used for each experiment (Fig. 3.8B).

3.4. Discussion

3.4.1 Accommodation-to-supply cycles

Our results demonstrate that the pattern of regional stratigraphic variability (*rsv*) in fluvio-deltaic systems changes systematically throughout an accommodation-to-supply (relative sea-level) cycle. Highest values of *rsv* have been observed in aggradational to retrogradational packages formed during sea-level rise. During such intervals, large-scale avulsions which affect the entire downstream portion of the sediment dispersal system are the dominant autogenic processes. The *rsv* reaches maxima in retrogradational packages, which represent periods in which the fluvial system is entirely unconstrained. Because *rsv* maxima reflect peaks in avulsion frequency occurring in the TST (Table 3.2), these are the intervals in which major depocentre shifts are most likely to occur. Consequently, the MFSs tend to separate time intervals in which the location of the active channel belt and its delta lobes were fixed. The large-scale compensational stacking pattern in fluvio-deltaic systems is therefore brought out most clearly by adopting the genetic sequence bounded by MFSs (Galloway, 1991), as seen in Figures 3.3A to 3.3C.

Regional stratigraphic variability is smaller in the FSST because channel-belt aggradation is low to absent, and incision during late falling stage inhibits large-scale avulsions (Table 3.2), thereby reducing the mobility of the distributary system. At late falling stages, the depocentre is confined to the immediate vicinity of the shelf-edge. The relative sea-level fall promotes rapid progradation (forced regression) which takes place by growth of the distributary network through mouthbar-induced bifurcations (Edmonds and Slingerland, 2007; Jerolmack, 2009). Hence, the bifurcation intensity reaches its peaks during the periods corresponding to (the late stage of) forced regression

(Fig. 3.5). This process does not have a major contribution to overall stratigraphic variability (*rsv*) as defined in this study, because progradation is localized and affects only the morphology of the terminal parts of the system. The values of *rsv* therefore primarily reflect the number of major avulsions, and the many bifurcations, crevasses and failed avulsions assume the role of background noise.

3.4.2 Relation between allogenic and autogenic forcing

Filtering and spectral analysis of the *rsv* signal permit the distinction of three types of variability corresponding to different frequency bands. The first type represents the long-term average (low-frequency) *rsv* which correlates strongly with rates of subsidence and sea-level fluctuation, and is thus allogenically induced. Post-processing of the synthetic stratigraphic record has allowed us to interpret the remaining variability of the *rsv* signal in terms of two autogenic components. The second type of variability (intermediate-frequency band) reflects large-scale avulsions with a median inter-avulsion period of ~3 kyr. More than 95% of all inter-avulsion periods range from 1 to 10 kyr (Fig. 3.6B). The third type of variability represents high-frequency autogenic noise associated with mouthbar-induced bifurcations and partial small-scale avulsions. The bifurcation intensity is modulated by the allogenic signal (rate of sea-level change), and is highest during late falling stage. However, its contribution to the total *rsv* is relatively small.

The intermediate frequency band is also modulated by the allogenic component of stratigraphic variability. The rate of relative sea-level rise is strongly correlated with avulsion frequency, because the rate of aggradation on the delta plain, which is a prerequisite for the development of channel-belt super-elevation driving major avulsions, varies systematically throughout a relative sea-level cycle. Moreover, a coupling between the rate of channel-belt aggradation and the frequency of major avulsions is suggested by a comparative analysis of various model runs, which seems to indicate that the ratio of solid to liquid discharge is positively correlated with avulsion frequency (Fig. 3.8B).

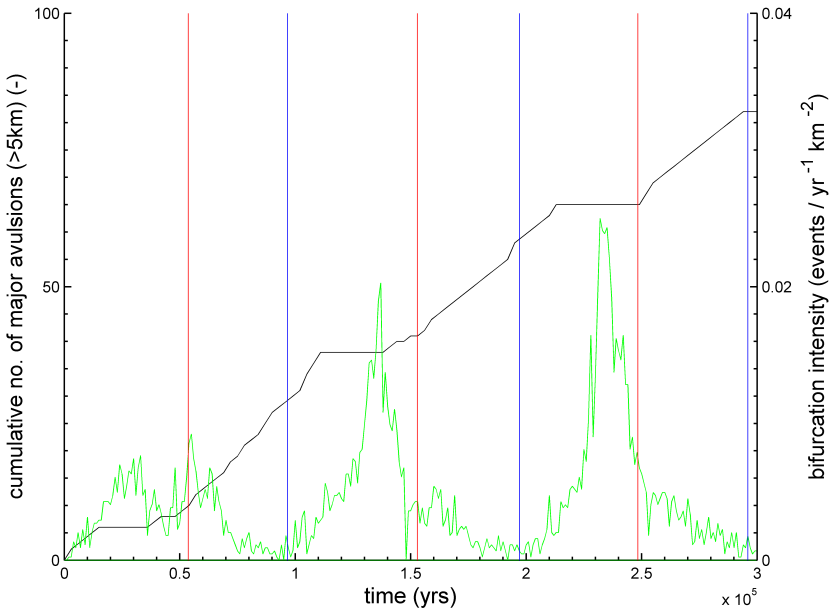

Figure 3.5: Cumulative frequency distribution of major avulsions (black) and bifurcation intensity (green). Isochronous bounding surfaces: MRS = red; MFS = blue.

ST	NE	D (kyr)	F	SP
LST	2	8	0,25	PA
TST	53	132	0,40	ARA
HST	3	11	0,27	AP
FSST	24	149	0,16	D
LST to HST	58	151	0,38	(A)

Table 3.2: Systems tracts and avulsion frequency. ST = Systems Tracts (LST = Lowstand ST; TST = Transgressive ST; HST = Highstand ST; FSST = Falling Stage ST); NE = total number of events; D (kyr) = total duration (kyr); F = avulsion frequency (kyr^{-1}); SP = stacking pattern (P = progradation; A = aggradation; R = retrogradation; D = degradation).

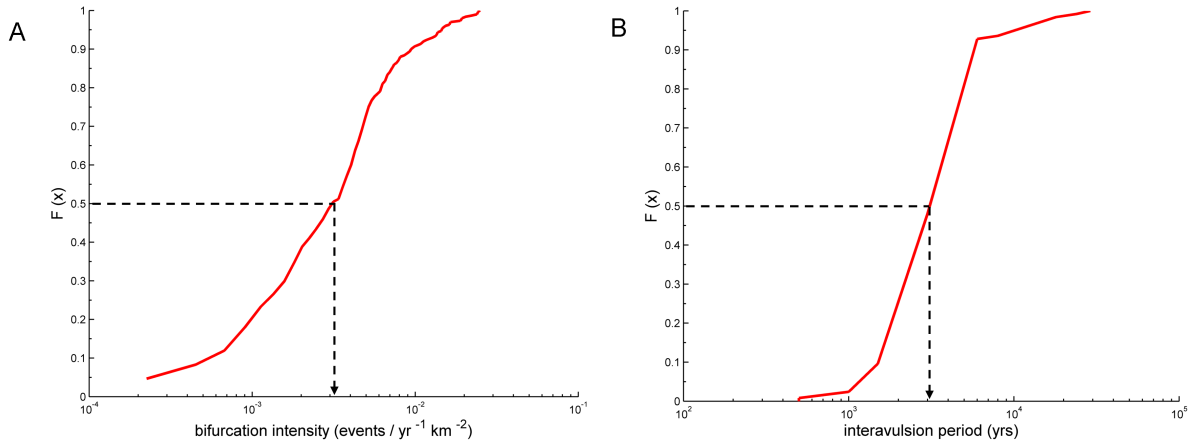

Figure 3.6: Cumulative distributions of: (A) bifurcation intensities and (B) inter-avulsion periods of major avulsions. Median values are indicated by black lines.

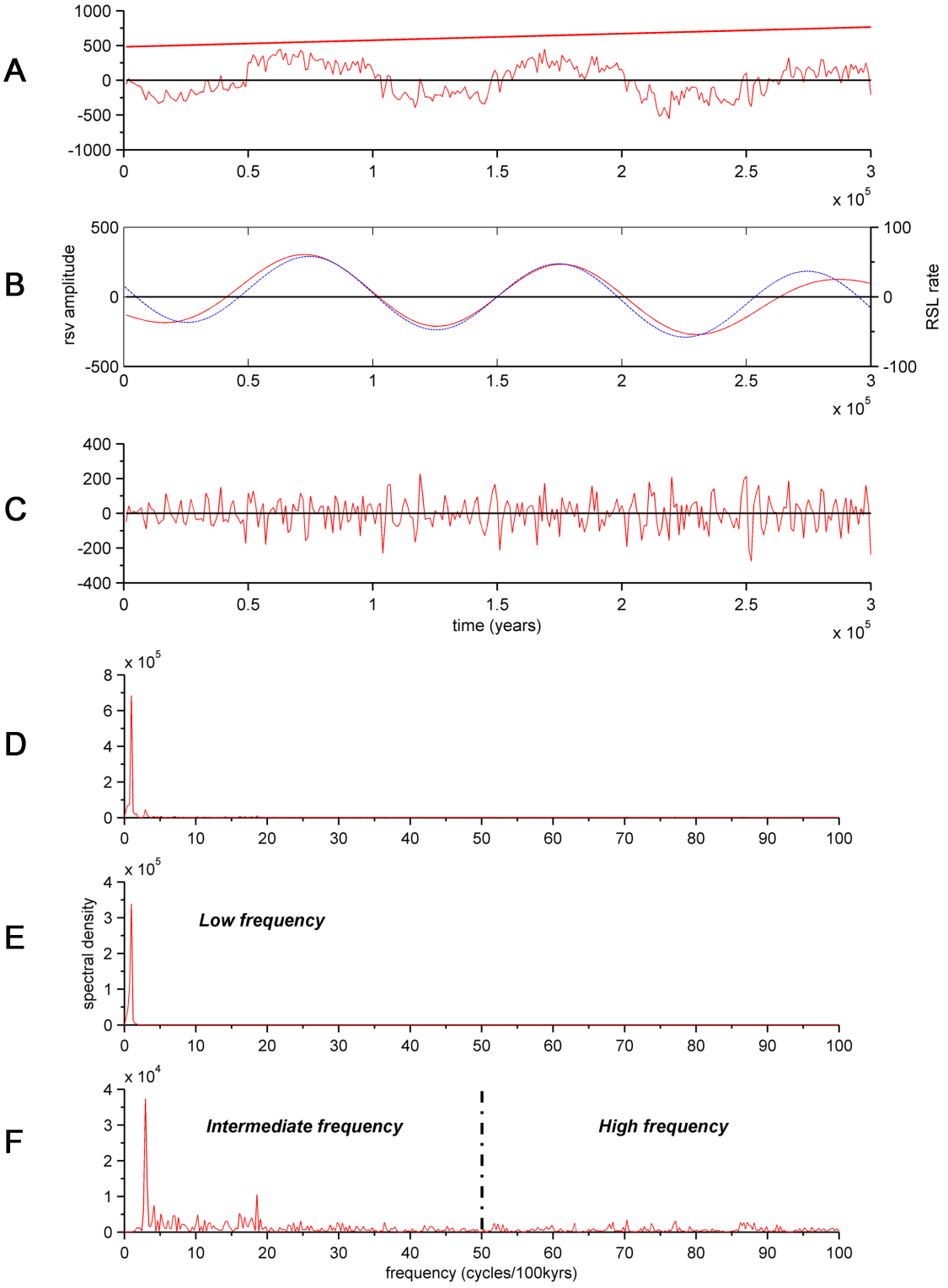

Figure 3.7: Processing of regional stratigraphic variability (base case). (A) Linear trend of rsv (red) and detrended signal in time domain. (B) Low-pass rsv and rate of sea level change (blue) in time domain. (C) high-pass rsv in time domain. (D) FFT of detrended rsv. (E) FFT of low-pass rsv. (F) FFT of high-pass rsv.

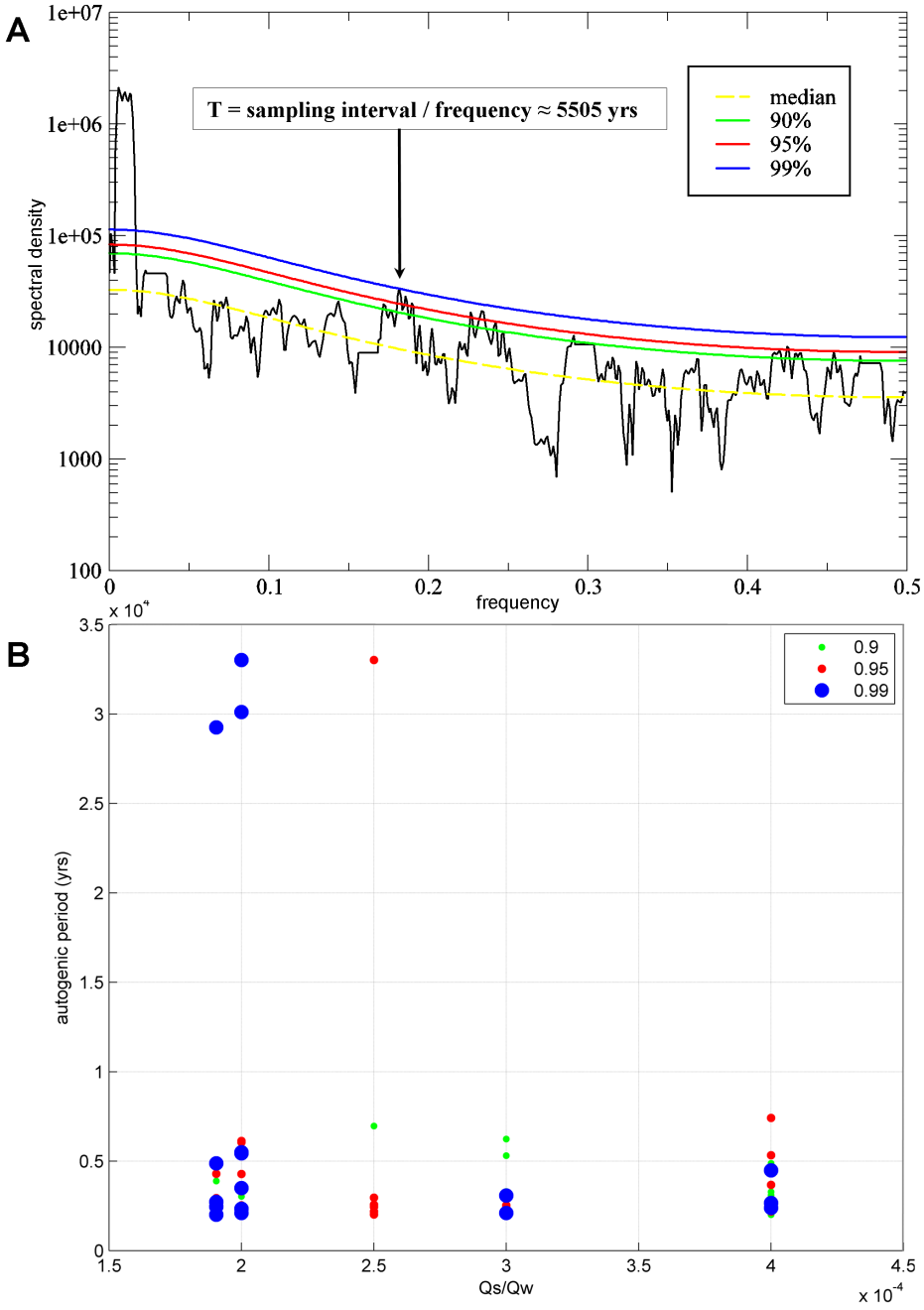

Figure 3.8: Spectral analysis of the rsv signal with the multi-taper method. (A) Spectral estimation of base-case scenario with confidence levels (90%, 95% and 99%). Black arrow indicates peak frequency exceeding 99% confidence level. (B) Significant periods plotted against Q_s/Q_w ratio.

The limited range of experimental conditions represented by our set of experiments does not warrant broad generalisations about the behaviour of the system under changing boundary conditions. Application of our results to the real world would have to be restricted to fluvial-

dominated deltas, because we did not take into account coastal dynamics. We expect that the influence of waves and tides in a receiving basin will manifest itself in various ways. Waves and associated longshore transport inhibit the formation of mouth bars and hence will reduce the bifurcation intensity, resulting in delta fronts with fewer distributaries. Wave resuspension will also reduce the rate of progradation, because fine-grained sediments are carried offshore and only the coarse-grained fraction of the sediments remains at the delta front. The SimClast model does not employ the concept of morphodynamic backwater (Jerolmack and Swenson, 2007; Edmonds et al., 2009) and we may therefore expect that the frequency of major avulsions will not be affected by the wave climate. Tidal currents are expected to have similar effects on bifurcation intensity, because they similarly rework mouth bars into longitudinal channel bars, but they also govern local accumulation of fine-grained sediments in estuaries by flocculation, so their net effect is more difficult to predict. Waves and tides will also exert a major influence on preservation of shelf deposits through formation of ravinement surfaces (Catuneanu and Zecchin, 2013). Extensive wave reworking during relative sea-level cycles may even out the signature of compensational stacking and reduce our capabilities to reconstruct the interplay of allogenic and autogenic forcing from the stratigraphic record, analogous to the shredding of environmental signals in river systems (Jerolmack and Paola, 2010). Lacustrine deltas are therefore the prime targets for investigating the interplay of allogenic and autogenic forcing on stratigraphy.

3.4.3 Real-world stratigraphy

Fluvial-dominated Quaternary systems such as the Deweyville units in Texas (present at places along Guadalupe, Nueces, Jacinto, Trinity, Neches, and Sabine Rivers) and the lower Mississippi River, as well as the Rhine-Meuse system, display stratigraphic patterns that appear to be quite similar to our modelling results. Periods of relative sea-level fall are marked by local incision and coeval deposition on the alluvial plain, and formation of amalgamated sandy fluvio-deltaic units in a falling-stage wedge (Törnqvist et al., 2000; Blum and Aslan, 2006; Blum et al., 2013). This field evidence confirms earlier conceptual models of aggradation during relative sea-level fall (Emery and Myers, 1996), and draws attention to the strongly diachronous nature and complicated genesis of the Sequence Boundary (Kyrkjebø et al., 2004; Holbrook and Bhattacharya, 2012; Blum et al., 2013; Burgess and Prince, 2015). Figure 3.4A shows that aggradation and degradation on the alluvial plain go hand-in-hand while relative sea level is falling. The same message can be deduced from Figure 3.5, which shows that major avulsions are still taking place in the early falling stage. However, the average frequency of major avulsions during deposition of the FSST is much lower

than the frequencies recorded during deposition of the other systems tracts (Table 3.2). From a purely geometric point of view, the extent of aggradation during relative sea-level fall is controlled by the gradient of the shelf relative to the gradient of the river profile upstream of the highstand shoreline, and by the amplitude of the relative sea-level fall in the presence of a shelf break. Application of such concepts to the real world is not straightforward, because the response of the sedimentary system will also depend on the covariance of changes in relative sea level and climate during glacio-eustatic cycles, which govern the liquid and solid discharges of river systems and directly affect their stratigraphic responses. Despite these potential problems, the inferred behaviour of ancient systems (e.g. the Cretaceous 'Notom' and 'Last Chance' delta complexes of the Cretaceous Ferron Sandstone, Utah and the Cisco Group, north-central Texas) with fluvial-dominated delta fronts in their palaeo-transfer valleys appears to be consistent with our numerical experiments (Yang et al., 1998; Garrison et al., 2006; Li et al., 2011, Zhu et al., 2012).

3.5 Conclusions

A straightforward measure of overall stratigraphic variability has been defined and post-processing of synthetic fluvio-deltaic stratigraphy by various methods has allowed us to explain its behaviour in terms of allogenic forcing and autogenic processes. This study has shown that autogenic processes occurring in fluvio-deltaic systems are modulated by allogenic forcing, and therefore, the dominant types of autogenic process contributing to stratigraphic variability vary systematically throughout an accommodation-to-supply cycle (Fig. 3.9).

Low-frequency regional stratigraphic variability (*rsv*) as defined in this study correlates strongly with the rate of sea-level change and is thus allogenically induced. Minima of *rsv* are recorded during periods of forced regression, whereas maxima of *rsv* correspond to periods of transgression. More specifically, allogenic forcing governs the relative contributions of two classes of autogenic processes to the intermediate-to-high frequency bands.

The intermediate-frequency band of regional stratigraphic variability corresponds to major avulsions >5km from the coastline with a median inter-avulsion period of ~3 kyr. The frequency of this autogenic process is modulated by the low-frequency allogenic signal. Our results suggest that increasing the ratio of solid to liquid discharge shifts the intermediate component of variability to higher frequency domains.

The high-frequency band of regional stratigraphic variability is associated with partial or small-scale avulsions (<5km from the coastline) and mouthbar-induced bifurcations occurring at the

terminal parts of the sediment dispersal system. The bifurcation intensity is also modulated by the low-frequency allogenic signal, and varies throughout an accommodation-to-supply cycle in proportion to the rate of regression (progradation). In view of its small contribution to overall stratigraphic variability (as defined in this study), and the small spatial scale at which it is likely to manifest itself in the stratigraphic record, it may be regarded as autogenic noise.

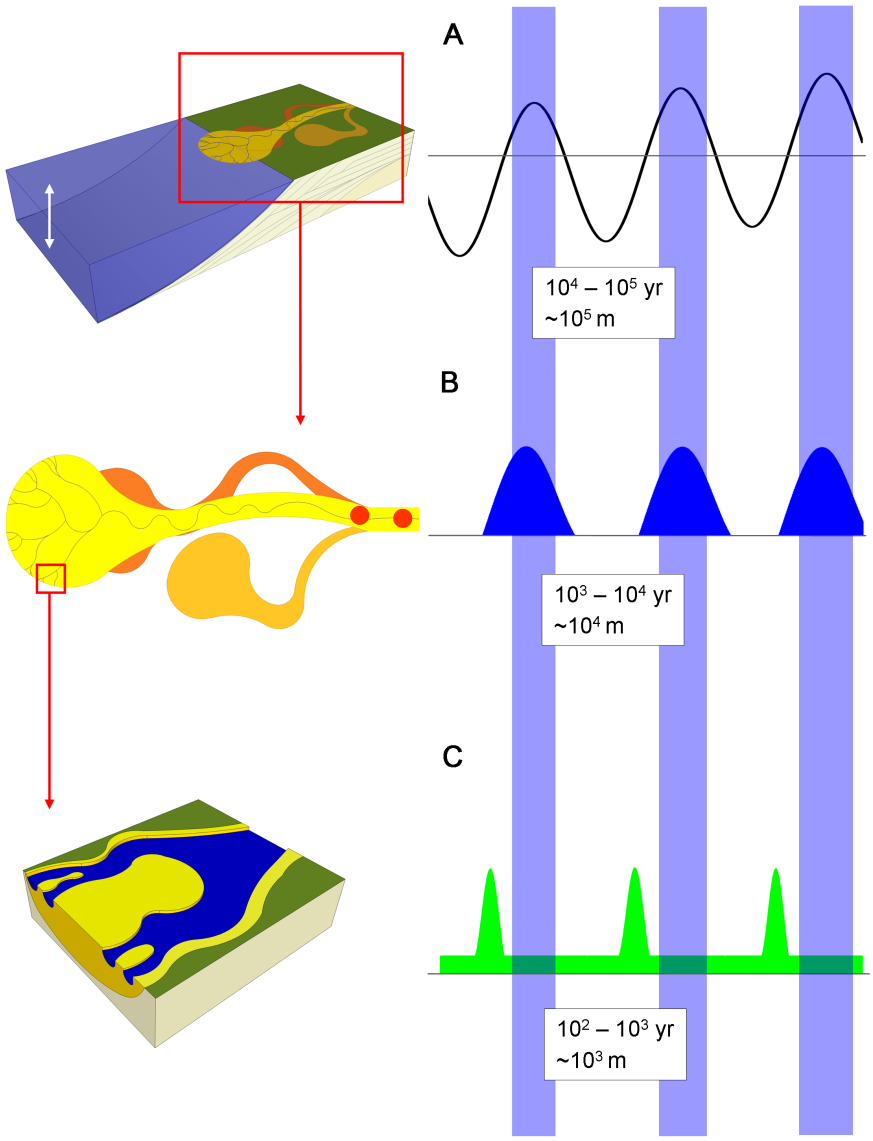

Figure 3.9: Conceptual model of spatio-temporal scales of stratigraphic variability in fluvio-deltaic systems. Light-blue bands correspond to TSTs. (A) Rate of sea-level change acts as allogenic modulator of autogenic variability at the system scale. (B) Frequency of major avulsions peaks in the TST and is zero in the late FSST. (C) Frequency of mouthbar-induced bifurcations occuring at the terminal part of the sediment dispersal system peaks in the late FSST and is much lower throughout the rest of the sequence.

The three characteristic time/space scales of the phenomena recognized in our synthetic stratigraphic record provide guidelines for predicting fluvio-deltaic stratigraphy in the context of co-existing autogenic and allogenic processes. The allogenic component is of high predictive value for sequence-stratigraphic studies that encompass the architectural arrangement of systems tracts and their bounding surfaces. The autogenic components of variability are relevant to reservoir-scale architecture studies (e.g. connectivity analysis). A better understanding of the relative importance of allogenic and autogenic processes is needed to develop an internally consistent multi-scale approach to stratigraphic prediction. Future efforts should focus on adapting our approach to analysis of synthetic stratigraphy to tackle real stratigraphic data (e.g. seismic cubes). We consider lacustrine deltas the most favourable targets for testing models of allogenically modulated autogenic variability.

Chapter 4

High-resolution sequence-stratigraphic architecture of fluvio-deltaic systems: inferences from the automated extraction of chronosomes [3]

Abstract

Multiscale simulation of fluvio-deltaic stratigraphy has been used to quantify the geometry and architectural arrangement of subseismic-scale fluvial-shelf sedimentary segments. We conducted numerical experiments of fluvial-shelf evolution by simulating accommodation-to-sediment-supply (A/S) cycles of varying wavelength and amplitude with the objective to produce 3-D stratigraphic records. A stack data structure was designed and implemented to analyze stratigraphic variability. The analysis permitted to extract chronostratigraphically constrained lithosomes (or chronosomes) and to quantify large-scale depositional connectivity throughout an A/S cycle. Chronosomes formed under conditions of channel-belt aggradation are systematically separated by abandonment surfaces associated with major avulsions. Late falling stage chronosomes demonstrate distinct architectural differences because they form when the coastline drops below the inherited shelf break in the absence of major avulsions. The earliest and late falling stage chronosomes demonstrate the highest large-scale depositional connectivity in proximal and distal areas, respectively. Lowstand and early transgressive chronosomes show moderate connectivity in medial and distal areas. Detailed investigation of the falling stage systems tracts showed that the spatial continuity of chronosomes may be disrupted by higher-frequency A/S cycles to produce 'stranded' coarse-grained segments. Lower-amplitude base level changes, representative of

[3] Based on: Karamitopoulos, P., Weltje, G.J., Dalman, R.A.F., in review. Process stratigraphy of fluvio-deltaic systems: inferences from numerical simulation and the automated extraction of chronosomes. Basin Research.

greenhouse periods, increase the magnitude of delta-lobe switching (M_{DLS}) and favor the development of system-wide abandonment surfaces, whose expression in real-world stratigraphy is likely to reflect the intertwined effects of high-frequency astronomical forcing and differential subsidence. Our approach allows quantification of sub-seismic sedimentary heterogeneity of fluvial-shelf deposits in a sequence stratigraphic framework and provides a coherent predictive model of lithofacies distribution throughout full A/S cycles.

4.1 Introduction

Fundamental notions of sequence stratigraphy resulted from observations of conspicuous patterns on continental-margin seismic lines (Payton, 1977; Mitchum et al., 1977; Vail et al., 1977). In this context, seismic reflection events are interpreted to outline basin-fill segments whose architectural arrangement is regulated by base level changes. This perspective has forged a series of two-dimensional sequence stratigraphic models which have been customarily used to subdivide sedimentary sequences into genetically related units aiming at landward and basinward prediction of lithological composition (Galloway, 1989; Posamentier and Vail, 1988; Hunt and Tucker, 1992; Wright and Marriott, 1993; Shanley and McCabe, 1994; Embry, 1995; Posamentier and Allen, 1999; Plint and Nummedal, 2000; Neal and Abreu, 2009). Due to the fact that these models are qualitative and cannot be easily verified, there exists a genuine need to: a) expand sequence stratigraphic analysis to three dimensions, b) provide quantifiable information regarding the system states and processes acting throughout an accommodation to sediment supply (A/S) cycle, c) accurately estimate net sediment accumulation rates and d) perform robust correlation analyses between sedimentation rate and the duration of sedimentary units in order to improve subsurface property prediction (Griffiths and Nordlund, 1993; Griffiths, 1996; Emery and Myers, 1996; Muto and Steel, 1997, 2004; Ritchie et al., 2004a, b; Catuneaunu et al., 2009; Bhattacharya, 2011; Holbrook and Bhattacharya, 2012; Karamitopoulos et al., 2014; Martinius et al., 2014; Miall, 2014; Tipper, 2015, 2016; Burgess, 2016; Hampson, 2016; Madof et al., 2016; Muto et al, 2016). Multi-scale simulation of fluvio-deltaic stratigraphy (SimClast: Dalman and Weltje, 2008, 2012) allows attaining the level of detail required to address each of these issues. Stratigraphic variability was analyzed by breaking down sedimentary A/S cycles (sequences) at the level of high-resolution fluvio-deltaic depositional units or chronosomes. The latter consist of channel-belt and delta-lobe sediments deposited in temporal continuity at a specific location within the basin (Schulz, 1982; Dalman et al., 2015).

4.2 Methods

4.2.1 Model description and experiments

A basin-scale numerical model of river-shelf evolution (Meijer, 2002) combined with a sub-grid parameterization of fluvio-deltaic processes and stratigraphy (SimClast: Dalman and Weltje, 2008, 2012) was used to obtain synthetic sedimentary sequences under the influence of time-variant external forcing in the form of sea-level cycles on a uniformly-subsiding (0.1 mm/yr) passive margin-adjacent topography (50×100 km) with grid cell size of 1×1 km (Fig. 4.1). Sedimentary processes relevant for this study are included by sub-grid parameterization of avulsions and mouthbar-induced bifurcations. Avulsions occur as a consequence of channel belt aggradation and increases in channel-belt elevation, whereas mouthbar-induced bifurcations dominate the terminal parts of the sediment dispersal system where delta lobes grow and topographic gradients are extremely low.

The initial topographic surface for all simulations was defined by running the model for 20 kyr under time-invariant forcing (Fig. 4.1A). Throughout the simulations, constant water discharge ($Q_w = 5{\times}10^9\ m^3/yr$) and sediment input ($Q_s = 1{\times}10^6\ m^3/yr$) (sand/clay ratio = 0.2) entered the transfer valley via a single-entry point (Fig. 4.1A). Two sets of numerical experiments were performed (Table 4.1): the first set consisted of 200-kyr model runs using low- and high-amplitude sea-level cycles representative of greenhouse and icehouse periods, respectively (Fig. 4.1B, green and blue curves, respectively) (Miller et al. 2005a). The second set consisted of 100-kyr model runs with a one phase sea-level fall and rise, and a scenario with a higher frequency signal (25 kyr periodicity) superimposed (Fig. 4.1C, blue and red curves, respectively). The former set of experiments aimed at quantitative description of channel network and stratal architecture as a function of fixed topography and base level changes, whereas the latter focused on the architectural arrangement of the falling stage systems tracts. In order to handle uncertainty, ten equiprobable realizations were obtained from base case scenario (RC1) by random perturbations to the initial surface.

Throughout the model runs, the net sediment accumulation record ($d(t_k)$) was stored in dynamic arrays so as to register deposition ($d(t_k)>0$), erosion ($d(t_k)<0$) and stasis ($d(t_k)=0$) for every grid cell throughout the simulation. A grid cell in stasis (which does not change its elevation) is in bypass if the site is occupied by an active channel or starved if the grid cell is far away from the active channel (Tipper, 2000, 2015). In order to maximize the preservation potential of modeled delta-

topset areas, all simulations were run in the absence of differential subsidence, coastal processes and bank-stabilizing vegetation.

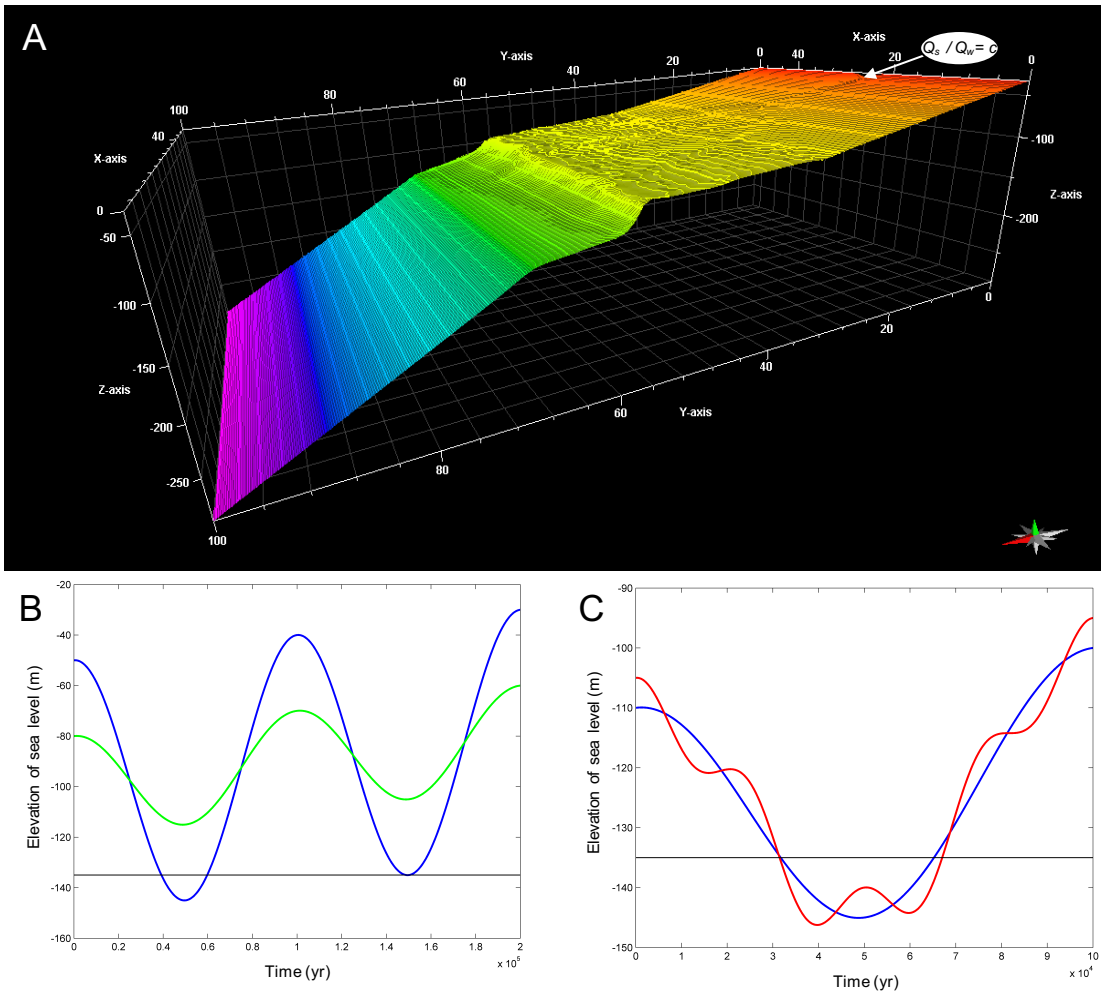

Figure 4.1: (A) Initial model topography and inflow point (white arrow); relative sea level curves of the first (B) and second set (C) of numerical experiments (black line in 1B indicates shelf break position). Scenario RC3 is the compound signal of RC3a and RC3b (see Table 1 for details).

Scenarios	Wavelength (kyr)	Amplitude (m)	Duration (kyr)
RC1 (Base Case)	100	50	200
RC2	100	15	200
RC3a	100	15	100
RC3b	25	10	100

Table 4.1: Input characteristics of reference base-level curves.

4.2.2 Post-processing

A stack data structure was designed to load synthetic stratigraphy (net sediment accumulation) in dynamic arrays (Fig. 4.3). The algorithm implements sequentially a series of post-processing methods, including: a) constrained cubic spline interpolation of cumulative net sediment accumulation, b) a first order central difference operator for the approximation of net sediment accumulation rates and c) a binary transformation and thresholding of the estimated rates. Finally, a cellular automaton simulation algorithm was used to outline the boundaries of the delta lobe chronosomes. An in-depth description of these methods follows in Appendix A.

The dominant channel branches and their associated major avulsion sites occurring more than 5 km from coastline were extracted using the method described in detail by Karamitopoulos et al. (2014). In addition, we estimated the Euclidian distance of the river mouth shift punctuated by a major avulsion, named here magnitude of delta-lobe switch (M_{DLS}). This metric is indicative of the impact of the major avulsions across the coastline (Fig. 4.2).

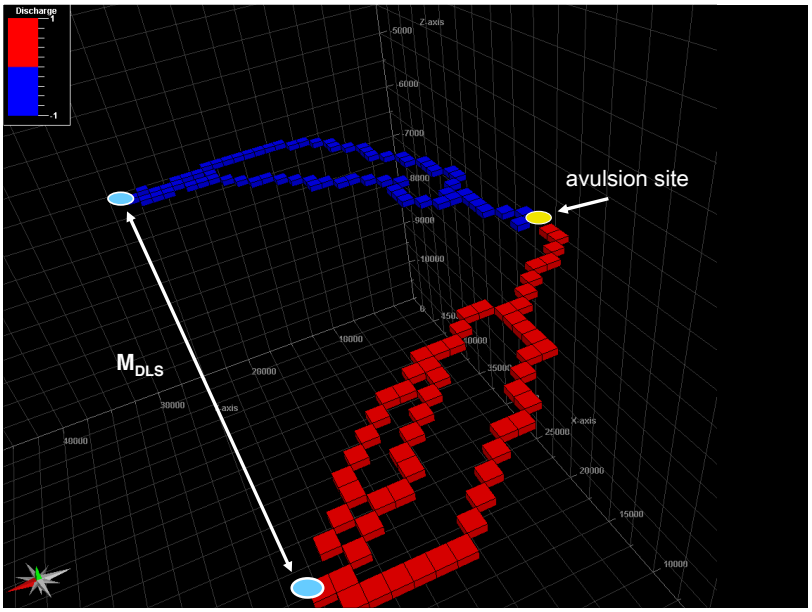

Figure 4.2: Channel network and major avulsion site (>5km from coastline) automated extraction. Red and blue grid cells correspond to abandoned and active channel respectively (modified from Karamitopoulos et al., 2014). Magnitude of delta-lobe switch (M_{DLS}) corresponds to river mouth shift distance at the coastline.

Large-scale depositional connectivity is quantified in this study by the total number of grid cells determined by the final states of the cellular automata post-processing operation (see Appendix A for further details). The metric is representative of the strike and longitudinal continuity of fluvio-deltaic chronosomes.

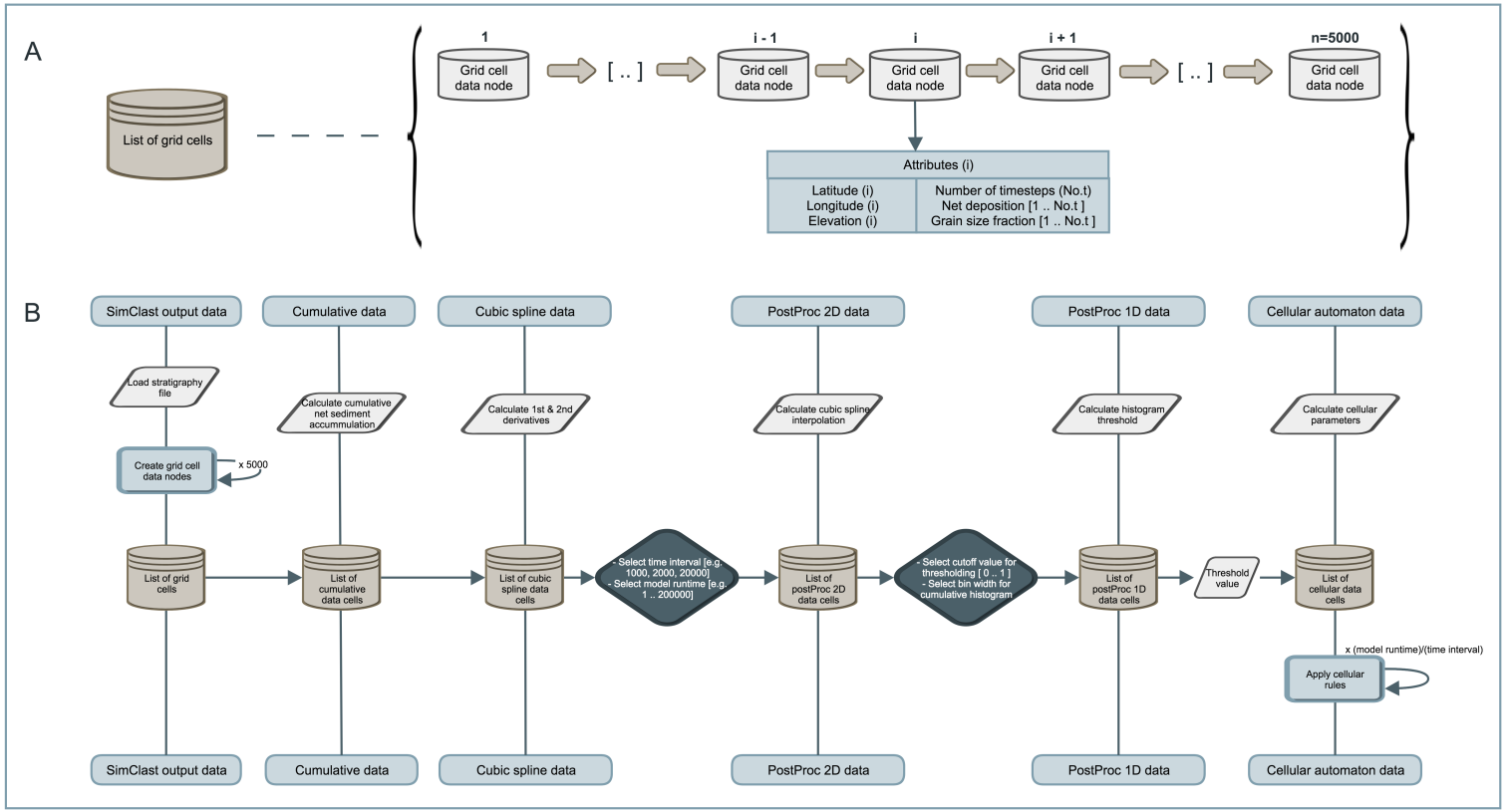

Figure 4.3: Flowchart illustrating the implementation of post-processing routine: (A) list of grid cells linked in a dynamic array structure; (B) generalized post-processor data flow. See appendix for full discussion.

4.3 Results

4.3.1 Systems tracts

The stratigraphic record of the base case scenario (RC1) was subdivided into systems tracts using the conventional two-dimensional sequence stratigraphic concepts (Frazier, 1974; Vail, 1987; Posamentier and Vail, 1988; Posamentier et al., 1988; Van Wagoner et al., 1988; Galloway, 1989; Hunt and Tucker, 1992; Emery and Myers, 1996; Helland-Hansen and Martinsen, 1996; Posamentier and Allen, 1999; Plint and Nummedal, 2000). In order to apply these concepts in three dimensions we assumed that sequence stratigraphic surfaces (with the exception of the sequence boundary) are considered to be system-wide isochronous surfaces separating sedimentary packages that have on average different stacking patterns longitudinally. In real-world stratigraphy, the three-dimensional (along-strike) expression of the latter surfaces will record a certain degree of diachroneity depending on differential subsidence and locally varying sediment supply rates (Catuneanu et al., 2009; Madof et al., 2016).

Maxima and minima of the estimated non-dimensional shoreline ratio curve (ratio of marine to non-marine grid cells) correspond to the ages of maximum flooding (MFS) and maximum regressive surfaces (MRS), respectively (Fig. 4.4, 4.5A). The ages of the basal surface of forced regression (BSFR) and correlative conformity (CC, sensu Hunt and Tucker, 1992) correspond to the highest and lowest values of the base level curve, respectively. These four chronostratigraphic surfaces allow us to firstly make a low-resolution sequence subdivision into the falling stage (FSST), lowstand (LST), transgressive (TST) and highstand (HST) systems tracts (Fig. 4.4) (Plint and Nummedal, 2000).

4.3.2 High-resolution sequence subdivision

Post-processing of the net sediment accumulation records ($d(t_k)$) was used to extract previously active delta-lobe chronosomes by estimating net sediment accumulation rates over 1 kyr time intervals (Fig. 4.5A) (see Appendix A for more details). The paleo-discharge network output was used accordingly to extract the dominant active channels throughout basin-fill evolution (Fig. 4.7A). The extraction of the dominant channels enables us to detect the downdip and strike coordinates of major avulsion sites (Fig. 4.6A) as well as their distribution in the Wheeler domain

(Fig. 4.6B). The latter figure clearly illustrates that the magnitude of a delta-lobe switch varies throughout the A/S cycle of the base case scenario.

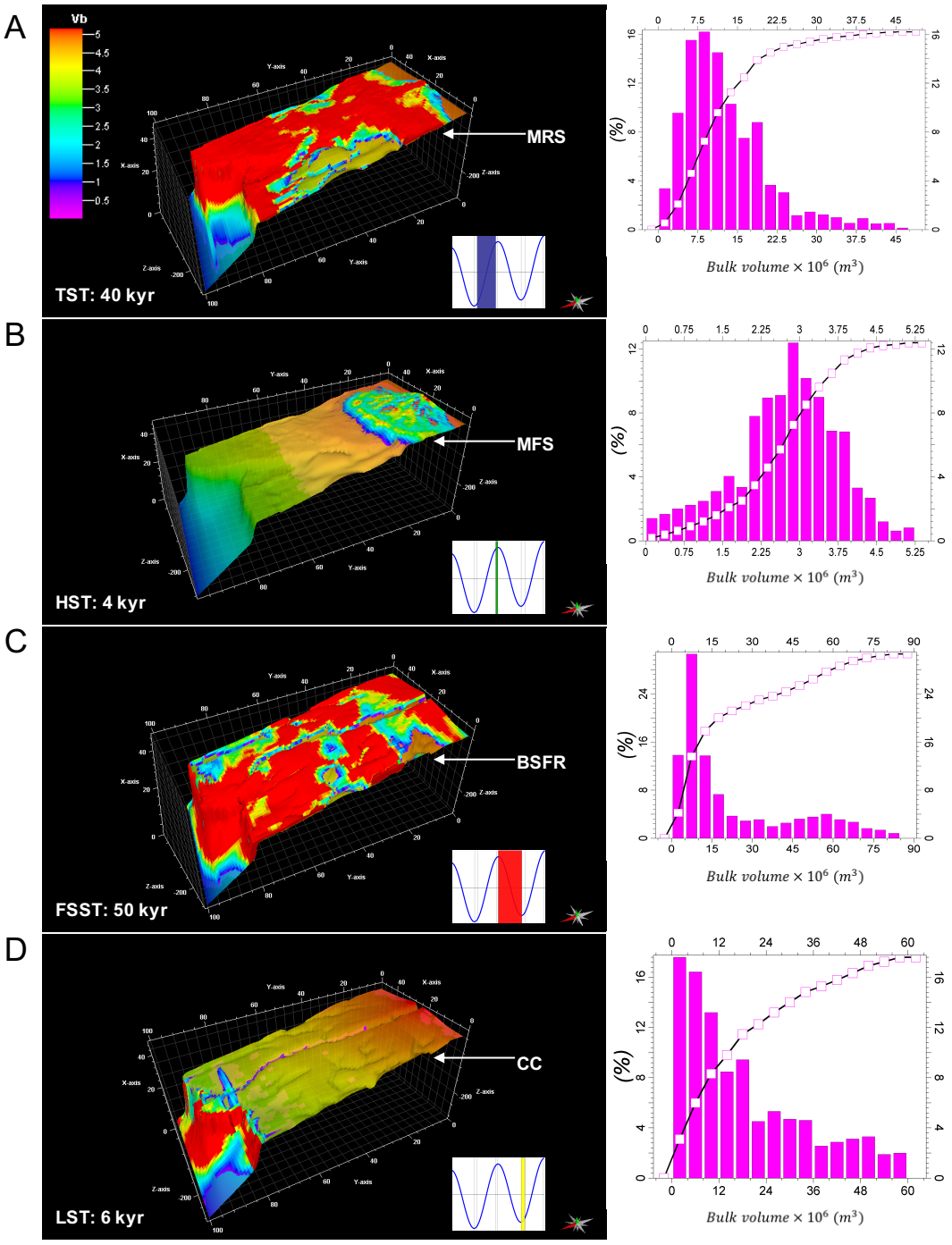

Figure 4.4: Systems tracts (in depth), histograms and cumulative histograms of sedimentary bulk volume (Vb): (A) transgressive systems tract (TST); (B) highstand systems tract (HST); (C) falling stage systems tract (FSST); (D) lowstand systems tract (LST).

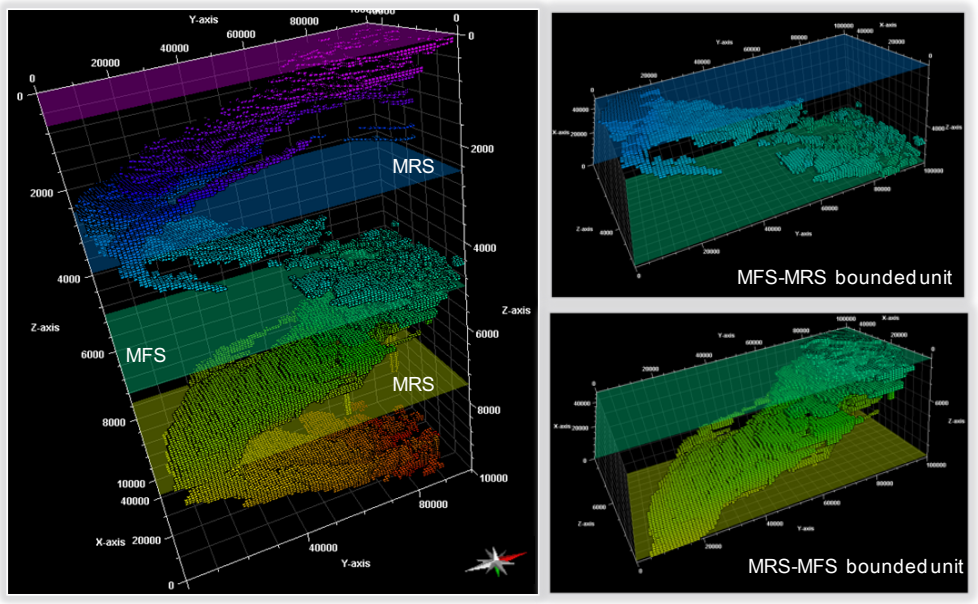

Figure 4.5: High-resolution sequence subdivision in space-time (Wheeler) domain using: automatically extracted chronosomes (1kyr resolution) (inverted).

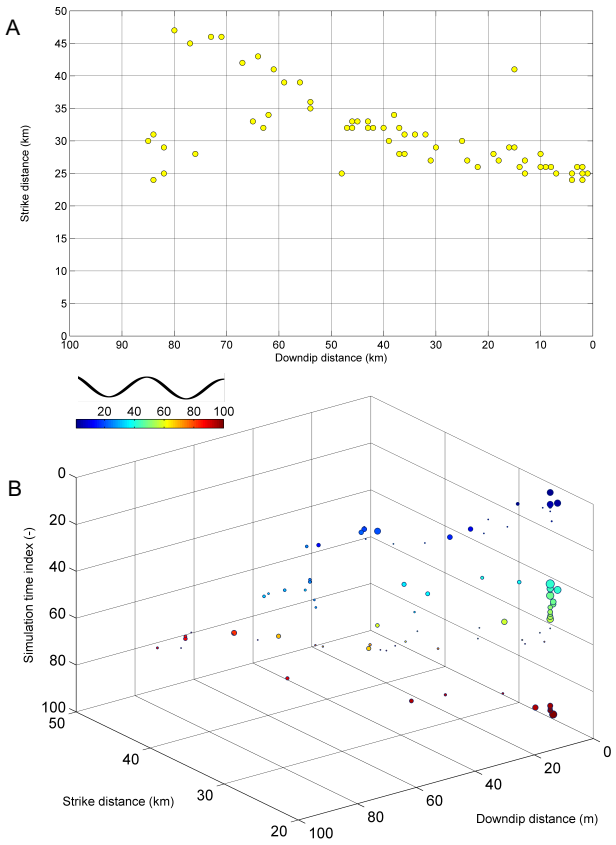

Figure 4.6: (A) Downdip and strike coordinates of major avulsion sites and (B) space-time (Wheeler) domain. The size of dot marker is indicative of the size of the estimated M_{DLS} values for base case scenario (RC1). The lower the simulation time index the younger the instance of a major avulsion occurrence.

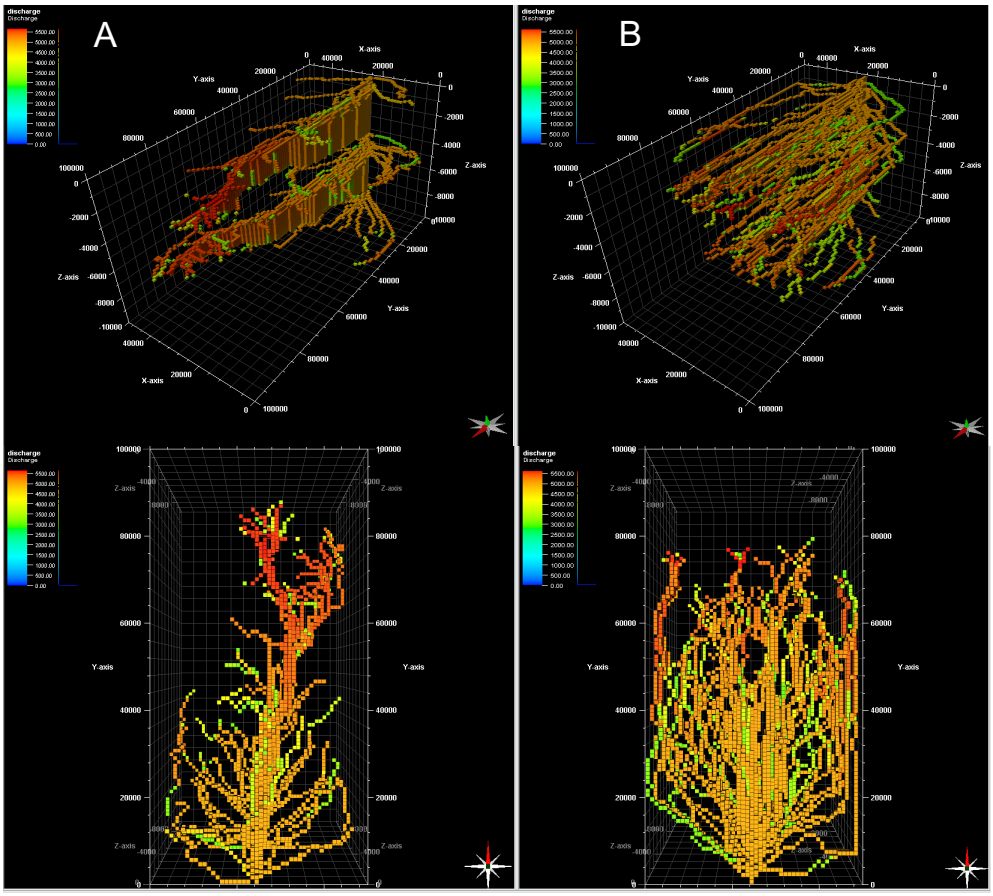

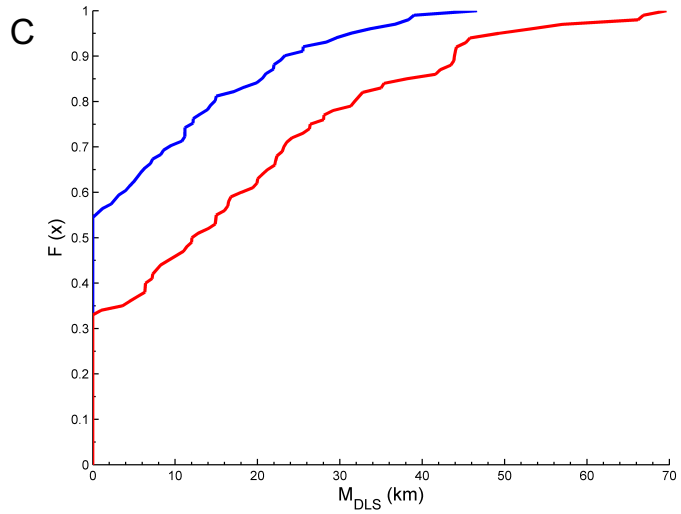

Figure 4.7: Development of channelized drainage network (2kyr resolution) exceeding a threshold value of 3 x 10^9 m^3yr^{-1}. Aside and top views of channelized drainage network of: (A) base-case ('icehouse') and (B) low- amplitude ('greenhouse') experiments. (C) Cumulative distributions of M_{DLS} for base case (blue) and low-amplitude (red) experiments.

4.4 Discussion

4.4.1 Morphodynamic evolution

The architecture of fluvial, delta-plain and cross-shelf sedimentary segments is governed by the relative position of the river mouth at the shoreline and the shelf-break exposure to subaerial processes. This is consistent with previous field, experimental and numerical studies concerned with the origin, formation and architectural arrangement of fluvial-shelf stratal units (Blum and Aslan, 2006; Holbrook et al., 2006; Strong and Paola, 2008; Martin et al., 2009; Blum and Hattier-Womack, 2009, Blum at al., 2013). High rates of base-level change as in the base case scenario, which represents icehouse periods, expose the shelf-break during late falling stage and initiate a phase of fixed drainage marked by incision and lack of major avulsions (Karamitopoulos et al., 2014, Fig. 4.7A). In real-world systems, the increased sediment discharge during late falling stage by the merging of adjacent drainage areas (Blum et al. 2013) will contribute to the high rate of progradation of late falling-stage chronosomes.

Conversely, low-amplitude sea-level change, representative of greenhouse periods (Fig. 4.1B: green curve), prevents shelf-break emergence during relative sea-level fall and hence the inherited topography (i.e. river and shelf gradients, shelf width) and the rate and amplitude of the A/S cycle regulate channel network evolution. This morphodynamic pattern favors residence of large sediment volumes along a limited shelf width range (both at highstand and lowstand coastlines) which may be remobilized by coastal processes to give massive accumulation of slope and basin-floor sediments (Posamentier and Kola, 2003, Blum and Womack, 2009, Somme et al., 2009, Blum et al., 2013, Gong et al., 2015, Sweet and Blum, 2016). Major avulsions with relatively large river mouth shifts dominate the entire sequence, in contrast with the icehouse pattern (Fig. 4.7A, 4.7B). Such low-amplitude base-level changes increase the magnitude and frequency of delta-lobe switches (M_{DLS}) (Fig. 4.7B, 4.7C).

4.4.2 Avulsion-based sequence subdivision and late FSST

Previous outcrop- and seismic-based studies have illustrated the offlapping and downlapping of stratal packages interpreted to be the product of a descending shoreline trajectory during the late falling stage of the A/S cycle (Plint and Nummedal, 2000; Neal and Abreu, 20009; Fielding, 2010; Li et al., 2011; Zhu et al., 2012; Fielding, 2015). The formation of the falling stage systems tract occurs during the time marked by the basal surface of forced regression and the surface marked by

the lowest point on the relative sea-level curve (correlative conformity sensu Hunt and Tucker, 1992), and thus corresponds in duration to the maximum stratigraphic gap represented by the composite sequence boundary (Fig. 4.8B). The abrupt decrease of major avulsions, which roughly coincides with the timing of shelf-break exposure, may be used to separate early from late falling stage deposits (Fig. 4.6, 4.8B). Owing to the relative absence of major avulsions, the architectural arrangement of late FSST chronosomes is fundamentally different (Fig. 4.8B). In contrast, delta-lobe units formed under conditions of channel-belt aggradation (i.e. lowstand, transgressive, highstand, early falling stage) may be subdivided into units bounded by delta-lobe abandonment surfaces associated with major avulsions (Fig. 4.8B, 4.8C) (Karamitopoulos et al., 2014; Dalman et al., 2015). These high-frequency units represent chronostratigraphically constrained lithosomes, or chronosomes (Schultz, 1982) for short.

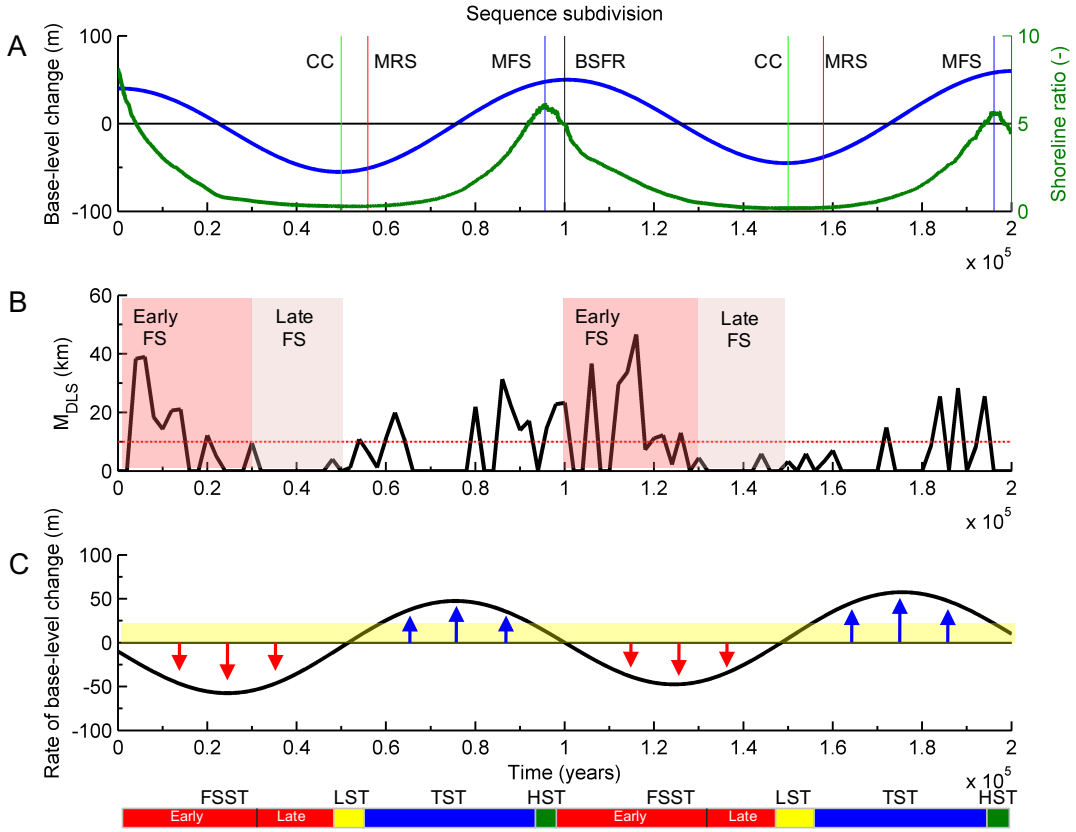

Figure 4.8: Sequence subdivision based on: (A) normalized relative sea-level (blue) and shoreline ratio (green) curves. Correlative conformity (CC) (green lines) and basal surface of forced regression (BSFR) (black line) surfaces were picked at the lowest and highest points on the relative sea-level curve. Similarly, red and blue lines mark times of maximum regressive and maximum flooding surfaces corresponding to the lowest and highest points on the shoreline ratio curve. (B) Extracted major avulsion sites for base case model. Timing and magnitude of M_{DLS} were used to differentiate between early and late falling stage systems tracts. Red dotted line corresponds to threshold of 10km along the coastline. (C) Rate of relative sea-level curve and schematic sedimentation rate (yellow). Inflection points on the curve indicate early and late stages of base-level rise (lowstand and highstand normal regressions respectively). Overview of low-resolution and avulsion-based sequence subdivision are shown at the bottom (modified from Catuneanu et al., 2009).

Precession-scale relative sea level fluctuations (25 kyr) superimposed on a full glacial-interglacial cycle (100 kyr) (Fig. 4.1C: red curve) may cause landward and seaward fluctuation of the mouthbar and shoreline areas and interrupt the net connection between fluvial distributary and beyond shelf-break sediments, causing fragmentation of the coarse units (Figure 4.9C). This stratigraphic response has been previously described as a 'stranded parasequence' by Plint and Nummedal (2000) and/or high-frequency cut and fill cycle (Zhu et al., 2012). Our simulations suggest that such 'stranded' sequences may represent the response to short episodes of stagnant or rising base level during an overall base-level fall.

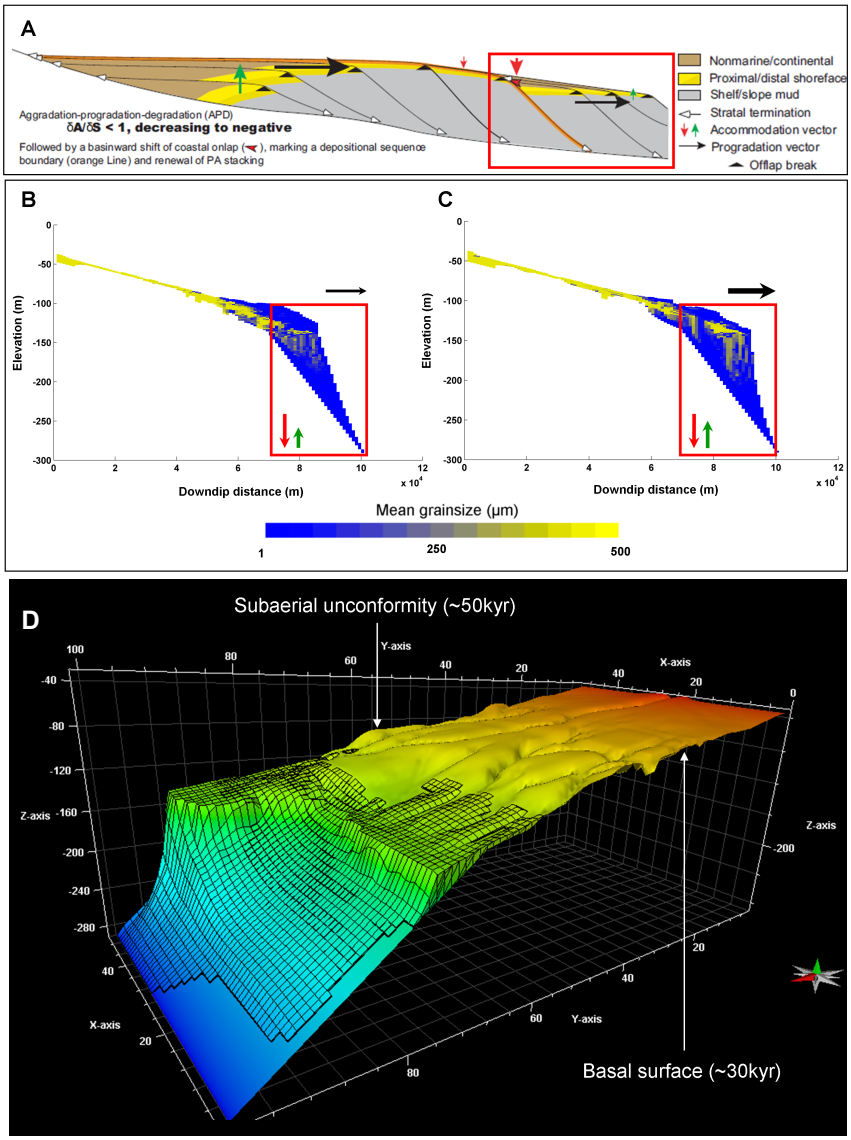

Figure 4.9: The falling stage systems tract: (A) idealized chronosome stacking pattern associated with changing A/S ratio (modified from Neal and Abreu, 2009). (B) and (C) Longitudinal central sections at a strike distance of 25 km for scenarios RC3a and RC3b, respectively. Note the isolated sandy units encased by fine-grained sediments form as a consequence of higher-frequency relative sea-level oscillation (D) Late falling stage chronosomes of scenario RC3a and bounding surfaces.

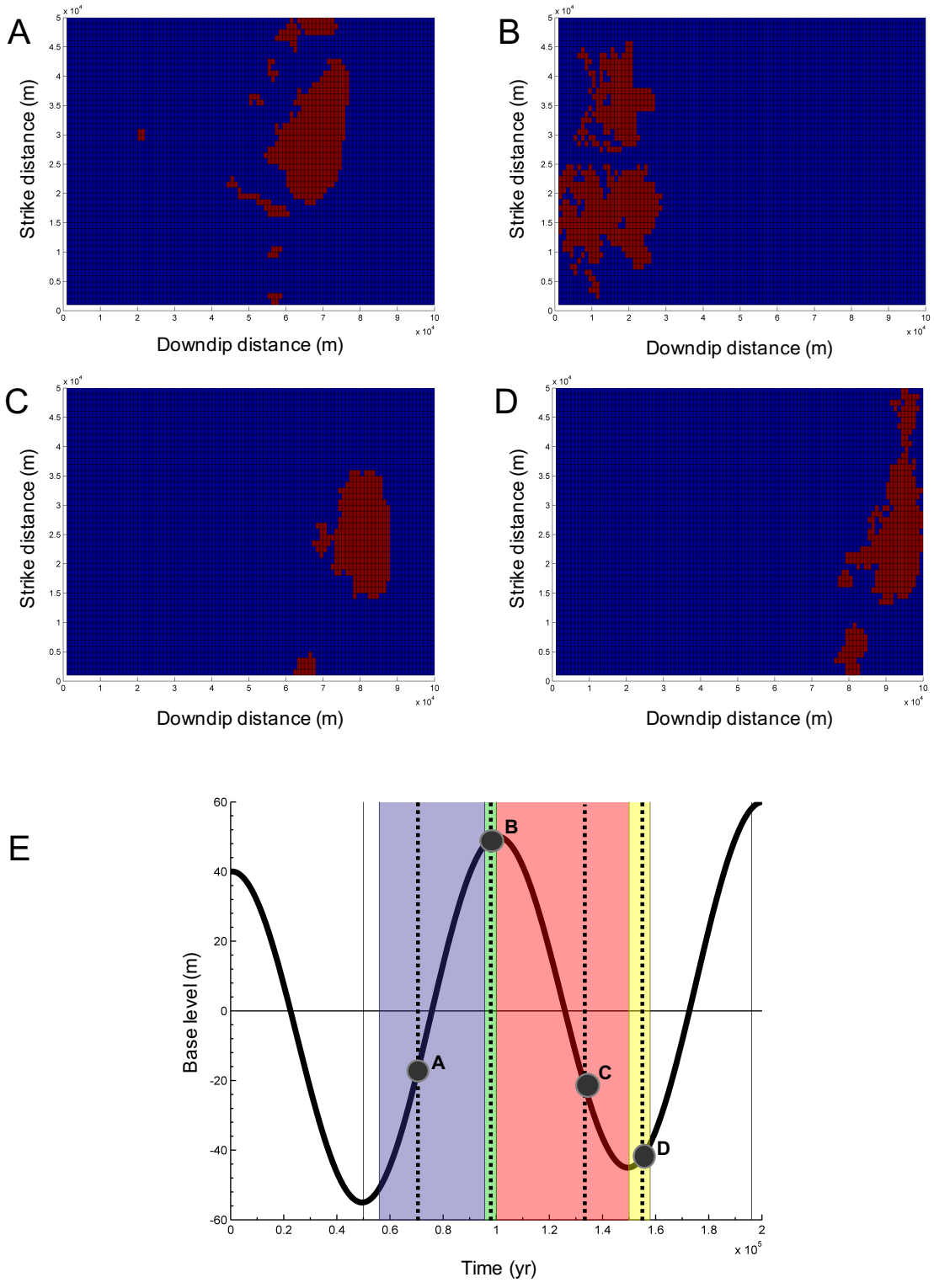

Figure 4.10: Examples of transgressive (A), (B) and regressive (C), (D) delta lobes (2 kyr) extracted from the base-case experiment. Black curve corresponds to the normalized base-level change.

4.4.3 Patterns of large-scale depositional connectivity

Large-scale depositional connectivity is quantified in this study by the total number of grid cells in the chronosomes as determined by the final states of the cellular automata post-processing operation (Fig. 4.10) (see Appendix A for further details). The metric is representative of the strike and longitudinal continuity of the extracted delta lobe chronosomes. The earliest and late falling stage chronosomes demonstrate the highest large-scale depositional connectivity in the proximal and distal areas, respectively (Figure 4.11). Avulsion frequency is increased during periods of relative sea level rise as a consequence of the combined effect of auto- and allogenic aggradation, which decreases large-scale depositional connectivity. Lowstand and early transgressive chronosomes demonstrate moderate depositional connectivity which is amplified in the vicinity of the shelf break owing to higher back-fill rates in the major trunk channel and the adjacent topographic lows.

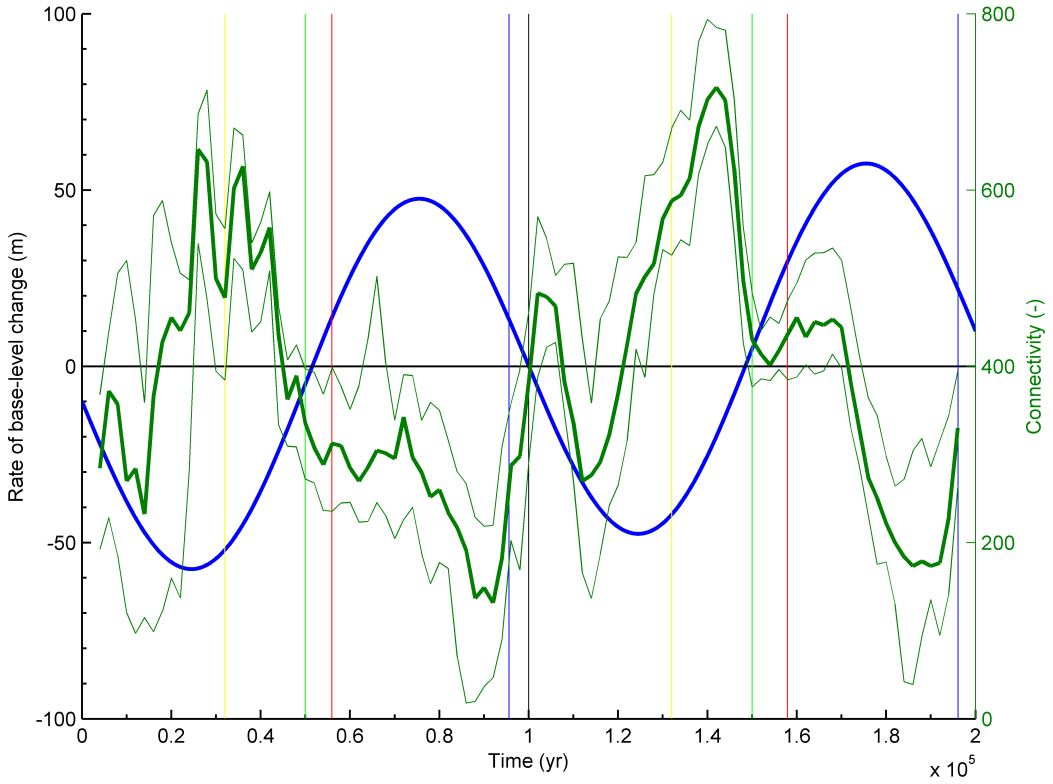

Figure 4.11: Median, P10 and P90 depositional connectivity (green lines in the middle, lower and upper parts respectively) and normalized rate of base-level change (blue) versus simulation time. Straight lines correspond to isochronous sequence stratigraphic surfaces as defined in this study (see text for further details).

4.5 Conclusions

The magnitude and frequency of delta-lobe switches varies throughout an A/S cycle. The stratigraphic expression of a delta-lobe switch marked by a major avulsion provides the key element for high-resolution avulsion-based subdivisions of fluvio-deltaic sequences into chronosomes. The timing of avulsion-induced abandonment surfaces in real-world stratigraphy will most likely be influenced by the intertwined perturbations of high-frequency astronomical forcing and differential subsidence. Late FSST deposits form in response to exposure of the shelf edge at the terminal parts of the incised-valley transfer system. The architectural arrangements of late FSST chronosomes, which develop during periods without major avulsions, are fundamentally different from those of the other chronosomes, which develop under conditions of (local) aggradation by means of rapid avulsion-induced depocentre shifts (Dalman et al., 2015). Metrics describing sedimentary heterogeneities in synthetic stratigraphy have been shown to increase the predictive capabilities of sequence stratigraphic interpretation at a sub-seismic scale. Our results indicate that a generic three-dimensional numerical sequence-stratigraphic description of sedimentary basin fills is needed to obtain a reliable basin-fill history reconstruction and improve the predictive capabilities of reservoir and aquifer characterization studies. This may be facilitated through coupling of sediment transport and subsidence models able to link surface to subsurface processes and basin-scale characteristics (i.e. tectonic fabric, crustal deformation). Further work will focus on population of the sequence stratigraphic framework with models of sedimentary architecture based on real-world stratigraphy.

Appendix A. Post-processing methods

A.1. Sediment accumulation vs time plots by constrained cubic spline interpolation

The depositional output for every grid cell was stored as stratigraphic thickness *D* (cumulative net sediment accumulation) versus simulation time records (Fig. A1A). The constrained cubic spline interpolation method (Kruger, 2003 (available from http://www.korf.co.uk/spline); Weltje and Roberson, 2011) was used to generate a smooth continuous record of cumulative thickness values. The method provides an explicit first order derivative at every point and ensures the smooth curve characteristics of linear interpolation while preventing the oscillatory (overshooting) behavior of cubic splines (Runge's phenomenon).

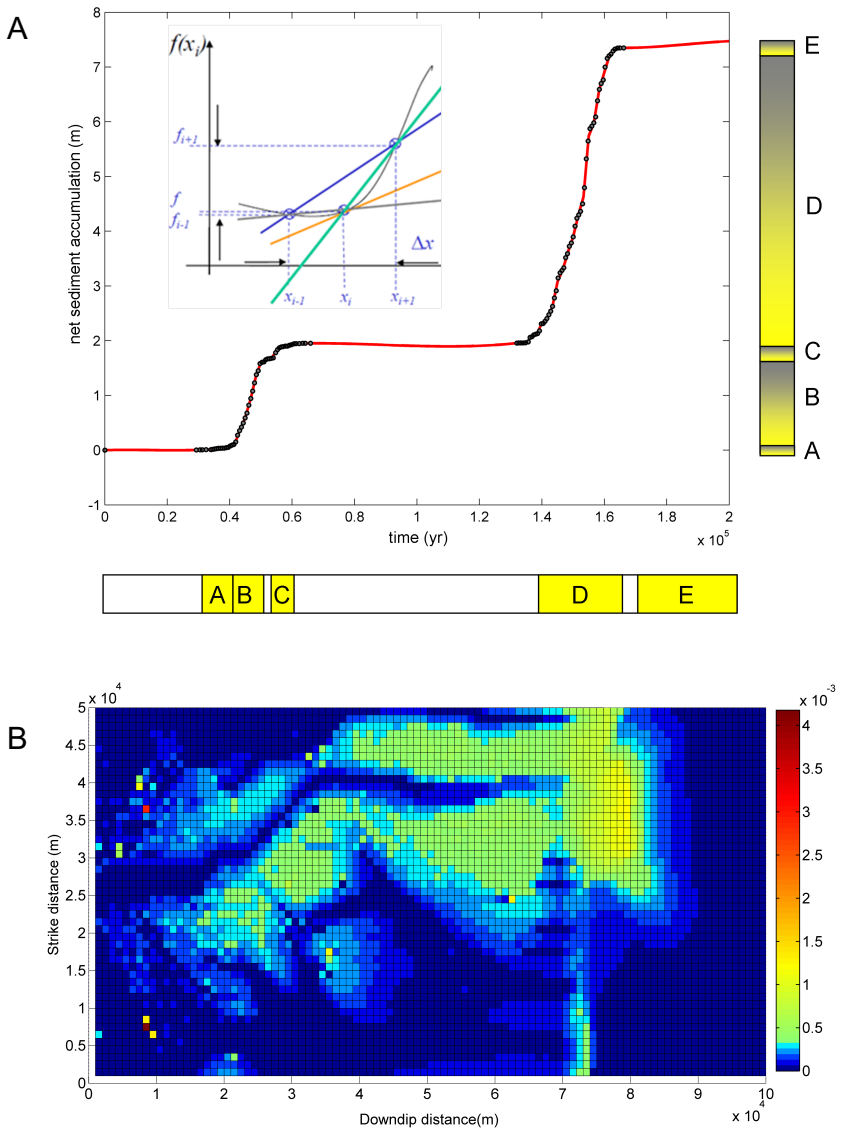

Figure A1: (A) Stratigraphic thickness (cumulative net sediment accumulation) vs simulation time at random cell. Fitted constrained cubic spline (red curve) used for interpolation between data points. Plateaus in the graph correspond to periods of stasis (bypass or non-deposition). Graph viewed as Cantor function below (modified after Plotnick, 1986, fig. 5). Inset: difference formulas for first-order derivatives forward (green), backward (gray) and central (blue) difference approximations. (B) Example of estimated net sediment accumulation rates (m/yr) during relative sea-level fall at ~20 kyr.

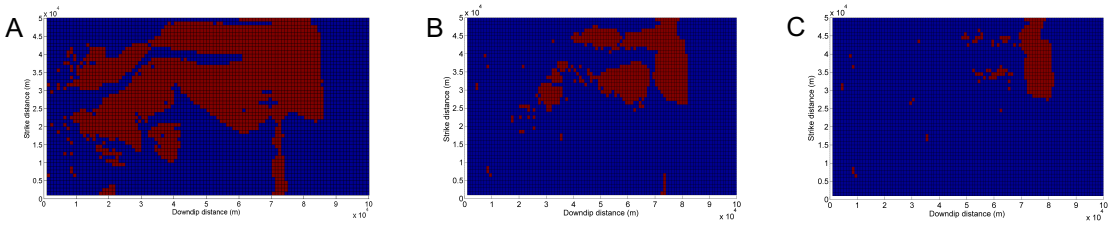

Figure A2: Net delta-lobe facies (red) extracted based on 60% (a), 80% (b) and 90% (c) of the overall sample population on the net sediment accumulation rate cumulative histogram.

A.2. Net sediment accumulation rate

The interpolation method was applied in order to approximate point-support rates *(R)* over a specified time interval (Tipper, 2016). Net sediment accumulation rate is estimated using a central difference operator of the cumulative net sediment accumulation function:

$$R_{s_i t_i} = \delta D_{s_i,t_i} = \delta D_{s_i,t_{i+\frac{1}{2}}} - \delta D_{s_i,t_{i-\frac{1}{2}}},$$

where s and t are space and time coordinates. The central difference instead of forward or backward operators was deployed in order to minimize the expected truncation error (Fig. A1A). Net sediment accumulation rates were estimated over kyr time-scale intervals which was assumed to be sufficient time for sites to receive the amount of sediment necessary to form discriminative delta-lobe units (Fig. A1B).

A.3. Delta-lobe initialization by binary transformation

The binary transformation (or thresholding) algorithm operates on the generated cumulative distribution of net deposition rates and aims to capture genetic delta-lobe units characterized by high net deposition rates. The assigned cut-off values correspond to the selected threshold population percentage of net sediment accumulation rates (Fig. A2). The P10 point (90% of the overall population) is the value for which 10% of the data points are higher. We assumed in this case that the P10 curve was an acceptable prediction. After the binary transformation operation, the values below threshold were nullified and therefore assigned as 'unpopulated' while the ones above became equal to 1 ('populated').

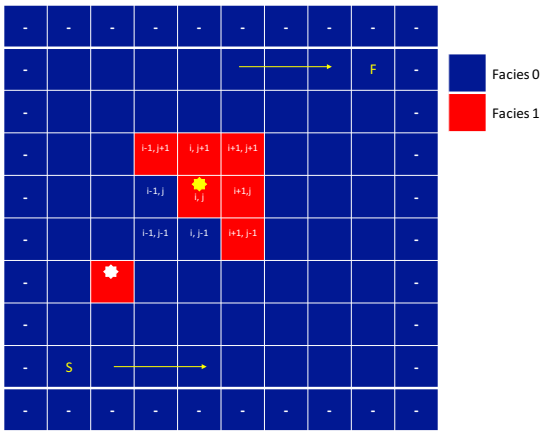

Figure A3: Example of cellular automaton simulation step displaying the occupant (red cell annotated with yellow star) that 'survives' for the next iteration and the one (red cell annotated with white star) which diminishes. Grid traversing direction indicated by yellow arrow(s).

A.4. Delta-lobe extraction by cellular automata

A cellular automaton is a simulation technique which traverses the grid cell nodes and modifies node (grid cell) states based on a set of rules governed by the current states of the neighboring cells (Von Neuman, 1966, Feynman, 1982; Wolfram, 2002). In the current study, the set of rules was assigned with the aim to preserve the emerged delta-lobe unit and discard stranded cells in the upstream part of the sediment dispersal system. A 'populated' grid cell 'survives' if the number of 'populated' neighboring cells is >= 4 (Fig. A3). An 'unpopulated' one is 'reborn' in the presence of more than 7 'populated' grid cells. This operation allows merging of 'unpopulated' inter-distributary depositional sites with the body of the fluvio-deltaic lobe so as to define its final shape (Fig. A4).

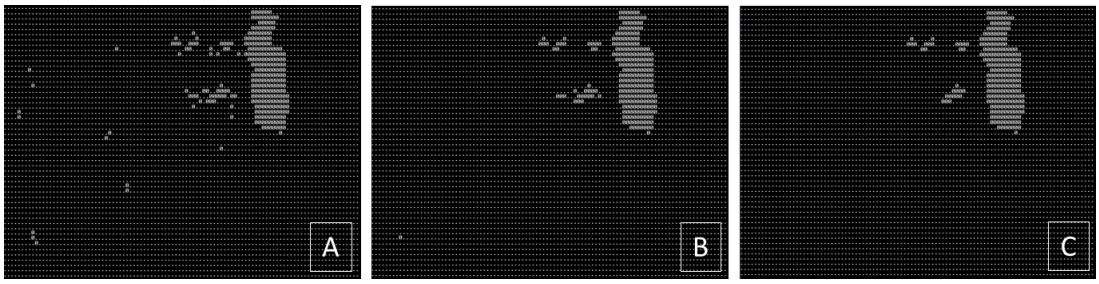

Figure A4: Graph illustrating the cleaning procedure of the cellular automaton algorithm using a set of rules (see text for more details) for the P10 case. White grid cells (zeros) correspond to the 'populated' whereas black grid cells (dots) are the unpopulated ones. Shape convergence in this example is achieved after two iterations. Initial and final states in (A) and (C) respectively.

Chapter 5

Dryland avulsion sequences: insights from data-model comparison within a terminal basin

Abstract

River avulsions are multiscale phenomena that regulate downstream distribution and architectural arrangement of channel-belt sediment bodies. Here, we used a model of bifurcation dynamics in order to explore the stratigraphic expression of the avulsion process in terminal fluvial systems and understand its control on basin-fill architecture. The model boundary and initial conditions (i.e. catchment area, smoothed initial topographic surface, grain size of sediment supply) were extracted from the Altiplano Basin (Bolivia), a modern-day dryland terminal basin filled by fluvio-lacustrine sediments. The water discharge and sediment load values were derived from global regression curves and the *BQART* equation, respectively. To evaluate the robustness of our simulations, the model was tested under increasing sediment load input values ranging from 0.003 m^3/sec to 0.095 m^3/sec. Low sediment load scenarios ($\leq$0.03 m^3/sec) are characterized by fixed drainage to the terminal part of the sediment dispersal system where symmetrical lacustrine deltas grow by means of mouthbar-induced bifurcations only. By contrast, strong alluvial-ridge aggradation during the high sediment load scenarios (>0.03 m^3/sec), creates favourable conditions for the initiation and stabilization of river avulsions.

Geographic and sedimentological data from Holocene fluvial sediments of the Rio Colorado river system were used to analyze river avulsions and to make a comparison between the observed and simulated channel-belt network evolutions, fluvial-fan dimensions and avulsion periods. The observed offset stacking of sediments is consistent with the high sediment load scenarios which are characterized by an architectural envelope that starts with a single-thread channel and gradually expands radially into multiple channels on account of alluvial-ridge aggradation, floodplain gradient increase and channel- floor elevation above the surrounding floodplain. The emergent

avulsive behavior formed a laterally extensive convex-upwards lobate topography with abandoned channel deposits arranged on either side of the main palaeoflow axis that extends ca. 10 km in the proximal part, ca. 50 km in the distal part and has a thickness of a few metres. These dimensions are in excellent agreement with the lateral and longitudinal extent of the fluvial forms in the upper and lower coastal plain of Rio Colorado river system. The simulated avulsion periods of the high load scenarios vary from 180 to 1200 yr and are consistent with the values reported from Rio Colorado river system (ca. 700 yr).

Avulsions in the high load scenarios are organised in three sequences with decreasing avulsion periods. During the first sequence, deposition is strongly progradational by means of mouthbar-induced bifurcations occurring at the lacustrine delta edge and a few nodal and local avulsions. The gradual lengthening of the fluvial profile reduces equilibrium gradient and induces upstream aggradation which marks the initiation of a new avulsion sequence that favors depocentre shifts to adjacent regions partially onlapping onto older existing fluvial fans or preferentially towards a completely new path (i.e. regional avulsion). During the third sequence, random avulsions fill with sediments the surrounding topographic lows while avoiding the interstitial alluvial ridges. Episodic peak discharge periods in the study area generate the sediment fluxes necessary to trigger the latter type owing to excessive amounts of rainfall in the drainage area forcing rapid flooding events. These results provide a large-scale framework for reservoir characterization and modelling studies of ancient fluvial stratigraphic units in which the radial extent of the fluvial system and the spatial organization of its isolated channel-belt sediment bodies as well as their reservoir quality distribution are largely controlled by avulsion-induced compensational stacking explored in this study.

5.1 Introduction

Channel-network evolution in dryland river systems is largely regulated by avulsion dynamics (Kelly and Olsen, 1993; Nichols and Fisher, 2007; Donselaar et al., 2013). Avulsion is a multiscale threshold process that may divert river flow outside the main (or parent) channel towards adjacent low-lying floodplain topography, and thus alter the downstream distribution of fluvial sediments (Leeder, 1978; Bridge and Leeder, 1979; Mackey and Bridge, 1995; Heller & Paola 1996; Jones & Schumm 1999; Mohrig et al., 2000; Slingerland and Smith, 2004; Hajek and Edmonds, 2014). Consequently, studies of modern and ancient dryland sediments deposited between the gravel-sand transition in the vicinity of orogenic belts and the terminal part of the sediment dispersal system

rely heavily on quantitative analysis of the mechanisms and frequency of avulsions (Bryant et al., 1995; Jerolmack and Mohrig, 2007; Donselaar et al., 2017, 2018).

Field studies of Quaternary and ancient fluvial systems provide a valuable, yet fragmented record of avulsion recurrences spanning a wide range of spatial (basin, architecture, event) and temporal scales (0.1 yr–10 yr, 1 kyr–10kyr, 100 kyr-Myr). (Jones & Hajek, 2007; Stouthamer et al., 2011; Hajek and Wolinsky, 2012; Edmonds et al., 2016). Experimental and field evidence demonstrated that avulsion frequency rises with increasing sedimentation rate and scales with the time needed to deposit unit thickness equal to one channel depth (Bryant et al. 1995, Heller & Paola 1996; Jerolmack and Mohrig, 2007). Makaske et al., 2002 advocated avulsion frequency of up to three per thousand years for settings which are characterized by high aggradation rates. Recent geographical research by Edmonds et al. (2016) suggested that 59% of recent avulsion events in Andean and Himalayan foreland basins were partial, with full avulsions averaging 11 yr in duration. Other authors suggested that the necessary normalized superelevation (ratio of alluvial ridge height to channel depth) period needed to drive avulsion may decrease in the presence of higher-magnitude trigger (i.e. episodic peak discharge periods) and/or optimal channel-floodplain hydrodynamic connectivity (Phillips, 2011; Morón et al., 2017b; Nicholas et al., 2018). In addition, the role of avulsions to the architectural arrangement of fluvial sedimentary packages, whose lateral dimensions and internal geometries are poorly resolved using conventional seismic and well-log data, remains still underexplored (Nichols and Fischer, 2007; Van Toorenenburg et al., 2016; Colombera et al., 2017).

Process-based numerical models provide optimal tools to explore the broad spatiotemporal ranges of the avulsion process and hence further our understanding of the spatial distribution and architectural arrangement of fluvial sedimentary packages. Here, we used a basin-scale advection-diffusion model (SimClast: Dalman and Weltje, 2008, 2012) in order to simulate channelized flow and investigate avulsion occurrences in low-gradient dryland river systems. Sedimentological and geographic data from Holocene fluvial sediments of the Rio Colorado river system were used to analyze avulsions, provide multiscale constraints for the simulations and to validate the model output (Fig. 5.1).

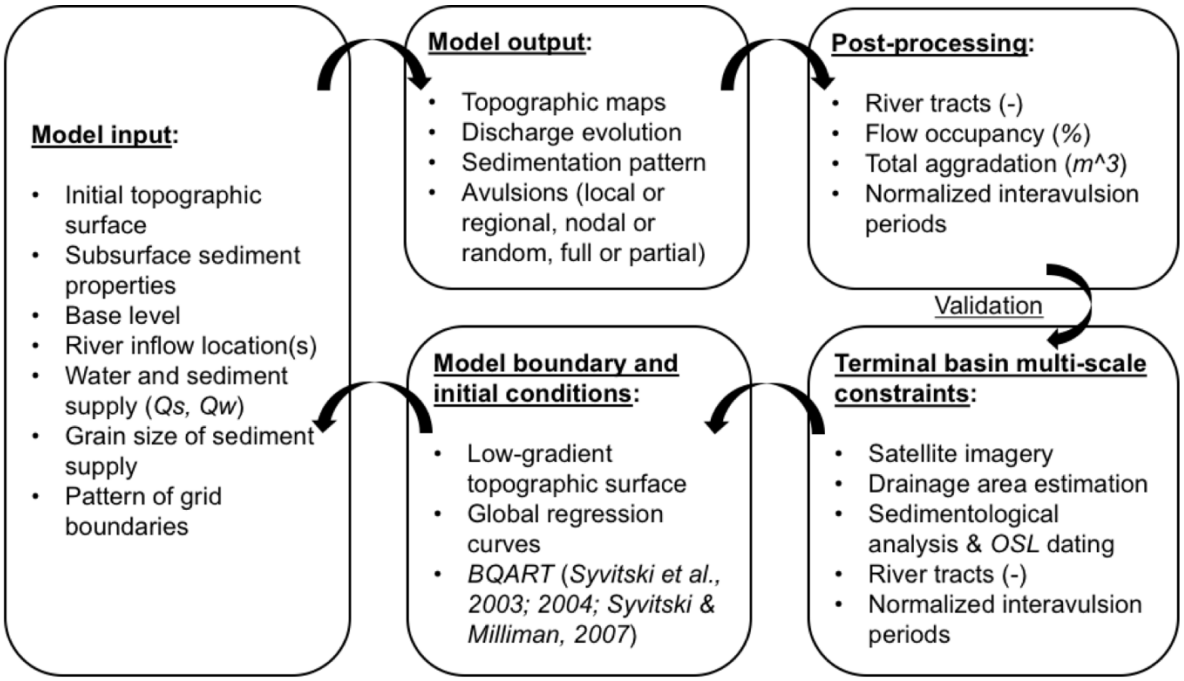

Figure 5.1: Flowchart illustrating the workflow that was used in this study.

The model output consists of multiple topographic maps, sedimentation pattern and water discharge. Post-processing enabled the clustering of channel deposits into avulsion-based river pathways (or tracts) and the quantification of flow occupancy, total aggradation and avulsion periods (cf. Mackey & Bridge, 1995; Ashworth et al., 2007; Van Dijk et al., 2009). The comparison between the observed and simulated basin-fills was based on channel network evolution, the fluvial-fan dimensions and normalized avulsion period estimates (avulsion period/total period of record).

5.2 Definitions: avulsion type, style, setup and threshold

Based on numerical experiments with a two-dimensional alluvial stratigraphic model, Leeder (1978) subdivided avulsion behaviour (or type) into nodal and random (Fig. 5.2A, B). The former originates from a relatively fixed area on the floodplain, whereas the latter may occur anywhere along the active channel. Heller and Paola (1996) characterized avulsions as local or regional based on the downstream distance over which the newly formed channel remains outside its former course (Fig. 5.2C, D). Slingerland and Smith (2004) recognized full or partial avulsions based on whether the entire flow, or only a portion of it, is transferred out of the main channel, respectively. They also summarized three avulsion style end-members based on distinct floodplain responses: avulsion

by annexation, in which a channel is captured or reoccupied, avulsion by incision and avulsion by progradation. Using R, i.e. the ratio of incision to progradation timescales (T_i/T_p), Hajek and Edmonds (2014) quantified the intermediate states between incisional and progradational avulsion styles while also underscoring the significance of floodplain morphodynamics to predispose sedimentation patterns in avulsive systems.

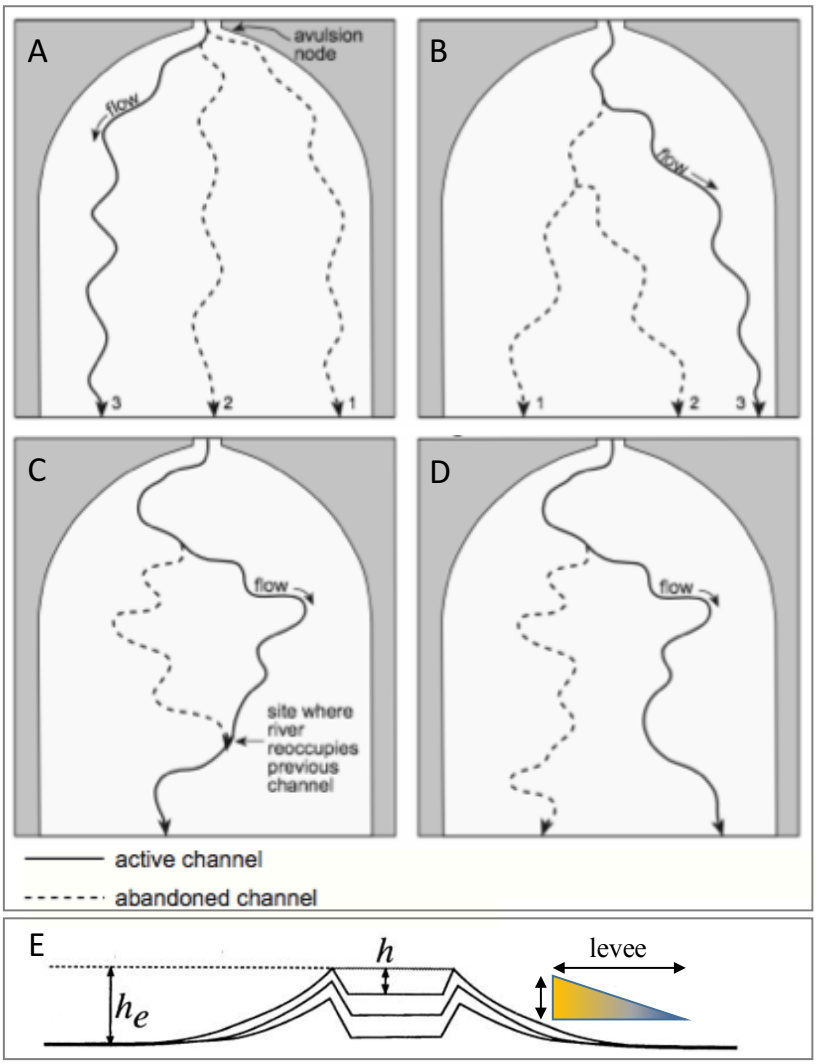

Figure 5.2: Avulsion types: Leeder (1978) recognized nodal (A) and random avulsions (B), Heller & Paola (1996) distinguished between local (C) and regional avulsion (D) (modified from Gouw et al., 2007). (E) Cross-sectional sketch of a channel showing avulsion setup (or conditions) as a function of a) levee growth and b) superelevation (h_e). The system becomes prone to avulse when h_e approximates flow depth (h), i.e. when $h \sim h_e$ (modified from Bryant et al., 1995).

Mohrig et al. (2000) summarized avulsion setup in terms of two different measures: (a) levee growth, which increases the ratio of cross-floodplain to along-river gradients, and (b) superelevation (Fig. 5.2E), which is 'the height between the water-surface elevation at bankfull discharge (i.e., levee height) to the minimum elevation of the adjacent flood plain (Heller and Paola,

1996). These two measures may be correlated if levee slope becomes steeper as the total amount of superelevation increases (i.e. the model of Slingerland and Smith, 1998)'. Avulsion thresholds control avulsion initiation and may either refer to short-term (annual to decadal) conditions under which a bifurcation or crevasse channel becomes stable or to long-term conditions that cause a successful (or full) regional avulsion at landscape/architecture scale (Hajek and Wolinsky, 2012). After avulsion initiation, the distributed flow adjacent to the parent channel will seek for gradient advantage on the floodplain (Hoyal and Sheets, 2009; Reitz et al., 2010). Ultimately, the stabilization of a newly formed crevasse channel is achieved by the appropriate combination of local conditions (i.e. cross-channel flow potential exceeding a certain threshold level, bed geometry at bifurcation sites, factors favoring floodplain incision) and an optimal downstream path at landscape-scale (Slingerland and Smith, 2004; Kleinhans et al., 2013; Hajek and Edmonds, 2014; Edmonds et al., 2016; Nienhuis et al., 2018). Finally, Jones and Schumm (1999) subdivided the conditions necessary for an avulsion into two main groups (or setups): (a) a long-term setup in which the channel gradually increases its susceptibility to avulsion and (b) a short-term trigger that initiates the avulsion (i.e. episodic peak discharge periods).

5.3 Methodology

5.3.1 Field area and avulsion history

Pristine dryland river systems in the Altiplano Basin (Bolivia) provided quantifiable information about the major sedimentary processes acting during their morphodynamic evolution. The Altiplano Basin is a high-altitude (3650 – 4200 m) internally drained semi-arid basin, with no direct connection to marine environment. The basin is filled by Cretaceous to Holocene fluvio-lacustrine sediments and aeolian accumulations of evaporite deposits (Donselaar et al., 2013; Li et al., 2014). Fluvial systems in such regions are characterized by sparse vegetation, long dry spells interrupted by events of high rainfall intensities with a very large inter-annual variability, ephemeral channelized flow with significant transmission losses and rapid evaporation of excess surface water (Powell, 2009; Thornes, 2009). Their geomorphic expressions are characterized by downstream decrease in river depth, absence of alluvial incision, offset stacking of fluvial sediments and convex-upwards lobate topographies. (Friend, 1979; North and Warwick, 2007; Li et al., 2014; Donselaar et al., 2017).

Satellite imagery and sedimentological analysis of the aggrading fluvial forms of the Rio Colorado river system (Altiplano Basin, Bolivia) enabled the historical restoration of the sediment routing system from the west flank of Andean Cordillera Oriental down to the terminal part of the sediment dispersal system where subaerial fluvial fans grow into shallow standing water (Fig. 5.3A, B, C). Alternating wetter and drier periods in the study area during the Pleistocene and Holocene epochs resulted in base level fluctuations and high sediment fluxes. The Holocene fluvio-lacustrine deposits have a maximum thickness of 3 m and overlie diatom-rich lacustrine clay deposits (Fig. 5.3D). Channel-network evolution was governed by aggrading alluvial ridges which favored the initiation and stabilization of river avulsions (Donselaar et al., 2013; Li, 2014, Van Toorenenburg et al., 2018). Avulsion-induced distributive flows filled over time the topographic lows of the lower coastal plain forming laterally extensive amalgamated sand bodies. Optically stimulated luminescence (OSL) dating of fluvial deposits obtained from point bar accretion surfaces provided an estimate of interavulsion periods ranging from 400 to 1300 yr (Fig. 5.3E). The Rio Colorado river system started flowing to its present location around 460 yr ago (Donselaar et al., 2017).

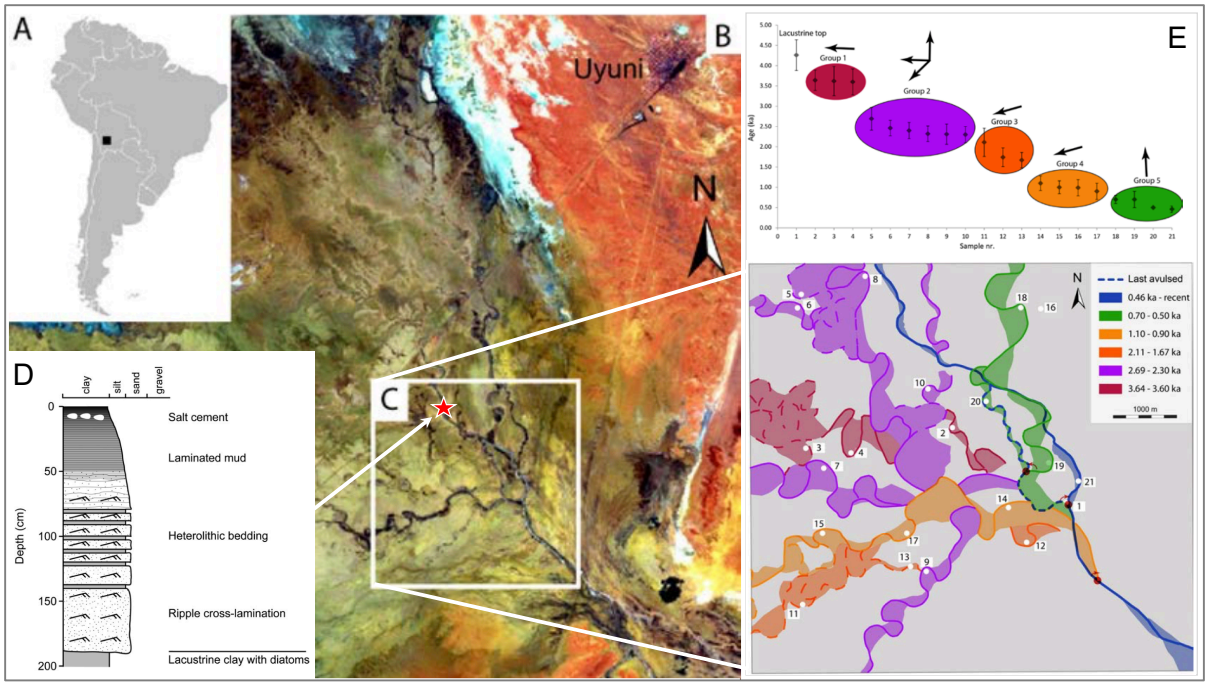

Figure 5.3: (A) Location of study area. (B) Landsat image of the Rio Colorado terminus ($25\times25\ km$). (C) Study area with exposed avulsion-associated river pathways. (D) Sedimentary log through point-bar, (E) OSL channel-belt age clusters (top), successive river pathways (or tracts) in the study area (bottom). Red points indicate avulsion sites and white dots are OSL control points (modified after Donselaar et al., 2013 and Donselaar et al., 2017) (see text for more details).

5.3.2 Multiscale constraints in a dryland terminal basin

From source to sink, Donselaar et al. (2013) subdivided the Rio Colorado river path into five segments: (1) upstream segment with small tributary channels, (2) confined segment with narrow gorges, (3) steeply dipping alluvial fan segment (bajada), (4) upper and (5) lower coastal plains that cover an area of 500 km^2 with a river gradient of 3m/36km and a divergent channel pattern (Fig. 5.4A). The total drainage area of the basin is ca. 15000 km^2 (Donselaar et al., 2013) and its surface uplift rate varies from 0.2 to 0.3 mm/yr (Gregory-Wodzicki, 2000).

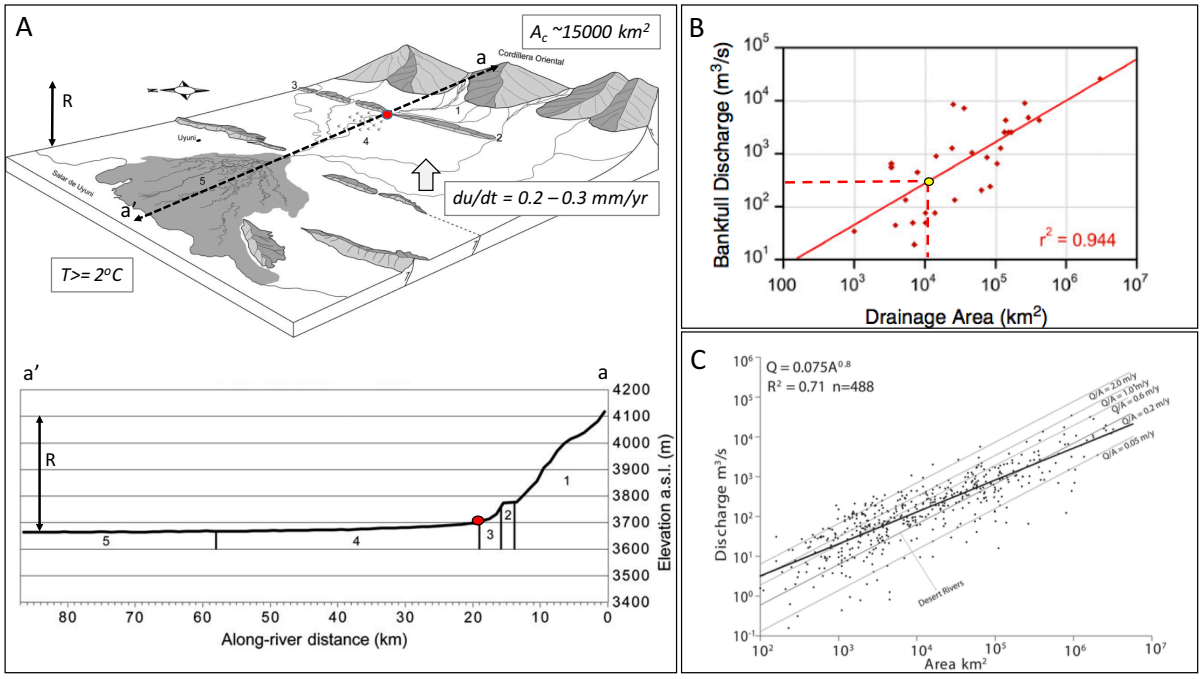

Figure 5.4: (A) block diagram of the Rio Colorado river system (top) and along-river profile with five river path segments (bottom) (modified after Donselaar et al., 2013). (B) global regression curve of estimated water discharge as a function of drainage area (modified after Blum et al., 2013). Yellow point indicates environmental parameters for Altiplano Basin. (C) Basin-averaged discharge and its power-law relationship with drainage area (after Syvitski & Milliman, 2007).

Mass balance and scale analysis enabled the approximation of the model boundary and initial conditions for the simulations. These included the low-gradient initial topography, subsurface sediment properties, base (lake) level, river inflow location and grain size of sediment supply. The water (Q_w) and sediment (Q_s) discharges were derived from global regression curves and the *BQART* equations, respectively (Fig. 5.4). Based on the regression of Q_w on catchment area (A_c), a water discharge of 500 m^3/sec was derived. This estimate lies in agreement with peak discharges obtained by model-based ratings (http://floodobservatory.colorado.edu/SiteDisplays/100127.htm) and the input water discharges used in a previous modelling study of an analogous river system in Lake Eyre Basin, Australia (Morón et al., 2018).

Sediment discharge was estimated using the *BQART* model (Syvitski et al., 2003; Syvitski and Milliman, 2007):

$$Q_S = \omega B Q_w^{0.31} A^{0.5} RT \qquad (1),$$

where Q_S is sediment discharge at the river mouth, ω is equal to 0.0006, Q_W is the estimated water discharge, B is the anthropogenic-geological influence factor (set equal to 1 since human influence, glacial influence and water trapping are negligible), R is the catchment maximum relief (ca. 0.45 km) and T which is basin-averaged temperature ($\geq 2°C$). By using these values, Q_S was found equal to 0.23 km^3/yr (7.29 m^3/sec). We assumed that only a small fraction of the estimated sediment discharge ($\leq 10\%$) reaches the entry point owing to the pronounced evapotranspiration (1500 mm/yr) which leads to high conveyance loss across the conveyor belt in the basin.

5.3.3 Numerical simulation of a terminal fluvial system

River avulsions in SimClast occur through the routing of a simplified bifurcation-stability routine and dispersive flow on the floodplain (Freeman, 1991). Basic assumption of the model is that channel-belt aggradation increases locally the ratio of cross-floodplain to along-river gradients (i.e. Slingerland & Smith, 1998), and thus creates favorable conditions for avulsions to occur. Crevassing is the triggering mechanism that initiates distributed flows outside the parent channel. The stability of a newly formed channel is tested by estimating water discharge (which is redistributed over the old channel and the crevasse channel) and the sediment transport capacity of the crevasse channel. If sediment load exceeds transport capacity, the river bank of the old channel will 'heal'. Conversely, the crevasse channel will incise, stabilize and follow the downstream path of the lower-laying inter-grid cell topography (Fig. 5.5).

Fluvial system evolution was simulated under time-invariant external forcing for a period of 4000 yr. Bifurcation and avulsion dynamics were tested under a wide range of sediment load scenarios (Table 1) in order to evaluate the robustness of the model results and fine-tune the model input. Low-gradient initial topography in the model represented the upper and lower coastal plain of the study area, whereas the grid cell size was set equal to 1×1 km, which is the finest spatial discretization at which the model can operate (Dalman and Weltje, 2008). Sandy and muddy sediments (20% and 80% of each by volume) were represented by two grain-size end-members (0.5 mm and 0.0001 mm, respectively).

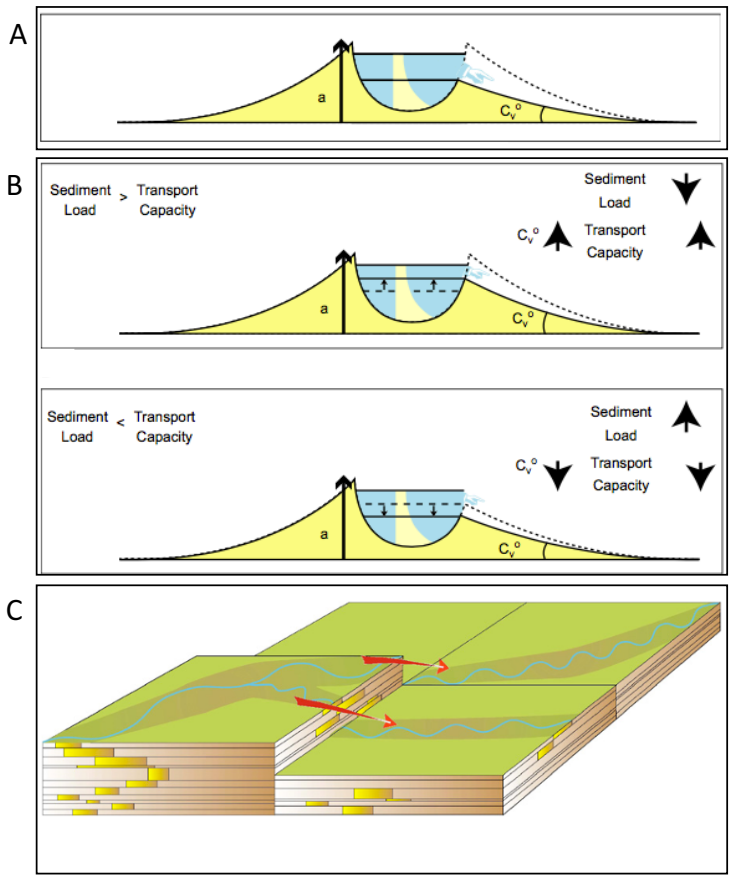

Figure 5.5: SimClast avulsion rules: (A) initiation by crevasse triggering, (B) conditions for crevasse termination (sediment load exceeds transport capacity) or stabilization (transport capacity exceeds sediment load). (C) oblique view of stabilized channel network after successful crevassing (modified after Dalman & Weltje, 2008).

Scenarios	Q_w (m^3/sec)	Q_s (m^3/sec)	Slope (-)
1	500	0.003	0.0015
2	500	0.015	0.0015
3	500	0.03	0.0015
4	500	0.06	0.0015
5	500	0.095	0.0015

Table 5.1: Input parameters used in numerical experiments.

Constant volumes of sediment entered the upper coastal plain of the basin through a single-entry point representing the boundary between the steeply dipping alluvial fan segment and the upper coastal plain. Bifurcation events and avulsion occurrences were extracted throughout the simulations. Dynamic parameters representative of water flow and sediment transport were estimated for every time step (1 yr) including the wetted area (or the cross-sectional area of flow)

a and the aggradation to progradation (*A/P*) ratio. The former was derived from an expression of the mass (and volume) conservation equation, assuming incompressible isochoric flow (constant density):

$$Q = U_1 a_1 = U_2 a_2 \qquad (1),$$

where *U* is decomposed, and represented by mean flow velocity using the Darcy-Weisbach Equation (Dalman and Weltje, 2008). The *A/P* ratio is indicative of alluvial aggradation and equals to the ratio of net sediment deposited above base level to the amount of sediments deposited below base level across the entire grid. As net sediment below the base level approaches zero, alluvial aggradation becomes infinite.

5.4 Results

The geomorphic end-products of the numerical experiments are illustrated in figure 5.6A. Low sediment load scenarios (≤0.03 m^3/sec) are characterized by straight channels and fixed drainage to the terminal part of the sediment dispersal system where symmetrical lacustrine deltas grow by means of mouthbar-induced bifurcations only. As shown in Fig. 5.6B, this geomorphic pattern changes over time in the high sediment load scenarios (>0.03 m^3/sec) as a consequence of high alluvial-ridge aggradation, deposition of higher-sinuosity channel-belt sediments and increase of cross-floodplain gradients. Such conditions favor the initiation and stabilization of avulsions.

Figure 5.7A illustrates the morphological and hydrodynamic development of the high-load scenario 5. During the early stage of the simulation, channels remained in place for long periods of time acting mostly as conduits for sediments to reach the coastline. The emergent avulsive behavior during later stages led to dispersion and offset stacking of sediments across the floodplain forming a laterally extensive convex-upwards lobate topography with abandoned channel deposits arranged on either side of the main palaeoflow axis (Fig. 5.7B).

The avulsions that were extracted during the simulation allow the subdivision of the simulated stratigraphy into 22 river tracts (or flow paths) and their associated deposits (Fig. 5.8, Fig. 5.9A). Avulsions that fell below the temporal resolution limit of the morphodynamic output (40 yr) were grouped in the same cluster. Avulsions included full (or stabilized), partial and failed avulsions. Post-processing of the channelized drainage evolution permitted the estimation of flow occupancy, defined by the percentage of simulation time a grid cell was occupied by an active channel and the

cumulative volume of total aggradation (Fig. 5.9B, C). Figure 5.10 illustrates the observed and simulated normalized avulsion periods. Low avulsion periods (<10 yr) are considered failed avulsions attributed to overestimation of bifurcation stability in the model.

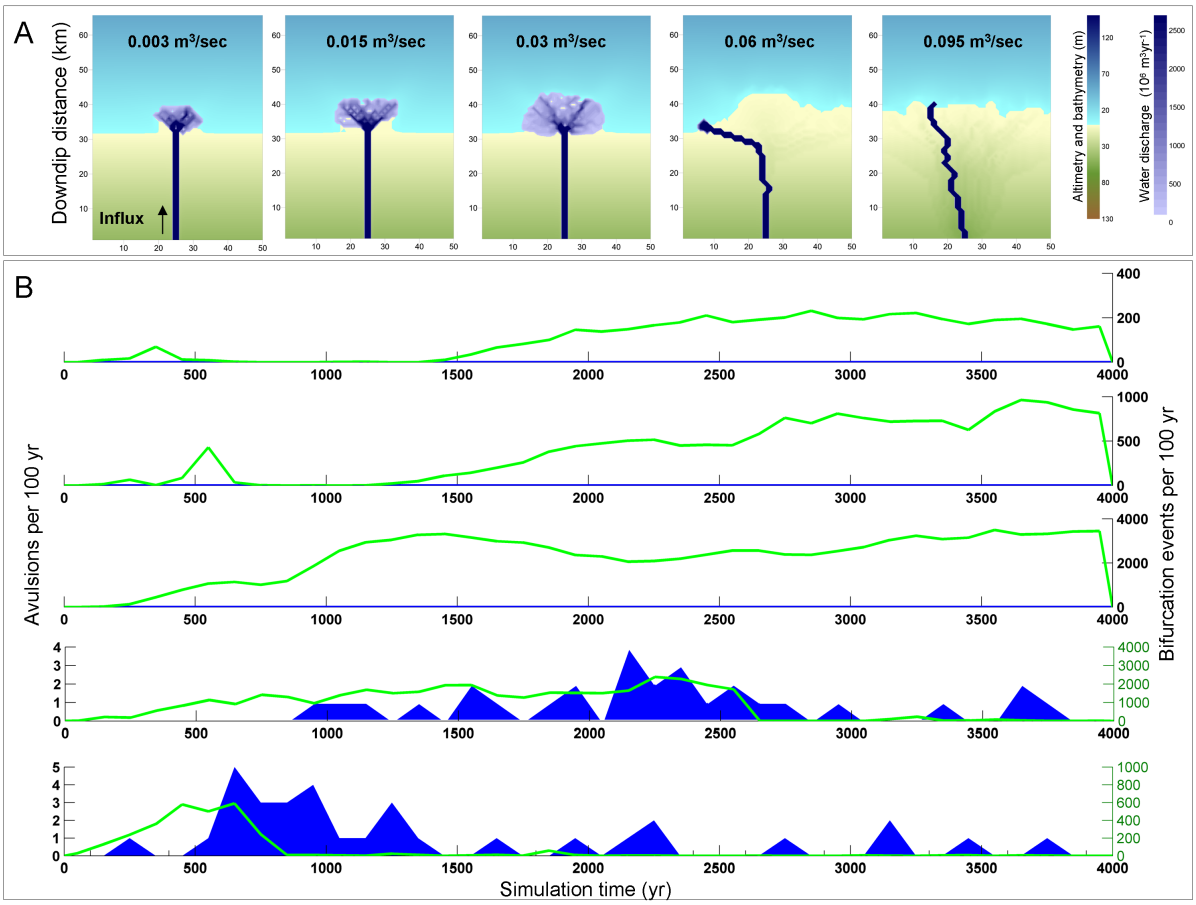

Figure 5.6: (A) Plan-view morphology snapshots of all numerical experiments (scenarios 1 to 5 from left to right). (B) Total avulsion occurrences (blue area) including full, partial and failed ones and bifurcation events (green line) per 100 yr (scenarios 1 to 5 are shown from top to bottom).

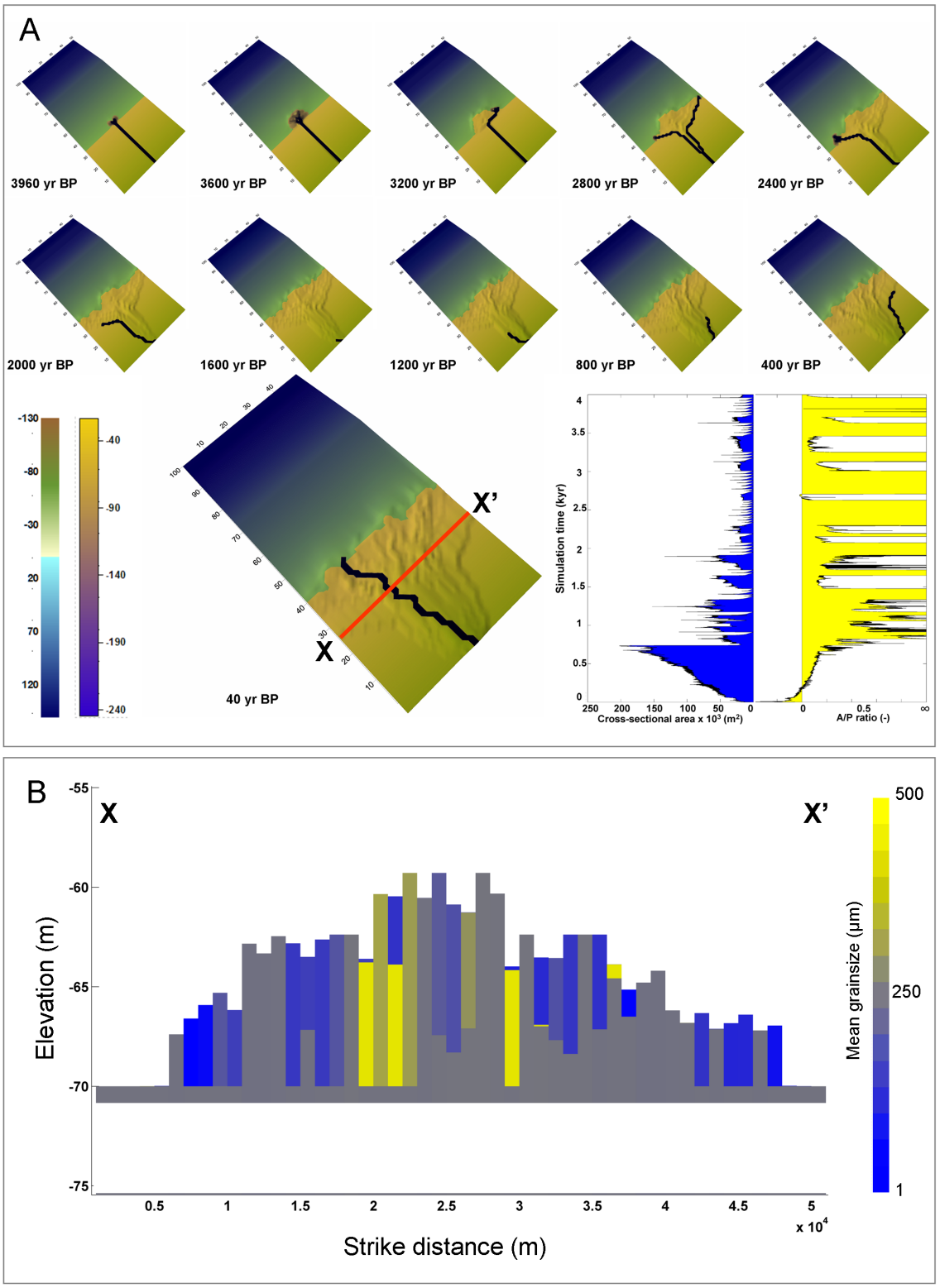

Figure 5.7: (A) Snapshots of simulated morphodynamic evolution of the high load scenario 5 (altimetry and bathymetry scales are superimposed for topographic relief intonation), inset: cross-sectional area and aggradation/progradation (A/P) ratio curves (see text for more details). (B) Strike section of synthetic stratigraphy (~25 km downdip) represented by median grain sizes.

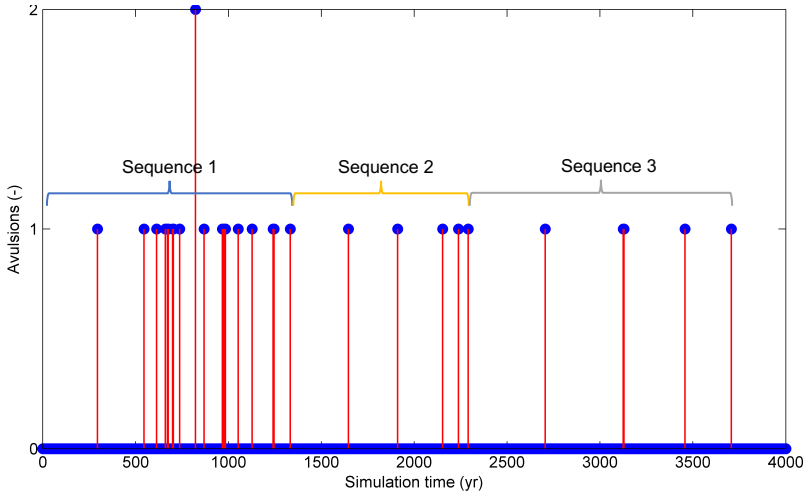

Figure 5.8: Extracted avulsion events (including full, partial and failed avulsions) and interpreted avulsion sequences. Time period between two successive occurrences marks the total inter-avulsion time that is available for alluvial-ridge aggradation.

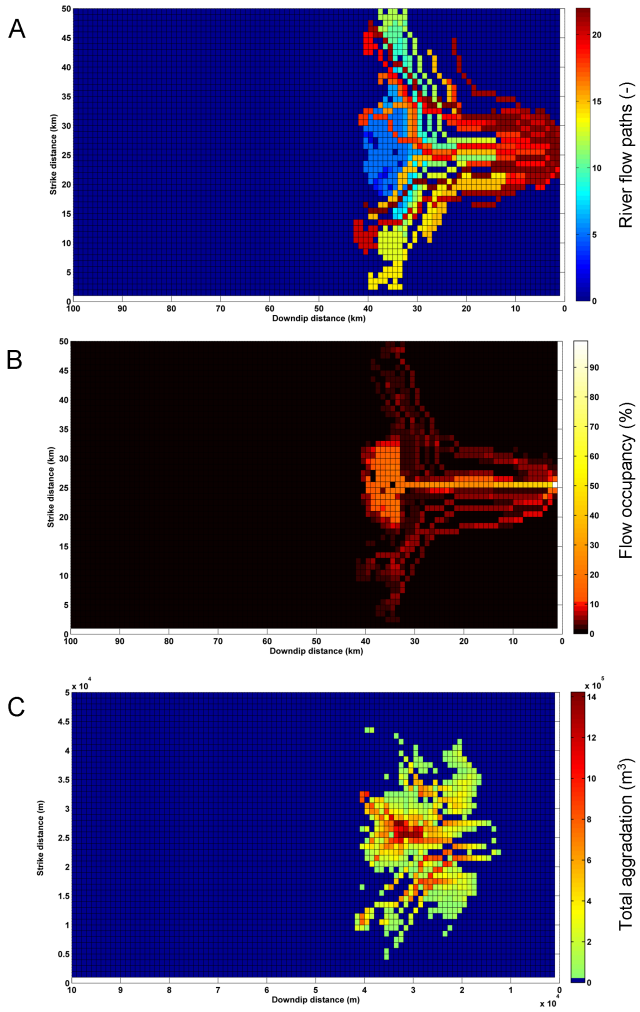

Figure 5.9: (A) Successive river flow paths. (B) Estimated flow occupancy. (C) Total aggradation.

5.5 Discussion

5.5.1 Morphodynamic evolution

The model output illustrates the relationship between morphodynamic evolution and spatio-temporal patterns of sedimentation (Fig. 5.7A). During the first stage of the simulation (4000-3200 yr BP) deposition is strongly progradational and marked by rapid increase of the cross-sectional channel area (Fig. 5.7A, inset). Under constant discharge rate, sediments reach the distal part of the lower coastal plain area forming a symmetrical lacustrine delta. At ca. 3200 yr BP, the system is punctuated by a significant decrease in cross-sectional channel area. The longitudinal outbuilding of the system lengthens its fluvial profile, reduces equilibrium gradient and induces upstream aggradation (Dalman et al., 2015). This in turn increases the cross-floodplain gradient relative to the slope downstream and prepares the ground for an avulsion which can be initiated by a flooding (or crevassing) event. In case of successful avulsion, the newly formed channel incises into the surrounding floodplain area while a juvenile lobate unit is deposited on a topographically lower-lying area downstream. The channels are backfilled with sediments and set up the system anew to an avulsion-prone state.

5.5.2 Data-model comparison and avulsion thresholds

The data-model comparison, which was conducted on the basis of channel-belt network evolution, the fluvial-fan geometry and probability density estimates of normalized avulsion periods, showed that the observations are in accordance with the high sediment load scenarios (Fig. 5.3, 5.4, 5.6A, 5.7A, B, 5.9). Rivers in the Altiplano Basin started with a low sinuosity (SI 1.29 to 1.64) single-channel trajectory bordered by small point bars and gradually evolved into high sinuosity (SI 1.80 to 2.29) streams with wide point bars with a large surface area (Donselaar et al., 2018). This is consistent with the modelled channelized flow (scenarios 4 and 5), which started with a straight single-thread channel and over time expanded radially on account of continuous growth of alluvial ridges, deposition of higher-sinuosity channel-belt sediments and the gradual increase of the ratio of cross-floodplain to along-river gradients. Compensational offset stacking of sediments formed a convex-upwards lobate topography which extends ca. 10 km in the proximal part, ca. 50 km in the distal part and is a few metres thick (2-5 m and 2-12 m for scenarios 4 and 5, respectively). Higher slopes occur in the vicinity of the main palaeoflow axis with a gradual down-valley decrease. These

dimensions are comparable to the lateral and longitudinal extent of the fluvial forms in the upper and lower coastal plain of Rio Colorado river system.

Figure 5.10 illustrates the probability density estimates of the observed and simulated normalized avulsion periods. The latter are based on a normal kernel function evaluated at equally-spaced points covering the range of observed and modelled data. For the simulated scenarios, the avulsion threshold between the failed avulsions (which include crevasse splays and healed breaches) and the successful (full) ones was defined by the intercept of the first two peaks of the probability distributions (~0.045, which equals an avulsion period of 180 yr). This threshold is supported by observations of avulsion type in the model simulations of similar low-angle river systems (Dalman & Weltje, 2008). The simulated avulsion periods in scenario 4 range from 180 to 1200 yr (corresponding to 0.045 and 0.3 normalized avulsion periods, respectively), whereas the estimated avulsion periods in the study area range from 400 to 1300 yr. The model results include a large number of local avulsions, which is likely not the case for the observed data, as these reflect substantial avulsions only. Evidence of local avulsions tends to be obscured by the subsequent evolution of the system which includes expansion of the alluvial ridge, so they are difficult to recognize in the field. Comparative analysis between scenarios 4 and 5 shows that a potential increase in sediment load (i.e. scenario 5) shifts avulsion recurrences to a higher-frequency domain.

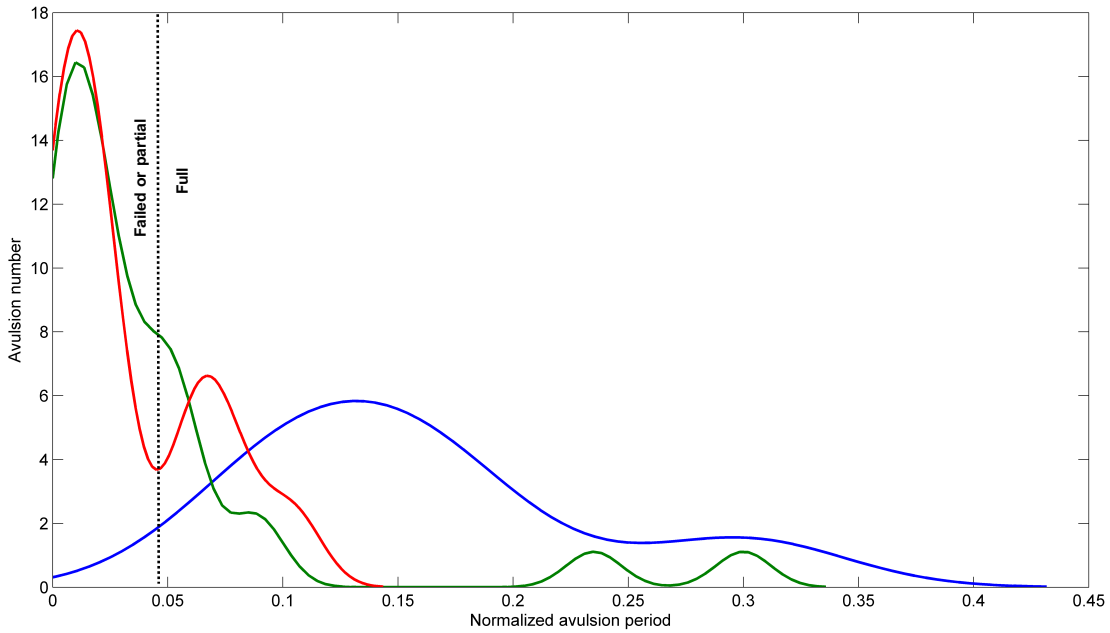

Figure 5.10: Probability density estimates of normalized avulsion periods (avulsion period/total period of record, i.e. Mackey and Bridge, 1995) for the observed (blue) and modelled periods. Green and red lines correspond to scenarios 4 and 5 respectively. Black dotted line indicates boundary between partial or failed avulsions and the full (stabilized) ones.

5.5.3 Avulsion sequences

Avulsions in the high load scenarios are organised in three sequences with decreasing avulsion periods (Fig. 5.8). This lies in accordance with previously interpreted avulsion sequences and architecture of river deltas (Mackey and Bridge, 1995; Stouthamer et al., 2011). During the first sequence, deposition is strongly progradational with predominantly mouthbar-induced bifurcations occurring at the lacustrine delta edge and a few nodal and local avulsions. The gradual lengthening of the fluvial profile reduces equilibrium gradient and induces upstream aggradation which marks the initiation of a new avulsion sequence which drives depocentre shifts to adjacent regions partially onlapping onto older existing fluvial fans or towards a completely new course driven by regional avulsions. During the third sequence, random avulsions feed with sediments the surrounding topographic lows while avoiding the interstitial alluvial ridges (Fig. 5.11A). Episodic peak discharge periods generate the sediment fluxes necessary to trigger the latter type owing to excessive amounts of rainfall in the drainage area forcing rapid flooding events. Previous authors have described the latter type as sheet flows separating them from sheet floods owing to their high precipitation intensity and the lack of channelized drainage (Hogg, 1982). Periods of intense rainfall in the Altiplano Basin are expected to create conducive conditions for high-magnitude mass fluxes able to impose a first-order control on downstream sediment dispersal and therefore alter the manifestation of the avulsion process from distal to proximal areas, yet further evidence is needed to substantiate this statement.

5.5.4 Architecture of dryland fluvial successions

Various hypotheses supported by morphodynamic modelling and field studies gave new insights on the formation and architectural arrangement of channel-belt sediment bodies (Leeder, 1978; Bridge and Leeder, 1979; Mackey and Bridge, 1995; Kraus and Aslan, 1999; Mohrig et al., 2000; Gouw, 2007; Hajek et al., 2010). In this study, the spatial organization of the abandoned channel belts reflects the adjustment of active river tracts to the inherited (local) base level, a phenomenon known as compensational stacking (Sheets et al., 2002; Straub et al., 2009; Wang et al., 2011; Hajek and Wolinsky, 2012), and plays a key role on the arrival site of the newly avulsed channel (Edmonds et al., 2016). These conditions create an envelope of predictive architecture which starts with a single-thread channel, and gradually expands radially into multiple channels on account of continuous growth of alluvial ridges and avulsion-induced compensational stacking. Recent field research focusing on crevasse-splay architectural elements in the same area advocated that avulsion

initiation is favored locally by alluvial-ridge development associated with compensational stacking of crevasse splay deposits and channel floor elevation above the floodplain (Van Toorenenburg et al., 2018).

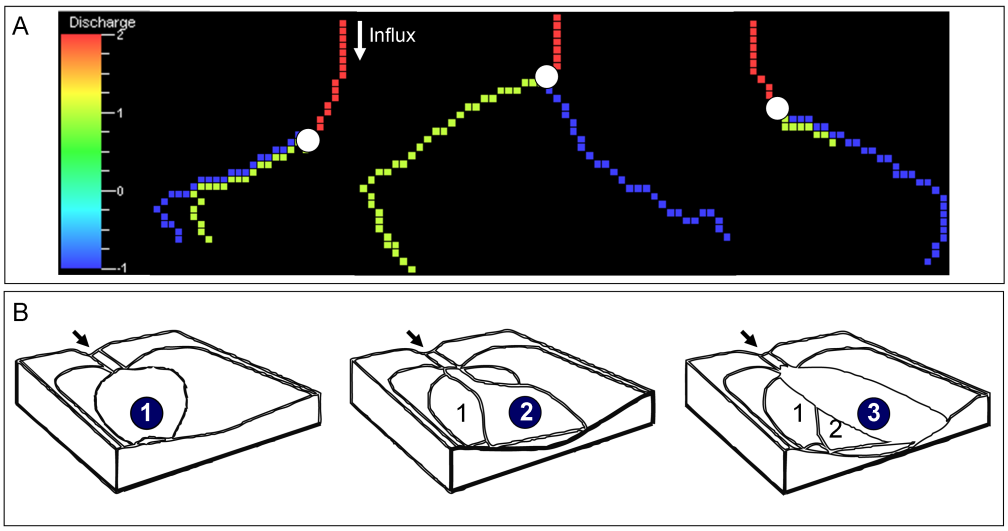

Figure 5.11: (A) Extracted avulsion types representative of the three sequences in scenario 5. Red, green and blue lines correspond to the conveyor, abandoned and active channels. White dots highlight the avulsion sites. (B) Avulsion-driven compensational stacking of sediments filling a topographic low (modified after Straub et al., 2009).

5.5.5 Preservation of a terminal fluvial system

Over the short term, the spatial variation in flow occupancy plays a key role in the sequestration and preservation of the fluvial-fan channel deposits (Fig. 5.8). Long flow occupancy periods in the proximal area corresponds to low total aggradation because the conveyor belt constantly reworks and distributes sediment downstream (Fig. 5.8C). By contrast higher abundance of channel-belt volumes are found across the medial to distal areas. This is consistent with previous experimental observations showing channelized flows occupying a particular route in the basin without filling it (Sheets et al., 2002; Ashworth et al., 2007; Van Dijk et al., 2009). Short-term sequestration and preservation runs against common stratigraphic evidence which suggests that high relative volumes of channel deposits typically lie in the proximal sectors of fluvial-fan bodies. Therefore, we distinguish between topographic fluvial fans, which are fans defined by surface topography at some instance in time, and the final preserved fluvial fans in the stratigraphic record. Over the long term, the preservation of sediments of terminal fluvial system is regulated by the regional subsidence pattern, and therefore periods of base-level rise (Miall, 1996). Under constant base (or lake) level conditions, the progradation of terminal fluvial system may be translated into a fixed rise of base

level across the entire coastal plain which induces aggradation upstream (Dalman et al., 2015). Additional accommodation space may be provided by the higher compaction rates of floodplain fines relative to the coarser grain-size fraction. By contrast, intense floods may abruptly destroy accommodation space and generate recognizable sedimentary signals in sink areas (i.e. storm intensity correlatable to mean grain size signature, cf. Romans et al., 2016). Finally, in the case of a high-magnitude base level rise, low-stand fluvial fan deposits simply drown without reworking, and are draped with lacustrine high-stand mud.

5.6 Conclusions

This study investigates the role of avulsions to sediment sequestration and architectural arrangement of channel-belt sediment bodies in dryland terminal basins. A series of numerical experiments was performed with a model of bifurcation dynamics, in order to investigate further the role of the avulsion process in low-gradient dryland river systems and predict the architectural arrangement of ancient fluvial sedimentary packages. The model boundary and initial conditions were extracted from sedimentological data from the Altiplano Basin (Bolivia) which also served for model validation. The observed offset stacking of sediments in the basin is consistent with the high sediment load scenarios which are characterized by an envelope of predictive architecture starting with a single-thread channel, and gradually expanding radially into multiple channels on account of continuous growth of alluvial ridges and avulsion-induced compensational stacking. The geomorphic end-product is a convex-upwards lobate topography with abandoned channel deposits arranged on either side of the main palaeoflow axis that extends over 10 km in the proximal part, 50 km in the distal part and has a thickness of a few metres. This is comparable to the lateral and longitudinal extent of the fluvial forms in the upper and lower coastal plain of Rio Colorado river system. In addition, the simulated avulsion periods of the high load scenario 4 range from 180 to 1200 yr and show a good fit with the ones extracted from Rio Colorado river system (ca. 700 yr).

Avulsions in high load scenarios are organised in three sequences with decreasing avulsion periods (Fig. 5.8). During the first sequence, deposition is strongly progradational with predominantly mouthbar-induced bifurcations occurring at the lacustrine delta edge and a few nodal and local avulsions. The gradual lengthening of the fluvial profile reduces equilibrium gradient and induces upstream aggradation which marks the initiation of a new avulsion sequence that drives depocentre

shifts to adjacent regions partially onlapping onto older existing fluvial fans or towards a completely new course on account of regional avulsions. During the third sequence, random avulsions fill with sediments the surrounding topographic lows while avoiding the interstitial alluvial ridges. This multiscale integrated approach provides a large-scale framework for reservoir characterization and modelling studies of ancient fluvial stratigraphic units in which the radial extent of the fluvial system and the spatial organization of its isolated channel-belt sediment bodies as well as their reservoir quality distribution are largely controlled by avulsion-induced compensational stacking (Fig. 5.11, 5.12).

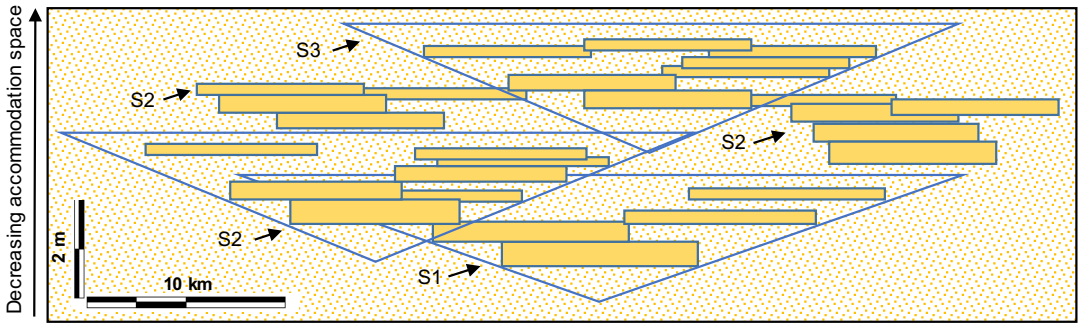

Figure 5.12: Model of alluvial architecture that predicts interconnectedness of composite beds (or channel fill successions) formed under avulsion-induced compensational stacking. Background represents fine-grained deposits.

Future efforts should focus on minimizing the high degree of uncertainty in predicting avulsion timing and locations by simulating preferential erosion of alluvial ridges as well as the differential suspension behavior of various sediment fractions. In the same direction, use of geochemical proxies may enable palaeochannel network reconstruction and identification of avulsion sites in ancient fluvial strata. High-resolution seismic tomography and ground penetration radar profiles supported by petrographic observations may not only improve the stratigraphic framework and lithofacies proportions in the study area but also narrow the uncertainty ranges of the environmental input parameters used to more reliably reconstruct the sedimentary evolution of a terminal fluvial system and thus enable a more robust comparison between numerical, experimental, recent and ancient avulsion sequences.

Chapter 6

Reservoir geology at the crossroads of process-based forward stratigraphic modelling and geostatistical lithology prediction: a synthesis[4]

Abstract

Subsurface resource exploration and development relies on geological information about the geometries, internal architecture and reservoir properties of prospective targets. This information is needed to predict reservoir quality distribution and thus support the decision-making process from prospect evaluation to resource base estimation and design of the appropriate development scenarios. The current workflow for building geological reservoir models is based on stochastic geometric interpolation methods and statistical considerations derived from seismic and well data. Quantitative descriptions of outcrop analogues and petrographic data if present, can help to bridge the spatial scale gap of the different subsurface data types used to build the model. Hitherto, the quality of the current workflow has not been objectively assessed and as is demonstrated in this paper, the lack of data cannot be held responsible for the suboptimal performance and uncertainty of geostatistical reservoir models. In this respect, we provide an overview of the main challenges in modelling channelized reservoirs and propose an alternative workflow for reducing uncertainty of static reservoir models by implementing basin-scale geological constraints derived from a process-based stratigraphic model. Model calibration allows to separate out model realizations which are geologically unrealistic and to provide stratigraphic model ensembles which are

[4] Based on: Weltje, G.J., Dalman, R.A.F., Karamitopoulos, P, Sacchi, Q., published. Reducing the uncertainty of static reservoir models: implementation of basin-scale geological constraints. 75th EAGE Conference & Exhibition incorporating SPE EUROPEC. DOI: 10.3997/2214-4609.20130913.

consistent with the palaeogeographic layout and basin-fill history. These ensembles may in turn be used as geologically-guided conditioning data for stochastic algorithms. The geostatistical reservoir models which are constrained to maintain quantitative coherence with the large-scale geological setting have higher predictive power relative to the ones that use local well data only. Potential integration of process-based model optimization and data assimilation techniques within a closed-loop reservoir management framework promises to improve field development decisions and enhance field-wide production performance.

6.1 Introduction

In the context of uncertainty, risk and benefit, optimal exploitation of subsurface water and energy resources relies on the accuracy of geological reservoir models which permit the spatial distribution of porosity and permeability to be predicted. Most reservoir models are based on stochastic geometric interpolation methods (Deutsch, 2002), as well as on statistical considerations derived from well data. These methods provide solutions which are locally optimal, but are rarely constrained using sedimentological knowledge about reservoir architecture, paleogeographic layout and basin-fill history (Weltje et al., 2013). Process-based stratigraphic modelling provides convenient tools to simulate sediment dispersal systems over a wide range of spatial and temporal scales and to capture the spatial distribution of lithology at the time of deposition, thus allowing basin- to architectural element-scale data types to be integrated at the reservoir scale (Cross and Lessemger, 1999; Granjeon and Joseph, 1999; Paola, 2000; Meijer, 2002; Wijns et al., 2004; Karssenberg et al., 2001, 2007; Imhof and Sharma, 2006; Charvin et al., 2009, 2011; Hajek and Wolinsky, 2012; Falivene et al., 2014; Sacchi et al. 2015, 2016; Skauvold and Eidvik, 2018).

This chapter addresses the main challenges in modelling channelized reservoirs and proposes a workflow for inverting the stratigraphic output derived from SimClast, a process-based stratigraphic model (Dalman and Weltje, 2008, 2012), in order to reduce uncertainty associated with spatial predictions of geostatistical reservoir models. We argue that geostatistical lithology prediction should go hand in hand with process-based stratigraphic modelling, because geostatistical reservoir models which are constrained to maintain quantitative coherence with the large-scale geological setting are superior in terms of predictive power relative to those that use local well data only (Weltje et al., 2013; Sacchi et al. 2015, 2016). The proposed workflow may be applied in data-rich and data-poor environments in the shallow and deep subsurface in order to increase the probability of success throughout all the phases of subsurface resource exploitation, from reserves estimation during exploration to enhanced recovery during production.

6.2 Geostatistical reservoir modelling

The current workflow for obtaining static reservoir models relies on integration of quantitative well and seismic data by geostatistical (geometric-stochastic) methods. Kriging-like procedures are used to build a "best-guess" static reservoir model, from which an ensemble of equiprobable realisations is produced by conditional simulation. Conditional simulation implies that the large-scale geometry of a reservoir (and its enveloping geological unit) as derived from seismic data is respected and well data are honoured.

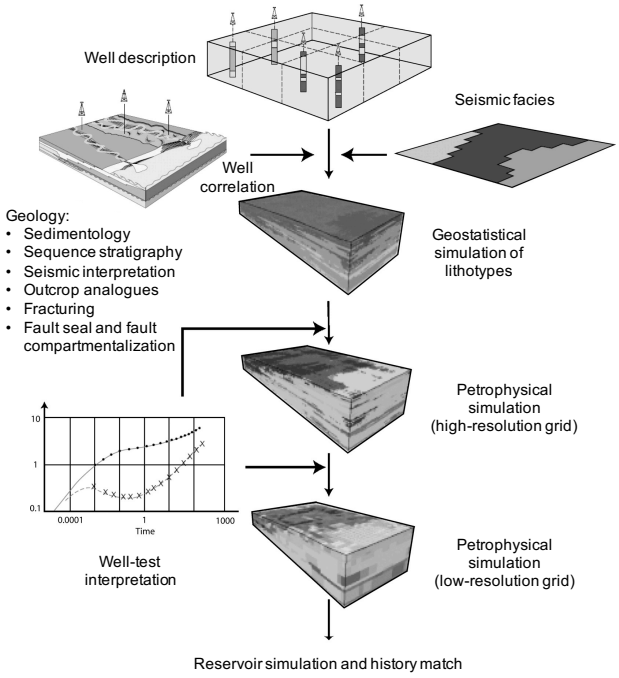

Figure 6.1: Conventional workflow for building static reservoir models (modified from Ravenne, 2002; originally from Doligez et al., 1999a).

Each realisation is transformed into a continuous 3-D porosity and permeability field by appropriate averaging (upscaling) procedures to serve as boundary conditions for dynamic models of reservoir behaviour (Fig. 6.1). Uncertainties associated with reservoir behaviour are modelled by regarding the ensemble of equiprobable realisations obtained by conditional simulation as a representative sample of a population of subsurface models that is consistent with the observations (Deutsch, 2002). In this classic approach to geological reservoir modelling, the aim is to mimic the present-

day spatial distribution of geological entities without taking into account how a particular spatial distribution of lithology (porosity and permeability) has been generated.

This "product-based" approach to prediction of reservoir architecture does not provide much opportunity to incorporate knowledge of the physical laws which govern basin filling into the modelling workflow. Integration of basin-scale geological knowledge into reservoir models is usually limited to the use of "soft constraints" such as regional property trends (net-to-gross) or main channel-belt orientations derived from seismic attribute analysis. The limited assimilation of basin-scale information does not permit detailed assessment of the contributions made by different data sources to the overall uncertainty of a reservoir model. The above point would be of merely academic interest if geometric-stochastic reservoir models can accurately predict lithology at unsampled locations, and therefore, form a reliable basis for production forecasts and planning of infill wells. As will be shown below, this does not appear to be the case, which implies that current reservoir-modelling practice should be improved.

6.3 Geostatistical model performance

The performance of conventional geometric-stochastic reservoir modelling software was tested in a modern environment with extensive well control (Janszen, 2008). The purpose of the study was to examine if the "static" model could be used to predict downhole lithology at unsampled locations. A modern fluvio-deltaic system (Po Delta, Italy) was selected (Fig. 6.2A), for which an extensive database in the form of cored wells and cone penetration tests (CPTs) was made available by the geological survey of Emilia-Romagna. Stefani and Vincenzi (2005) recognized in the boreholes carried out in the Codigoro area six facies-associations and depositional environments including alluvial plain, coastal plain, lagoon, pro-delta, beach-ridge and marsh (Fig. 6.2A, B). Most of the facies distributions were limited to certain sequence stratigraphic intervals marked by key sequence stratigraphic surfaces. The validity of this framework was constrained by ^{14}C dating from two boreholes.

The data set used for the modelling exercise consisted of 154 wells (CPTs and cores) in which four lithology classes were represented as a function of depth below the present-day surface. There are several different ways to determine lithology from CPT data (Lunne, 1997). The method used for this research was developed by Cheng-Hou et. al. (1990) and utilizes physical parameters, i.e. pore pressure ratio, cone resistance and the equivalent water pressure of a water column with the same height as the depth of the cone to indicate the coarseness (N_h) of sediments at a certain point. Furthermore, to distinguish silty soils from peats the friction-ratio (FR) was used as a percentage. The friction ratio is defined by the sleeve friction (f_s) per unit area of the cone to the cone tip resistance (q_c) corresponding to the soil resistance per unit area to penetration. When the ratio is smaller than 2% we deal with a silty soil while when the friction-ratio is higher than 2% it is probably peat (Janszen, 2008). The calculated value of coarseness and the friction ratio form an indication of the rheological properties of the soil (e.g. strength, compaction) and therefore may be translated into lithology. It is also possible to recognize coarsening and fining-upward sequences (similar to Gamma Ray logs) by the shape of the CPT-curves. However, the strongest criterion was the original interpretation of boreholes nearby the CPT where direct observations of sediment were made by the Geological Survey of the Regione Emilia Romagna. The facies of the interpreted lithologies (sand, silt, clay, peat) may then be inferred from their location within the proposed sequence stratigraphic framework by Stefani and Vincenzi (2005).

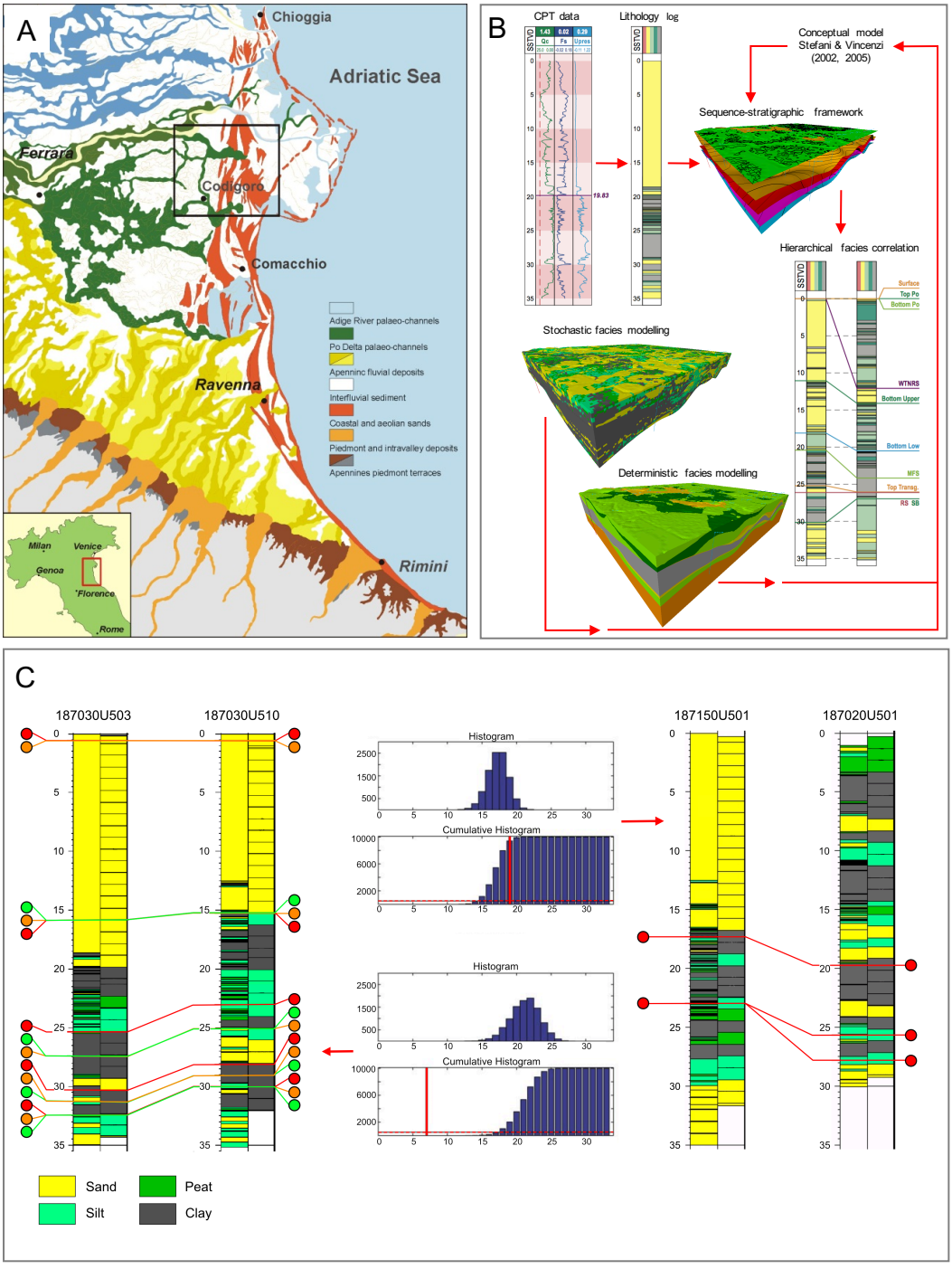

Figure 6.2: Geostatistical model performance: (A) Modern Po Delta, Italy: complex interfingering of fluvial and coastal sands (after Stefani & Vincenzi, 2005). (B) Workflow testing the performance of a conventional geometric-stochastic reservoir model in a modern environment with extensive well control (after Janszen et al., 2007). (C) Levenshtein distance of true and predicted wells compared to vertically randomized realisations (modified from Janszen, 2008) (see text for more details).

A digital elevation model of the Po plain was combined with a geomorphological map to define the top surface, and a regional map of the late Pleistocene sequence boundary, which dates back to 19

kyr BP, was used to delineate the bottom of the simulated reservoir interval, which comprises the transgressive and highstand systems tracts. Reservoir architecture in the study area is complicated, because it corresponds to the lower delta plain to delta-front area of the Po river, where fluvial sands (oriented perpendicular to the coastline) merge into shore-parallel coastal sands of the wave-dominated paleo-Po delta front. Lithologies were modelled using object-based simulation (for the fluvial channel belts) and sequential indicator simulation (for the coastal-plain deposits and delta-front sands). After upscaling, the final model had a vertical resolution of 1 meter (Fig. 6.2B).

Lithology prediction in the upscaled model was carried out by cross validation, i.e. leaving out one well and predicting its lithology based on the other 153 wells. Each well was represented by a string of coded lithologies. Differences between wells were quantified by the Levenshtein distance, which equals the minimum number of edits (insertions, deletions, replacements) needed to transform one string into another. Local probability distributions of the Levenshtein distance were determined by a permutation test. The target string (the actual well lithology) was compared to 10,000 randomized sequences of the same lithologies and the 5th percentiles of distances thus obtained was taken as the critical value (Fig. 6.2C). The cross-validation tests showed that in most cases, models based on 153 wells could not predict the sequence of lithologies in the target well. Successful prediction, defined as a significantly better match than a random guess at the 5% significance level, was only achieved in the simplest of cases, i.e., wells dominated by coastal sands which are laterally continuous in the shore-parallel direction. A second (less severe) test, in which local probability distributions of the Levenshtein distance were determined by comparing the target string to randomized versions of the predicted well gave essentially the same results. The cross-validation tests thus indicate that conditional simulation on the field scale is insufficient to guarantee geological feasibility in complex fluvial reservoirs, even in data-rich environments. The fact that a predicted well does not differ significantly from a random guess implies that it is not possible to estimate lateral continuity of lithologies, which severely hampers reliable estimation of horizontal permeability in the upscaled model.

It also follows that the geometric-stochastic model cannot be used as a reliable guide to planning of infill wells during the late production phase, when the commercial impact of uncertainties becomes increasingly high (Fig. 6.3).

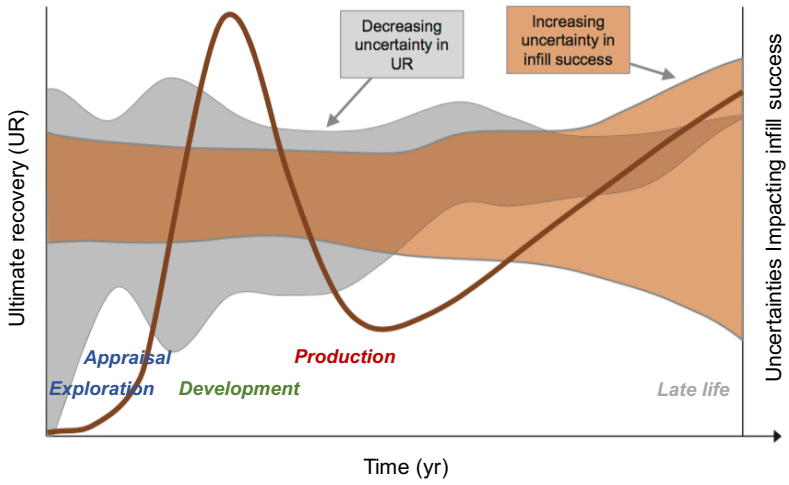

Figure 6.3: Decreasing and increasing uncertainty in ultimate recovery and infill success, respectively. Commercial impact of uncertainties throughout the field's life cycle (brown line). Uncertainty increases sharply at the point of project sanction (i.e. appraisal and development phases) and during the late production phase (modified from Bentley, 2016).

The modern Po delta study is of particular interest because tests of common reservoir-modelling workflows in data-rich environments are scarce. Indeed, the usual situation is the opposite, because models of the subsurface have to be constructed from a comparatively small well-data base. The fact that one has no choice but to use all available data to build a model comes at a high price, because it implies that the predictive capability of a model cannot be evaluated. Although the quality of the current workflow for geological reservoir modelling of industry targets has not been objectively assessed according to formal criteria, our results indicate that the performance of conventional static reservoir models leaves much to be desired. As shown above, the lack of data cannot be held responsible for the suboptimal performance of geostatistical models, and solutions to improving their performance have to be sought elsewhere.

6.4 Basin-scale forward models

Stratigraphic forward models are well established in exploration geology as a tool to predict spatially averaged gross lithology trends at a resolution suitable for direct comparison to subsurface data, specifically seismic, because they are able to capture first-order heterogeneity (Deutsch and Wang, 1996; Burgess et al., 2006; Burgess, 2012). A popular approach to modelling of clastic reservoirs is based on topographic diffusion, which may be combined with advective transport for more accurate representation of channelized flow (e.g. Granjeon and Joseph, 1999; Meijer, 2002;

Hajek and Wolinsky, 2012). Inputs for such models are initial basin topography (including locations of sediment entry points), relative sea-level history, and the liquid and solid discharges at entry points. Sediment supply from each entry point may vary through time, in terms of bulk volume, grain-size distribution, and mineral composition, depending on the degree of sophistication of the model. In typical applications, such models are run several times (preferably many) to determine their sensitivity to initial and boundary conditions, after which they are used to predict the large-scale spatial distributions of lithology in a sequence-stratigraphic framework (Burgess et al., 2006; Hutton and Syvitski, 2008).

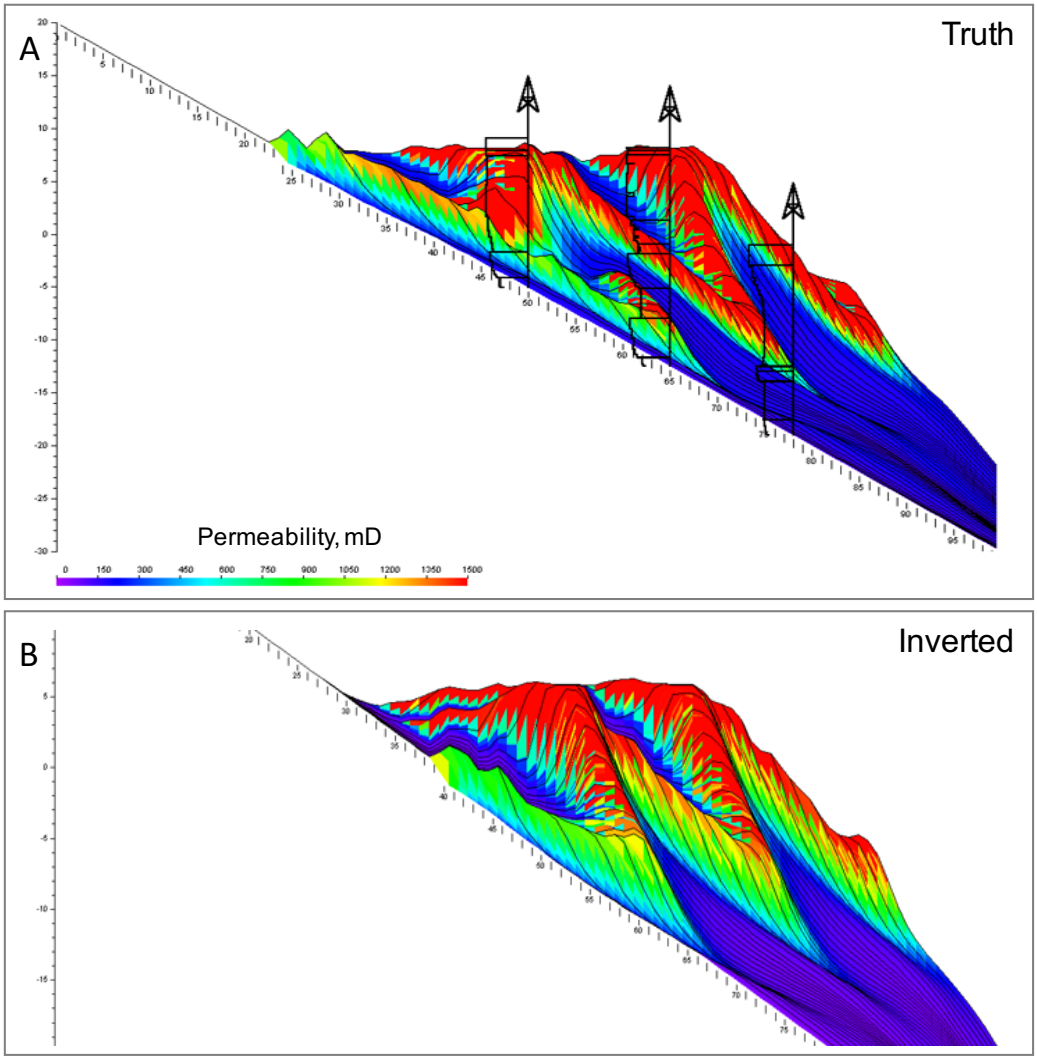

Figure 6.4: Conditioning of a two-dimensional forward model (BARSIM: Storms et al., 2002): (A) Inverted and (B) true longitudinal cross-sections (Geel & Weltje, 2003). Red, green and blue colors correspond to mud, silt and sand, respectively. Six-parameter inversion (sea level, sediment supply); best-fit solution out of ~50.000 realisations using a genetic algorithm for the minimization of the Levenshtein distance. Target data were K profiles of three wells.

It is important to note that these models cannot provide detailed sedimentological heterogeneity at sub-seismic resolution. Downscaling of model output requires knowledge of architecture and primary textural/compositional heterogeneity of the deposits to permit detailed predictions of reservoir behaviour (Griffiths et al., 2001). Direct prediction of lithological heterogeneity at the reservoir scale requires a high spatial resolution coupled with advanced physical descriptions of sediment transport, which take into account various grain populations (size/shape/density classes). In process-based models such as Delft3D (http://oss.deltares.nl/web/delft3d) and Sedsim (Tetzlaff and Harbaugh, 1989; Martinez and Harbaugh, 1993; Griffiths et al., 2001), sediment transport is directly coupled to hydrodynamics, which significantly increases realism of model output as well as computational overhead. Process-based models are notoriously difficult to condition to well data, because they display strongly nonlinear behaviour and tend to have many parameters, which quite often cannot be constrained in applications to ancient reservoirs. In addition, it is not entirely clear how the objective function should be formulated, and the occurrence of erosion surfaces indicates that the stratigraphic record is incomplete. Inversion of stratigraphic models is therefore often carried out by global optimisation (Bornholdt et al., 1999; Cross and Lessenger, 1999; Sharma and Imhof, 2007). Because such strategies require many model runs, process-based models are rarely used to conduct basin-scale, long-term simulation studies needed for probabilistic stratigraphic modelling (Wijns et al., 2004). Successful inversion of small-scale, simplified process-based models has been reported by Karssenberg et al. (2001, 2007), Geel and Weltje (2003), and Charvin et al. (2009, 2011). An acceptable fit of such models to well data may require many thousands of model runs (Fig. 6.4), which renders them prohibitively expensive.

6.5 Reservoir modelling workflow

As discussed above, the current approach to geostatistical reservoir modelling is insufficiently powerful to provide meaningful lithology predictions. The central problem of geostatistical modelling is that it relies on the assumption that well data contain enough information about the spatial arrangement of lithologies to provide meaningful solutions to the filling of inter-well space based on statistical considerations alone. Given that well data never lead to unique solutions, and requirements of geological realism are not directly incorporated into the geostatistical workflow, it seems safe to assume that each solution set contains a fair proportion of geometric-stochastic

realisations which are not "geologically realistic" in the light of sedimentological knowledge about reservoir architecture, the paleogeographic layout, and the history of basin filling. If such solutions could be identified and "weeded out", the degree of non-uniqueness of static models could be reduced by narrowing down their solution spaces.

Process-based geological reservoir modelling based on stratigraphic inversion may be used to supply more geological knowledge to the current workflow, but it has not yet matured to an "off-the-shelf" tool. Currently, only process-based models at the scale of one stratigraphic zone (or reservoir zone, depending on how the zone is defined) exist i.e. SBED^{TM} software (Wen et al., 1998; Elfenbein et al., 2005). Development of techniques to create geologically reasonable models of the subsurface which can be efficiently inverted and conditioned to well data is therefore still a major challenge. As long as the vast computational overhead and detailed specification of input parameters needed in forward stratigraphic modelling cannot be reduced, the uncertainty associated with the initial and boundary conditions of basin-scale geological models is not propagated into reservoir models. This shortcoming is intrinsic to all modelling workflows which treat exploration and production of hydrocarbons as separate activities, i.e., carried out by different teams (Fig. 6.5).

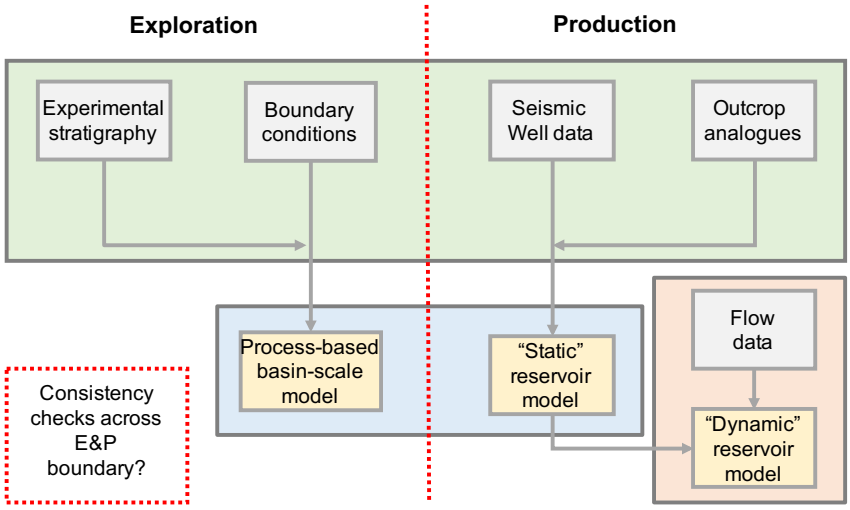

Figure 6.5: Diagram illustrating the exploration and production connection problem: limited consistency checks across the E&P boundary do not permit the use of process-based basin-scale models for reservoir-scale lithology prediction.

During the early stage of a project's lifecycle (i.e. exploration and appraisal phases), decisions and operations take place in a data-poor environment as subsurface data are expensive. The exploration geoscientist analyses and fuses all available multiscale, incomplete and imperfect datasets (i.e. seismic, well-log data, complemented by outcrop analogues along with information obtained by

process-based basin-scale models) to produce a 'best-guess' static reservoir model, which is used in turn to design the appropriate development scenarios. The accuracy of this model as lithology predictor cannot be evaluated by cross-validation techniques, because it was built with all available data. Hence, it cannot be excluded that the model is highly inaccurate. At later stage (i.e. development and production phases) and in light of new well and production data, consistency checks (or model updates) across the 'exploration-production boundary' are likely to be very limited, which in turn leaves the reservoir engineering team anchored among static reservoir models whose accuracy is essentially untested, and possibly questionable. An efficient way to condition reservoir models to basin-scale geological information would be a major step forward.

6.6 Alternative workflow for reservoir modelling

An alternative reservoir modelling workflow is demonstrated in which basin-scale process-based simulations are combined with a) evaluations of the overall 3D reservoir architecture (chronosomes) and b) local stochastic predictions of reservoir architecture. This workflow allows regional and local information to be genetically linked with the conditioning data (seismic, wells), and thus more effectively upscale reservoir properties to flow simulation grid-cell sizes, while preserving the inherent small-scale statistical structure. Many of the problems related to inversion of basin-scale models and reservoir-architecture (lithology) prediction can be avoided by using a computationally efficient low-resolution basin-scale model which uses large grid cells in which small-scale phenomena such as channels are represented by sub-grid elements. The SimClast model (Dalman and Weltje, 2008, 2012), has been designed with this objective in mind: enhance our understanding of clastic sedimentary systems as a whole, and to provide a new data type, representative of the spatial distribution of potential water- and/or energy-bearing permeable volumes of sediments and sedimentary rocks at the time of deposition, at a resolution directly comparable to subsurface data. The model is run with the intent to approximate large-scale basin-fill properties (based on geological/geophysical background information about palaeotopography, sea level, sediment supply, subsidence, and so forth). The model simulates hillslope and fluvial sediment transport (channel-belt and levee geometry, bifurcations and avulsions, fluvial style) and the resulting basin-scale stratigraphic architecture. The model keeps track of the gross lithology and the evolving drainage pattern within each of the 1 by 1 km size grid cells of the SimClast model without specifying the exact locations of channel belts.

Sacchi et al. (2015, 2016) showed a way to combine basin-scale process-based simulations with local stochastic predictions of reservoir architecture. This was accomplished by stratigraphic inversion of the basin-scale models using synthetic seismic, and integrated the gross lithology trends as soft constraints in a multipoint (MPS) geostatistical model conditioned to well data.

Uncertainty over channel-belt occurrence probability at basin scale was reduced at selected monitoring locations on account of averaging over a subset of the most likely (100/2000) best fit scenarios. Further analysis and comparison of the local sand probability curves at reservoir scale obtained with and without process-based stratigraphic constraints were used to verify the effectiveness of the proposed methodology (Fig. 6.6).

Different realisations of a reservoir volume, each consistent with the basin-scale model, may be generated by MPS models by including the averaged channel-occurrence probability in the reservoir volume, or if desired, by including a set of pseudo-wells based on the simulated stratigraphy of the grid blocks surrounding the reservoir area. Pseudo-wells may be constructed from the cell-averaged lithology and depositional style of grid blocks (Fig. 6.6B). If the size of the grid cells in the basin-scale model is large relative to the widths of individual channel belts, stochastic- geometric post-processing may be used to examine the effects of variable channel-belt connectivity on reservoir behaviour (Fig. 6.6C), so as to give a more geologically plausible assessment of uncertainty. Reservoir models which can be constrained to maintain quantitative coherence with the large-scale geological setting approximated by a basin-scale model are potentially superior to models which use only local well data (Fig. 6.6D). Hence, this approach promises a simultaneous increase in the geological credibility of stochastically simulated fluvial reservoir models and a significant reduction of the time needed to attain an acceptable level of fit to observations relative to direct inversion of basin-scale models. Geological information on the basin history is thus directly incorporated into the field-scale model, which narrows down the range of possible scenarios (realisations) that would be considered equally probable from a purely geostatistical point of view.

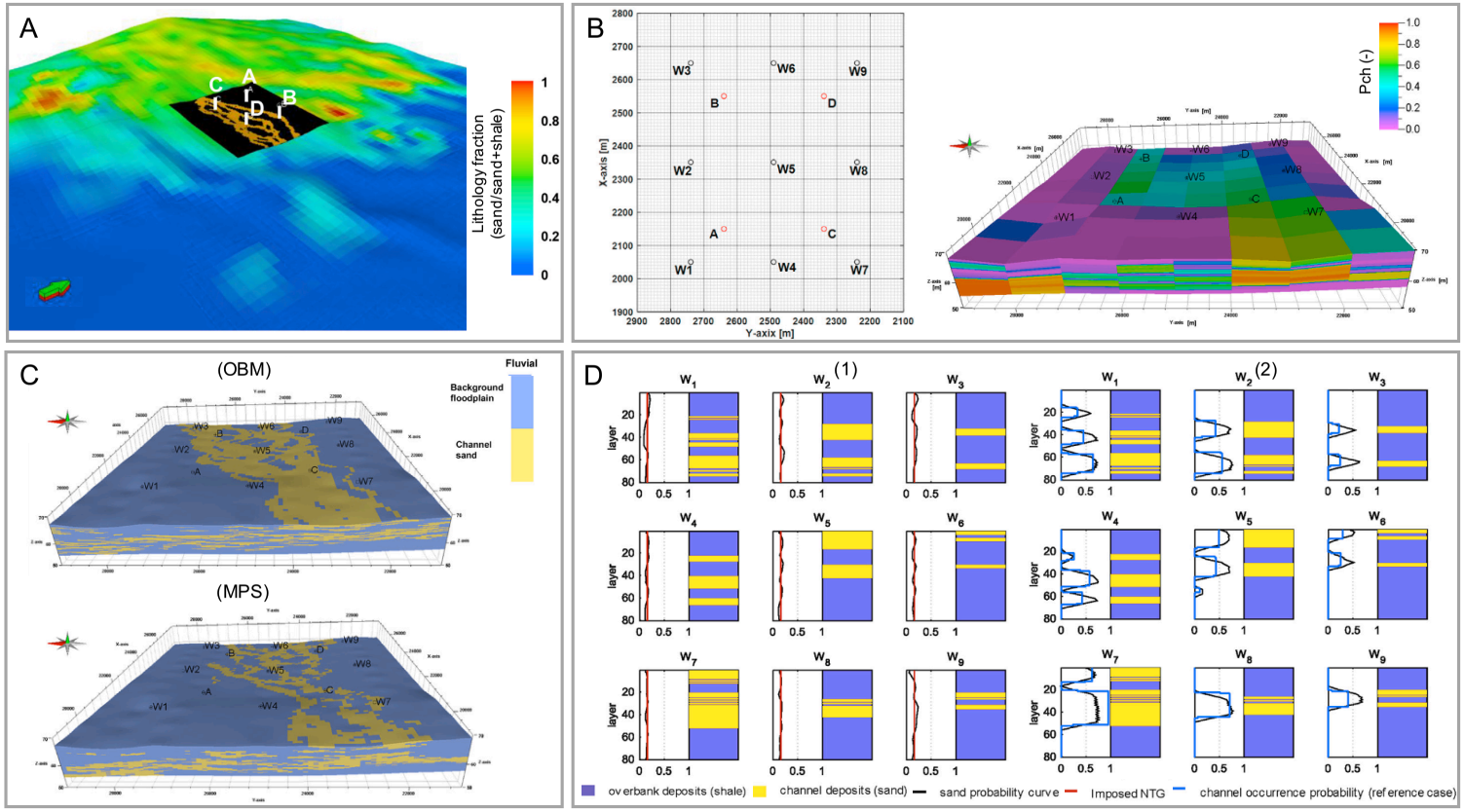

Figure 6.6: (A) Basin-scale model in terms of net to gross and fluvial architecture at reservoir scale. Reference wells A to D are also displayed (Sacchi et al., 2015). (B) 3D channel occurrence probability distribution at the basin scale in the reservoir area for the reference case. (C) Simulations with the geostatistical object modeling (top) and multipoint geostatistics approaches (bottom) of the 3D fluvial architecture at the reservoir scale for the reference case. (D) Monitoring locations W1-W9: sand probability curves unconditioned (1) and conditioned (2) to the channel occurrence probability distribution as calculated from a statistically representative number (100) of realisations (MPS approach). Each plot two columns: in the first column, the sand probability curve (black line) is plotted against the imposed N/G (red line) (1) or channel occurrence probability of the reference case (2). The second column represents the lithological sequence at reservoir scale for the base case scenario (Sacchi et al., 2016).

Here we demonstrate how the previous methodology may be significantly improved by evaluating the overall 3D reservoir architecture rather than monitoring the lithology at defined reservoir locations. Post-processing algorithms (chapter 4) allow automatic extraction of genetically related channel-belt and delta lobes (chronosomes) and their representations in space-time domain (Fig. 6.7). This intermediate construction stage facilitates automatic sequence-stratigraphic interpretation of basin fills, because it allows straightforward mapping of (near) isochronous boundaries between reservoir units, such as maximum flooding and regressive surfaces (Fig. 6.7C). In this way, the assessment of the uncertainty based on sand probability from a joint distribution of the sand volumes is possible, rather than from a marginal distribution only.

Our approach has two major advantages for conditioning relative to other schemes: (1) The low-resolution model is computationally efficient; (2) Channel belts may be fitted to local data (wells) by post-processing of model output. The first point is relevant for fitting basin-scale models to seismic; the second comes into play when a suitable geological scenario has been identified. Note that our approach to lithology prediction makes use of the same data as the conventional workflow, but in a more efficient way. In addition, the partitioning of the overall uncertainty into contributions at the basin and reservoir scales may be quantitatively assessed, and the information content of all available data may be quantified.

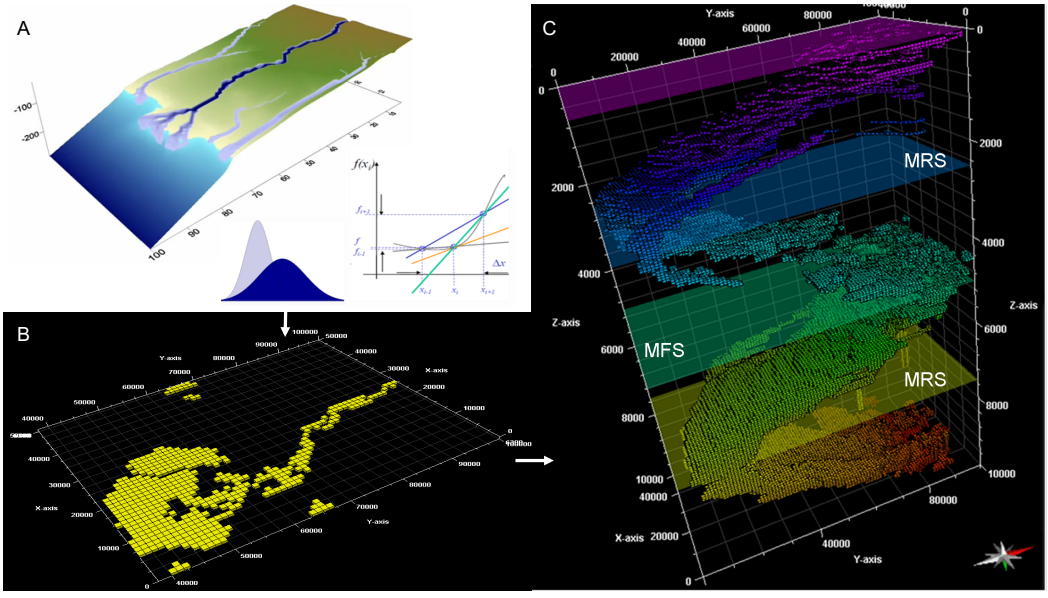

Figure 6.7: (A) A delta developing on the SimClast grid during run time (cell size 1 by 1 km), with high-resolution object- based channel-belt stratigraphy (sub-grid scale) obtained by stochastic post-processing methods. (B) Extracted channel belt and delta facies. (C) Automated sequence-stratigraphic interpretation at reservoir scale: extracted delta lobe facies and isochronous bounding surfaces (MFS and MRS) in time-space representation (x, y, t; Wheeler diagram).

6.7 The role of reservoir sedimentology

Reservoir sedimentology is the branch of applied sedimentology concerned with the quantitative description and prediction of the geometry, spatial distribution and reservoir properties of subsurface sedimentary units. Using a variety of datasets (i.e. seismic, well-log, outcrop and petrographic data), the practicing reservoir sedimentologist aims at capturing anisotropy and heterogeneity of sedimentary units at different scales in order to model uncertainties associated with reservoir quality distribution. Reservoir sedimentology regards also information about the impact of prominent depositional and post-depositional processes on reservoir properties. Having knowledge of the physical processes and environmental conditions at the time of deposition is important because their associated lithofacies and inherited particle-size characteristics (i.e. grain size and sorting) largely control matrix permeability. Analysis of sediment fabric, grain surface texture, nature of contacts, composition and pore structure can reveal sediment provenance as well as diagenetic and tectonic overprints.

The study of post-depositional (i.e. diagenetic) processes is of equally high relevance because diagenesis controls porosity and permeability changes by grain rearrangement, compaction, clay infiltration (i.e. dissolution and kaolinitization of detrital silicates, illite pore lining, chlorite/smectite coatings) and cementation (i.e. quartz, calcite, dolomite, pyrite, siderite) (Morad et al., 2000, 2010; Ajdukiewicz and Lander, 2010; Taylor et al., 2010; Bjørlykke, 2015). In this respect, process-oriented diagenesis models (and their close cousins, the reactive transport models) provide important insights into the understanding of spatial variations in diagenetic reactions and have accurately predicted sandstone reservoir quality in a variety of basins where compaction and quartz cementation involving certain framework grains and clay minerals are the main diagenetic processes (Worden et al., 2018).

In this study, we focused on channelized reservoirs and summarized the role of reservoir sedimentology in terms of three hierarchical sedimentary architecture levels/scales and their associated depositional processes and sedimentary products (Hajek and Wolinsky, 2012). Basin scale is the scale of sequence stratigraphy and includes processes that control the distribution of depositional environments such as allogenic forcing and mass balance (e.g. accommodation/supply). A previous study on the prediction of stratigraphic compartmentalization of marginal marine reservoirs (Ainsworth, 2010), yielded a hierarchical sequence stratigraphic framework on the basis of accommodation to coarse sediment supply (A/S) ratio and fluvial and coastal processes (Fig. 6.8). Based on observational changes in stacking pattern, sequence

stratigraphy provides a framework to subdivide sedimentary successions into genetically related sedimentary packages bounded by erosional and conformable surfaces and/or chronostratigraphically constrained lithosomes (chronosomes) (Fig. 6.9A). Figure 6.9B illustrates in two dimensions the subdivision of a fluvial succession into a high A/S fluvial system at the top and a low one below (Swift and Thorne, 1991; Thorne and Swift, 1991a, b; Muto and Steel, 1997).

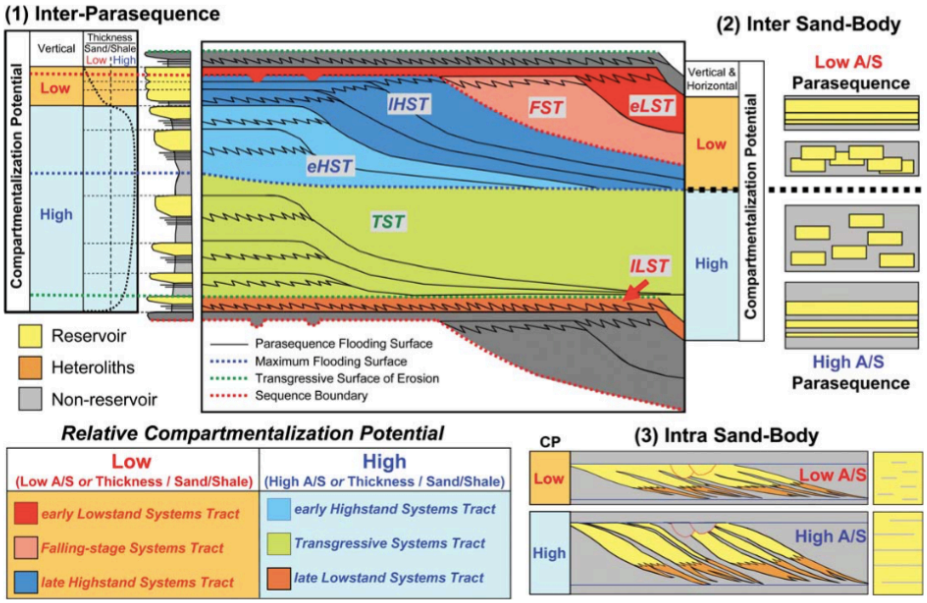

Figure 6.8: Sequence stratigraphy as a predictive tool for stratigraphic compartmentalization potential in marginal marine systems. Note that high compartmentalization potential equates to high A/S ratios and low compartmentalization potential to low A/S ratios at all hierarchical levels. Also note that high thickness divided by sand/shale ratios equate to high compartmentalization potential and low thickness divided by sand/shale ratios equate to low compartmentalization potential (CP) (after Ainsworth, 2010).

The second architecture level refers to system-specific architecture scale processes which regulate landscape formation and evolution, and are either allogenic (e.g. climatic) or autogenic in origin. Architecture scale processes dominate over intervals of 10^2-10^4 years and include avulsions and channel-floodplain interactions. Sedimentary products at this level include channel-belt sandstone stacks within fluvial successions, individual channel segments, levees, crevasse splays, overbank and floodplain sheets (Fig. 6.9C). Finally, event scale processes refer to short-lived processes which are prominent at daily to decadal time scales and produce landforms or beds (Fig. 6.9D). Processes include crevassing, levee building, mouth bar-induced bifurcations, as well as tidal and wave reworking in coastal areas. Lithofacies internal features (laminae) and pore structure are the resultant products at this stratigraphic level (Fig. 6.9E, 6.9F).

At the largest scale (basin scale), channel-belt geometries which are typically larger than the field extent remain still very difficult to predict without detailed knowledge of the paleogeography, location of sediment entry points, sediment calibre, fluvial style, and basin history (tectonics and climate). The prime data source at the largest scale is seismic data. Data acquisition from subsurface and outcrop sedimentary units, ranging from architectural-element to pore scales, is commonly used to deal with scale levels 2 and 3. In the previous section, we provided an alternative workflow which more effectively uses the available seismic and well data to tackle reservoir sedimentology problems at the two largest scales. The smallest scale, which brings its own problems, lies beyond the scope of the thesis and will not be discussed further.

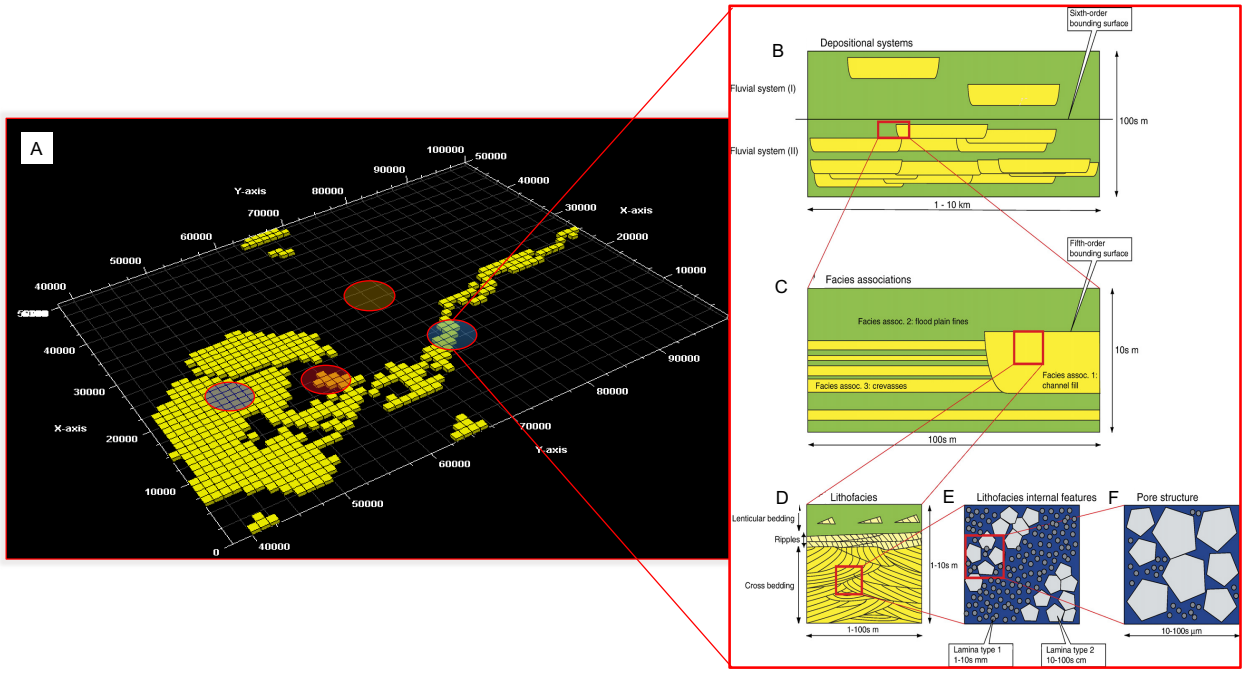

Figure 6.9: Multiscale characterization of fluvio-deltaic reservoirs: different scale and type of heterogeneities that affect reservoir quality distribution and fluid flow behaviour as captured by the analysis of process-based modelling results (this thesis) and outcrop and subsurface data (practice of daily geomodeler industry life) (after Keogh et al., 2007, modified from Weber, 1986, Haldorsen, 1986, Dreyer et al., 1990).

6.8 Conclusions

The proposed workflow for conditioning reservoir models to well data is a two-step operation: (1) a low-resolution basin-scale model is inverted to approximate overall basin-fill properties (based on geological a-priori information about relative sea-level changes, sediment supply, and palaeogeography; (2) the reservoir-scale architecture of selected parts of the basin fill is generated by post-processing algorithms which perform conditional simulation by taking into account a set of pseudo wells acting as boundary conditions for the reservoir model. Pilot tests have illustrated the feasibility of the proposed approach (Karamitopoulos et al., 2014; Dalman et al., 2015; Sacchi et al. 2015, 2016). The implementation of geological constraints on reservoir models is expected to improve estimation of sand-body connectivity and dynamic reservoir behaviour, and will therefore contribute to reduction of non-uniqueness in current static reservoir models. Furthermore, the uncertainty associated with each basin-scale parameter can be propagated all the way through to reserve estimation. Ultimately, a powerful combination of data assimilation techniques and process-based geological model optimization in a closed-loop reservoir management framework (Jansen et al., 2009) may activate continuous consistency checks across the 'exploration-production boundary' and thus maximize reservoir performance in terms of recovery efficiency. The approach outlined above thus permits geological reservoir modelling to be integrated in a closed-loop reservoir management process (Fig. 6.10).

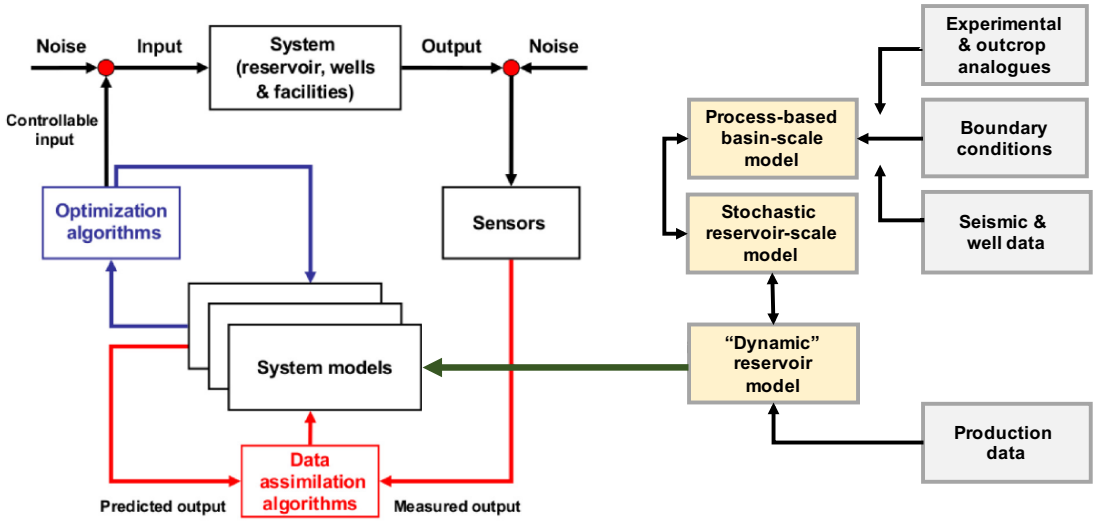

Figure 6.10: Process-based geological reservoir models enhancing system models of the closed-loop reservoir management process (modified from Jansen et al., 2009).

6.9 Future study

Although this study has provided new insights concerning the application of process-based stratigraphic models to simulate sedimentary architecture of fluvio-deltaic systems and improve lithology prediction, there are several questions remain to be addressed. As shown, numerical models in forward and inverse mode provide attractive tools for simulating earth surface processes over a wide range of temporal and spatial scales while allowing full access to the response (model output) formed under known initial and boundary conditions. In this perspective, the predictive capabilities of process-based stratigraphic models may be further increased by: a) including more complex syn- and post-depositional processes and b) more accurately approximating the initial and boundary conditions of prospective sedimentary basins.

The first part can be tackled by coupling hydrogeological, sediment transport and subsidence numerical models in order to link surface processes to substrate characteristics, i.e. the interplay of unsaturated (vadose) zone recharging, groundwater table fluctuation and subsidence and has been poorly explored as a controlling mechanism for sedimentary architecture and avulsion dynamics. In addition, the incorporation of peatland dynamics modules may contribute to capturing the effects of peat deposition and compaction on the sedimentary architecture of fluvio-deltaic systems (Van Asselen et al., 2009). Coastal dynamics modules able to simulate waves, tides and alongshore drift may account for sediment erosion, redistribution and deposition, and thus making possible to analyze backwater effects on avulsion dynamics and the spatial distribution of lithofacies internal features (laminae) (Fagherazzi et al., 2008; Kleinhans et al., 2010; Chatanantavet et al., 2012; Ganti et al., 2016). Future efforts should also focus on compaction and pore structure evolution. In siliciclastic sedimentary systems, depositional processes control the composition of sediments which tends to be a function of grain-size (i.e. SiO_2/ Al_2O_3 ratios typically decrease with decreasing grain size or decreasing textural maturity within a given size range) (Weltje & Von Eynatten 2004). At the time of deposition, the interconnected pore volume is regulated by sediment sorting which will preferentially enrich specific materials in certain grain-size fraction. The inclusion of modules that simulate post-depositional (early-diagenetic) processes (i.e. coupling of process-based stratigraphic models to reactive transport models) may contribute to the understanding of pore structure evolution of sediments after deposition, from fabric initiation following packing and grain-rearrangement to the spatial relationships of early diagenetic products within a sequence (Morad et al., 2012). The proposed improvements may better our understanding on the architectural arrangement of chronosomes, as well as to contribute to environmental mitigation strategies, i.e.

simulate river systems under different groundwater extraction scenarios (Erban et al., 2014; Minderhoud et al., 2017). The application of software able to take advantage of parallel computing capabilities of computer clusters may tackle the increasing computational overhead when coupling models that implement additional, more complex geological processes.

The second part can be tackled by integrating multiscale, multi-type datasets including satellite and geophysical/geological data supported by absolute and relative dating techniques in order to construct detailed chronostratigraphic frameworks for stratigraphic levels or zones of interest and analyse long-term source-sink sediment budgets. Geochemical proxies may enable palaeodischarge estimation and palaeochannel network reconstruction (Bhattacharya et al., 2016), and thus help to trace avulsion sites and sequences in ancient fluvial strata. Palaeotopography can be estimated using geodynamic modeling (Allen and Allen, 2013) or interpreted from thermochronometry (Reiners et al., 2017), whereas temperature variations may be estimated using climate proxies i.e. palaeosols. Data integration may thus steer the reconstruction of prospective sedimentary basins (Madof et al., 2019) and help to constrain basin-fill evolution scenarios (Sømme et al., 2009, 2013a, b; Gvirtzman et al., 2014; Hawie et al., 2017). The development of alternative model calibration/matching routines may help to more efficiently separate out model realizations which are geologically unrealistic, and thus narrow down the range of possible scenarios from the model outset. At the scale of groundwater, hydrocarbon and geothermal reservoirs, the integration of boreholes, geophysical and outcrop data, supported by dynamic reservoir data should be pursued to unravel details on internal sedimentary architecture (laminae-scale) and its effects on porosity and permeability estimation.

References

Abrahamsen, P, Hauge, R., Odd Kolbjørnsen, O., (Eds.) 2012. Geostatistics Oslo 2012. Springer, Dordrecht, 559pp. https://doi.org/10.1007/978-94-007-4153-9.

Agterberg, F., 2014. Geomathematics: Theoretical Foundations, Applications and Future Developments. Springer, Cham, 553pp. https://doi.org/10.1007/978-3-319-06874-9.

Ainsworth, R.B., 2006. Sequence stratigraphic-based analysis of reservoir connectivity: influence of sealing faults – a case study from a marginal marine depositional setting. Pet. Geosci. 12, 127-141.

Ainsworth, R.B., 2010. Prediction of stratigraphic compartmentalization in marginal marine reservoirs. From: Jolley, S.J., Fisher, Q.J., Ainsworth, R.B., Vrolijk, P J. & Delisle, S. (Eds.), Reservoir Compartmentalization. Geol. Soc. London Spec. Publ. 347, 199-218.

Ajdukiewicz, J.M., Lander, R.H., 2010. Sandstone reservoir quality prediction: the state of the art. AAPG Bull. 94, 1083-1091.

Allen, J. R.L., 1965. Fining-upwards cycles in alluvial successions. Geol. J., 4, 229-246.

Allen, J.R.L., 1978. Studies in fluviatile sedimentation: an exploratory quantitative model for the architecture of avulsion-controlled alluvial suites. Sed. Geol., 21, 129-147.

Allen, J.R.L., 1979. Studies in fluviatile sedimentation: an elementary model for the connectedness of avulsion-related channel sand bodies. Sed. Geol. 24, 253-267.

Allen, P.A., 1997. Earth Surface Processes. Blackwell Science Ltd. 404pp.

Allen, P.A., 2008. Time scales of tectonic landscapes and their sediment routing systems. In: Earth's Dynamic Surface: Catastrophe and Continuity in Landscape Evolution (ed. by K. Gallagher, S.J. Jones and J. Wainwright). Geol. Soc. London, Spec. Publ. 296, 7–28.

Allen, P.A., 2017. Sediment Routing Systems: The Fate of Sediment from Source to Sink. Cambridge: Cambridge University Press. doi:10.1017/9781316135754.

Allen, P.A, Allen. J.R. 2013. Basin Analysis: Principles and Application to Petroleum Play Assessment (version 3rd ed.). 3rd ed. Chichester, West Susex, UK: Wiley-Blackwell. 632pp.

Allen, P.A., Collinson, J.D., 1986. Lakes. In: Sedimentary Environments and Facies (ed. by H.G. Reading), Blackwell Scientific Publications, Oxford, 63–94.

Allen, P.A., Densmore, A.L., 2000. Sediment flux from an uplifting fault block. Basin Res. 12, 367-380.

Allen, P.A., Heller, P.L., 2012. The timing, distribution and significance of tectonically generated gravels in terrestrial sediment routing systems. In: Tectonics of Sedimentary Basins: Recent Advances (ed. by C. Busby and A. Azor Pérez), Wiley-Blackwell, 111–130, 647pp.

Allen, P.A., Hovius, N., 1998. Sediment supply from landslide- dominated catchments: implications for basin-margin fans. Basin Res. 10, 19–35.

Allen, P.A., Armitage, J. J., Carter, A., Duller, R.A., Michael, N.A., Sinclair, H.D., Whitchurch, A.L., Whittaker, A.C., 2013. The Qs problem: Sediment volumetric balance of proximal foreland basin systems. Sedimentology, 60, 102-130.

Anderson, M.P., Woessner, W.W., 1992. Applied Groundwater Modeling-Simulation of Flow and Advective Transport. Academic Press, Inc., San Diego, CA, 381pp.

Andrews, E.D., 1980. Effective and banfull discharges of streams in the Yampa river basin, Colorado and Wyoming. J. Hydrol. 46, 311-330.

Armstrong, M., Dowd, P.A., 1993 (Eds.) Geostatistical Simulations: Proceedings of the Geostatistical Simulation Workshop, Fontainebleau, France, 27–28 May 1993. Kluwer Academic Publishers.

Arnold, D., Demyanov, V., Rojas, T., 2019. Uncertainty quantification in reservoir prediction: Part 1-Model realism in history matching using geological prior definitions. Math. Geosci. 51, 209-240.

Arpat, G.B., Caers, J., 2007. Conditional Simulation with Patterns**.** Math. Geol. 39, 177-203.

ASCE., 1966. Nomenclature for Bed Forms in Alluvial Channel. Report of the Task Force on Bed Forms in Alluvial Channels of the Committee on Sedimentation. J. Hydraul. Div. Amer. Soc. Civil Eng. 92, 51-64.

Ashmore, P.E., 1991a. How do gravel-bed rivers braid? Can. J. Earth Sci. 28, 326-341.

Ashmore, P.E., 1991b. Channel morphology and bed load pulses in braided, gravel-bed streams. Geogr. Ann. 68, 361-371.

Ashworth, P.J., Best, J.L., Jones, M.A., 2007. The relationship between channel avulsion, flow occupancy and aggradation in braided rivers: insights from an experimental model. Sedimentology 54, 497–513.

Aslan, A., Autin, W.J., 1999. Evolution of the Holocene Mississippi River floodplain, Ferriday, Louisiana: insights on the origin of fine-grained floodplains. J. Sed. Res. 69, 800-815.

Atkinson, P.M., Lloyd, C.D., (Eds.) 2010. geoENV VII – Geostatistics for Environmental Applications. Springer, Dordrecht. https://doi.org/10.1007/978-90-481-2322-3.

Autin, W.J., Burns, S.F., Miller, B.J., Saucier, R.T., Snead, J.I., 1991. Quaternary geology of the Lower Mississippi Valley. In: Morrison, R.B. (Ed.), Quaternary Nonglacial Geology:

Conterminous U.S. In: The Geology of North America, vol. K-2. Geological Society of America, Boulder, Colorado, pp. 547-581.

Barrell, J., 1917. Rhythms and the measurement of geologic time. Geol. Soc. Am. Bull. 28, 745–904.

Bates, C., 1953. Rational theory of delta formation. AAPG Bull. 37, 2119-2162.

Bates, R.L., Jackson, J.A., 1987. Glossary of Geology, third ed. American Geological Institute, Alexandria, Virgina.

Bentley, M., 2016. Modelling for comfort? Pet. Geosci. 22, 3-10.

Berner, R.A., Berner, E.K., 1997. Silicate weathering and climate. In: Tectonic Uplift and Climate Change (ed. by W. Ruddiman), Plenum Press, New York, 353-365.

Besag, J., 1986. On the Statistical Analysis of Dirty Pictures. Journal of the Royal Statistical Society: Series B (Methodological), 48, 259-279.

Bhattacharya, J.P., 2006. Deltas. In: Walker, R.G., Posamentier, H. (Eds.): Facies Models revisited. SEPM Spec. Publ. 84, 237-292.

Bhattacharya, J.P., 2011. Practical problems in the application of the sequence strati- graphic method and key surfaces: integrating observations from ancient fluvial– deltaic wedges with Quaternary and modelling studies. Sedimentology 58, 120-169.

Bhattacharya, J.P., Copeland, P., Lawton, T.F., Holbrook, J., 2016. Estimation of source area, river paleo-discharge, paleoslope, and sediment budgets of linked deep-time depositional systems and implications for hydrocarbon potential. Earth Sci. Rev. 153, 77-110.

Bhattacharya, J.P., Walker, R.G., 1992. Deltas. In: Facies Models: Response to Sea Level Change (R.G. Walker and N.P. James, Eds.). Geological Association of Canada, St Johns, NF, 157–177.

Bjørlykke, K., 2015. Petroleum Geoscience: From Sedimentary Environments to Rock Physics-Second Edition. Springer, 662pp.

Blair, T.C, McPherson, J.G., 1994. Alluvial fans and their natural distinction from rivers based on morphol- ogy, hydraulic processes, sedimentary processes, and facies. J. Sed. Res. A64, 451-490.

Blum, M.D., Aslan, A., 2006. Signatures of climate vs. sea- level change within incised valley-fill successions: Quaternary examples from the Texas Gulf Coast. Sed. Geol. 190, 177-211.

Blum, M.D., Hattier-Womack, J., 2009. Climate change, sea-level change, and fluvial sediment supply to deepwater systems. In Kneller, B., Martinsen, O.J., McCaffrey, B. (Eds.), External Controls on Deep Water Depositional Systems: Climate, Sea-Level, and Sediment Flux. SEPM Spec. Publ. 92, 15–39.

Blum, M.D., Törnqvist, T.E., 2000. Fluvial response to climate and sea-level change: a review and look forward. Sedimentology, 47 (Supplement), 1-48.

Blum, M.D., Martin, B.J., Milliken, K., Garvin, M., 2013. Paleovalley systems: insights from quaternary analogs and experiments. Earth Sci. Rev. 116, 128–169.

Boggs, S., Jr., 1995. Principles of Sedimentlogy and Stratigraphy, 2nd ed.: Englewood Cliffs, NJ, Prentice Hall, 774 pp.

Bornholdt, S., Nordlund, U., Westphal, H., 1999. Inverse stratigraphic modelling using genetic algorithms. In: Harbaugh, J.W. et al. (Eds.), Numerical Experiments in Stratigraphy: Recent Advances in Stratigraphic and Sedimentologic Computer Simulations. SEPM Spec. Publ. 62, 85-90.

Bowman, S.A., Vail, P.A., 1999. Interpreting the stratigraphy of the Baltimore Canyon Section, Offshore New Jersey with PHIL, a stratigraphic simulator. In Numerical Experiments in Stratigraphy: Recent Advances in Stratigraphic and Sedimentologic Computer Simulations (Eds J.W. Harbaugh, L.W. Watney, E.C. Rankey, R. Slingerland, R.H. Goldstein and E.K. Franseen), SEPM Spec. Publ., 62, 117-138.

Boyd, R., Dalrymple, R.W., Zaitlin, B.A., 1992. Classification of clastic coastal depositional environments. Sed. Geol. 80, 139–150.

Bratvold, R. B., Holden, L., Svanes, T., Tyler, K., 1995. STORM: Integrated 3D Stochastic Reservoir Modeling Tool for Geologists and Reservoir Engineers. Society of Petroleum Engineers. doi:10.2118/27563-PA.

Braun, J., 2005. Quantitative constraints on the rate of landform evolution derived from low-temperature thermochronology. Reviews in Mineral Geochemistry, 58, 351-374.

Bridge, J.S., 2003. Rivers and Floodplains: Forms, Processes and Sedimentary Record, Blackwell Publishing Ltd., Oxford, 491pp.

Bridge, J.S., Leeder, M.R., 1979. A simulation model of alluvial stratigraphy. Sedimentology 26, 617-644.

Brierley, G.J., Ferguson, R.J., Woolfe, K.J., 1997. What is a fluvial levee? Sed. Geol. 114, 1-9.

Bristow, C.S., 1999. Gradual avulsion, river metamorphosis and reworking by underfit streams: a modern example from the Brahmaputra river in Bangladesh and a possible ancient example in the Spanish Pyrenees. In: N.D. Smith and J. Rogers (Eds.), Fluvial Sedimentology VI. Int. Assoc. Sedimentol. Spec. Publ. 28, 221-230.

Bryant, M., Falk, P., Paola, C., 1995. Experimental study of avulsion frequency and rate of deposition. Geology, 23, 365-368.

Bull, W.B., 1977. The alluvial fan environment. Progress in Physical Geography, 1, 222–270.

Bull, W.B., 1991. Geomorphic Responses to Climate Change. Oxford University Press, New York.

Bull, W.B., Schick, A.P., 1979. Impact of climatic change on an arid watershed: Nahal Yael, Southern Israel. Quatern. Res. 11, 153–171.

Burgess, P.M., 2012. A brief review of developments in stratigraphic forward modelling 2000-2009. In: Roberts, D.G., Bally, A.W. (Eds.), Regional Geology and Tectonics: Principles of Geologic Analysis, Elsevier, p. 378-404.

Burgess, P.M., 2016. RESEARCH FOCUS: The future of the sequence stratigraphy paradigm: Dealing with a variable third dimension. Geology 44, 335-336.

Burgess, P.M., Lammers, H.M, Van Oosterhout, C., Granjeon, D., 2006. Multivariate sequence stratigraphy: Tackling complexity and uncertainty with stratigraphic forward modeling, multiple scenarios and conditional frequency maps. AAPG Bull. 90, 1883-1901.

Caers, J, Zhang, T., 2004. Multiple-point geostatistics: a quantitative vehicle for integration geologic analogs into multiple reservoir model, integration of outcrop and modern analog data in reservoir models. AAPG Mem. Doi: https://doi.org/10.1306/M80924C18.

Carlston, C.W., 1965. The relation of free meander geometry to stream discharge and its geomorphic implications. Am. J. Sci. 263, 864-885.

Carter, R.M., 1998. Two models: global sea-level change and sequence stratigraphic architecture. Sed. Geol., 122, 23–36.

Carter, R.M., 2005. A New Zealand climatic template back to c. 3.9 Ma: ODP Site 1119, Canterbury Bight, south-west Pacific Ocean, and its relationship to onland successions. J. Roy. Soc. NZ 35, 9-42.

Carvajal, C., Steel, R. 2012. Source-to-Sink Sediment Volumes within a Tectono-Stratigraphic Model for a Laramide Shelf-to-Deep-Water Basin: Methods and Results. In Tectonics of Sedimentary Basins (eds C. Busby and A. Azor). Blackwell Publishing Ltd., Oxford, 131–151.

Catuneanu, O., 2006. Principles of Sequence Stratigraphy. Elsevier, Amsterdam. 375pp.

Catuneanu, O., Zecchin, M., 2013. High-resolution sequence stratigraphy of clastic shelves II: controls on sequence development. Mar. Pet. Geol. 39, 26-38.

Catuneanu, O., Abreu, V., Bhattacharya, J.P., Blum, M.D., Dalrymple, R.W., Eriksson, P.G., Fielding, C.R., Fisher, W.L., Galloway, W.E., Gibling, M.R., Giles, K.A., Holbrook, J.M., Jordan, R., Kendall, C.G.St.C., Macurda, B., Martinsen, O.J., Miall, A.D., Neal, J.E., Nummedal, D., Pomar, L., Posamentier, H.W., Pratt, B.R., Sarg, J.F., Shanley, K.W., Steel, R.J., Strasser, A., Tucker, M.E., Winker, C., 2009. Towards the standardization of sequence stratigraphy. Earth-Sci. Rev. 92, 1-33.

Catuneanu, O., Galloway, W.E., Kendall, C.G.St.C., Miall, A.D., Posamentier, H.W., Strasser, A., Tucker, M.E., 2011. Sequence stratigraphy: methodology and nomenclature. Newsl. Stratigr. 44, 173-245.

Cazanacli, D., Smith, N.D., 1998. A study of morphology and texture of natural levees-Cumberland Marshes Saskatchewan, Canada. Geomorphology, 25, 43-55.

Charvin, K., Gallagher, K.L., Hampson, G., Labourdette, R., 2009. A Bayesian approach to inverse modelling of stratigraphy, part I: method. Basin Res. 21, 5-25.

Charvin, K., Hampson, G.J., Gallagher, K.L., Storms, J.E.A., Labourdette, R., 2011. Characterization of controls on high-resolution stratigraphic architecture in wave-dominated shoreface shelf parasequences using inverse numerical modeling. J. Sed. Res. 81, 562-578.

Chatanantavet, P., Lamb, M.P., Nittrouer, J.A., 2012. Backwater controls of avulsion location on deltas. Geophys. Res. Lett. 39, L01402.

Cheng-Hou, Z., Greeuw, G., Jekel, J., Rosenbrand, W., 1990. A New Classification Chart for Soft Soils using the Piezocone Test. Eng. Geol. 29, 31-47.

Christie-Blick, N. 1991. Onlap, offlap, and the origin of unconformity-bounded depositional sequences. Mar. Geol. 97, 35-56.

Clemensten, R., Hurst, A.R., Knarud, R., More, K.H., 1989. A computer program for evaluation of fluvial reservoirs, *in* Buller, A. T., et al. (Eds.), North Sea Oil and Gas Reservoirs II, Proceedings of the North Sea Oil and Gas Reservoirs Conference. Graham and Trotman, London, p. 373–385.

Clevis, Q., de Boer, P., Wachter, M., 2003. Numerical modelling of drainage basin evolution and three-dimensional alluvial fan stratigraphy. Sed. Geol. 163, 85-110.

Coleman, J.M., 1969. Brahmaputra River: channel processes and sedimentation. Sed. Geol. 3, 129-239.

Coleman, J.M., Wright, L.D., 1975. Modern river deltas: variability of processes and sand bodies. In: Deltas, Models for Exploration (M.L. Broussard, Ed.). Houston Geological Society, Houston, TX, pp. 99–149.

Colombera, L., Mountney, N.P., Russell, C.E., Shiers, M.N., McCaffrey, W.D., 2017. Geometry and compartmentalization of fluvial meander-belt reservoirs at the bar-form scale: Quantitative insight from outcrop, modern and subsurface analogues. Mar. Petrol. Geol. 82, 35-55.

Cowell, P.J., Stive, M.J.F., Niedoroda, A.W., de Vriend, H.J., Swift, D.J.P., Kaminsky, G., Capobianco, M., 2003. The coastal tract (Part 1): A conceptual approach to aggregated modelling of low-order coastal change. J. Coastal Res. 19, 812-827.

Cowell, P.J., Stive, M.J.F., Niedoroda, A.W., Swift, D.J.P., de Vriend, H.J., Buijsman, M.C., de Boer, P.L., 2003. The coastal tract (Part 2): Applications of aggregated modeling of low-order coastal change. J. Coastal Res. 19, 828-848.

Cressie, N. 1990. The origins of kriging. Math. Geol. 22, 239-252.

Cressie, N., 1991. Statistics for spatial data. John Wiley & Sons, New York, 900pp.

Cross, T., Lessenger, M., 1999. Construction and application of stratigraphic inverse model. In: Harbaugh, J.W. et al. (Eds.), Numerical Experiments in Stratigraphy: Recent Advances in Stratigraphic and Sedimentologic Computer Simulations. SEPM Spec. Publ. 62, 69-83.

Cross, T.A., Lessenger, M.A, 1998. Correlation Strategies for Clastic Wedges: AAPG Search and Discovery Abstract #90937.

Dade, W.B., Friend, P.F., 1998. Grain size, sediment-transport regime and channel slope in alluvial rivers. J. Geol. 106, 661-675.

Dadson, S.J., Hovius, N., Chen, H., Dade, W.B., Hsieh, M., Willet, S.D., Hu, J., Horng, M., Chen, M., Stark, C., Lague, D., Lin, J., 2003. Erosion of the Taiwan orogen. Nature, 426, 648–651.

Dalman, R.A.F., Weltje, G.J., 2008. Sub-grid parameterisation of fluvio-deltaic processes and architecture in a basin-scale stratigraphic model. Comput. Geosci. 34, 1370-1380.

Dalman, R.A.F., Weltje, G.J., 2012. SimClast: An aggregated forward stratigraphic model of continental shelves. Comput. Geosci. 38, 115-126.

Dalman, R.A.F., Weltje, G.J., Karamitopoulos, P., 2015. High-resolution sequence stratigraphy of fluvio–deltaic systems: Prospects of system-wide chronostratigraphic correlation: Earth Planet. Sci. Lett. 412, 10-17.

Dalrymple, R.W., 1992. Tidal Depositional Systems. In: Walker, R.G., James, N.P., Eds., Facies Models: Response to Sea Level Change, Geological Association of Canada, Newfoundland, 195-218.

Dalrymple, R.W., Zaitlin, B.A., Boyd, R., 1992. Estuarine facies models: conceptual basis and stratigraphic implications. J. Sed. Petrol. 62, 1130–1146.

Daly, C., Caers, J., 2010. Multi-point geostatistics – an introductory overview. First Break, 28, 39-47.

Dana, J.D., Rice, W.N., 1897. Revised Text-book of Geology. American Book Company, New York.

Daniel, J.F., 1971. Channel movement of meandering Indiana streams. USGS Prof. Pap. 732A.

Desbarats, A.J., Bachu, S., 1994. Geostatistical analysis of aquifer heterogeneity from the core scale to the basin scale: A case study. Water Resour. Res. 30, 673-684, doi:10.1029/93WR02980.

Dettinger, M.D., Ghil, M., Strong, C.M., Weibel, W., Yiou, P., 1995. Software expedites singular-spectrum analysis of noisy time series, Eos, 76, 12-21.

Deutsch, C.V., 1989. DECLUS: A Fortran 77 program for determining optimum spatial declustering weights. Comput. Geosci. 15, 325-332.

Deutsch, C.V., 2002. Geostatistical Reservoir Modeling. Oxford University Press, Oxford, 376pp.

Deutsch, C.V., Journel, A.G. 1998. GSLIB. Geostatistical Software Library and User's Guide, 2nd ed., 369 pp.

Deutsch, C.V., Tran, 2002. FLUVSIM: a program for object-based stochastic modeling of fluvial depositional systems. Comput. Geosci. 28, 525-535.

Deutsch, C.V., Wang, L., 1996. Hierarchical object-based stochastic modeling of fluvial reservoirs. Math. Geol. 28, 857-880.

Deveugle, P.E.K., Jackson, M.D., Hampson, G.J., Farrell, M.E., Sprague, A.S., Stewart, J., Calvert, C.S., 2011. Characterization of stratigraphic architecture and its impact on fluid flow in a fluvial-dominated deltaic reservoir analog: Ferron Sandstone Member, Utah. AAPG Bull. 95, 693–727.

Dimitrakopoulos, R., 1994. (Ed.) Geostatistics for the next century: An International Forum in Honour of Michel David's Contribution to Geostatistics, Montreal, 1993. Kluwer Academic Publishers, Dordrecht. 499pp.

Dimitrakopoulos, R., Desbarats, A.J., 1993. Geostatistical modelling of gridblock permeabilities for 3D reservoir simulators. SPE Reservoir Engineering, 8, 13-18.

Doligez, B., Beucher, H., Geffroy, F., Eschard, R., 1999a. Integrated reservoir characterization: improvement in heterogeneities stochastic modelling by integration of additional external constraints. In Reservoir Characterization-Recent Advances, Schatzinger and Jordan (Eds.), AAPG Mem. 71, 333- 342.

Donselaar, M. E., Overeem, I. (2008) Connectivity of fluvial point-bar deposit: An example from the Miocene Huesca fluvial fan, Ebro Basin, Spain. AAPG Bull. 92, 1109-1129.

Donselaar, M.E., Cuevas Gozalo, M.C., Moyano, S., 2013. Avulsion processes at the terminus of semi-arid fluvial systems: Lessons from the Río Colorado, Altiplano endorheic basin, Bolivia. Sed. Geol. 283, 1-14.

Donselaar, M.E., Cuevas Gozalo, M.C., Van Toorenenburg, K.A., Wallinga, J., 2018. Self-organizing avulsions in an endorheic dryland river system. 20th International Sedimentological Congress, Quebec, Canada.

Donselaar, M.E., Cuevas Gozalo, M.C., Wallinga, J., 2017. Avulsion history of a Holocene semi-arid river system: outcrop analogue for thin-bedded fluvial reservoirs in the Rotliegend feather edge. 79th EAGE Conference & Exhibition, Paris, France, 12-15 June 2017.

Dreyer, T., Scheie, A., Walderhaug, O., 1990. Mini-permeameter-based study of permeability trends in channel sand bodies. AAPG Bull. 74, 359–374.

Dreyer, T., Falt, L.-M., Hoy, T., Knarud, R., Steel, R., Cuevas, J.-L.,1993. Sedimentary architecture of field analogues for reservoir information (SAFARI): a case study of the fluvial Escanilla formation, Spanish Pyrenees. In: Flint, S.S., Bryant, I.D. (Eds.), The Geological Modelling of Hydrocarbon Reservoirs and Outcrop Analogues. Blackwell Scientific Publications, pp. 57–80.

Dubrule, O., 1989. A Review of Stochastic Models for Petroleum Reservoirs. In: Armstrong M. (eds) Geostatistics. Quantitative Geology and Geostatistics, vol 4. Springer, Dordrecht.

Duller, R.A., Whittaker, A.C., Fedele, J.J., Whitchurch, A.L., Springett, J., Smithells, R., Fordyce, S., and Allen, P.A., 2010. From grain size to tectonics, J. Geophys. Res. 115, F03022.

Edmonds, D.A., Slingerland, R.L., 2007. Mechanics of river mouth bar formation: Implications for the morphodynamics of delta distributary networks. J. Geophys. Res. 112, F02034.

Edmonds, D.A., Hajek, E.A., Downton, N., Bryk, A.B., 2016. Avulsion flow-path selection on rivers in foreland basins. Geology 44, 695-698.

Edmonds, D.A., Hoyal, D.C.J.D., Sheets, B.A., Slingerland, R.L., 2009. Predicting delta avulsions: implications for coastal wetland restoration. Geology 37, 759-762.

Einsele, G., 2000. Sedimentary Basins: Evolution, Facies and Sediment Budget, Second Edition, Springer, Berlin.

Elfenbein, C., Ringrose, P.S., Christie, M., 2005. Small-scale reservoir modeling tool optimizes recovery offshore Norway. October World oil. 45-50.

Embry, A.F., 1995. Sequence boundaries and sequence hierarchies: problems and proposals, in Steel, R.J., Felt, V.L., Johannessen, E.P., Mathieu, C. (Eds.), Sequence stratigraphy on the Northwest European Margin. Norw. Petrol. Soc. Spec. Publ. 5, 1-11.

Embry, A.F., Johannessen, E.P., 1992. T-R sequence stratigraphy, facies analysis and reservoir distribution in the uppermost Triassic– Lower Jurassic succession, western Sverdrup Basin, Arctic Canada. In: Arctic Geology and Petroleum Potential (ed. by T.O. Vorren, E.

Bergseger, O.A. Dahl-Stamnes *et al*.), Special Publication, 2, Norwegian Petroleum Society, 121–146.

Emery, D., Myers, K., 1996. Sequence Stratigraphy. Blackwell, Oxford. 297pp.

Emiliani, C., 1955. Pleistocene temperatures. J. Geol., 63, 538-578.

Erban, L.E., Gorelick, S.M., Zebker H.A., 2014. Groundwater extraction, land subsidence, and sea-level rise in the Mekong Delta, Vietnam. Environ. Res. Lett. 9 (084010).

Esposito, C.R., Leonardo, D.D., Harlan, M., Straub, K.M., 2018. Sediment storage partitioning in alluvial stratigraphy: the influence of discharge variability. J. Sed. Res. 88, 717-726.

Fagherazzi, S., Overeem, I., 2007. Models of Deltaic and Inner Continental Shelf Landform Evolution. Annu. Rev. of Earth Planet. Sci. 35, 685-715.

Fagherazzi, S., Edmonds, D.A., Nardin, W., Leonardi, N., Canestrelli, A., Falcini, F., Jerolmack, D. J., Mariotti, G., Rowland, J.C., Slingerland, R.L., 2015. Dynamics of river mouth deposits, Rev. Geophys. 53, 642–672.

Falivene O., Frascati A., Gesbert S., Pickens J., Hsu Y., and Rovira A., 2014. Automatic calibration of stratigraphic forward models for predicting reservoir presence in exploration. AAPG Bull. 98, 1811-1835.

Fielding, C.R., 2010. Planform and facies variability in asymmetric deltas: facies analysis and depositional architecture of the Turonian Ferron sandstone in the Western Henry mountains, south-central Utah, USA. J. Sed. Res. 80, 455-479.

Fielding, C.R., 2015. Anatomy of falling-stage deltas in the Turonian Ferron sandstone of the western Henry mountains syncline, Utah: growth faults, slope failures and mass transport complexes. Sedimentology 62, 1–26.

Fielding, C. R., Alexander, J., Newman-Sutherland, E., 1997. Preservation of in situ, arborescent vegetation and fluvial bar construction in the Burdekin River of north Queensland, Australia. Palaeogeog., Palaeoclimatol., Palaeoecol. 135, 123-144.

Felletti, F., Bersezio, R., Giudici, M. 2006. Geostatistical Simulation and Numerical Upscaling, to Model Ground-Water Flow in a Sandy-Gravel, Braided River, Aquifer Analogue. J. Sed. Res. 76, 1215-1229.

Feynman, R.P., 1982. Simulating physics with computers. Int. J. Theor. Phys. 21, 467-488.

Frazier, D.E., 1967. Recent deltaic deposits of the Mississippi River: their development and chronology. Trans. - Gulf Coast Assoc. Geol. Soc. 17, 287-315.

Frazier, D.E., 1974. Depositional episodes: their relationship to the Quaternary stratigraphic framework in the northwestern portion of the Gulf Basin. University of Texas at Austin, Bureau of Economic Geology, Geological Circular, 4, 28pp.

Freeman, T., 1991. Calculating catchment area with divergent flow based on a regular grid. Comput. Geosci. 17, 413-422.

Friend, P.F., Slater, M.J., Williams, R.C., 1979. Vertical and lateral building of river sand- stone bodies, Ebro Basin, Spain. J. Geol. Soc. 136, 39–46.

Galloway, W.E., 1975. Process framework for describing the morphologic and stratigraphic evolution of deltaic depositional systems. In: Deltas, Models for Exploration (ed. by M.L. Broussard), Houston Geological Society, Houston, 87–98.

Galloway, W.E., 1989. Genetic stratigraphic sequences in basin analysis. I. Architecture and genesis of flooding-surface bounded depositional units. AAPG Bull. 73, 125-142.

Galy, V., France-Lanord, C., Beyssac, P., Faure, P., Kudrass, H., Palhol, F., 2007. Efficient organic carbon burial in the Bengal fan sustained by the Himalayan erosional system. Nature, 450, 407-410.

Ganti, V., Chadwick, A.J., Hassenruck- Gudipati, H.J., Lamb, M.P., 2016. Avulsion cycles and their stratigraphic signature on an experimental back- water-controlled delta. J. Geophys. Res. Earth Surf., 121, 1651–1675.

Garrison, J.R., Van Den Bergh, T.C.V., 2006. Effects of sedimentation rate, rate of relative rise in sea level, and duration of sea-level cycle on the filling of incised-valleys: examples of filled and "overfilled" incised valleys from the upper Ferron Sandstone, Last Chance Delta, East-Central Utah, U.S.A. In: *Dalrymple, R.W, Leckie, D.A., Tillman,* R.W. (Eds.): Incised Valleys in Time and Space, SEPM Spec. Publ. 85, 239-279.

Gawthorpe, R.L., Leeder, M.R., 2000. Tectono-sedimentary evolution of active extensional basins. Basin Res. 12, 195–218.

Geel, C.R., Weltje, G.J., 2003. A strategy for automated stratigraphic inversion of process-based models. In: Symposium on Analogue and Numerical Forward Modelling of Sedimentary Systems, 9-11 October 2003, Utrecht, The Netherlands, Abstracts, p. 26.

Geman, S. Geman, D. 1984. Stochastic Relaxation, Gibbs Distributions, and the Bayesian Restoration of Images," in IEEE Transactions on Pattern Analysis and Machine Intelligence, vol. PAMI-6, no. 6, 721-741.

Ghil, M., Allen, R.M., Dettinger, M.D., Ide, K., Kondrashov, D., Mann, M.E., Robertson, A., Saunders, A., Tian, Y., Varadi, F., Yiou, P., 2002. Advanced spectral methods for climatic time series. Rev. Geophys. 40, 1-41.

Gibling, M.R., Rust, B.R., 1990. Ribbon sandstones in the Pensylvanian Waddens Cove Formation, Sydney Basin, Atlantic Canada: the influence of siliceous duricrusts on channel-body geometry. Sedimentology 37, 45-65.

Gómez-Hernandez, J., Rodrigo-Ilarri, J., Rodrigo-Clavero, M.E., Cassiraga, E., Vargas-Guzmán, J.A., 2017. Geostatistics Valencia 2016. Springer, Cham. 974pp.

Gómez-Hernandez, J., Soares, A., Froidevaus, R., (Eds.) 1999. geoENV II-Geostatistics for environmental applications. Kluwer Academic Publishers, Dordrecht.

Gong, C., Steel, R.J., Wang, Y., Lin, C., Olariu, C., 2016. Shelf-margin architecture variability and its role in sediment-budget partitioning into deep-water areas. Earth-Sci. Rev. 154, 72-101.

Goovaerts, P., 1997. Geostatistics for Natural Resources Evaluation. Oxford University Press, 483pp.

Gouw, M.J.P., 2007. Alluvial architecture of fluvio-deltaic successions: a review with special reference to Holocene settings, Neth. J. Geosci. 86, 211-227.

Gran, K., Paola, C., 2001. Riparian vegetation controls on braided stream dynamics. Water Resour. Res., 37, 3275– 3283.

Granjeon, D., Joseph, P., 1999. Concepts and applications of a 3-D multiple lithology, diffusive model in stratigraphic modeling. In: Harbaugh, J.W. et al. (Eds.), Numerical Experiments in Stratigraphy: Recent Advances in Stratigraphic and Sedimentologic Computer Simulations, SEPM Spec. Publ. 62, 197- 210.

Gregory-Wodzicki, K.M., 2000. Uplift history of the Central and Northern Andes: A review. Geol. Soc. Am. Bull. 112, 1091-1105.

Griffiths, C.M., 1996. A stratigraphy for the 21st Century: First Break 14, 383-389.

Griffiths, C.M., Nordlund, U., 1993. Chronosome and quantitative stratigraphy. Geoinformatics 4, 327-336.

Griffiths, C.M., Dyt, C., Paraschivoiu, E., Liu, K., 2001. SedSim in hydrocarbon exploration. In: D. Merriam, J.C. Davis, (Eds.), Geologic Modeling and Simulation: Kluwer Academic, New York, 352 p.

Gvirtzman, Z., Csato, I., Granjeon, D., 2014. Constraining sediment transport to deep marine basins through submarine channels: The Levant margin in the Late Cenozoic. Marine Geology, 347, 12-26.

Hajek, E.A., Edmonds, D.A., 2014. Is river avulsion style controlled by floodplain morphodynamics? Geology 42, 199-202.

Hajek, E.A., Heller, P.L., Sheets, B.A., 2010. Significance of channel-belt clustering in alluvial basins. Geology, 38, 535–538.

Hajek, E.A., Straub, K.M., 2017. Autogenic Sedimentation in Clastic Stratigraphy. Annu. Rev. Earth Planet. Sci., 45, 681–709.

Hajek, E.A., Wolinsky, M.A., 2012. Simplified process modelling of river avulsion and alluvial architecture: connecting models and field data. Sed. Geol. 257, 1-30.

Haldorsen, H.H., 1986. Simulator Parameter Assignment and the Problem of Scale in Reservoir Engineering. In: Lake, L.W., Caroll, H.B. (Eds.), Reservoir Character ization. Academic Press, Orlando, p. 293-340.

Haldorsen, H.H., Chang, D.M., 1986. Notes on Stochastic Shales: From Outcrop to Simulation Model. In Proceedings of the Reservoir Engineering Technical Conference, April 29-May 1. Dallas, TX, edited by L.W. Lake and H.B. Carroll, Academic Press, Orlando, Fla., 1986.

Haldorsen, H., Damsleth, E., 1990, Stochastic Modeling: J. Petrol. Technol., 42, 404-412.

Hampson, G.J., 2000. Discontinuity surfaces, clinoforms, and facies architecture in a wave-dominated shoreface-shelf parasequence. J. Sed. Res. 70, 325-340.

Hampson, G.J., 2016. Towards a sequence stratigraphic solution set for autogenic processes and allogenic controls: Upper Cretaceous strata, Book Cliffs, Utah, USA. J. Geol. Soc. London 173, 817-836.

Haq, B.U., Hardenbol, J., Vail, P.R., 1987. Chronology of fluctuating sea levels since the Triassic (250 Myr ago to present). Science, 235, 1156-1167.

Harding, A., Strebelle, S., Levy, M., Thorne, J., Xie, D., Leigh, S., Preece, R. 2005. Reservoir Facies Modelling: New Advances in MPS. In: Leuangthong O., Deutsch C.V. (eds) Geostatistics Banff 2004. Quantitative Geology and Geostatistics, 14, 559-568.

Hawie, N., Deschamps, R., Granjeon, D., Nader, F.H., Gorini, C., Müller, C., Montadert, L., Baudin, F., 2017. Multi-scale constraints of sediment source to sink systems in frontier basins: a forward stratigraphic modelling case study of the Levant region. Basin Res. 29, 418-445.

Hay, W.W., 1998. Detrital sediment fluxes from continents to oceans. Chem. Geol. 145, 287–323.

Heffern, E.L., Reiners, P.W., Naeser, C.W., Coates, D.A., 2008. Geochronology of clinker and implications for evolution of the Powder River Basin landscape, Wyoming and Montana. Geol. Soc.Am. Rev.Eng. Geol. 18, 155–175.

Helland-Hansen, W., Gjelberg, J.G., Conceptual basis and variability in sequence stratigraphy: a different perspective. Sed. Geol. 92, 31-52.

Heller, P.L., Paola, C. 1992. The large scale dynamics of grain-size variation in alluvial basins; 2, application to syntectonic conglomerate. Basin Res. 4, 91–102.

Heller, P.L., Paola, C., 1996. Downstream changes in alluvial architecture: an exploration of controls on channel stacking patterns. J. Sed. Res. 66, 297-306.

Heward, A.P., 1981. A review of wave-dominated clastic shoreline deposits. Earth Sci. Rev. 17, 223-276.

Hoeksema, R.J., Kitanidis, P.K., Analysis of potential variability of properties of selected aquifers. Water Resour. Res. 21, 563-572.

Hogg, S.E., 1982. Sheetfloods, sheetwash, sheet flow, or . . . Earth Sci. Rev. 18, 59–76.

Holbrook, J., Bhattacharya, J.P., 2012. Reappraisal of the sequence boundary in time and space: case and considerations for an SU (subaerial unconformity) that is not a sediment bypass surface, a time barrier, or an unconformity. Earth Sci. Rev. 113, 271-302.

Holbrook, J., Scott, R.W., Oboh-Ikuenobe, F.E., 2006. Base-level buffers and buttresses: a model for upstream versus downstream control on fluvial geometry and architecture within sequences. J. Sed. Res. 76, 162-174.

Hovius, N., 1998. Controls on sediment supply by large rivers. In: Relative Role of Eustasy, Climate and Tectonics in Continental Rocks (ed. by K.W. Shanley and P.J. McCabe), SEPM Spec. Publ. 59, 3–16.

Hovius, N., 2000. Macroscale process systems of mountain belt erosion. In: Geomorphology and Global Tectonics (ed. by M.A. Summer eld), John Wiley & Sons Ltd., Chichester. 77–105.

Howard, A.D., 1994. A detachment limited model of drainage basin evolution. Water Resour. Res. 30, 739–752.

Hoyal, D.C.J.D., Sheets, B.A., 2009. Morphodynamic evolution of experimental cohesive deltas. J. Geophys. Res. 114, F02009.

Huang, H.Q., Nanson, G.C., 1997. Vegetation and channel variation; a case study of four small streams in southeastern Australia. Geomorphology 18, 237-249.

Hübscher, C., Betzler, C., Reiche, S., 2016. Seismo-stratigraphic evidences for deep base level control on middle to late Pleistocene drift evolution and mass wasting along southern Levant continental slope (Eastern Mediterranean). Mar. Petrol. Geol. 77, 526-534.

Hunt, D., Tucker, M.E., 1992. Stranded parasequences and the forced regressive wedge systems tract: deposition during base-level fall. Sed. Geol. 81, 1-9.

Hunt, D., Tucker, M.E., 1995. Stranded parasequences and the forced regressive wedge systems tract: deposition during base-level fall-reply, Sed. Geol. 95, 147-160.

Hutton, E.W.H, Syvitski, J.P.M., 2008. Sedflux 2.0: an advanced process response model that generates 3D stratigraphy. Comput. Geosci. 34, 731-753.

Imhof, M., Sharma, A.K., 2006. Quantitative seismostratigraphic inversion of a prograding delta from seismic data. Mar. Petrol. Geol. 23, 735-744.

Jansen, J.D., Douma, S.G., Brouwer, D.R., Van den Hof, P.M.J., Bosgra, O.H. and Heemink, A.W., 2009. Closed-loop reservoir management. Paper SPE 119098 presented at 2009 SPE Reservoir Simulation Symposium, The Woodlands, Texas, U.S.A, 2-4 February.

Janszen, A., 2008. High-resolution geological modelling of deltaic reservoir architecture in the shallow subsurface of the Po plain, Italy. MSc Thesis, Delft University of Technology, AES/AW/08-01, 82 p.

Janszen, A., Moscariello, A., Bennet., R., 2007. A high-resolution, geological model of a wave-dominated delta: cone penetration tests from the shallow subsurface of the Po Delta, (Italy). EP Journal of Technology, 7006, 6, 20-27.

Jerolmack, D.J., 2009. Conceptual framework for assessing the response of channel networks to Holocene sea level rise. Quatern. Sci. Rev. 28, 1786-1800.

Jerolmack, D.J., Mohrig, D., 2007. Conditions for branching in depositional rivers. Geology 35, 463-466.

Jerolmack, D.J., Paola, C., 2007. Complexity in a cellular model of river avulsion. Geomorphology 91, 259-270.

Jerolmack, D.J., Paola, C., 2010. Shredding of environmental signals by sediment transport. Geophys. Res. Lett. 37, L19401.

Jerolmack, D.J., Swenson, J.B., 2007. Scaling relationships and evolution of distributary networks on wave-influenced deltas. Geophys. Res. Lett. 34, L23402.

Jervey, M.T., 1988. Quantitative geological modeling of siliciclastic rock sequences and their seismic expressions. In: Sea Level Changes: An Integrated Approach (ed. by C.K. Wilgus, B.S. Hastings, C.G.St.C. Kendall, H.W. Posamentier, C.A. Ross and J.C. Van Wagoner). SEPM Spec. Publ. 42, 47–69.

Johnson, H.D., Baldwin, C.T., 1986. Shallow siliciclastic seas. In: Sedimentary Facies and Environments (ed. by H.G. Reading), Blackwell Scientific Publications, Oxford, 229–282.

Johnson, J.G., Murphy, M.A., 1984. Time-rock model for Siluro-Devonian continental shelf, western United States. Geol. Soc. Am. Bull. 95, 1349-1359.

Jolley, S.J., Fisher, Q.J., Ainsworth, R.B., 2010. Reservoir compartmentalization: an introduction. From: Jolley, S. J., Fisher, Q. J., Ainsworth, R. B., Vrolijk, P. J. & Delisle, S. (Eds.), Reservoir Compartmentalization. Geol. Soc. London Spec. Publ. 347, 1–8.

Jones, H.L., Hajek, E.A., 2007. Characterizing avulsion stratigraphy in ancient alluvial deposits. Sed. Geol. 202, 124-137.

Jones, H.L., Schumm, S.A., 1999. Causes of avulsion: an overview. Spec. Publ. Int. Assoc. Sedimentol. 28, 171-178.

Journel, A.G., 1986. Geostatistics: Models and tools for the earth sciences. Math. Geol. 18, 119-140. https://doi.org/10.1007/BF00897658.

Journel, A.G., Alabert, F., 1989. Non-Gaussian data expansion in the earth science. Terra Nova l, 123-134.

Journel, A.G., Alabert, F., 1990. New method for reservoir mapping. Jour. Petrol. Technol. 42, 212-218.

Journel, A.G., Gundeson, R., Gringarten, E., Yao, T., 1998. Stochastic modelling of a fluvial reservoir: a comparative review of algorithms. J. Petrol. Sci Eng. 21, 95-121.

Karamitopoulos, P., Weltje, G.J., Dalman, R.A.F., 2014. Allogenic controls on autogenic variability: inferences from analysis of synthetic stratigraphy. Basin Res. 26, 767-779.

Karssenberg, D.J., Bridge, J.S., 2008. A three-dimensional numerical model of sediment transport, erosion and deposition within a network of channel belts, floodplain and hill slope: extrinsic and intrinsic controls on floodplain dynamics and alluvial architecture. Sedimentology 55, 1717-1745.

Karssenberg, D.J., De Vries, M., Bridge, J. S., 2007. Conditioning a process-based fluvial-stratigraphy model to well data by inverse estimation of model inputs using a genetic algorithm. AAPG Search and Discovery Article #90063, AAPG Annual Convention, Long Beach, California.

Karssenberg, D.J., Törnqvist, T.E., Bridge, J.S., 2001. Conditioning a process-based model of sedimentary architecture to well data. J. Sed. Res. 71, 868-879.

Kelly, S.B., Olsen, H., 1993. Terminal fans-a review with reference to Devonian examples. In: Fielding C.R. (Ed.), Current Research in Fluvial Sedimentology. Sed. Geol. 85, 339-374.

Keogh, K.J., Martinius, A.W., Osland, R., 2007. The development of fluvial stochastic modelling in the Norwegian oil industry: a historical review, subsurface implementation and future directions. Sed. Geol., 202, 249-268.

Khan, I.A., Bridge, J.S., Kappelman, J., Wilson, R., 1997. Evolution of Miocene fluvial environments, eastern Potwar plateau, northern Pakistan. Sedimentology, 44, 221-251.

Kim, W., Paola, C., Swenson, J.B., Voller, V.R., 2006. Shoreline response to autogenic processes of sediment storage and release in the fluvial system. J. Geophys. Res. 111, F04013.

Kim, W., Paola, C., Voller, V.R., Swenson, J.B., 2006. Experimental measurements of the relative importance of controls on shoreline migration. Geophys. Res. Lett. 34, L23402.

Kleinhans, M.G., Ferguson, R.I., Lane S.N., Hardy, R.J., 2013. Splitting rivers at their seams: bifurcations and avulsion, Earth Surf. Proc. Land. 38, 47-61.

Kleinhans, M.G., Jagers, H.R.A., Mosselman E., Sloff, C.J., 2008. Bifurcation dynamics and avulsion duration in meandering rivers by one-dimensional and three-dimensional models. Water Resour. Res. 44, W08454.

Kleinhans, M.G., Weerts, H.J.T., Cohen, K.M., 2010. Avulsion in action: reconstruction and modelling sedimentation pace and upstream flood water levels following a Medieval tidal-river diversion catastrophe (Biesbosch, The Netherlands, 1421-1750 AD), Geomorphology 118, 65-79.

Knighton, A.D., 1998. Fluvial Forms and Processes: A New Perspective. Arnold. London.

Koltermann, C.E., Gorelick, S.M., 1996. Heterogeneity in Sedimentary Deposits: A Review of Structure-Imitating, Process-Imitating, and Descriptive Approaches, Water Resour. Res. 32, 2617– 2658.

Kraus, M.J., 1987. Integration of channel and floodplain suites. II. Vertical relations of alluvial palaeosols. J. Sed. Petrol. 57, 602-612.

Kraus, M.J., Aslan, A., 1999. Palaeosol sequences in floodplain environments: a hierarchical approach. Spec. Publ. Int. Assoc. Sedimentol. 27, 303-321.

Kraus, M.J., Wells, T.M., 1999. Recognizing avulsion deposits in the ancient strati- graphic record. In: Smith, N.D., Rogers, J. (Eds.), Fluvial Sedimentology VI. In: Spec. Publ. Int. Assoc. Sedimentol., vol. 28, pp. 251-268.

Krige, D.G., 1951. A Statistical Approaches to Some Basic Mine Valuation Problems on the Witwatersrand. Journal of the Chemical, Metallurgical and Mining Society of South Africa, 52, 119-139.

Kyrkjebø, R., Gabrielsen, R.H., Faleide, J.L., 2004. Unconformities related to the Jurrasic-Cretaceous synrift-post-rift transition of the northern North Sea. J. Geol. Soc. London 161, 1-17.

Leeder, M.R., 1978. A quantitative stratigraphic model for alluvium, with special reference to channel deposit density and interconnectedness. In: Miall, A.D. (ed.): Fluvial Sedimentology. Can. Soc. Petrol. Geol. Mem. 5, 587-596.

Leeder, M.R., 2011. Sedimentology and Sedimentary Basins: From Turbu- lence to Tectonics, Second Edition, Wiley-Blackwell, 768pp.

Leopold, L.B., Maddock, T., 1953. Hydraulic geometry of stream channels and some physiographic implications. USGS Prof. Pap. 252.

Leopold, L.B., Wolman, M.G., Miller, J.P., 1964. Fluvial Processes in Gemorphology. Freeman, San Fransisco.

Lesser, G.R., Roelvink, J.A., van Kester, J.A.T.M., Stelling, G.S., 2004. Development and validation of a three-dimensional morphological model. Coast. Eng. 51, 883-915.

Leuangthong, O., Deutsch, C.V., 2003. Stepwise conditional transformation for simulation of multiple variables. Math. Geol. 35, 155-173.

Li, J., 2014. Terminal fluvial systems in a semi-arid endorheic basin, Salar de Uyuni (Bolivia) (PhD thesis): https://doi.org/10.4233/uuid:0dac02b5-7004-4aa4-99aa-237adadfab1f.

Li, J., Donselaar, M.E., Hosseini Aria, S.E., Koenders, R., Oyen, A.M., 2014. Landsat imagery-based visualization of the geomorphological development at the terminus of a dryland river system. Quatern. Int. 352, 100–110.

Li, Q., Yu, L., Straub, K.M., 2016. Storage thresholds for relative sea-level signals in the stratigraphic record. Geology, 44, 179–182.

Li, W., Bhattacharya, J.P., Zhu, Y., 2011. Architecture of a forced regressive systems tract in a Turonian Ferron "Notom Delta", southern Utah, U.S.A. Mar. Petrol. Geol. 28, 1517-1529.

Li, W., Bhattacharya, J.P., Zhu, Y., Garza, D., 2010. Evaluating delta asymmetry using three-dimensional facies architecture and ichnological analysis, Ferron 'Notom Delta', Capital Reef, Utah, USA. Sedimentology, 58, 478-507.

Liu, X.M., Xu, J.M., Zhang, M.K., Huang, J.H., Shi, J.C., Yu, X.F., 2004. Application of geostatistics and GIS technique to characterize spatial variabilities of bioavailable micronutrients in paddy soils. Env. Geol. 46, 189-194.

Lunne, T., Robertson, P.K., Powell, J.J.M., 1997. Cone Penetration Testing in Geotechnical Practice. Blackie Academic & Professional, London, 312 p.

MacDonald, A.C., Halland, E.K., 1993. Sedimentology and shale modeling of a sandstone-rich fluvial reservoir; upper Statfjord Formation, Statfjord Field, Northern North Sea. AAPG Bull. 77, 1016-1040.

Mackey, S.D., Bridge, J.S., 1995. Three-dimensional model of alluvial stratigraphy: theory and applications. J. Sed. Res. 65, 7-31.

Mackin, J.H., 1948. Concept of a graded river. Bull. Geol. Soc. Am. 59, 463-512.

Madof, A.S., Bertoni, C., Lofi, J., 2019. Discovery of vast fluvial deposits provides evidence for drawdown during the late Miocene Messinian salinity crisis. Geology, 47, 171-174.

Madof, A.S., Harris, A.D., Connell, S.D., 2016. Nearshore along-strike variability: Is the concept of the systems tract unhinged? Geology 44, 315-318.

Makaske, B., Smith, D.G., Berendsen, H.J.A., 2002. Avulsions, channel evolution and floodplain sedimentation rates of the anastomosing upper Columbia River, British Columbia. Sedimentology 49, 1049-1071.

Malmon, D.V., Dunne, T., Reneau, S.L., 2003. Stochastic theory of particle trajectories through alluvial valley floors. J. Geol. 111, 525–542.

Mariethoz, G., Caers, J., 2014. Multiple-Point Geostatistics: Stochastic Modeling with Training Images.

Marr, J.G., Swenson, J.B., Paola, C., Voller, V.R. 2000. A two-diffusion model of fluvial stratigraphy in closed depositional basins. Basin Res. 12, 381–398.

Martin, J., Sheets, B., Paola, C., Hoyal, D., 2009. Influence of steady base-level rise on channel mobility, shoreline migration, and scaling properties of a cohesive experimental delta. J. Geophys. Res. 114, F03017.

Martinez, P.A., 1987. Simulation of Sediment Transport and Deposition by Waves for Simulation of Wave vs. Fluvial-dominated Beach Environments: M.S. thesis, 406 p., Dept. of Applied Earth Sciences, Stanford University.

Martinez, P.A., Harbaugh, J.W., 1993. Simulating Nearshore Environments. Pergamon Press, Oxford, 265pp.

Martinius, A., Kaas, I., Næss, A., Helgesen, G., Kjærefjord, J.M., Leith, D.A., 2001. Sedimentology of the heterolithic and tide-dominated Tilje Formation (Early Jurassic, Halten Terrace, Offshore Mid-Norway). Norwegian Petroleum Society Special Publications, 10, 103-144.

Martinius, A.W., Elfenbein, C., Keogh, K.J., 2014. Applying accommodation versus sediment supply ratio concepts to stratigraphic analysis and zonation of a fluvial reservoir. Int. Assoc. Sedimentol. Spec. Publ. 46, 101-126.

Matheron, G., 1962. Traité de geostatisque appliquée, vol. I: Memoires du Bureau de Recherches Géologiques et Miniéres, no. 14, Editions Technip, Paris, 333 pp.

Matheron, G., Bencher, H., de Fouquet, C., Galli, A., Ouerillot, D., Ravenne, C., 1987, Conditional simulation of the geometry of fiuviodeltaic reservoirs: S.P.E. 62nd Annual Conference Dallas, Texas, p. 591-599.

McManus, D.A. 1975. Modern versus Relict Sediment on the Continental Shelf. GSA Bull. 86, 1154-1160.

Meijer, X.D., 2002. Modelling the drainage evolution of a river-shelf system forced by Quaternary glacio-eustasy: Basin Res. 14, 361-377.

Meybeck, M., 1987. Global chemical weathering of surficial rocks estimated from river dissolved loads. Am. J. Sci. 287, 401-428.

Miall, A.D., 1985. Architectural elements and boundaries: A new method of facies analysis applied to fluvial deposits. Earth-Sci. Rev. 22, 261-308.

Miall, A.D., 1996. The geology of fluvial deposits: New York, Springer, 582pp.

Miall, A.D., 2010. The Geology of Stratigraphic Sequences, Second Edition, Springer Verlag, 522pp.

Miall, A.D., 2014. Updating uniformitarianism: stratigraphy as just a set of 'frozen accidents'. Geol. Soc. London Spec. Publ. 404, 11-36.

Miall, A.D., 2014. Fluvial Depositional Systems. Springer Geology. 316pp.

Miller, K.G., Kominz, M.A., Browning, J.V., Wright, J.D., Mountain, G.S., Katz, M.E., Sugarman, P.J., Cramer, B.S., Christie-Blick, N., Pekar, S.F., 2005a. The Phanerozoic record of global sea-level change. Science 310, 1293-1298.

Milliman, J.D., Meade, R.H., 1983. Worldwide delivery of river sediment to the oceans. J. Geol. 91, 1–21.

Milliman, J.D., Syvitski, J.P.M., 1992. Geomorphic/tectonic control of sediment discharge to the ocean: the importance of small mountainous streams. J. Geol. 100, 525–544.

Minderhoud, P.S.J., Erkens, G., van Pham, H., Bui, V.T., Erban, L., Kooi, H., Stouthamer, E., 2017. Impacts of 25 years of groundwater extraction on subsidence in the Mekong delta, Vietnam. Environ. Res. Lett. 12 (064006).

Mitchum, R.M. Jr., Vail, P.R., Thompson III, S., 1977. Seismic stratigraphy and global changes of sea level; Part 2, The depositional sequence as a basic unit for stratigraphic analysis, in Payton, C.E., ed., Seismic stratigraphy; applications to hydrocarbon exploration. AAPG Mem. 26, 53-62.

Mohrig, D., Heller, P.L., Paola, C., Lyons, W.J., 2000. Interpreting avulsion process from ancient alluvial sequences: Guadalope–Matarranya system (northern Spain) and Wasatch Formation (western Colorado). Geol. Soc. Am. Bull. 112, 1787-1803.

Monestiez, P., Allard, D., Froidevaux, R. (Eds.) 2001. geoENV III—Geostatistics for environmental applications. Kluwer Academic Publishers, Dordrecht.

Morad, S., Al-Ramadan, K., Ketzer, J.M., De Ros, L.F., 2010. The impact of diagenesis on the heterogenity of sandstone reservoirs: a review of the role of depositional facies and sequence stratigraphy. AAPG Bull. 94, 1267-1309.

Morad, S., Ketzer, J.M., De Ros, L.F., 2000. Spatial and temporal distribution of diagenetic alterations in siliciclastic rocks: implications for mass transfer in sedimentary basins. Sedimentology 47, 95-120.

Morad, S., Ketzer, J., De Ros, L., 2013. Linking Diagenesis to Sequence Stratigraphy. John Wiley & Sons, Inc. 552pp. DOI:10.1002/9781118485347.

Morón, S., Amos, K.J., (2018) Downstream grain-size changes associated with a transition from single channel to anabranching. Sedimentology 65, 1590-1610.

Morón, S., Amos, K.J., Edmonds D.A., Payenberg T., Sun, X., Thyer, M., 2017. Avulsion triggering by El Niño–Southern Oscillation and tectonic forcing: The case of the tropical Magdalena River, Colombia. Geol. Soc. Am. Bull. 129, 1300-1313.

Mount, J. F., 1995. California rivers and streams: the conflict between fluvial process and land use. Berkeley: University of California Press.

Murray, A.B., Paola, C., 2003. Modelling the effect of vegetation on channel pattern in bedload rivers. Earth Surf. Proc. Land. 28, 131-143.

Muto, T., 2001. Shoreline autoretreat substantiated in flume experiments. J. Sed. Res. 71, 246-254.

Muto, T., Steel, R.J., 1997. Principles of regression and transgression: the nature of the interplay between accommodation and sediment supply. J. Sed. Res. 67, 994-1000.

Muto, T., Steel, R.J., 2002. Role of autoretreat and A/S changes in the understanding of deltaic shoreline trajectory: a semi-quantitative approach. Basin Res. 14, 303-318.

Muto. T., Steel, R.J., 2004. Autogenic response of fluvial deltas to steady sea-level fall: implications from flume-tank experiments. Geology 32, 401-404.

Muto, T., Steel, R. J., Burgess, P.M., 2016. Contributions to sequence stratigraphy from analogue and numerical experiments. J. Geol. Soc. London 173, 837-844.

Neal, J., Abreu, V., 2009. Sequence stratigraphy hierarchy and the accommodation succession method. Geology, 37, 779-782.

Nemec, W., 1995. The dynamics of deltaic suspension plumes. In: Oti, M., Postma, G. (Eds.) Geology of deltas. Balkema, Rotterdam, 31-93.

Nicholas, A.P., Aalto, R.E., Sambrook Smith, G.H., Schwendel, A.C., 2018. Hydrodynamic controls on alluvial ridge construction and avulsion likelihood in meandering river floodplains. Geol. Soc. Am. Bull. 46, 639-642.

Nichols, G.J., Fisher, J.A., 2007. Processes, facies and architecture of fluvial distributary system deposits. Sed. Geol. 195, 75–90.

Nienhuis, J.H., Törnqvist, T.E., Esposito, C.R., 2018. Crevasse splays versus avulsions: A recipe for land building with levee breaches. Geophys. Res. Lett. 45, 4058– 4067.

North, C.P., Warwick, G.L., 2007. Fluvial Fans: Myths, Misconceptions, and the End of the Terminal-Fan Model. J. Sed. Res. 77, 693-701.

Olariu, C., Bhattacharya, J.P., 2006. Terminal Distributary Channels and Delta Front Architecture of River-dominated delta systems. J. Sed. Res. 76, 212-233.

Olea, R.A., Fundamentals of semivariogram estimation, modelling, and usage, in J.M. Yarus and R.L. Chambers, eds., Stochastic modeling and geostatistics. Principles, methods, and case studies. AAPG Computer Applications in Geology 3, 27-35.

Orton, G.J., Reading, H.G., 1993. Variability of deltaic processes in terms of sediment supply, with particular emphasis on grain size. Sedimentology 40, 475–512.

Paola, C., 2000. Quantitative models of sedimentary basin filling. Sedimentology 47, 121-178.

Paola, C., Leeder, M. 2011. Environmental dynamics: Simplicity versus complexity. Nature, 469, 38-39.

Paola, C., Martin, J. 2012. Mass balance effects in depositional systems. J. Sed. Res. 82, 435-450.

Paola, C., Seal, R., 1995. Grain-size patchiness as a cause of selective deposition and downstream fining. Water Resour. Res. 31, 1395–1407.

Paola, C., Heller, P.L., Angevine, C.L., 1992. The large-scale dynamics of grain size variation in alluvial basins. 1. Theory. Basin Res. 4, 73–90.

Paola, C., Straub, K.M., Mohrig, D.C., Reinhardt, L., 2009. The "unreasonable effectiveness" of stratigraphic and geomorphic experiments, *Earth Sci. Rev.* 97, 1-43.

Parker, G., 1978a. Self-formed straight rivers with equilibrium banks and mobile bed. Part 1. The sand-silt river. J. Fluid Mech. 89, 109–125.

Parker, G., 1978b. Self-formed straight rivers with equilibrium banks and mobile bed. Part 2. The gravel river. J. Fluid Mech. 89, 127–146.

Parker, G., Paola, C., Whipple, K.X., Mohrig, D.C., 1998. Alluvial fans formed by channelized fluvial and sheet flow. I: Theory. J. Hydraul. Eng. 124, 985–995.

Payton, C.E., 1977. Seismic-stratigraphy - applications to the exploration of sedimentary basins: AAPG Mem. 26, 516p.

Phillips, J.D., 2011. Universal and local controls of avulions in southeast Texas Rivers. Geomorphology 130, 17-28.

Pickup, G., Warner, R.F., 1976. Effects of hydrologic regime on magnitude and frequency of dominant discharge. J. Hydrol. 29, 51-75.

Plint, A.G., Nummedal, D., 2000. The falling stage systems tract: recognition and importance in sequence stratigraphic analysis. In: Hunt, D., Gawthorpe, R.L., (Eds.), Sedimentary Response to forced regression. Geol. Soc. London Spec. Publ. 172, 1-17.

Posamentier, H.W., 2004. Future Trends in 3-D Seismic Analysis: The Integration of Seismic Stratigraphy and Seismic Geomorphology. Search and Discovery Article #40127.

Posamentier, H.W., Allen, G.P., 1999. Siliciclastic sequence stratigraphy: concepts and applications: SEPM Concepts in Sedimentology and Paleontology, 210pp.

Posamentier, H.W., Kolla, V., 2003. Seismic geomorphology and stratigraphy of depositional elements in deep-water settings. J. Sed. Res. 73, 367-388.

Posamentier, H.W., Vail, P.R., 1988. Eustatic controls on clastic deposition. II. Sequence and systems tract models. In: Wilgus, C.K., Hastings, B.S., Kendall, C.G.St.C., Posamentier, H.W., Ross, C.A., Van Wagoner, J.C. (Eds.), Sea Level Changes—An Integrated Approach. SEPM Spec. Publ. 42, 125-154.

Posamentier, H.W., Weimer, P., 1993. Siliciclastic sequence stratigraphy and petroleum geology - where to from here? AAPG Bull. 77, 731-742.

Posamentier, H.W., Allen, G.P., James, D.P., Tesson, M., 1992. Forced regressions in a sequence stratigraphic framework: concepts, examples and sequence stratigraphic significance. AAPG Bull. 76, 1687–1709.

Posamentier, H.W., Davies, R.J., Cartwright, J.A., Wood, L., 2007. Seismic geomorphology-an overview. Geol. Soc. London Spec. Publ. 277, 1-14.

Posamentier, H.W., Jervey, M.T., Vail, P.R., 1988. Eustatic controls on clastic deposition. I. Conceptual framework. In: Wilgus, C.K., Hastings, B.S., Kendall, C.G.St.C., Posamentier, H.W., Ross, C.A., Van Wagoner, J.C. (Eds.), Sea Level Changes-An Integrated Approach. SEPM Spec. Publ. 42, 110-124.

Postma, G., 1990. Depositional architecture and facies of river and fan deltas: a synthesis. In: Coarse-grained Deltas (ed. by A. Colella and D.B. Prior), Int. Assoc. Sedimentol. Spec. Publ. 10, 13–27.

Postma, G., Kleverlaan, K., Cartigny, M.J., 2014. Recognition of cyclic steps in sandy and gravelly turbidite sequences, and consequences for the Bouma facies model. Sedimentology, 61, 2268-2290.

Powel, E.J., Kim, W., Muto, T., 2012. Varying discharge controls on timescales of autogenic storage and release processes in fluvio-deltaic environments: Tank experiments. J. Geophys. Res. 117, F02011.

Powel, J.W., 1875. Exploration of the Colorado River of the West and its Tributaries. Smithsonian Inst, Washington, D.C.

Powell, D.M., 2009. Dryland rivers: processes and forms. In Parsons A.J., Abrahams, A.D. (Eds.) Geomorphology of Desert Environments, 2nd ed., 831pp.

Power, M.E., Dietrich, W.E., Sullivan, K.O., 1998. Experimentation, observation and inference in river and watershed investigations, in Resetarits, W.J., and Bernardo, J., eds., Experimental Ecology: Issues and Perspectives: Oxford, U.K., Oxford University Press, p. 113–132.

Pyrcz, M.J., Deutsch, C.V., 2014. Geostatistical Reservoir Modeling. Second Edition. Oxford University Press, 448 pp.

Qayyum, F., Betzler, C., Catuneanu, O., 2017. The Wheeler diagram, flattening theory, and time. Mar. Petrol. Geol. 86, 1417-1430.

Qian, N., 1990. Fluvial processes in the lower Yellow River after levee breaching at Tong-waxiang in 1855. Int. J. Sed. Res. 5, 1-13.

Ravenne, C., 2002. Stratigraphy and Oil: a Review - Part 2: Characterization of Reservoirs and Sequence Stratigraphy: Quantification and Modeling. Oil & Gas Science and Technology - Rev. IFP, 57, 311-340.

Ravenne, C., Vially, R., Riché, P. Trémoliéres, P., 1987. Sédimentation et tectonique dans le bassin marin Eocène supérieur-Oligocène des Alpes du Sud. Revue de l'Institut Français du Pétrole, 42.

Reading, H.G. (ed.), 1996. Sedimentary Environments: Processes, Facies and Stratigraphy, Third Edition, Blackwell Publishing Ltd., Oxford, 688pp.

Reading, H.G., Collinson, J.D., 1996. Clastic coasts. In: Sedimentary Environments: Processes, Facies and Stratigraphy, Third Edition (ed. by H.G. Reading), Blackwell Publishing Ltd., 154–231.

Rebesco, M., Camerlenghi, A., 2008. Contourites. Elsevier.

Reitz, M.D., Jerolmack, D.J., Swenson, J.B., 2010. Flooding and flow path selection on alluvial fans and deltas. Geophys. Res. Lett. 37, L06401.

Reiners, P.W., Carlson, R.W., Renne, P.R., Cooper, K.M., Granger, D.E., McLean, N.M., Schoene, B., 2017. Geochronology and Thermochronology. Wiley-Blackwel. doi:10.1002/9781118455876.

Reiners, P.W., Ehlers, T.A., Zeitler, P.K., 2005. Past, present and future of thermochronology. In: Thermochronology (ed. by P.W. Reiners and T.A. Ehlers) Reviews in Mineralogy and Geochemistry, 58, 1–18.

Reynolds, A.D., 1999. Dimensions of paralic sandstone bodies. AAPG Bull. 83, 211-229.

Ripley, B.D., 1989. The use of spatial models as image priors. In: Possolo A. (ed.) Spatial Statistics & Imaging. IMS Lecture Notes, 29 pp.

Ritchie, B.D., Gawthorpe, R.L., Hardy, S., 2004a. Three-dimensional numerical modelling of deltaic depositional sequences 1: influence of the rate and magnitude of sea-level change. J. Sed. Res. 74, 203-220.

Ritchie, B.D., Gawthorpe, R.L., Hardy, S., 2004b. Three-dimensional numerical modelling of deltaic depositional sequences 2: influences of local controls. J. Sed. Res. 74, 221-238.

Romans, B.W., Normark, W.R., McGann, M.M., Covault, J.A., Graham, S.A., 2009. Coarse-grained sediment delivery and distribution in the Holocene Santa Monica Basin, California:

implications for evaluating source-to-sink flux at millennial time scales. Geol. Soc. Am. Bull. 121, 1394-1408.

Romans, B.W., Castelltort, S., Covault, J.A., Fildani, A., Walsh, J.P., 2016. Environmental signal propagation in sedimentray systems across timescales. Earth Sci. Rev. 153, 7-29.

Ruddiman, W.F., 2001. Earth's Climate: Past and Future. W.H. Freeman & Sons, New York.

Sacchi, Q., Borello, E.S., Weltje, G.J., Dalman, R.A.F., 2016. Increasing the predictive power of geostatistical reservoir models by integration of geological constraints from stratigraphic forward modelling. Mar. Petrol. Geol. 69, 112-126.

Sacchi, Q., Weltje, G.J., Verga, F., 2015. Towards process-based geological reservoir modelling: Obtaining basin-scale constraints from seismic and well data. Mar. Petrol. Geol. 61, 56-68.

Sadler, P.M., 1981. Sediment accumulation rates and the completeness of stratigraphic sections. J. Geol. 89, 569-584.

Sadler, P.M., Strauss, D.J., 1990. Estimation of completeness of strati- graphical sections using empirical data and theoretical models. J. Geol. Soc. 147, 471-485.

Sanchez-Villa, X., Carrera, J., Gomez-Hernandez, J. (Eds.) 2004. geoENV IV—Geostatistics for environmental applications. Kluwer Academic Publishers, Dordrecht.

Schultz, E.H., 1982. The chronosome and supersome: terms proposed for low-rank chronostratigraphic units. Bull. Can. Pet. Geol. 30, 29-33.

Schumm, S.A., 1968. River adjustment to altered hydrologic regimen – Murrumbidgee River and paleochannels. USGS Prof. Pap. 589.

Schumm, S.A., 1969. River Metamorphosis. J. Hydraul. Div. Amer. Soc. Civil Eng. 95, 255-274.

Schumm, S.A., 1993. River response to baselevel change: implications for sequence stratigraphy. J. Geol. 101, 279-294.

Schumm, S.A., Mosley, M.P., Weaver, W.E., 1987. Experimental Fluvial Geomorphology. Wiley, New York.

Seybold, H., Abrdade, J.S., Hermann, H.J., 2007. Modeling river delta formation. Proc. Natl. Acad. Sci. USA, 104, 16804-16809.

Shackleton, N.J., Opdyke, N.D., 1973. Oxygen isotope and palaeo-magnetic stratigraphy of equatorial Pacific core V28-238: oxygen isotope temperatures and ice volumes in a 10^5 and 10^6 year scale. Quatern. Res. 3, 39-55.

Shackleton, N.J., Opdyke, N.D., 1976. Oxygen isotope and paleomagnetic stratigraphy of Pacific core V28-239 late Pliocene to latest Pleistocene. Geol. Soc. Am. Mem. 145, 449-464.

Shanley, K.W., McCabe, P.J., 1993. Alluvial architecture in a sequence stratigraphic framework: a case history from the Upper Cretaceous of southern Utah, USA. In: Flint, S.S., Bryant, I.D.

(Eds.), The Geological Modelling of Hydrocarbon Reservoirs and Outcrop Analogues. In: Spec. Publ. Int. Assoc. Sedimentol. 15, 21-56.

Sharma, A.K., Imhof, M.G., 2007. Quantitative stratigraphic inversion: numerical study. Extended Abstracts SEG Annual Meeting, San Antonio, pp. 1500-1504.

Sheets, B., Hickson, T.A., Paola, C., 2002. Assembling the stratigraphic record: depositional patterns and time-scales in an experimental alluvial basin. Basin Res. 14, 287-301.

Skauvold, J., Eidvik., J., 2018. Data assimilation for a geological process model using the ensemble Kalman filter. Basin res. 30, 730-745.

Slingerland, R., Smith, N.D., 1998. Necessary conditions for a meandering-river avulsion. Geology 26, 435-438.

Slingerland, R., Smith, N.D., 2004. River avulsions and their deposits. Annu. Rev. Earth Planet. Sci. 32, 257-285.

Slingerland, R.H., Harbaugh, J.W., Furlong, K.P., 1994. Simulating Clastic Sedimentary Basins. Prentice Hall Publishers, Eaglewood Cliffs, USA, 220pp.

Sloss, L.L., 1950. Paleozoic stratigraphy in the Montana area. AAPG Bull. 34, 423–451.

Sloss, L.L., 1962. Stratigraphic models in exploration. J. Sed. Petrol. 32, 415–422.

Smith, D.G., 1976. Effect of vegetation on lateral migration of anastomosed channels of a glacier meltwater river. Geol. Soc. Am. Bull. 87, 857-860.

Smith, N.D., Cross, T.A., Dufficy, J.P., Clough, S.R., 1989. Anatomy of an avulsion. Sedimentology 36, 1-23.

Soares, A. (Ed.), 1993. (Geostatistics Troia'92, vols 1 and 2. Kluwer Academic Publishers, Dordrecht.

Soares, A., Gomez-Hernandez, J., Froidevaux, R. (Eds.), 1997. geoENV I—Geostatistics for environmental applications. Kluwer Academic Publishers, Dordrecht.

Soares, A, Pereira, M.J., Dimitrakopoulos, R. (Eds.), 2008. geoENV VI—Geostatistics for environmental applications. Springer, Dordrecht.

Sømme, T.O., Helland-Hansen, W., Martinsen, O.J., Thurmond, J.B., 2009. Relationships between morphological and sedimentological parameters in source-to-sink systems: a basis for predicting semi-quantitative characteristics in subsurface systems. Basin Res. 21, 361-387.

Sømme, T.O., Jackson, C.A.L., Vaksdal, M. 2013b. Source-to-sink analysis of ancient sedimentary systems using a subsurface case study from the Møre–Trøndelag area of southern Norway: Part 1 – depositional setting and fan evolution. Basin Res. 25, 489-511.

Sømme, T.O., Martinsen, O.J., Lunt, I., 2013a. Linking offshore stratigraphy to onshore paleotopography: The Late Jurassic–Paleocene evolution of the south Norwegian margin. Geol. Soc. Am. Bull. 125, 1164-1186.

Sømme, T.O., Piper, D.J.W., Deptuck, M.E., Helland-Hansen, W., 2011. Linking onshore-offshore sediment dispersal in the Golo source-to-sink system (Corsica, France) during the late Quaternary. J. Sed. Res. 81, 118-137.

Stefani, M., Vincenzi, S., 2002. Geologic- Stratigraphic Map of the Po Delta Central Area, Foglio 187 – Codigoro della Carta 1:50.000 del I.G.M. Servizio Geologico, Sismico, e dei Suoli, Bologna, Italy.

Stefani, M., Vincenzi, S., 2005. The Interplay of Eustasy, Climate and Human Activity in the Late Quaternary Depositional Evolution and Sedimentary Architecture of the Po Delta System. Mar. Geol., 222-223, 19-48.

Storms, J.E.A., Weltje, G.J., Van Dijke, J.J., Geel, C.R., Kroonenberg, S.B., 2002. Process-response modeling of wave-dominated coastal systems: simulating evolution and stratigraphy on geological timescales. J. Sed. Res. 72, 226-239.

Stouthamer, E., Berendsen, H.J.A., 2001. Avulsion frequency, avulsion duration, and interavulsion period of Holocene channel belts in the Rhine-Meuse delta, The Netherlands. J. Sed. Res. 71, 589-598.

Stouthamer, E., Berendsen, H.J.A., 2007. Avulsion: The relative roles of autogenic and allogenic processes. Sed. Geol. 198, 309-325.

Stouthamer, E., Cohen, K.M., Gouw, M.J.P., 2011. Avulsion and its implications for fluvial–deltaic architecture: insights from the Holocene Rhine–Meuse delta. In: Davidson, S.K., Leleu, S., North, C.P. (Eds.), From River to Rock Record: The Preservation of Fluvial Sediments and Their Subsequent Interpretation. In: SEPM Spec. Publ. 97, 215-232.

Straub, K.M., Paola, C., Mohrig, D., Wolinsky, M.A., George, T., 2009. Compensational stacking of channelized sedimentary deposits. J. Sed. Res. 79, 673-688.

Straubhaar, J., Renard, P., Mariethoz, G. Froidevaux, R., Besson, O., 2011. An Improved Parallel Multiple-point Algorithm Using a List Approach. Math. Geosci. 43. 305-328.

Strebelle, S., 2002. Conditional simulation of complex geological structures using multiple-point statistics. Math. Geol. 34, 1-21.

Strong, N., Sheets, B., Hickson, T., Paola, C., 2005. Mass balance framework for quantifying downstream changes in fluvial architecture. Int. Assoc. Sedimentol. Spec. Publ. 35, 243–253.

Summerfield, M.A., Hulton, N.J., 1994. Natural controls of fluvial denudation rates in major world drainage basins. J. Geophys. Res. 99, 13871-13883.

Sweet, M.L., Blum, M.D., 2016. Connections between fluvial to shallow marine environments and submarine canyons: implications for sediment transfer to deep water. J. Sed. Res. 86, 1147-1162.

Swenson, J.B., 2005. Relative importance of fluvial input and wave energy in controlling the timescale for distributary-channel avulsion. Geophys. Res. Lett. 32, L23404.

Swenson, J.B., Voller, V.R., Paola, C., Parker, G., & Marr, J.D., 2000. Fluvio-deltaic sedimentation: A generalized Stefan problem. European Journal of Applied Mathematics, 11, 433-452.

Swift, D.J.P., 1974. Continental shelf sedimentation. In: The Geology of Continental Margins (ed. by C.A. Burk and C.L. Drake), Springer- Verlag, Berlin, 117–135.

Swift, D.J.P., Thorne, J.A., 1991. Sedimentation on continental margins, I: a general model for shelf sedimentation. In: Shelf sand and sandstone bodies (Ed. by D.J.P. Swift, G.F. Oertel, R.W. Tillman and J.A. Thorne). Int. Assoc. Sedimentol. Spec. Publ. 14, 3-31.

Syvitski, J.P.M., Milliman, J.D., 2007. Geology, geography and humans battle for dominance in the delivery of fluvial sediment to the coastal ocean. J. Geol. 115, 1-19.

Syvitski, J.P.M., Peckham, S.D., Hilberman, R.D., Mulder, T., 2003. Predicting the terrestrial flux of sediment to the global ocean: a planetary perspective. Sed. Geol. 162, 5-24.

Talbot, M.R., Allen, P.A., 1996. Lakes. In: Sedimentary Environments: Processes, Facies and Stratigraphy, Third Edition (ed. by H.G. Reading), Blackwell Publishing Ltd., 83–124.

Taylor, T.R., Giles, M.R., Hathon, L.A., Diggs, T. N., Braunsdorf, N.R., Birbiglia, G.V., Kittridge, M.G., Macaulay, C.I., Espejo, I.S., 2010. Sandstone diagenesis and reservoir quality prediction: Models, myths, and reality. AAPG Bull. 94, 1093-1132.

Tetzlaff, D.M., Harbaugh, J.W., 1989. Simulating Clastic Sedimentation. Computer methods in the geosciences 7, Van Nostrand Reinhold, New York, 202pp.

Tetzlaff, D.M., 2004b. Modeling costal sedimentation through geologic time. J. Coast. Res. 20, 343-350.

Thorne, J.A., Swift, D.J.P., 1991a. Sedimentation on continental margins, I1: application of the regime concept. In: Swift, D.J.P., Tillman, R.W., Oertel, G.F., Thorne, J.A. (Eds.), Shelf sand and sandstone bodies: geometry, facies and sequence stratigraphy. lnt. Assoc. Sedimentol. Spec. Publ. 14, 33-58.

Thorne, J.A., Swift, D.J.P., 1991b. Sedimentation on continental margins, VI: A regime model for dcpositional sequences, their component systems tracts, and bounding surfaces. In: Swift,

D.J.P., Tillman, R.W., Oertel, G.F., Thorne, J.A. (Eds.), Shelf sand and sandstone bodies: geometry, facies and sequence stratigraphy. lnt. Assoc. Sedimentol. Spec. Publ. 14, 188-243.

Thornes, J.B., 2009. Catchment and Channel Hydrology. In: Parsons A.J., Abrahams, A.D. (Eds.) Geomorphology of Desert Environments, 2nd ed., 831pp.

Tipper, J.C., 2000. Patterns of stratigraphic cyclicity. J. Sed. Res. 70, 1262-1279.

Tipper, J.C., 2015. The importance of doing nothing: stasis in sedimentation systems and its stratigraphic effects. In: Smith, D.G., Bailey, R.J., Burgess, P.M., Fraser, A.J. (Eds.), Strata and Time: Probing the Gaps in Our Understanding. Geol. Soc. London Spec. Publ. 404, 105-122.

Tipper, J.C., 2016. Measured rates of sedimentation: What exactly are we estimating, and why? Sed. Geol. 339, 151-171.

Tomer, A., Muto, T., Kim, W., 2011. Autogenic hiatus in fluviodeltaic successions: geometrical modeling and physical experiments. J. Sed. Res. 81, 207-217.

Törnqvist, T.E., 1994. Middle and late Holocene avulsion history of the River Rhine (Rhine–Meuse delta, Netherlands). Geology 22, 711-714.

Törnqvist, T.E., *Bridge, J.S.,* 2002. *Spatial variation of overbank aggradation rate and its influence on avulsion frequency.* Sedimentology 49, 891-*905.*

Törnqvist, T.E., Wallinga, J., Murray, A.S., De Wolf, H., Cleveringa, P., De Gans, W., 2000. Response of the Rhine-Meuse system (West-central Netherlands) to the last Quaternary glacio-eustatic cycles: A first assessment. Global Planet. Change 27, 89-111.

Vail, P.R., Audemard, F., Bowman, S.A., Eisner, P.N., Perez-cruz, C., 1991. The stratigraphic signatures of tectonics, eustasy and sedimentology - an overview. In: Einsele, G., Ricken, W. & Seilacher, A. (eds) Cycles and Events in Stratigraphy. Springer-Verlag, Berlin, 617-659.

Vail, P.R., Mitchum, R.M., Thompson III, S., 1977, Seismic stratigraphy and global changes of sea level; Part 4, Global cycles of relative changes of sea level. In: Payton, C.E. (Ed.), Seismic stratigraphy; applications to hydrocarbon exploration. AAPG Mem. 26, 83–97.

Van Asselen, S., Stouthamer, E., Van Asch, T.W.J., 2009. Effects of peat compaction on delta evolution: a review on processes, responses, measuring and modelling. Earth Sci. Rev. 92, 35-51.

Van Dijk, M., Postma, G., Kleinhans, M.G., 2009. Autocyclic behaviour of fan deltas: an analogue experimental study. Sedimentology 56, 1569-1589.

Van Toorenenburg, K.A., Donselaar, M.E., Weltje, G.J., 2018. The life cycle of crevasse splays as a key mechanism in the aggradation of alluvial ridges and river avulsion. Earth Surf. Proc. Land. 43, 2409– 2420.

Van Toorenenburg, K.A., Donselaar, M.E., Noordijk, N.A., Weltje, G.J., 2016. On the origin of crevasse-splay amalgamation in the Huesca fluvial fan (Ebro Basin, Spain): Implications for connectivity in low net-to-gross fluvial deposits. Sed. Geol. 343, 156-164.

Van Wagoner, J.C., Beaubouef, R.T., Hoyal, D.C.J.D., Dunn, P.A., Adair, N.L., Abreu, V., Li, D., Wellner, R.W., Awwiller, D.N., Sun., T., 2003. "Energy Dissipation and the Fundamental Shape of Siliciclastic Sedimentary Bodies"., Abstract AAPG/SEPM: Siliciclastic sequence stratigraphy - Going Beyond parasequences; Technical Program AAPG Annual Meeting 2003.

Van Wagoner, J.C., Mitchum Jr., R.M., Campion, K.M., Rahmanian, V.D., 1990. Siliciclastic Sequence Stratigraphy in Well Logs, Core, and Outcrops: Concepts for High-Resolution Correlation of Time and Facies. In: American Association of Petroleum Geologists Methods in Exploration Series, vol. 7. 55pp.

Van Wagoner, J.C., Posamentier, H.W., Mitchum, R.M., Vail, P.R., Sarg, J.F., Loutit, T.S., Hardenbol, J., 1988. An overview of the fundamentals of sequence stratigraphy and key definitions. In: Wilgus, C.K., Hastings, B.S., Kendall, C.G.St.C., Posamentier, H.W., Ross, C.A., Van Wagoner, J.C. (Eds.), Sea-Level Changes – An Integrated Approach. In: Society of Economic Paleontologists and Mineralogists, Special Publication, 42, 39-45.

Ventra, D., Clarke., L.E., 2018. Geology and geomorphology of alluvial and fluvial fans: current progress and research perspectives, 440. https://doi.org/10.1144/SP440.16.

Von Neumann, J., 1966. Theory of Self Reproducing Automata: University of Illinois Press, 418pp.

Walling, D.E., Webb, B.W., 1996. Erosion and sediment yield: a global overview. In: Erosion and Sediment Yield: Global and Regional Perspectives (ed. by D.E. Walling and B.W. Webb), Int. Assoc. Hydrol. Sci. Publ. 236, 3–19.

Wang, Y., Straub, K.M., Hajek, E.A., 2011. Scale-dependent compensational stacking: An estimate of autogenic time scales in channelized sedimentary deposits. Geology, 39, 811–814.

Weber, K.J., 1986. How heterogeneity affects oil recovery. In: Lake, L.W., Carroll, H.B. (Eds.), Reservoir Characterisation. Academic Press, pp. 487-544.

Weber, K.J., Van Geuns, L.C., 1990. Framework for constructing clastic reservoir simulation models. J. Petrol. Technol. 42, 1248-1297.

Webster, R. Oliver, M.A., 2001. Geostatistics for Environmental Scientists (Statistics in Practice). John Wiley and Sons, Ltd., Chichester, 330pp.

Weltje, G.J., Roberson, S., 2012. Numerical methods for integrating particle-size frequency distributions. Comput. Geosci. 44, 156-167.

Weltje, G.J., Von Eynatten, H., 2004. Quantitative provenance analysis of sediments. Sed. Geol. 171, 1-11.

Weltje, G.J., Dalman, R.A.F., Karamitopoulos, P., Sacchi, Q., 2013. Reducing the uncertainty of static reservoir models: implementation of basin-scale geological constraints. 75th EAGE Conference & Exhibition incorporating SPE EUROPEC. SPE-164821-MS.

Weltje, G.J., Meijer, X.D., de Boer, P.L., 1998. Stratigraphic inversion of siliciclastic basin fills: a note on the distinction between supply signals resulting from tectonic and climatic forcing. Basin Res. 10, 129-153.

Wen, R.-J., Martinius, A.W., Næss, A., Ringrose, P.S., 1998. Three-dimensional simulation of small-scale heterogeneity in tidal deposits e a process-based stochastic simulation method. In: Buccianti, A., Nardi, G., Potenza, R. (Eds.), Proceedings of the 4th Annual Conference of the International Association of Mathematical Geology (IAMG), pp. 129-134. Ischia. De Frede, Napoli.

Wendebourg, J., Harbaugh, J.W., 1997. Simulating Oil Entrapment in Clastic Sequences, Volume 16 (1st Edition). Pergamon, 198pp.

Werner, B.T., 1999. Complexity in natural landform patterns. Science, 284, 102-104.

Wheeler, H.E., 1964. Base level, lithosphere surface, and time-stratigraphy. Geol. Soc. Am. Bull. 75, 599-610.

Whipple, K.X., Trayler, C.R., 1996. Tectonic control on fan size: the importance of spatially variable subsidence rates. Basin Res. 8, 351–366.

Williams, G.P., 1978. Bankfull discharge in rivers. Water Resour. Res. 14, 1141-1154.

Willis, B.J., Behrensmeyer, A.K., 1994. Architecture of Miocene overbank deposits in northern Pakistan. J. Sed. Res. 64, 60-67.

Wijns, C., Poulet, T., Boschetti, F., Dyt, C., Griffiths, C.M., 2004. Interactive inverse methodology applied to stratigraphic forward modelling. In: Curtis, A., Wood, R. (Eds.), Geological Prior Information: Informing Science and Engineering. Geol. Soc. London Spec. Publ. 239, 147-155.

Wolfram, S., 2002. A New Kind of Science: Wolfram Media, Champaign, III, 1197pp.

Wolinsky, M.A., Edmonds, D.A., Martin, J., Paola, C., 2010. Delta allometry: Growth laws for river deltas. Geophys. Res. Lett. 37, L21403.

Wolman, M.G., Miller, J.P., 1960. Magnitude and frequency of forces in geomorphic processes. J. Geol. 68, 54-74.

Worden, R.H., Armitage, P.J., Butcher, A.R., Churchill, J.M., Csoma, A.E., Hollis, C., Lander, R.H., Omma, J.E., 2018. Petroleum reservoir quality prediction: overview and contrasting approaches from sandstone and carbonate communities. From: Armitage, P. J., Butcher, A. R., Churchill, J. M., Csoma, A. E., Hollis, C., Lander, R. H., Omma, J. E. & Worden, R. H. (Eds.), Reservoir Quality of Clastic and Carbonate Rocks: Analysis, Modelling and Prediction. Geol. Soc. London Spec. Publ. 435, 1–31.

Wright, L.D., 1977. Sediment transport and deposition at river mouths: a synthesis. Geol. Soc. Am. Bull. 88, 857–868.

Wright, L.D., Coleman, J.M., 1974. Mississippi River mouth processes; effluent dynamics and morphologic development. J. Geol. 82, 751–778.

Wright, V.P., Marriott, S.B., 1993. The sequence stratigraphy of fluvial depositional systems: the role of floodplain sediment storage: Sed. Geol. 86, 203–210.

Xu, W., Tran, T.T., Srivastava, R.M., Journel, A.G., 1992. Integrating seismic data in reservoir modelling: the collocated cokriging alternative. Soc. Petr. Eng., Am. Inst. Min., Metall. Petr. Eng., SPE 24742.

Yang, W., Kominz, M.A., Major, R.P., 1998. Distinguishing the roles of autogenic versus allogenic processes in cyclic sedimentation, Cisco Group (Virgilian and Wolfcampian), north-central Texas. Geol. Soc. Am. Bull. 110, 1333-1353.

Yarus, J.M., Chambers, R.L., 1994. Stochastic Modeling and Geostatistics: Principles, Methods and Case Studies. AAPG, Computer Applications in Geology, 3, 379pp.

Zecchin, M., 2007. The architectural variability of small-scale cycles in shelf and ramp clastic systems: the controlling factors. Earth Sci. Rev. 84, 21-55.

Zecchin, M., 2010. Towards the standardization of sequence stratigraphy: is the parasequence concept to be redefined or abandoned? Earth Sci. Rev. 102, 117-119.

Zecchin, M., Catuneanu, O., 2013. High-resolution sequence stratigraphy of clastic shelves I: units and bounding surfaces. Mar. Petrol. Geol. 39, 1-25.

Zhang, J., Burgess, P.M., Granjeon, D., Steel, R., 2019. Can sediment supply variations create sequences? Insights from stratigraphic forward modelling. Basin Res. 31, 274– 289.

Zhu, Y., Bhattacharya, J.P., Li, W., Lapen, T.J., Jicha, B.R., Singer, B.S., 2012. Milankovitch-scale sequence stratigraphy and stepped forced regressions of the Turonian Ferron Notom Deltaic Complex, South-central Utah, U.S.A. J. Sed. Res. 82, 723–746.

Summary

Process-based stratigraphic models provide attractive tools to simulate sedimentary system dynamics spanning a wide range of spatial and temporal scales and segments of the sediment routing system while allowing full access to the model responses, i.e. the spatial distribution of lithologies as a function of the intervening processes and environmental conditions at the time of deposition. Apart from improving our understanding regarding the evolution of sedimentary systems under pre-specified allogenic forcing mechanisms and intrinsic dynamics, process-based stratigraphic models can be used to improve basin-fill history reconstructions and increase the geological credibility of static reservoir models by integrating regional information to local-scale heterogeneities. The realism and predictive power of the model responses and geological model realizations may be quantitatively assessed by comparison with the geophysical/geological data available.

In this thesis, fluvio-deltaic stratigraphy was acquired by employing a basin-scale forward stratigraphic model that includes sub-grid parameterizations of alluvial and marine processes for efficient simulation of basin-fill architecture. Chapter 2 focuses on the role of fluvial system dynamics, specifically avulsions, in the formation of delta lobes under time-invariant forcing. A feedback loop linking major avulsion, delta-plain aggradation, and delta-lobe switching is responsible for depocentre shifts and the generation of compensational stacking patterns in fluvio-deltaic systems. These stacking patterns occur in all settings where delta-plain accommodation is sufficient to permit local top-set aggradation. The stratigraphic expression of a depocentre shift is an isochronous surface (abandonment surface), which allows the subdivision of the sedimentary record into a series of units representing intervals during which channel belt and delta lobe were forming at a fixed location in the basin, so-called chronosomes. The recognition of system-wide chronosomes allows potentially high-resolution chronostratigraphic correlation of marine to continental deposits.

Chapter 3 investigates the role of autogenic processes (avulsions and mouth-bar induced bifurcations) throughout a sequence, i.e. a cycle of accommodation to sediment supply (A/S) rates. A measure of the overall stratigraphic variability is defined and post-processing of synthetic fluvio-deltaic stratigraphy by various methods allowed to explain its behaviour in terms of allogenic forcing and autogenic processes. Autogenic processes occurring in fluvio-deltaic systems are modulated by allogenic forcing, and therefore, the dominant types of autogenic process contributing to stratigraphic variability vary systematically throughout an accommodation-to-

supply cycle. In Chapter 4, synthetic stratigraphic records were obtained by simulating A/S cycles of varying wavelength and amplitude. A series of post-processing methods was developed and applied to extract chronostratigraphically constrained lithosomes (or chronosomes). Metrics describing sedimentary heterogeneities in synthetic stratigraphy at sub-seismic scale show to increase the predictive capabilities of sequence stratigraphic interpretation. This chapter also documents the linkage of avulsion events in a sequence stratigraphic context.

Chapter 5 demonstrates the application of a process-based stratigraphic forward model to a real-world setting (Altiplano Basin, Bolivia). A series of numerical experiments was performed with the model, in order to investigate the role of the avulsion process in low-gradient dryland river systems and predict sedimentary architecture. The model boundary and initial conditions (i.e. catchment area, smoothed initial topographic surface, grain size of sediment supply) were extracted from satellite images and sedimentological data obtained from Altiplano Basin (Bolivia) which also served for model validation.
The observed offset stacking of sediments in the area of interest is consistent with the high sediment load experiments which are characterized by an envelope of predictive architecture starting with a single-thread channel, and gradually expanding radially into multiple channels on account of continuous growth of alluvial ridges and avulsion-induced compensational stacking. This multiscale integrated approach provides a large-scale framework for reservoir characterization and modelling studies of ancient fluvial stratigraphic units in which the radial extent of the fluvial system and the spatial organization of its isolated channel-belt sediment bodies as well as their reservoir quality distribution are largely controlled by avulsion-induced compensational stacking.

Chapter 6 presents a modelling workflow that allows the construction of static reservoir models that maintain quantitative coherence with the large-scale geological setting of the reservoir. Based on geological/geophysical background information about palaeotopography, sea level, sediment supply, subsidence and so forth, the process-based stratigraphic model is run with the intent to approximate large-scale basin-fill properties. Subsequently, the model may be stochastically optimised by dedicated post-processing software to mimic sub-grid (reservoir-scale) properties of selected parts of the basin fill. This approach allows us to narrow down the range of possible scenarios (realisations) from the outset, which results in more reliable uncertainty estimates associated with reservoir models. Pilot studies suggest that the improvement of geological credibility of stochastically simulated fluvial reservoir models may go hand-in-hand with a significant reduction of the computational effort of inverting basin-scale process-based

stratigraphic forward models. The implementation of geological constraints on object-based models is expected to improve estimation of sand-body connectivity and dynamic reservoir behaviour, and will therefore contribute to reduction of the non-uniqueness in current static reservoir models. The partitioning of the overall uncertainty into contributions at the basin and reservoir scales may be quantitatively assessed, and the information content of all available data may be quantified. The approach outlined above thus permits geological reservoir modelling to be integrated in a closed-loop reservoir management process.

Although this thesis does not cover all processes occurring at the different segments of sediment routing system from source to sink, it provides an integrated approach that may be easily extended to reduce uncertainties related to basin-fill history reconstruction capturing the large-scale depositional fabric of potential geothermal and hydrocarbon reservoirs.

List of publications

Karamitopoulos, P., Weltje, G.J., Dalman, R., in review. Process stratigraphy of fluvio-deltaic systems: inferences from numerical simulation and the automated extraction of chronosomes. Basin Res.

Wendebourg, M., Verweij, J.M., Karamitopoulos, P., 2017. Using grain size analysis to study facies distribution and paleo-environment in the Southern North Sea delta of the Dutch offshore. 79th EAGE Conference and Exhibition.

Karamitopoulos, P., Verweij H., Fattah, R.A., Nelskamp, S., Dalman, R.A.F., 2016. Modelling siliciclastic stratigraphic traps in paralic sedimentary sequences: integrating stratigraphic forward modelling results in a basin modelling workflow. AAPG Hedberg Conference, The Future of Basin and Petroleum Systems Modelling, Santa Barbara, California.

Dalman, R., Weltje, G.J., Karamitopoulos, P., 2015. High-resolution sequence stratigraphy: prospects of system-wide chronostratigraphic correlation. Earth Planet. Sci. Lett. 412, 10-17.

Karamitopoulos, P., Weltje, G.J., Dalman, R.A.F., 2014. Allogenic controls on autogenic variability in fluvio-deltaic systems: inferences from analysis of synthetic stratigraphy. Basin Res. 26, 767-779.

Weltje, G.J., Dalman, R.A.F., Karamitopoulos, P, Sacchi, Q., 2013. Reducing the uncertainty of static reservoir models: implementation of basin-scale geological constraints. 75th EAGE Conference & Exhibition incorporating SPE EUROPEC.

Karamitopoulos, P., Weltje, G.J., Dalman, R.A.F., 2012. Stratigraphic variability in fluvio-deltaic sedimentary systems: Inferences from numerical experiments. Nederlands aardwetenschappelijk congres 11, Veldhoven, The Netherlands.

Karamitopoulos, P., Weltje, G.J., Dalman, R.A.F., 2011. Allogenic forcing of autogenic processes: inferences from an aggregated process-based model of fluvio-deltaic systems. American Geophysical Union, Fall Meeting 2011, abstract id. EP21A-0656.